

ACCELERATOR COMPLEX U70 OF IHEP: STATUS AND UPGRADES

S. Ivanov, on behalf of the U70 staff[#]
Institute for High Energy Physics (IHEP) of NRC “Kurchatov Institute”
Protvino, Moscow Region, 142281, Russia

Abstract

The report overviews present status of the Accelerator Complex U70 of IHEP–Protvino. It is a sequel to prior status reports [1] delivered to RuPAC-2008, -2010, -2012, and outlines the recent machine-related activity and upgrades in run-by-run chronological ordering.

GENERALITIES

Layout of the entire Accelerator Complex U70 of IHEP–Protvino is shown in Fig.1. It comprises four machines — 2 linear (I100, URAL30) and 2 circular (U1.5, U70) accelerators.

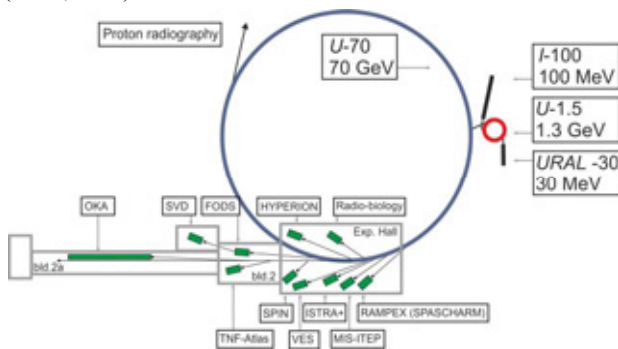


Figure 1: Accelerator Complex U70, beam transfer line network and fixed-target experimental facilities included. Proton mode (default) — cascade of URAL30–U1.5–U70, light-ion (carbon) mode — that of I100–U1.5–U70.

The points of attraction to the efforts spent during the period under report to be spotted in the scheme above are:

- Quality of stochastic slow extraction of 50–60 GeV protons to BTL#21 and the OKA facility;
- Extractions of the top-energy (24.1 GeV/u) carbon ions to BTL#22 (which is also an incidental fragment separator) and the FODS or SVD facilities;
- Stochastic slow extraction of the intermediate-energy (456 MeV/u ca) carbon ions via the new BTL#25 to the Interim Radio-Biological Work-bench;
- Launching beam-commissioning of the new Proton Radiography Facility (along the upward arrow, via a fast extraction);
- Re-equipment of the U-70 ring magnet main power supply plant with the up-to-date static thyristor AC-DC converters.

[#] N. Tyurin, Yu. Fedotov, O. Zyatkov, A. Minchenko, A. Maksimov, A. Afonin, E. Ludmirsky, O. Lebedev, D. Demihovskiy, V. Lapygin, A. Ermolaev, Yu. Milichenko, I. Tsygankov, I. Sulygin, N. Ignashin, S. Sytov, Yu. Antipov, D. Hmaruk, and G. Kuznetsov.

The light-ion program proceeds smoothly. Its advances are listed in Table 1.

Table 1: Light-ion program milestones

	Deuterons $^2\text{H}^+$	Carbon $^{12}\text{C}^{6+}$
U1.5	16.7–448.6 MeV/u March 30, 2008	16.7–455.4 MeV/u December 08, 2010
U70	23.6 GeV/u April 27, 2010	34.1 GeV/u April 24, 2011
		Slow extraction at 455 MeV/u April 24, 2011
		24.1 GeV/u (300 GeV full) in BTL#22 and the FODS facility April 27, 2012
		Validation tests of all top-energy extractions with the ion beam April 24, 2013

STATISTICS

Since RuPAC-2012, the U70 complex operated for five runs in total. Table 2 lists their calendar data. There were two runs in a row during the spring of 2014, which is uncommon.

Figure 2 shows beam availability data during machine development (MD) and fixed-target experimental physics program (XPh) with averages accumulated over 2002–13. The extracted beam is delivered to experimental facilities with the 82.2% availability, on average.

Runs 2013-2 and 2014-1, 2 are all excluded from the statistics since these were the MD runs entirely, without a pronounced top-energy physical program.

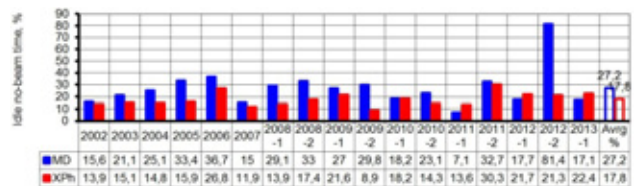


Figure 2: Beam availability statistics.

Details of the routine operation and upgrades are given on a run-by-run basis in what follows.

RUN 2012-2

As it can be seen from Fig. 2, the unfortunate feature of this run was a failed MD program followed by a squeezed

STATUS AND PERSPECTIVES OF THE VEPP-2000 COMPLEX*

Yu.A. Rogovsky[#], D.E. Berkaev, I.A. Koop, E.A. Perevedentsev, Yu.M. Shatunov, D.B. Shwartz,
BINP SB RAS and Novosibirsk State University, Novosibirsk, Russia

A.S. Kasaev, A.N. Kyrpotin, A.P. Lysenko, V.P. Prosvetov, A.L. Romanov, A.I. Senchenko,
P.Yu. Shatunov, A.N. Skrinsky, I.M. Zemlyansky, Yu.M. Zharinov,
BINP SB RAS, Novosibirsk, Russia

Abstract

The VEPP-2000 is a modern electron-positron collider at BINP. Last season in 2012–2013 was dedicated to the energy range of 160÷520 MeV per beam. The application of round colliding beams concept along with the accurate orbit and lattice correction yielded the high peak luminosity of $1.2 \cdot 10^{31} \text{ cm}^{-2} \text{ s}^{-1}$ at 500 MeV with average luminosity of $0.9 \cdot 10^{31} \text{ cm}^{-2} \text{ s}^{-1}$ per run. The peak luminosity limited only by beam-beam effects, while average luminosity – by present lack of positrons in whole energy range of 160÷1000 MeV. To perform high luminosity at high energies with small dead time the top-up injection is needed. At present new electron and positron injection complex at BINP is commissioned and ready to feed VEPP-2000 collider with intensive beams with energy of 450 MeV. Last calendar 2014 year was dedicated to the full/partial upgrade of complex's main parts.

VEPP-2000 OVERVIEW

The VEPP-2000 collider [1] exploits the round beam concept (RBC) [2]. This approach, in addition to the geometrical factor gain, should yield the significant beam–beam limit enhancement. An axial symmetry of the counter-beam force together with the X – Y symmetry of the transfer matrix between the two IPs provide an additional integral of motion, namely, the longitudinal component of angular momentum $M_z = x'y - xy'$. Although the particles' dynamics remains strongly nonlinear due to beam–beam interaction, it becomes effectively one-dimensional.

The RBC at VEPP-2000 was implemented by placing two pairs of 13 T superconducting final focusing solenoids into two interaction regions (IR) symmetrically with respect to collision points. There are several combinations of solenoid polarities that satisfy the RBC requirements, with different type of eigenmodes of betatron oscillations. Finally it was found that only 'flat' combinations (+– +– or +– –+) provide enough dynamic aperture (DA) for effective collider operation. This optics satisfies the RBC approach if the betatron tunes lie on the coupling resonance $\nu_1 - \nu_2 = 2$ to provide equal emittances via eigenmodes coupling.

The layout of the VEPP-2000 complex as it worked until 2013 is presented in Fig. 1. The complex consisted of the injection chain (including the old beam production

system and Booster of Electrons and Positrons (BEP) with an energy limit of 800 MeV) and the collider itself with two particle detectors, Spherical Neutral Detector (SND) and Cryogenic Magnetic Detector (CMD-3), placed into dispersion-free low-beta straights. The main design collider parameters are listed in Table 1.

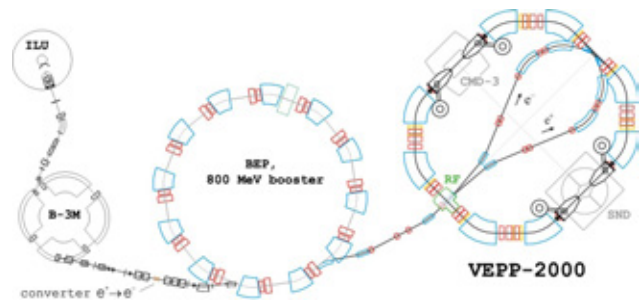


Figure 1: VEPP-2000 complex layout.

Table 1: VEPP-2000 main parameters @ $E = 1 \text{ GeV}$.

Parameter	Value
Circumference (C)	24.3883 m
Energy range (E)	200÷1000 MeV
Number of bunches	1×1
Number of particles per bunch (N)	1×10^{11}
Betatron functions at IP ($\beta_{x,y}^*$)	8.5 cm
Betatron tunes ($\nu_{x,y}$)	4.1, 2.1
Beam emittance ($\epsilon_{x,y}$)	$1.4 \times 10^{-7} \text{ m rad}$
Beam–beam parameters ($\xi_{x,y}$)	0.1
Luminosity (L)	$1 \times 10^{32} \text{ cm}^{-2} \text{ s}^{-1}$

The density of magnet system and detectors components is so high that it is impossible to arrange a beam separation in the arcs. As a result, only a one-by-one bunch collision mode is allowed at VEPP-2000.

BEAM DIAGNOSTICS

Diagnostics is based on 16 optical CCD cameras that register the visible part of synchrotron light from either end of the bending magnets and give full information about beam positions, intensities and profiles. In addition to optical beam position monitors (BPM) there are also four electrostatic pickups in the technical straight sections, two photomultipliers for beam current measurements via the synchrotron light intensity, and one beam current transformer as an absolute current monitor.

*Work is supported by: 1) the Ministry of Education and Science of the Russian Federation, Nsh-4860.2014.2; 2) the RFBR grant 14-02-31501
[#]rogovsky@inp.nsk.su

STATUS OF INJECTION COMPLEX VEPP-5

P. Logatchev, A. Petrenko, D. Bolkhovityanov, D. Nikiforov, A. Leviceh, A. Barnyakov, A. Novikov, V. Gambaryan, K. Astrelina, Budker INP, Novosibirsk, Russia
 A. Starostenko, F. Emanov, Budker INP, Novosibirsk; NSU, Novosibirsk, Russia

Abstract

The VEPP-5 Injection Complex [1] will supply BINP RAS colliders with electron and positron beams. Primary launch have been performed: electron and positron beams were obtained, injection to damping ring have been done, as well as storage of electrons and positrons. Now both transport channel to the electron/positron colliders VEPP-2000 and VEPP-4M are fully assembled and therefore test extractions of electron beam with energy of 360 MeV into beam lines to users are being performed. Main users require a reliable and trouble proof source of particles, thus reliability and stability of operation are a paramount tasks.

INTRODUCTION

VEPP-5 Injection Complex consists of 270 MeV driving electron linac, 510 MeV positron linac and damping ring (See Fig.1). Both linear accelerators are based on four accelerating modules, each one feeds by one SLAC klystron (5045). Two first modules have three accelerating structures and second two — four structures. First accelerating structures of both linacs have an enhanced average acceleration gradient of 20 MeV/m and other regular sections up to 17–20 MeV/m. Both linacs can operate up to 50 Hz repetition rate. Damping ring stores and cools down both electron and positron beams (See Figure 3). It is equipped with 50 Hz injection system.



Figure 2: Linear accelerators.



Figure 3: Damping ring.

Table 1: Designed parameters of Injection Complex

Maximum Beam Energy (MeV)	510
Max. number of electrons in the beam	$2 \cdot 10^{10}$
Max. number of positrons in the beam	$2 \cdot 10^{10}$
Energy spread in the beam (%)	0.07
Longitudinal beam sigma (mm)	4
Vertical emittance (mm mrad)	0.005
Horizontal emittance (mm mrad)	0.023
Dumping times vert./horis. (ms)	17/11
Extraction rate (Hz)	1

Designed parameters of VEPP-5 Injection Complex are presented in Table 1. At the parameters listed above Injection Complex will be able to cover all needs of BINP $e^+ e^-$ colliders for nearest future. This will greatly improve the VEPP-2000 and VEPP-4M performance, because of significant increase of positron production rate and will help to reach their maximum luminosity.

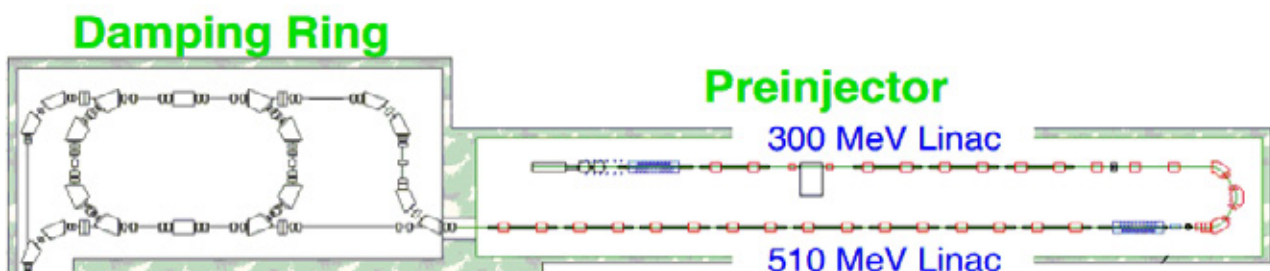


Figure 1: Injection complex.

COMMISSIONING 2 MEV COOLER IN COSY AND NOVOSIBIRSK

V. B. Reva, V.V. Parkhomchuk, BINP, Novosibirsk, and NSU, Novosibirsk, Russia
 M.I. Bryzgunov, A.V. Bublely, A.D. Goncharov, V.M. Panasyuk, BINP, Novosibirsk, Russia
 Vsevolod Kamerdzhev, FZJ, Jülich, Juergen Dietrich, HIM, Mainz

Abstract

The 2 MeV electron cooling system for COSY-Julich was proposed to further boost the luminosity in presence of strong heating effects of high-density internal targets. The 2 MeV cooler is also well suited in the start up phase of the High Energy Storage Ring (HESR) at FAIR in Darmstadt. It can be used for beam cooling at injection energy and for testing new features of the high energy electron cooler for HESR. The COSY cooler is designed on the classic scheme of low energy coolers like cooler CSRm, CSRe, LEIR that was produced in BINP before. The electron beam is transported inside the longitudinal magnetic field along whole trajectory from an electron gun to a collector. The 2 MeV electron cooler was installed in the COSY ring in the spring 2013. Electron beam commissioning and first studies using proton and deuteron beams were carried out. Electron cooling of proton beam up to 1662 MeV kinetic energy was demonstrated. Maximum electron beam energy achieved so far amounted to 1.25 MeV. Voltage up to 1.4 MV was demonstrated. The cooler was operated with electron current up to 0.5 A.

SETUP DESCRIPTION

Electron cooling is very useful technique for obtaining high-quality ion beams with high-intensity and low momentum spread [1]. In this method, the phase-space density of an ion beam is increased with a Coulomb interaction of a “hot” ion beam with a “cold” electron beam. Therefore, the ion beam repeatedly transfers its thermal energy to the electron beam moving with the same velocity.

There are many experiments and theoretical calculation that shows the useful of the magnetized cooling. These experiments and calculation was done in the different scientific centres in the world. The 2 MeV cooler at COSY is the first device utilizing the idea of magnetized cooling in this energy range, being an important step towards relativistic electron cooling required for the HESR at FAIR. Furthermore, it has been shown, that the 2 MeV cooler, if installed in the HESR, can be used without changes for the heavy ion operation modes [2,3].

First ideas was formulated in 2003 and a first report was published in 2005 [4]. The construction of the 2 MeV electron cooler for COSY began at the Budker Institute of Nuclear Physics (BINP) in 2009 and ended 2012. In spring 2013 the cooler was installed in the COSY ring. First beam cooling results were obtained in October 2013 by the joint BINP-COSY team. Further beam cooling experiments followed during a two-week period of dedicated beam time beginning of 2014. At that time a

first attempt to use electron and stochastic cooling in the same machine cycle was made. Furthermore, electron cooling of proton/deuteron beam into a barrier bucket was demonstrated. The design of the cooler and its main parameters are described in [5].

The schematic design of the setup is shown in Fig.1. The electron beam is accelerated by an electrostatic generator that consists of 33 individual sections connected in series. Each section has two high-voltage power supplies with maximum voltage 30 kV and current 1 mA. The electron beam is generated in electron gun immersed into the longitudinal magnetic field. After that the electron beam is accelerated, moves in the transport line to the cooling section where it will interact with protons of COSY storage ring. After interaction the electron beam returns to electrostatic generator where it is decelerated and absorbed in the collector.

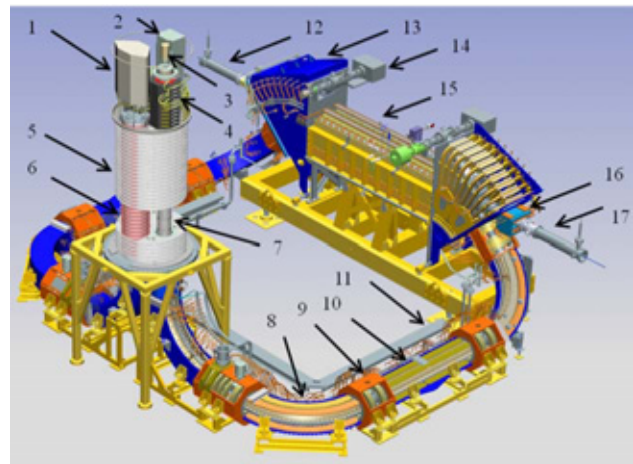


Figure 1: 3D design of 2 MeV COSY cooler. Collector PS is 1, SGF system is 2, ion pump of collector is 3, collector with magnetic system is 4, HV section is 5, cascade transformer is 6, acceleration tube is 7, bend 90 degrees is 8, straight section is 9, line section is 10, cable path is 11, input of the proton beam is 12, toroid 45 is 13, vacuum pump is 14, cooling section is 15, ion dipole is 16, output of the ion beam is 17.

The optics of 2 MeV cooler for COSY is designed close to the classical low-energy coolers. The motion of the electron beam is magnetized (or close to magnetized conditions) along whole trajectory from a gun to a collector. This decision is stimulated by requirement to operate in the wide energy range from 25 keV to 2 MeV. So, the longitudinal field is higher than transverse component of the magnetic fields. The bend magnets and linear magnets of the cooler are separated by a section

ON THE WAY TO A RELATIVISTIC ELECTRON COOLER

J. Dietrich[#], TU Dortmund and Helmholtz Institut Mainz, Germany

K. Aulenbacher, M. Bruker, A. Hofmann, Helmholtz-Institut Mainz, Germany

V. Kamerzhiev, Forschungszentrum Jülich, Germany

M. Bryzgunov, V. Parkhomchuk, V. Reva, BINP SB RAS, Novosibirsk, Russia

Abstract

A 4-8 MeV relativistic electron cooling system for the HESR storage ring, which is part of the future GSI facility FAIR, is needed to further boost the luminosity even with strong heating effects of high-density internal targets. In addition, the upgrade to 8 MeV of the relativistic electron cooler is essential for the future Electron Nucleon Collider (ENC at FAIR) project. Using the experience of the 2 MeV electron cooler at COSY, which has the highest energy of all coolers that were made based on the idea of magnetised cooling and transport of the electron beam up to now, a new concept for powering the solenoids at high voltage is proposed.

INTRODUCTION

The use of electron coolers in the range of electron beam energy lower 400 keV is well established and state of the art. For higher electron energies there exists up to now only one machine – the Recycler Electron Cooler (REC) of Fermilab with a terminal voltage of 4.4. MV [1]. The cooler was installed into the Recycler during the summer of 2005 and was operating until the end of 2011 when the Tevatron was shut off. The cooling opened the possibility for several times higher, record luminosities. The REC overcame not only the great challenge of operating 4.4 MV pelletron accelerator in the recirculation mode with up to 1A beams, but also resolved the hard issue of high quality beam transport through non-continuous magnetic focusing beamline [2]. The next unique high energy electron cooler -the 2 MV COSY electron cooler- was commissioned in 2013 at Juelich [3]. Development of high energy electron coolers is a technical challenge due to the engineering problems like high voltage generation, power transmission to the gun and collector in the accelerator “head” and the power transmission to the magnetic coils at the accel/decel tubes for magnetised electron beam transport. Today there is a need for further development. In the high energy storage ring HESR for antiprotons at the FAIR facility in Darmstadt a 4.5 MV electron cooler is planned [4]. The proposed concept of the polarised Electron-Nucleon Collider (ENC) integrates the 15 GeV/c HESR of the FAIR project for protons/deuterons and an additional 3.3 GeV electron ring [5]. A new 8.2 MV electron cooler is an essential part in this concept. In the NICA collider project of JINR Dubna a 2.5 MV electron cooler is foreseen with one electron

beam per each ring of the collider [6]. There are some special features of high energy cooling. The cooling rate decreases with $\beta^{-4}\gamma^{-5}$ [7]. To obtain a maximum friction force the “waveiness” of the magnetic force line should be as small as possible to get a smaller contribution to the effective electron velocity [8]. To get a high cooling rate magnetised electron cooling is necessary. All low-energy (3-400 keV) electron coolers are based on magnetised cooling. The electron beam transport and alignment of electron and ion beam is done with continuous magnetic field. Strong magnetic field completely suppresses transverse temperature of electron beam, so that effectiveness of cooling is determined by a very low longitudinal temperature of electrons. Non-magnetised cooling relies on the fact that rms velocity spread of electrons is comparable or smaller than the one of ions which need to be cooled. For the REC (non-magnetised case) cooling times of about one hour was sufficient. The new coolers for COSY and the new future projects should provide a few orders of magnitude more powerful longitudinal and transverse cooling. This requires new technical solutions. The basic idea of the 2MeV COSY cooler and for the future HESR and NICA collider coolers is to use a high magnetic field along the orbit of the electron beam from the electron gun to the collector. Faster cooling times are essential for the future projects. The technical problems for electrostatic accelerator at 8-10 MV and needed electron beam currents up to 3 A is a great challenge. An alternative can be a low frequency linac with bunched electron beam. Today this system achieved electron peak currents of about 10 A [9].

In order to solve critical technical issues of a future relativistic electron cooler based on an electrostatic accelerator the Helmholtz-Institut Mainz promotes collaborations with other Institutes such as Forschungszentrum Juelich (FZJ), Budker Institute of Nuclear Physics Novosibirsk (BINP), Russia and Lehrstuhl fuer Technische Thermodynamik und Transportprozesse, University Bayreuth. One of the challenges in case of the electrostatic accelerator is the powering of HV-solenoids for the magnetised electron beam transport. The HV-solenoids are located on different electrical potentials inside a high voltage vessel, which is why they needed a floating power supply. A novel idea from Budker institute is to use small turbines for high voltage generation, for power of the magnetic coils in-side the high voltage vessel and for powering of

[#]juergen.dietrich@tu-dortmund.de

MECHANISM OF COMPRESSION OF POSITRON CLOUDS IN THE SURKO TRAP OF THE LEPTA FACILITY*

E. Ahmanova, A. Kobets, I. Meshkov, O. Orlov, A. Sidorin, S. Yakovenko, JINR, Dubna, Russia
M.K. Eseev[#], NAFU after name M.V. Lomonosov, Arkhangelsk, Russia

Abstract

Results from experimental studies of plasma storage in the Surko trap at the LEPTA facility are presented. The number of stored particles is found to increase substantially when using the so-called "rotating wall" (RW) method, in which a transverse rotating electric field generated by a cylindrical segmented electrode cut into four pairs is applied to the positrons storage region.

The conditions of transverse compression of the plasma bunch under the action of the rotating field and buffer gas are studied. The optimal storage parameters are determined for these experimental conditions. Mechanisms of the action of the rotating field and buffer gas on the process of positron clouds storage are presented.

INTRODUCTION

Experiments with antimatter required the development of methods of storage, confinement and manipulate of clouds of antiparticles. For these purposes, generally used a electromagnetic trap. One method of increasing the efficiency of storage: increase in the lifetime of charged clouds inside the trap in a rotating electric field. The effect of «The Rotating Wall» (RW) was detected in experiments on the storage of a plasmoid ions [1]. Then, similar results were obtained for both the electron and positron plasma [2, 3]. The method of the rotating field is used to generate antihydrogen in projects ATHENA/ALPHA [4, 5]. Successful use of this method allowed us to begin the study of the properties of antimatter and exotic atomic and molecular systems. Determining if there is storage of the frequency and the direction of rotation of the field in a plane transverse to the axis of the trap. The dependence of the efficiency savings from RW-field parameters is resonant. There are several mechanisms [6-9] action of the rotating field compression and holding a bunch of charged particles trapped. Until now, the explanation of this phenomenon causes a heated discussion.

THE SURKO TRAP OF THE LEPTA FACILITY

The LEPTA facility [10] is designed for generating high flow orthopositronium opportunity to carry out precision measurements of the characteristics of positronium. In the storage ring can be made of two kinds of particles injection. The electron beam creates an

electron gun to clear the circulating electron beam collector exists, positron beam is injected from the source of positrons passing through positron trap. Optimization of the process of accumulation of positrons in the trap is one of the basic conditions of work. This is an open the trap Malmberg-Penning type with a longitudinal magnetic field. Retention of charged particles in the longitudinal direction of the accumulation is carried out by the electrostatic field created by trap electrodes. With the storage of positrons injection from the source (^{22}Na) of a continuous stream necessary to ensure the selection of the energy of motion for the "rolling" in the potential well inside the trap. For these purposes, Surko [11] proposed the use of a buffer gas. Thus modified trap began to wear his name. It is used to the LEPTA facility (see Fig. 1).

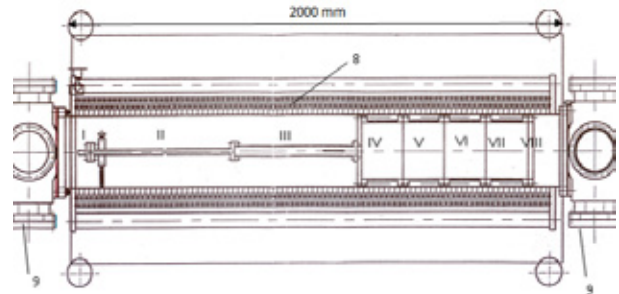


Figure 1: Scheme the Surko traps (longitudinal section). I - VIII - electrodes 8 - solenoid 9 - Vacuum posts.

MECHANISM OF COMPRESSION OF POSITRON CLOUDS

In [12] proposed a mechanism of the effect of a RW-field on the transverse size and lifetime of the storage trapped cloud based 3D model of the dynamics of charged particles. The experiments datas were presented on research independion frequency of the rotating field with a longitudinal oscillation bounce-frequency, which show the validity of this model. The essence of the proposed mechanism is reduced to the necessity of matching the frequency of the rotating field f_{RW} , frequency magnetron motion of particles in the trap f_- and the frequency of the longitudinal oscillations of the bounce f_z :

$$f_{RW} = Nf_- = Lf_z. \quad (1)$$

Here N, L — integers. The values of the longitudinal oscillation frequency bounce-determined depth and size of the potential well, retaining particles within the area of accumulation. The values of the magnetron frequency is

ULTRAHIGH VACUUM IN SUPERCONDUCTING SYNCHROTRONS

A.M.Bazanov, A.V.Butenko, A.R.Galimov, A.V.Nesterov, A.V.Smirnov[#]
JINR, Dubna, 141980, Russia

Abstract

The achievement of ultrahigh vacuum conditions in the range of 10^{-10} – 10^{-12} Torr is a very complicated task for charged particle accelerators. For the superconducting accelerators the main rest gas is the hydrogen which does not freeze effectively on the chamber wall even under the liquid helium temperature. A fast ramp of the magnetic field in the superconducting synchrotrons leads to the heating of the vacuum chamber and the additional evaporation of the hydrogen from the vacuum wall. Non-evaporable getters under the liquid nitrogen temperature are planned to the pumping of the hydrogen and achievement of the necessary vacuum conditions in the new accelerator complex of the NICA project at JINR.

VACUUM GAS COMPOSITION

In the atmosphere conditions the main gas components are nitrogen and oxygen. Other gases like water, argon, CO_2 occupy less than 1% of the air volume. The gas composition at vacuum condition is varied depending on many factors: choice of material, cleaning, baking, pumping system design, type of pumps, temperature, photon, electron or ion bombardment of the surface and many others.

Water is the main gas in unbaked metal chambers. The water outgassing does not depend significantly on the nature of metals, on surface treatments and on temperature (for temperatures lower than 110°C). At present no methods, except heating, exist to remove water from unbaked metals.

At the ultrahigh vacuum condition H is the main gas desorbed by baked metals. The outgassing of hydrogen is an intrinsic property of metals and the value of the outgassing rate of hydrogen is stable at room temperature. The diffusion model predicts values for the hydrogen outgassing that are in accord with experimental observations. Firing decreases the hydrogen outgassing rate by more than 2 orders of magnitude.

Gas molecules are dissolved into the bulk of materials during the production processing and during their permanence in air. In vacuum, the lighter molecules diffuse and, after reaching the surface, they are released. Only hydrogen atoms have enough mobility in metals to attain the surface where they recombine to form H_2 . The models that take into account all the steps in the outgassing process are quite complicated and, in general, they give only asymptotic solution for limit conditions.

[#]smirnov@jinr.ru

PUMPING SYSTEMS

Different pumping systems are used for the achievement of ultrahigh vacuum conditions in particle accelerators. Ion sputter pump cannot effectively remove hydrogen from the rest gas and can be used in the combination with other pumping systems. Turbomolecular pumps has a minimum limit about 10^{-11} Torr and can be used as preliminary pumping system only. Titanium sublimation pumps require the periodical activation at high temperature and cannot be used with superconducting accelerators at the cryogenic temperature.

Cryosorption pumps are the most popular pumping systems for the achievement of the ultrahigh vacuum conditions at superconducting accelerators. Cryocondensation is based on the mutual attraction of similar molecules at low temperature. The key property is the saturated vapour pressure, i.e. the pressure of the gas phase in equilibrium with the condensate at a given temperature. It limits the attainable pressure. Only Ne, H_2 and He have saturated vapour pressures higher than 10^{-11} Torr at 20 K (Figure 1). The vapour pressure of H_2 at 4.3 K is in the 10^{-7} Torr range, at 1.9 K lower than 10^{-12} Torr.

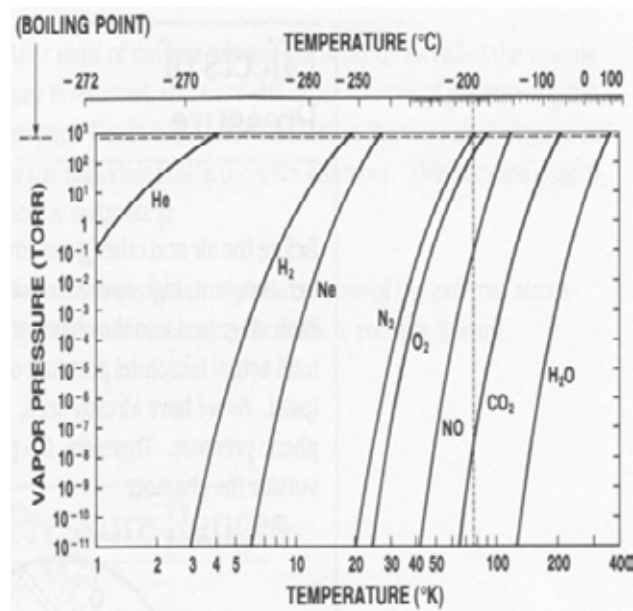


Figure 1: Vapour pressure of common gases.

Cryosorption is based on the attraction between molecules and substrate. This interaction is much stronger than that between similar molecules. Gas molecules are pumped at pressures much lower than the saturated vapour pressure providing the adsorbed quantity is lower than one monolayer. Porous materials in cryosorption

RF SYSTEM OF THE BOOSTER OF NICA FACILITY

G.Ya.Kurkin[#], A.M.Batrakov, S.A.Krutikhin, Ya.G.Kruchkov, S.V.Motygin, A.M.Pilan,
Budker Institute of Nuclear Physics, SB RAS, Novosibirsk, Russia

G.A.Fatkin, Budker Institute of Nuclear Physics, Novosibirsk State University, Novosibirsk, Russia

Abstract

The project NICA is being constructed in JINR, Dubna to provide collisions of heavy ion beams in the energy range from 1 to 4.5 GeV/u at the luminosity level of $1 \cdot 10^{27} \text{ cm}^{-2} \cdot \text{s}^{-1}$. One of the elements in the collider injection chain is the Booster – a cycling accelerator of ions $^{197}\text{Au}^{32+}$. The injection energy of particles is 6.2 MeV/u, extraction energy is 600 MeV/u.

Two RF station are to provide 10 kV of acceleration voltage. Frequency range of operation of the stations in the injector chain is from 634 kHz to 2400 kHz [1, 2]. The provisions are made for autonomous mode of operation in the frequency range of 0.5 – 5.5 MHz at the same accelerating voltage. Amorphous metal rings produced in Russia are used in the RF cavities.

RF stations are created in the Budker Institute of Nuclear Physics, SB RAS, Novosibirsk. The stations are tested in the operative mode and have been delivered to the customer in September 2014. Main design features and parameters of RF cavity power generator and control system of the stations are described in the paper.

INTRODUCTION

Acceleration of particles in the Booster will be made in two stages.

- Adiabatic capture and acceleration at the fourth harmonic of revolution frequency up to the energy of electronic cooling of 100 MeV/U.
- Acceleration of particles at the first harmonic up to energy of 600 MeV/U.

Between the acceleration stages the electronic cooling of beam is made for a time of ~ 1 sec with RF switched off.

During both acceleration stages the operational frequency range lays within the limits of 0.5 - 2.5 MHz.

On the customer request for autonomous operation of Booster the frequency range is extended to 0.5 - 5.5 MHz at the same gap voltage of 10 kV. The duration of the acceleration cycle in this mode is 1.5 sec, the repetition time of a cycle is 6 sec. It is supposed, that after acceleration of ions their slow extraction from Booster for physical experiments will be carried out.

THE ACCELERATING CAVITY

The accelerating cavity is formed by two pieces of the short-circuited coaxial lines divided by the accelerating gap (Fig.1). A vacuum-tight ceramic insulator 6 is installed in the gap. Only the stainless steel beam pipe and the gap ceramic are under vacuum, the remaining cavity is operated in air.

Main parameters of RF cavity are given in table 1.

Table 1: RF station main parameters

Parameter	Value
Frequency range, MHz	0.5 – 5.5
Gap voltage, kV	5.0
Beam pipe diameter, mm	160
Residual gas pressure, Torr	$< 5.5 \cdot 10^{-11}$
Outside station diameter, m	1.2
Installation length, m	1.4
Real part of conductance at the cavity gap, Ohm	> 1000

To increase the shunt impedance of RF cavities in the frequency range from hundreds kilohertz and in excess of ten megahertz a space between conductors of the coaxial is filled with a material with large magnetic permeability.

The choice usually is between ferrites and amorphous magnetic alloys. The last material is used in modern designs more often.

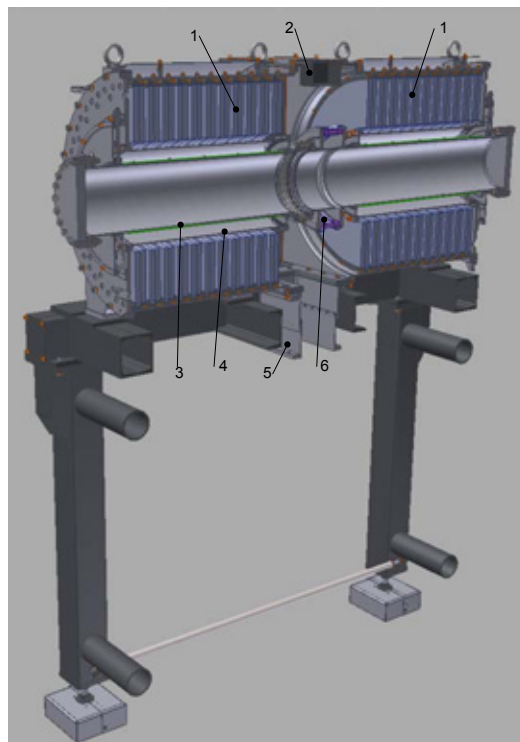


Figure 1: Accelerating cavity of RF station. 1. Amorphous alloy rings. 2. Gap voltage pickup. 3. Beam pipe. 4. Coaxial inner conductor. 5. Connecting nipple. 6. Ceramic insulator.

PARTICLE AND ACCELERATOR PHYSICS AT THE VEPP-4M COLLIDER

V. Kiselev for the VEPP-4 team [1]
 BINP, Novosibirsk 630090, Russia

Abstract

VEPP-4M electron-positron collider is now operating with KEDR detector for high-energy physics experiments in the 1.5–4.0 GeV beam energy range to study production of hadrons in continuum and for precise measurement of R constant. In parallel with these experiments, the VEPP-4M scientific team carries out a number of accelerator physics investigations. Here are some of them: stabilization of the guide field of VEPP-4M with an accuracy of 10^{-6} using a special feedback system, development of the method of RF orbit separation of electron and positron beams at VEPP-4M instead of usual electrostatic orbit separation for CPT-theorem testing experiment, finding ways to increase luminosity of VEPP-4M. The paper discusses the recent results, present status and prospective plans for the facility.

nuclear physics experiments is operating at VEPP-3. Some physical technical characteristics of the complex make it possible to design experiments that are unique not only for Russia but for the world as a whole.

Table 1: Main Parameters of VEPP-4M

Parameters	Values	Units
Circumference	366	m
Tunes Q_H/Q_V	8.54/7.58	
Mom. compaction	0.017	
Max. energy	5.5	GeV
Nat. chromaticity C_H/C_V	-13/-20	
RF-frequency	181.8	MHz
Harmonic number	222	
RF power	0.3	MW
RF voltage	5	MV
No. of bunches per beam	2	
Interaction point		
β_V function	0.05	m
β_H function	0.75	m
D_H function	0.80	m

INTRODUCTION

The VEPP-4M is the modernized VEPP-4 collider, which was commissioned for the first time in 1977. At present, the complex [2] includes (Fig. 1) a Positron injector, VEPP-3 booster accumulator with beam energy in the range from 350 MeV to 2 GeV, VEPP-4M electron-positron collider with beam energy E in the range from 0.9 to 5.5 GeV (Table 1), and KEDR universal magnetic detector [3].

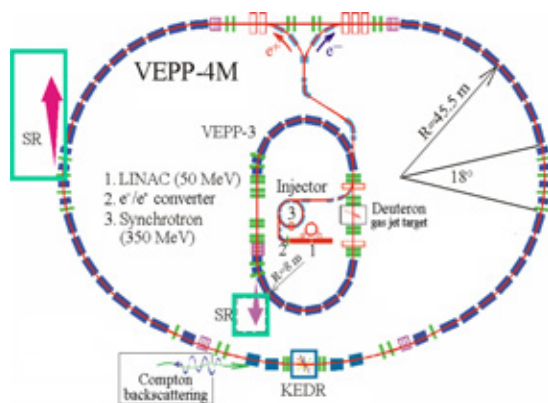


Figure 1. The layout of the VEPP-4 complex.

In addition to the KEDR detector, the experimental spacing of the collider contains a system for registering scattered electrons and positrons for two-photon physics. The VEPP-3 and VEPP-4 facilities are equipped with user stations for studies on the extracted SR beams. A Deuteron unit with the internal polarized gas target for

HIGH-ENERGY PHYSICS

The luminosity of VEPP-4M is a bit lower than the corresponding value in new-generation colliders. For this reason, the KEDR physical program is directed at precision measurements of the parameters of fundamental particles. The following advantages are used in this case: a broad energy range of the center of mass at the complex ($2E = 2-10$ GeV), the methods and techniques that have been developed for the precision determination of the beam energy [4, 5], the fine energy and spatial resolution in a LKr calorimeter (3.5% and 1 mm, $E = 1.8$ GeV), and the high resolution in the system of scattered electrons (10^{-2}). A number of HEP experiments have been carried out at the VEPP-4 complex over the years of its operation since 1980: spectroscopy of the c and b states, including precision measurements of the masses of fundamental particles (the particles from J/ψ , $\psi(2S)$, $\psi(3770)$ and Y families, and D mesons), as well as of the lepton masses and total widths of narrow resonances (Γ_{ee} and Γ_{tot}); measurement of the tau lepton mass proceeding from the threshold behavior of the production cross section (near $E = 1777$ MeV); the unique measurement of fundamental parameter R in the wide energy range of $2E = 2-10$ GeV at one facility; and studies of two-photon physics (full cross section of the $\gamma\gamma \rightarrow$ hadrons process and charge parity states) [6-12].

ACCELERATOR TECHNOLOGIES DEVELOPMENT AT ITEP

N.N.Alexeev, V.A.Andreev, A.A.Golubev, A.A.Kolomiets, A.M.Kozodaev, T.V.Kulevoy,
V.I.Nikolaev, Ju.A.Satov, V.A.Schegolev, A.V.Shumshuruv, A.B.Zarubin,
ITEP, B. Cheremushkinskaya 25, 117218, Moscow, Russia

Abstract

Restart of scientific activity at ITEP associated with join it to the pilot project of NRC “Kurchatov Institute” is the occasion for summing up of intermediate results and existing capability of accelerator physics and technologies development in the institute. School of accelerators construction at ITEP has old traditions and refers on studying, invention, mastering and implementation to operation of technological features of proton and ion beams generation, transportation, acceleration, accumulation, extraction and space-time formation for usage of accelerated beams in physical experiments and applied research works. Historical survey and current state of accelerator science activity at ITEP are presented.

INTRODUCTION

The heyday of the accelerator areas in the country can be attributed to the mid 70-ies of the last century, when the proton synchrotron U-70 in Protvino occupied a leading position in the world and attempts were made to maintain this leading position in almost all areas of development accelerator science and technology. It was difficult to find such physical Institute, which would not have or were not going to have an accelerator facility for experiments in nuclear physics and physics of elementary particles or the practical use of the accelerated beams for applied purposes. In ITEP at that time, it was reconstructed the country's first alternating gradient synchrotron U-7, was created new experimental setups, was implemented proton therapy, were studied and begin to be realised new ideas for creating a linear accelerator with radio-frequency quadrupole focusing of the accelerated beam, were developed intensively technology of ion sources, was discussed actively the idea of creating high-current accelerators for use in electronuclear installations and in experiments on heavy ion fusion. Created in those years in ITEP scientific-technical potential, technology base and high school for training of specialists were allowed to retain up to the present time the leading position of the Institute in the development of accelerator science and technology, despite the constantly changing not for the better conditions for the development and implementation of promising projects.

Historical analysis of distance travelled from emergence of accelerator subjects in ITEP to the current state of Affairs and possible directions in the future use and development of existing scientific and practical groundwork is the basis for the search of optimal ways of combining the efforts of stakeholders in the revival of the accelerator industry in the country to a new level of

technological development and expansion of the practical use of charged particle beams

FIRST ACCELERATOR IN ITEP

The first accelerator appeared at ITEP in 1948, three years after the establishment of the Institute It was a cyclotron capable of accelerating protons to an energy of 6.2 MeV, deuterons up to 12.5 MeV and the α -particle up to 24 MeV, with relatively high current of the accelerated beam: current of deuteron at work on the inner target was reached 600 μ A, the current of extracted beam was 70 μ A. The cyclotron has successfully operated more than 20 years and was dismantled in 1972. If it was known then, where we will come in 40 years, it would have to be preserved.

HISTORY OF THE FIRST ALTERNATING GRADIENT SYNCHROTRON IN RUSSIA

In Russia the principle of alternating gradient focusing became aware of the messages that appeared in the October 1952 American popular science magazine Scientific American. On the initiative M.S.Kozodaev, drew attention to the importance of this message and entrusted to A.A.Tyapkina to check the correctness of this idea, in early January 1953, a meeting was organized in the office of the Minister of medium machine building M.G.Pervukhina [1], which was attended by all the leading accelerator scientists at that time in the country: V.I.Veksler, A.A.Kolomensky, M.S.Rabinovich, V.V.Vladimirsky, and other. In spite of serious doubts as to the correctness of this principle, expressed at the meeting, it was approved the proposal of V.V.Vladimirsky to build on the territory of the ITEP proton synchrotron U-7 on energy 7 GeV to check the beam stability at alternating gradient focusing, and, if successful, to begin the design of the 70 GeV accelerator U-70 and finding a place for its construction.

Design of U-7 (Fig.1) and U-70 began under the leadership V.V.Vladimirsky in 1953, and in 1961 the U-7 was put into operation with electrostatic injector [2].



Figure 1: General view of U-7 Accelerator in ITEP

SUPERCONDUCTING UNCLOSED SHIELDS IN HIGH ENERGY PHYSICS

E. Kulikov, G. Dorofeev, V. Drobin, H. Malinovski, A. Smirnov, JINR, Dubna, Russia

Abstract

This paper presents the experimental and theoretical results of studying the unclosed shields made from LTS (low temperature superconductor) and HTS (high temperature superconductor) materials to obtain a homogeneous magnetic field in solenoids. There is a comparison of LTS and HTS shields, the construction peculiarities are described. HTS shield was proposed to obtain the required magnetic field homogeneity (about 10^{-5}) in the 6 meters length solenoid of the electron cooling section which will be installed in the heavy ion collider of the NICA project (JINR, Russia).

INTRODUCTION

The main requirement at the development of the electron cooling system for charged-particle beams of the NICA collider is to form a highly homogeneous magnetic field [1,2]. At the same time the electron cooling system solenoid will be multisectional with a magnetic field up to 0.2 T. Generation of a highly homogeneous magnetic field using unclosed superconducting shields is the most promising direction to solve this problem.

It is known that low-temperature superconductors can be used for these purposes [3,4,5]. Still, the need of cooling to the liquid helium temperature (4.2 K) forms a major disadvantage of the shield and raises exploitation costs.

For this reason the idea of an HTS shield, which works under 77K, is even more attractive. This paper presents the comparison between conventional LTS shields and HTS shields requiring a fundamentally different winding technology, their construction peculiarities are described as well. It also contains data on characteristic homogeneity of magnetic fields which appear in HTS shield in the gap between two magnetic dipoles.

LTS SHIELD

Investigations on unclosed shields were first carried out in the 1970s; the shields were made of low temperature NbTi alloy superconductor [3]. First papers lacked a clear physical model and had pure experimental nature. Thus there was no unified approach like the one described in our papers [4,5] to the problem of unclosed superconducting shields.

The LTS shield structure is formed by multilayer winding of superconducting foil on a cylindrical frame [4,5] (Fig.1).

A characteristic property of the technology is cross arrangement of superconducting foil pieces to the frame. Shield layers are isolated with condenser paper.

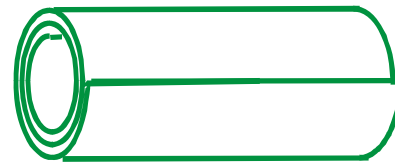


Figure 1: The scheme of spiral winding.

The carried out experiments and numeric researches proved high efficiency of conventional LTS shield usage to improve the magnetic field homogeneity in a straight solenoid [5]. Data analysis showed that the existence of an area with the homogenous magnetic field longitudinal component resulted from screening the external field's radial component by the superconducting unclosed shield.

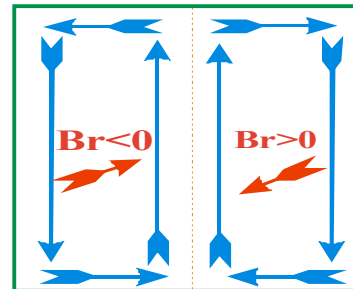


Figure 2: The unfolded shield with effective shielding currents on its surface.

In particular on the end of the shield the shielding currents flow in the same direction as the major solenoid currents, while in the center they have an opposite direction which explains the formation of typical homogenous field areas. (See in Fig.2.)

The derived results formed a basis for works upon the next technical solution – the unclosed HTS shield.

2-G HTS SHIELD

A 12-mm wide 2-G HTS (Re)BCO produced by Super Power and SuperOx was used as a base element of the construction. Its critical current – up to 300 A (i.e. 2.5×10^6 A/sm²), the field of one tape full magnetization is about 25 mT.



Figure 3: Structure of 2-G HTS tape (Re)BCO.

OPERATING FREQUENCY AND ACCELERATING STRUCTURE GEOMETRY CHOSE FOR THE HYBRID TRAVELLING WAVE ELECTRON LINEAR ACCELERATOR

I.D. Sokolov, R.Yu. Alekhanov, E.A. Savin, National Research Nuclear University MEPhI (Moscow Engineering Physics Institute), Moscow, Russia

Abstract

For the compact electron linear accelerating structure based on the hybrid scheme which consists from SW biperiodic structure buncher and TW DLS with magnetic couple TW accelerating part, the best option for the operating frequency and cells geometry has been chosen. Comparative calculations for the DLS cells with magnetic couple and without it, on the different operating frequencies and with the different couple coefficient were carried out. The best option will be manufactured, measured and used in the accelerator structure.

ELECTRO-DYNAMICS PARAMETERS

In this paper we use some specified parameters to describe the efficiency of the accelerating structures [1].

Coupling coefficient – describes the width of the dispersion curve $k_c = \frac{|f_{\pi} - f_0|}{f_{\pi/2}}$, where $f_{\pi}, f_0, f_{\pi/2}$ – are the frequencies $\pi, 0, \pi/2$ respectively;

Phase velocity $v_{ph} = \frac{\omega}{k_z}$, where ω is the circular frequency and k_z is the longitudinal wave number;

Group velocity $v_{gr} = \frac{d\omega}{dk_z}$;

Shunt Impedance per unit length $r_{sh} = \frac{(\int_0^z E_z dz)^2}{P_{loss} * l}$;

T – transit time factor ;

Q - quality factor $Q = \frac{\omega W}{P_{loss}}$, where W -is the stored energy and P_{loss} –is the dissipated power in walls;

α – attenuation coefficient $\alpha = \frac{\omega}{2v_{gr}Q}$;

Normalized electric field strength $\frac{E_z \lambda}{\sqrt{P}} = \sqrt{\frac{2\pi \lambda r_{sh}}{Q \beta_{gr}}}$.

DIAPHRAGM-LOADED STRUCTURE

Diaphragm – loaded structure (DLS) [2] (see Fig.1) is the most common geometry type for using it in travelling wave electron linear accelerator. But the disadvantage of this geometry is small coupling coefficient and small group velocity i.e. structure filling time. But the shunt impedance is relatively high.

For working mode $2\pi/3$ ($D = \beta \lambda \theta / 2\pi$) electro dynamical parameters of the DLS with different a/λ at S band – 2997.2 MHz were calculated [3] and compared (see Table 1.). All data are in this table are matched with the DLS catalogue [4].

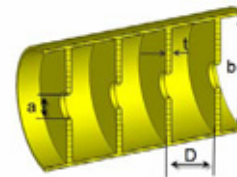


Figure 1: DLS geometry.

Table 1. S band different DLS geometry

Parameter	Value			
a/λ	0.06	0.08	0.1	0.12
$k_c, \%$	0.008	0.03	0.09	0.19
$r_{sh}, \text{MOhm/m}$	111	106	102	96
Q	13800	13800	13800	13800
T	0.61	0.62	0.63	0.64
$E_{acc}, \text{MV/m}$	37	36	35	34
β_{gr}	0.00007	0.0002	0.0008	0.0016
α, M^{-1}	33	11	2.8	1.5
K_E	2.22	2.33	2.46	2.59
$E\lambda/P^{1/2}, \text{Ohm}^{1/2}$	8500	4900	2400	1700

From the Table 1 results we can see, that the group velocity is very small, i.e. it is needed to increase coupling coefficient by inventing a magnetic coupling.

MAGNETIC COUPLED DIAPHRAGM-LOADED STRUCTURE

By putting radial slits in the maximum magnetic field concentration area we increase the connection between the cells [5] thereby obviously we increase the value of the coupling coefficient. Construction and dimensions of DLS-M are presented on Fig. 2. DLS-M was constructed and tuned for S-band -2997.2 MHz and L-band -1818 MHz, working on $2\pi/3$ mode. To design a linac that uses DLS-M as an accelerating structure it is necessary to find its optimal dimensions in order to obtain the best electro-dynamic parameters (EDP). The most significant parameters are: shunt impedance per unit length r_{sh} , normalized electric field strength $E\lambda/P^{1/2}$ and overvoltage K_E . These parameters dependencies from coupling coefficient, group velocity and a/λ are presented on Fig. 3 and Figure 4 for different frequencies. Data calculations are present in Tables 2-5 for the S-band and L-band. On the Fig.5 is shown the comparison of the dispersion

THREE ELECTRODE ELECTRON GUN WITH THE DECREASED ANODE VOLTAGE GEOMETRY OPTIMIZATION

S.V. Matsievskiy, E.A. Savin, National Research Nuclear University MEPhI (Moscow Engineering Physics Institute), Moscow, Russia

Abstract

With the rapid growth of demand for compact particle accelerators, used in number of different fields (medicine, security, etc.), there is a need for more compact and simple in production particle accelerator parts. One of such parts, electron gun injector for linear accelerator, is considered in this paper.

Modifications to the initial design, such as anode potential decrease and change of geometrical properties of cathode are described, optimal operating mode is calculated.

INITIAL MODEL CALCULATION

On figure 1 an existing electron gun with buncher cell are shown. In this case, buncher cell has an electric potential and acting as anode. Potential difference between anode and heated cathode forces electrons to emit from cathode. Control electrode is used to focus electron beam from cathode and to control electron emission intensity by altering electric field value near the cathode surface.

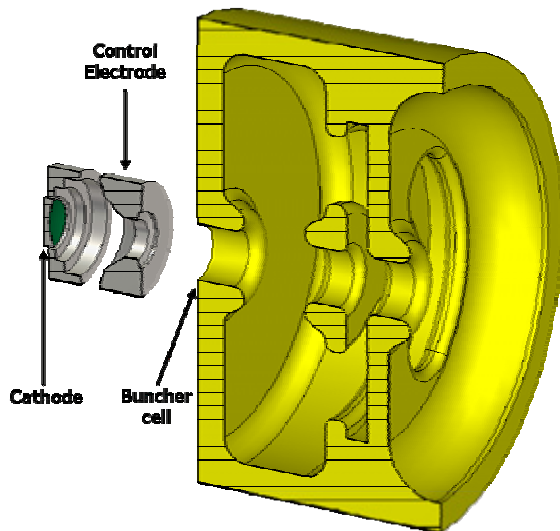


Figure 1: Cross-section of electron gun with buncher cell.

To validate the calculation method of electron gun, model of existing one was built. It consisted of spherical cathode with potential set to zero, control electrode with potential of 12.9 kV and 50 kV anode. On the figure 2 calculation output data is presented. Purple lines represent equipotential lines of electric field inside of the gun. Green lines are the electron trajectories.

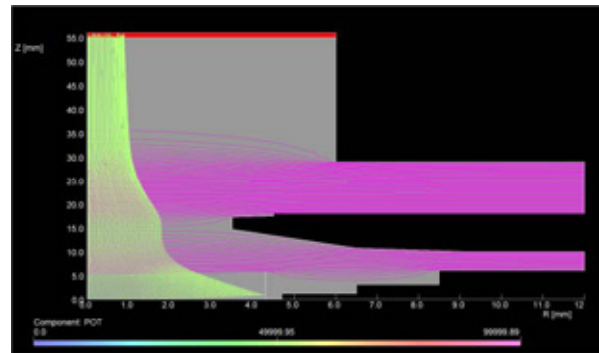


Figure 2: Initial model output data.

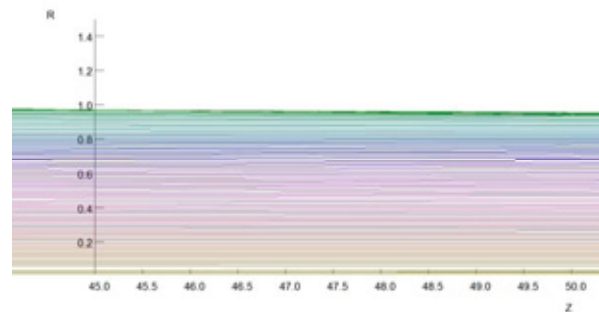


Figure 3: Electron trajectories near crossover.

Calculation results of existing gun model coincided with beam parameters measurement. Calculation method is suitable for modified gun calculations.

MODEL WITH DECREASED ANODE VOLTAGE

Beam width in the crossover dependence of anode potential was investigated. The plot of beam radius r over anode potential U_1 is shown on the figure 4. As shown on figure 4, beam width is decreasing in reverse ratio to anode potential. For simplification of electron gun design due to the isolation requirement reduction, compromise potential of 30 kV on the anode was chosen.

BEAM DYNAMICS CALCULATION IN THE INDUCTION LINEAR ACCELERATOR

D.S. Bazyl, E.A. Savin, National Research Nuclear University “MEPhI”, Moscow, Russia
A.A. Zavadtsev, D.A. Zavadtsev, OOO “NANO INVEST”, Moscow, Russia

Abstract

The geometry of the linear induction electron accelerator (LIA), which will be used for high current acceleration, has been calculated. For the different currents values the optimum focusing magnetic field and has been obtained. Also a current in the compensative coil near the cathode has been calculated. The cathode electrode geometry was changing to achieve minimum beam oscillations during the acceleration.

INTRODUCTION

Electric field which is created by ferromagnetic rings having windings mounted along the beam axis is used for the acceleration of particles in this type of machine. As soon as the accelerating field structure excited in the tubes is similar to the electrostatic field excited by applying a potential difference between the span tubes, to simplify the calculation in this model fields is excited by an electrostatic field.[1] Schematic version of model of the accelerator is shown on the Figure 1. Basic parameters of the accelerator are shown in Table 1.

Injector is a flat grid-controlled cathode, located in the first accelerating gap. Grid voltage is up to 200 V. Voltage on the grid draws electrons which are then accelerated in the first gap. One inductor is connected to each accelerating gap. The pulse duration of the accelerating field is ~ 10 ns. The modules will contain a delay pulse-matching acceleration. The calculation was carried out in a constant acceleration field.

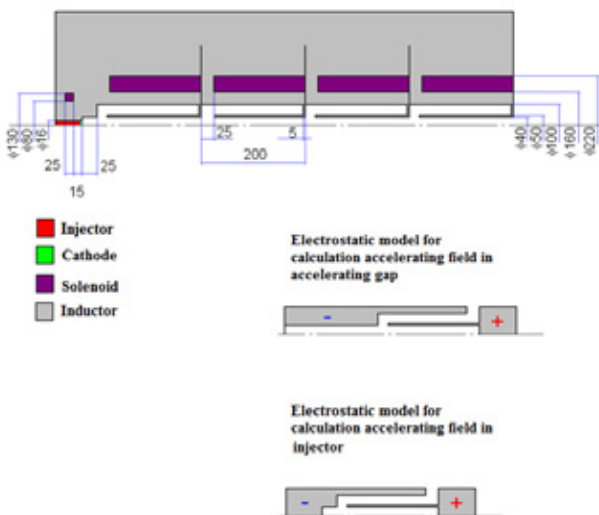


Figure 1: Schematic model for calculating the induction accelerator.

Table 1: Parameters of the accelerator.

Energy of the accelerated electrons, MeV	8
Injection energy, eV	200
The injection current, A	10
The diameter of the injected beam, mm	16
Accelerating voltage in each gap, kV	100

The calculations have started with a small number of modules but with further simulations their number was gradually increased.

Each inductor comprises one focusing coil. The compensating coil is positioned in the injector. The purpose of this coil is to compensate the field at the cathode. Its current is selected so that the total magnetic field at the cathode is zero.

SIMULATIONS

Several electro dynamical parameters were found by using simulations in CST PIC solver.

Simulations of the Electric Fields

When appropriate boundary conditions [2] are installed, the distribution of electric fields in the injector (Figure 2,3), corresponding to reality.

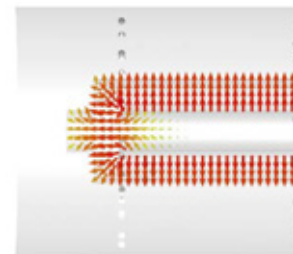


Figure 2: accelerating field in the injector.

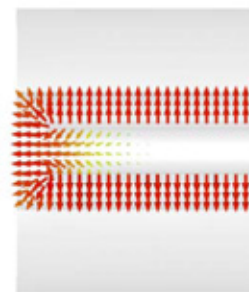


Figure 3: accelerating field in the accelerating gap.

TRANSIT CODE FOR BEAM DYNAMIC SIMULATION

A.A. Kolomiets, A.S. Plastun, T.E. Tretyakova, FSBI «SSC RF ITEP», Moscow, Russia

Abstract

Multiparticle computer code TRANSIT for simulation of intense ion beams in linacs and transport systems is presented. The code is based on experience in design of ion linacs in ITEP. TRANSIT summarizes the most actual and modern methods and algorithms for integration of motion equations including space charge forces. It is being used in ITEP for design and simulation of conventional RFQs, spatially periodic RF focusing linacs, beam transport systems, RF deflectors, etc. The paper presents general description of TRANSIT code and some achieved results.

INTRODUCTION

Development of codes for beam dynamic simulation in ITEP has been started in the early 80s [1]. It was concerned with design of first RFQ proton linacs in ITEP [2]. The simulation code was a tool for study of high intensity beam dynamics in RFQ linacs. It had to describe motion of beam particles accurately and in the most natural approach. Initially external field of RFQ channel was approximated by 2-term 3-D potential, but self-field of the beam was calculated by combined "particle-particle" (PP) and "particle-in-cell" (PIC) method. It was expected as the most adequate method for beam interaction solver, but it was replaced by conventional PIC method in following versions due to technique difficulties. Coulomb field of each macroparticle was expressed by Lienard–Wiechert potentials. The beam had initial truncated normal (gaussian) distribution of space charge density as the most natural. Macroparticle motion solver was operated on predictor-corrector scheme. This code was called PROTON.

Further upgrades of the code allow user to choose PP or PIC methods, simulate multi-component ion beams with different charge-to-mass ratios in different elements of the channel: RFQ cells, quadrupoles, drift spaces, drift tube linacs, etc. External fields can be based on 3-D interpolation of data from ASCII files. The code POLE [x] was used to simulate 3-D field in RFQ cells and the code ALFIL - to simulate 3-D field in DTL cells. These upgrades were caused by application of the code for simulations of UNILAC [3]. This upgraded code was called DYNAMION. Thus it was able to simulate beam dynamics from plasma border inside the ion source up to the end of the linac.

Further versions of the code have been developed in GSI [4] and ITEP independently due to separate applications. To avoid a confusion the code developing in ITEP was called TRANSIT. This paper presents general description of TRANSIT code and some achieved results.

MOTION SOLVER

Motion Equations

One of the most important effect in linear accelerators is emittance growth of accelerated ion beam. It is mainly expressed by redistribution of space-charge density of the beam and halo formation due to nonlinear external and self fields. Unfortunately finite difference approximation of particle motion can produce the artificial emittance growth. The rate of artificial growth is defined by resolution of finite difference approximation (i.e. integration step) and order of numeric method. There are methods that doesn't cause the artificial growth - symplectic methods [5]. The most simple and natural one is "symplectic Euler method", which is used in TRANSIT. Symplectic Euler methods is shown below:

$$\begin{aligned}\vec{v}_{i+1} &= \vec{v}_i + \Delta t \cdot \vec{A}(\vec{v}_{i+1}, \vec{r}_i), \\ \vec{r}_{i+1} &= \vec{r}_i + \Delta t \cdot \vec{v}_{i+1}, \\ \vec{A} &= \frac{q}{m} \sqrt{1 - \frac{v^2}{c^2}} \left\{ \vec{E} + \frac{1}{c} [\vec{v} \vec{H}] - \frac{1}{c^2} \vec{v}(\vec{v} \vec{E}) \right\}.\end{aligned}$$

Here \vec{v} is vector of particle velocity, \vec{r} - radius-vector of a particle, \vec{A} - acceleration vector, q - particle charge, m - particle mass, E and H - vectors of external and self electromagnetic field, c - speed of light.

In addition elementary transfer matrices of every particle are evaluated for each integration step during simulation. The multiplication of elementary matrices defines common transfer matrix of focusing lattice. It provides the analysis of beam dynamics proposed in [6].

Beam frame

TRANSIT is able to simulate beam dynamics through the channel consisted from various number of elements. Element is a part of a channel with specifically defined field distribution (3-D mapping, series, etc.) or drift space. Length and aperture radius (especially for self-field calculations) have to be defined for each element.

To reduce calculating time for multi-element channel the moving frame has been proposed for TRANSIT. Beam frame is 3-D space domain around the reference particle. Frame has length of $\beta\lambda$ and transverse sizes equal to aperture radius. Frame moves with reference particle during simulation. Beam frame can include only part of all elements. of a channel at every moment of time. Special algorithm of interaction between lost particles and beam frame has been proposed for accurate and authentic simulation.

External Fields

One of the most important feature of TRANSIT code is 3-D mapping of external field from ASCII file. Motion

ISBN 978-3-95450-170-0

BEAM DYNAMICS CALCULATIONS IN THE MULTI-BEAM GENERATOR CAVITY

S.V. Matsievskiy, E.A. Savin, N.P. Sobenin, National Research Nuclear University MEPhI (Moscow Engineering Physics Institute), Moscow, Russia

A.A. Zavadtsev, OOO “Nano Invest”, Moscow, Russia

Abstract

In the previously designed, calculated and tuned structure of the compact generator-cavity the beam dynamics for the different geometry options has been calculated. The influence of injected beam parameters to the output power value has been overviewed. Also the geometry of the beam tubes and couple coefficient between cavity and the output waveguide has been optimized to reach the maximum output power value.

INTRODUCTION

The inductive output tube klystron combine two superior characteristics of gridded tube and high-frequency klystron. A grid is used to provide simple control of electron beam. Cavity of klystron couple bunches of modulated beam to the RF field. This combination makes a smaller, lower cost, high-frequency, high-power tube. To increase power of device without significant size change multiple electron beams coupled to one RF cavity.

RESONATOR TUNING

RF power is generated is multi-beam klystron by drawing power from the electron beams, and storing it in cylindrical resonator, operating on TM₀₂₀ mode at 2856 MHz. Beam drift tubes are located in maximums of electrical field. Electrical field distribution in resonator model is shown on figures 1 and 2.

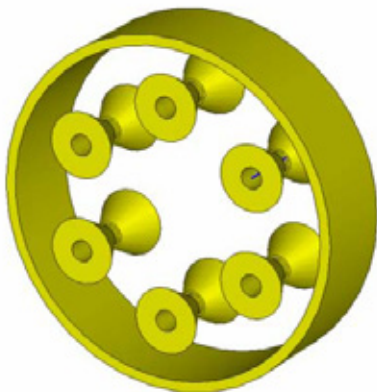


Figure 1: Resonator of multi-beam klystron.

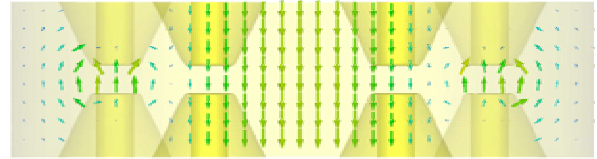


Figure 2: Electric field distribution in multi-beam klystron resonator (side view).

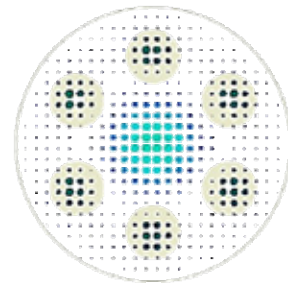


Figure 3: Electric field distribution in multi-beam klystron resonator (top view).

For this resonator geometry, shunt impedance on the axis of each beam tube is 2.95 MOhm/m, which gives a total impedance of the model 17.7 MOhm/m.

WAVEGUIDE IRIS TUNING

For power input, standard waveguide 72.1mm x 34mm is used.

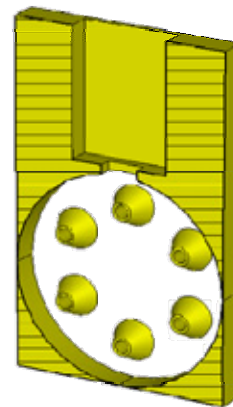


Figure 4: Multi-beam klystron resonator and waveguide, connected by iris.

Maximum power transition from resonator to waveguide was acquired by tuning waveguide iris. On the figure 6 plot of normalized output port power over iris

ADVANCED OPTIMIZATION OF AN LOW-ENERGY ION BEAM DYNAMICS AT LINAC FRONT-END WITH RF FOCUSING

V.S. Dyubkov,*

National Research Nuclear University “MEPhI”, Moscow, Russian Federation

Abstract

A design and development of a linac front-end, that guarantees the required beam, quality is an issue of the day. A linac with RF focusing by means of the accelerating field spatial harmonics is suggested as an alternative to RFQ system. Simulation results of the low-energy proton beam dynamics at linac, that takes into account main linac parameter optimization, based on advanced dynamical acceptance calculation, are presented and discussed.

INTRODUCTION

Projects based on accelerator driven systems are developed in about twenty countries around the world. In order to ensure the safety and stability of this systems it is used well-tried and proven engineering solutions. The initial part of a linear accelerator-driver is a section with spatially homogeneous quadrupole focusing (RFQ), as a general rule. However, a grave drawback of classical RFQ structures is the relatively low acceleration rate that often leads to an increase of the accelerator driver total length. In addition, main losses of the particles typically occur in initial parts of the RFQ sections.

Proton and ion accelerators with RF focusing by means of field spatial harmonics are offered as almost only adequate alternative to the well-proven and reliable RFQ systems for many years [1–3]. Analytical method to control the beam envelope at linac with RF focusing was developed previously to minimize particle losses [4]. The goals of this work are to present results of beam dynamics advanced optimization, which allows one to define main parameters of structure with RF focusing by means of nonsynchronous spatial harmonic which guarantee high acceleration rate under high current transmission.

ANALYTICAL RESULTS

Let's present some results obtained earlier in [4]. One first expresses RF field in an axisymmetric periodic resonant structure as Fourier's representation by spatial harmonics of a standing wave assuming that the structure period is a slowly varying function of a longitudinal coordinate z

$$E_z = \sum_{n=0}^{\infty} E_n I_0(k_n r) \cos\left(\int k_n dz\right) \cos \omega t,$$

$$E_r = \sum_{n=0}^{\infty} E_n I_1(k_n r) \sin\left(\int k_n dz\right) \cos \omega t,$$

where E_n is the n th harmonic amplitude of RF field on the axis; $k_n = (\mu + 2\pi n)/D$ is the propagation wave number for the n th RF field spatial harmonic; μ is the phase advance per D ; D is the resonant structure geometric period; ω is the RF frequency; I_0, I_1 are modified Bessel functions of the first kind.

On averaging over rapid oscillation period one can present the motion equation in the smooth approximation in the following matrix form

$$\ddot{\Upsilon} + \Lambda \dot{\Upsilon} = -L\Phi_{\text{ef}}, \quad (1)$$

where the dot above stands for differentiation with respect to the independent longitudinal coordinate ξ and

$$\Upsilon = \begin{pmatrix} \psi \\ \delta \end{pmatrix}, \quad \Lambda = \begin{pmatrix} 3\kappa & 0 \\ 0 & \kappa \end{pmatrix}, \quad L = \begin{pmatrix} \frac{\partial}{\partial \psi} \\ \frac{\partial}{\partial \delta} \end{pmatrix}.$$

Here $\psi = \tau - \tau^*$ ($\tau = \omega t$, τ^* is a normalized motion time of the reference particle at the laboratory coordinate system), $\xi = 2\pi z/\lambda$, $\delta = 2\pi r/\beta_s \lambda$, $\kappa = \ln'_{\xi} \beta_s$. Φ_{ef} plays role of an effective potential function (EPF) describing a beam interaction with the polyharmonic field of the system subject to the incoherent particle oscillations.

For example, we consider there are two spatial harmonics at the linac. One of it is the synchronous harmonic with $s = 0$, and another one is the nonsynchronous (focusing) with $n = 1$. In this case one has

$$\begin{aligned} \Phi_{\text{ef}} = & \frac{e_0}{2\beta_s} [I_0(\delta) \sin(\psi + \varphi^*) - \psi \cos \varphi^* - \sin \varphi^*] \\ & + \frac{e_0^2}{64} [I_0^2(\delta) + I_1^2(\delta) - 1] \\ & + \frac{5e_0^2}{256} [I_0^2(3\delta) + I_1^2(3\delta) - 1] \\ & - \frac{e_0^2}{32} [I_0(\delta) \cos \psi - 1] - \frac{5e_0^2}{128} [I_0(3\delta) \cos \psi - 1] \\ & - \frac{e_0 e_1}{32} \{ [I_0(\delta) + I_0(3\delta)] \cos(\psi + 2\varphi^*) - 2 \cos 2\varphi^* \} \\ & + \frac{e_0 e_1}{32} \{ [I_0(\delta) I_0(3\delta) + I_1(\delta) I_1(3\delta)] \cos 2(\psi + \varphi^*) \\ & - \cos 2\varphi^* \}, \end{aligned}$$

where $e_n = e E_n Z \lambda / 2\pi \beta_s^2 m_0 c^2$, φ^* is the reference particle phase.

In order to guarantee effective acceleration under small particle loss it is necessary to optimize a changing of synchronous particle phase & field amplitude so that the Eq. 1 has stable solution for a number of initial conditions.

* vsdyubkov@mephi.ru

THE USER FRIENDLY INTERFACE FOR BEAMDULAC-RFQ CODE

P.O. Larin, S.M. Polozov, National Research Nuclear University MEPhI (Moscow Engineering Physics Institute), Moscow, Russia

Abstract

The BEAMDULAC [1] beam dynamics simulation code is under development at MEPhI Department of Electrophysical Facilities since 1999. Such code includes versions for beam dynamics study in a number of accelerating structures as RFQ, DTL, APF, transport channels, etc. The motion equation for each particle is solved self-consistently in the external fields and the inter-particle Coulomb field simultaneously. The BEAMDULAC code utilizes the cloud-in-cell (CIC) method for accurate treatment of the space charge effects. The external field can be represented analytically, as a series or on the grid. The absence of user-friendly interface was the main disadvantage of the code. Last year such interface was developed and will present in the report.

INTRODUCTION

A number of codes for beam dynamics study as DYNAMION, TRACE, PARMELA, COBRA and etcetera are well known. Any one of codes has own field of use, own abilities and disabilities, a different methods for motion equation and Poisson equation solving are used.

The BEAMDULAC code is developing at Department of Electrophysical Facilities of MEPhI by E.S. Masunov, N.E. Vinogradov and S.M. Polozov through 1999. This code was early designed for self-consistent beam dynamics study in RF focusing linacs as axisymmetric radio frequency focusing (ARF, [2]), ribbon radio frequency focusing (RRF, [3]) accelerators and undulator linear accelerators (UNDULAC, [4-8]). 2D and 3D versions were developed for axisymmetric structures and for ribbon beams respectively.

Later new code versions were developed to simulate the beam dynamics in RFQ or DTL linacs, transport channels [1]. Especially versions for electron linacs were designed. The beam dynamics taking into account beam loading and Coulomb field can be studied with the help of these codes [9].

But all code versions have one serious disadvantage. They are compiled as dos operation system application and have not user friendly interface. Now we start to solve such problem and the interface for BEAMDULAC-RFQ version was modified first.

BEAMDULAC CODE AND USED ALGORITHMS AND METHODS

The BEAMDULAC code utilizes the cloud-in-cell (CIC) method for accurate treatment of the own beam space charge effects that are especially important for high-intensity beams. The motion equation of each particle is

solved in the external fields and the inter-particle Coulomb field simultaneously. The charge density is deposited on the grid points using the CIC technique. To determine the potential of the Coulomb field the Poisson equation is solved on the grid with periodic boundary conditions at both ends of the domain in the longitudinal direction. The aperture of the channel is represented as an ideally conducting surface of rectangular or circular cross-section. Therefore the Dirichlet boundary conditions are applied in transverse boundaries of the simulation domain. In such approach the interaction of the bunch space charge with the accelerating channel boundaries is taken into account. This allows considering of the shielding effect which is sufficiently important for transverse focusing in the narrow channel. The fast Fourier transform (FFT) algorithm is used to solve the Poisson equation on a 3D grid. The Fourier series for the space charge potential obtained can be analytically differentiated and thus each component of the Coulomb electrical field can be found as a series with known coefficients. The Coulomb defocusing force is the main factor limiting the beam current in high-intensity linacs. In our code the space charge field can be calculated with the same precision as the Coulomb potential without numerical differentiation. Time is used as an independent variable and standard fourth-order Runge-Kutta method is applied for integration of the motion equation. The external fields in BEAMDULAC code can be represented by three different methods: analytically, as a series of space harmonics (the field amplitude is representing as a polynomial coefficient series) and in a "real field" which can be defined on 2D or 3D grid by electrostatics simulation codes or experimental measurement [10].

Especially versions of code were developed to study the ion beam dynamics with different charge to mass ratio in low energy transport systems, RF bunchers and linacs, as an example for simultaneous acceleration of positive and negative ions and beam space charge neutralization study [1, 8].

The RF field induced by the beam in the accelerating structure depends on the beam velocity as well as the current pulse shape and duration. The influence of the beam loading can reduce the external field amplitude and induce the irradiation in the wide eigen frequency modes. Therefore we should to solve the motion equations simultaneously with Maxwell's equations for accurate simulation of beam dynamics. The method of beam loading effect treatment was developed by E.S. Masunov [11]. It provides to define eigen modes amplitude variation equations in stationary and transient cases for standing and traveling wave periodical structures. Such technique was used for BEAMDULAC-BL code version development [9].

THE INTERACTIVE COMPUTER ENVIRONMENT FOR DESIGNING AND TUNING OF CHARGED PARTICLE BEAMS TRANSPORT CHANNELS

G.P. Averyanov¹, Yu. A. Bashmakov^{1,2}, V.A. Budkin¹, V.V. Dmitrieva¹, I.O. Osadchuk¹

¹National Research Nuclear University «MEPhI», Moscow, Russia

²P.N. Lebedev Physical Institute of RAS, Moscow, Russia

Abstract

This paper considers the application package that simulates transport channel of relativistic charged particles. The package provides an interactive mode for the user. It is possible to observe the main parameters of the beam crossing the channel on the PC screen such as envelope and cross-section of the beam at different sections of the channel while changing the main control parameters of the real channel. Enabling of procedures of mathematical programming provides express optimization of control parameters of the channel. The designed package is compact, has a modular structure and can be easily adapted to different software platforms. MATLAB integrated environment is used as instrumental environment, which has a freeware version of this system - SCILAB. Package testing was carried out on the electron synchrotron “Pakhra” during the recalibration of the channel of the accelerator working in different modes, which are determined by conducted experiments.

INTRODUCTION

A simulation model of the channel is created on the basis a MATLAB environment and its open-source counterpart SCILAB. One of the main advantages of these software environments is the programming efficiency of matrix operations, which are the basic mathematical tools for calculating the magneto-optical systems. In this environment is developed KATRAN representing an integrated modular open structure, adaptable to the calculation of a specific transportation channel of relativistic charged particles [2].

KATRAN STATE DIAGRAM

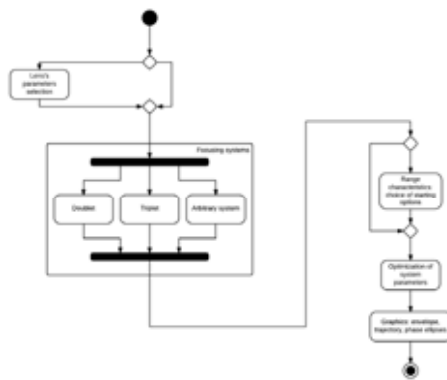


Figure 1: KATRAN state diagram.

The complete cycle of study of the properties and the calculation of the focusing system begins with the

selection of the quadrupole lens. Preliminary review of its envelop characteristics will allow in further calculations to select working variant the system parameters. In general, this process is iterative by nature. You must select a variant of the system fully provide the required launch parameters, using perhaps more "weak" lenses. Module KATRAN named "Range characteristics" allows consider depending focal lengths of the system (the lens, doublet, triplet, etc.) one by one. Building a envelop characteristics provides a visual representation of the degree of influence of the individual parameters of the system on its focusing properties. Figure 2 shows, as an example, the dependence of the focal length of the triplet from the first lens's magnetic field with a parameter - the distance between the first and second lenses. As can be seen from the figure, the focus of the charged particles at the same time in the two transverse planes (vertical and horizontal) is possible in a limited range of parameters of quadrupole lenses and system as a whole (the focal lengths in both planes have positive values).

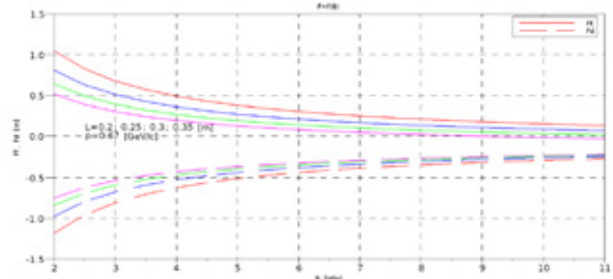


Figure 2: Dependency of focal lengths of the triplet from magnetic field of the first lens with a parameter - the distance between the first and second lenses.

KATRAN allows us to consider these characteristics of the various focusing systems. When considering the envelop characteristics of focusing systems and calculation of parameters of the transport channel numerical methods used for finding optimal solutions (search simplex method).

In general, the objective function F_t , used for the calculation of the magneto-optical system can be written as

$$F_t = \sqrt{\sum_n a_i ((\phi_i(\bar{x}) - x_i^c) / x_i^{norm})^2}. \quad (1)$$

MATHEMATICAL OPTIMIZATION MODEL OF LONGITUDINAL BEAM DYNAMICS IN KLYSTRON-TYPE BUNCHER*

I.D. Rubtsova[#], SPbSU, Saint-Petersburg, Russia

Abstract

The paper presents recurrent integral-differential beam evolution model. This model is convenient for mathematical description of specific dynamic processes with due account of particle interaction and electric fields excitation by moving beam. On the basis of this model the problem of beam dynamics optimization is formalized as trajectory ensemble control problem. Analytical expression for quality functional gradient is obtained. Theoretical results are applied for solving problem of beam dynamics optimization in klystron-type buncher.

RECURRENT INTEGRAL-DIFFERENTIAL BEAM EVOLUTION MODEL

Let us consider beam dynamics description by recurrent system of integral-differential equations. Finite iteration process is introduced. At every iteration beam evolution is described by the equations of the following form:

$$\frac{d\mathbf{x}^{(k)}}{d\tau} = \mathbf{f}^{(k)}(\tau, \mathbf{x}^{(k)}, \mathbf{u}, \mathbf{H}^{(k-1)}(\mathbf{u})) = \mathbf{f}_1(\tau, \mathbf{x}^{(k)}, \mathbf{u}, \mathbf{H}^{(k-1)}(\mathbf{u})) + \int_{M_{\tau, \mathbf{u}}^{(k)}} \mathbf{f}_2(\tau, \mathbf{x}^{(k)}, \mathbf{y}_\tau^{(k)}) \rho^{(k)}(\tau, \mathbf{y}_\tau^{(k)}) d\mathbf{y}_\tau^{(k)}, \quad (1)$$

$$\frac{\partial \rho^{(k)}}{\partial \tau} + \frac{\partial \rho^{(k)}}{\partial \mathbf{x}^{(k)}} \mathbf{f}^{(k)}(\tau, \mathbf{x}^{(k)}, \mathbf{u}, \mathbf{H}^{(k-1)}(\mathbf{u})) + \rho^{(k)} \operatorname{div}_{\mathbf{x}} \mathbf{f}^{(k)}(\tau, \mathbf{x}^{(k)}, \mathbf{u}, \mathbf{H}^{(k-1)}(\mathbf{u})) = 0 \quad (2)$$

with initial conditions

$$\mathbf{x}^{(k)}(0) = \mathbf{x}_0 \in M_0, \rho^{(k)}(0, \mathbf{x}) = \rho_0(\mathbf{x}). \quad (3)$$

Here $\tau \in [0, T]$ is independent variable; T is fixed; k is iteration number ($1 \leq k \leq K$); $\mathbf{x}^{(k)}$ (or $\mathbf{y}^{(k)}$) is n -vector of phase coordinates; $\mathbf{u}(\tau)$ is r -vector of control; $\mathbf{f}_1(\tau, \mathbf{x}^{(k)}, \mathbf{u}, \mathbf{H}^{(k-1)}(\mathbf{u}))$ and $\mathbf{f}_2(\tau, \mathbf{x}^{(k)}, \mathbf{y}^{(k)})$ are n -vector functions; $\mathbf{H}^{(k-1)}(\mathbf{u})$ is the matrix containing the values $H_{s_j}^{(k-1)}(\mathbf{u})$, $s = \overline{1, S}$, $j = \overline{1, J_2}$ of functionals defined on beam trajectories at previous iteration; $\rho^{(k)}(\tau, \mathbf{x}^{(k)})$ is phase density corresponding to dynamic system (1); $M_{\tau, \mathbf{u}}^{(k)} = \{\mathbf{x}_\tau^{(k)} = \mathbf{x}^{(k)}(\tau, \mathbf{x}_0, \mathbf{u}) : \mathbf{x}_0 \in M_0\}$, M_0 is open

bounded initial phase domain; $\rho_0(\mathbf{x})$ is initial phase density; it is supposed $\int_{M_0} \rho_0(\mathbf{x}_0) d\mathbf{x}_0 = 1$.

The components of every matrix $\mathbf{H}^{(l)}$, $l = \overline{1, K}$ are the values of functionals

$$H_{s_j}^{(l)}(\mathbf{u}) = \int_0^T \int_{M_{\tau, \mathbf{u}}^{(l)}} C_{s_j}(\tau, \mathbf{x}_\tau^{(l)}, \overline{\mathbf{x}}^{(l)}(\tau), \mathbf{u}) \rho^{(l)}(\tau, \mathbf{x}_\tau^{(l)}) d\mathbf{x}_\tau^{(l)} d\tau, \quad (4)$$

$s = \overline{1, S}$, $j = \overline{1, J_2}$; here $\overline{\mathbf{x}}^{(l)}(\tau) = \int_{M_{\tau, \mathbf{u}}^{(l)}} \mathbf{x}_\tau^{(l)} \rho^{(l)}(\tau, \mathbf{x}_\tau^{(l)}) d\mathbf{x}_\tau^{(l)}$ is

average phase vector at l -th iteration. Note that $\mathbf{H}^{(0)} = \mathbf{0}$.

The resulting beam evolution is to be achieved at the last iteration number K .

Beam evolution model suggested is based on formalization and generalization of iterative method of beam dynamics simulation in floating-drift klystron with due account of Coulomb repulsion and RF fields excitation in resonators. According to this method excited fields are represented via induced current Fourier decomposition [1]. Vector-function $\mathbf{f}_1(\tau, \mathbf{x}^{(k)}, \mathbf{u}, \mathbf{H}^{(k-1)}(\mathbf{u}))$ is determined by the method of RF fields description. Functional values (4) represent induced current Fourier harmonics in resonators (excluding modulator) and are used to express excited fields at next $(l+1)$ -th iteration and thus to determine vector-function $\mathbf{f}_1(\tau, \mathbf{x}^{(l+1)}, \mathbf{u}, \mathbf{H}^{(l)}(\mathbf{u}))$ in dynamics equation (1). Vector function $\mathbf{f}_2(\tau, \mathbf{x}, \mathbf{y})$ is defined by particle interaction accounting (in view of space-charge forces representation given in [2]).

It should be noted that model (1)-(4) may be convenient for wide class of beam evolution iterative descriptions with due account of beam dynamics dependence on the functionals defined on beam trajectories at previous iteration. These functionals approximate the fields generated by moving beam itself.

Beam evolution modeling with due account of the fields mentioned (in particular, Coulomb forces) may be performed in different ways [2-14]. Analytical representation of these fields allows to formalize beam dynamics optimization problem and to obtain quality criterion gradient analytical expression [2,11,12].

OPTIMIZATION PROBLEM

Let us introduce quality criterion of the dynamic process (1)-(4) as a function of functionals defined on beam trajectories at finite iteration:

*Work supported by St. Petersburg State University, grant 9.38.673.2013 #rubtsova05@mail.ru

SECOND ORDER METHOD FOR BEAM DYNAMICS OPTIMIZATION *

O.I. Drivotin, D.A. Starikov, St. Petersburg State University, St. Petersburg, Russia

Mathematical methods of beam dynamics optimization was developed in the works of D.A. Ovsyannikov (see [1]). These methods are based on numerical calculation of the first derivatives on accelerator structure parameters of functional estimating quality of a beam. They allow to find accelerator structures with satisfactory parameters and also to improve existing structures. The present paper is devoted to new method based on numerical calculation of the second derivatives of the functional. This method can be considered as an extension of the methods of first order.

BEAM DYNAMICS CONTROL PROBLEM

Consider a beam describing by the particle distribution density $\varrho(x)$ in the phase space Ω , $x \in \Omega$. Let at the initial moment t_0 the particle distribution density [2] is given on some p -dimensional surface $S : \varrho(t_0, x) = \varrho_{(0)}(x) = \varrho_{(0)1\dots p}(x) dx^1 \wedge \dots \wedge dx^p$, $p \leq \dim \Omega$, where x^i , $i = \overline{1, p}$, are coordinates on S_0 which can be taken also as some of coordinates in the phase space.

Assume that the particle trajectories are described by the differential equation

$$\frac{dx}{dt} = f(t, x, u),$$

where t is trajectory parameter, $t \in [t_0, T]$, u is control function, $u(t) \in U \subset R^r$. Assume that vector f is defined in a domain $[t_0, T] \times \Omega \times U$, and that the solution of the Cauchy problem for this equation with initial condition $x(t_0) = x_0$ uniquely exists for any x_0 under consideration.

Let introduce functional characterizing quality of the controlled process

$$\Phi(u) = \int_{\Omega} g(x_T) \varrho(T, x_T), \quad (1)$$

where $g(x)$ is a piecewise continuous function, and integral on Ω means in fact integration over image of initial surface S_0 of corresponding differential form satisfying to the Vlasov equation [2]. The problem of minimizing of functional (1) on control function u from U is called the terminal problem of beam control with account of particle distribution density.

METHOD FORMULATION

Equation for the first variation of x has the form

$$\frac{d\delta x^i}{dt} = \frac{\partial f^i}{\partial x^j} \delta x^j + \delta u f^i, \quad \delta x^i(t_0) = 0, \quad (1)$$

* Work supported by St. Petersburg State University grant #9.38.673.2013

where

$$\delta_u f^j = \frac{\partial f^j}{\partial u^k} \delta u^k$$

(summation is meant on coincident indices). The solution of the problem (1) can be written as

$$\delta x^i(t) = \int_{t_0}^t G_j^i(t, t') \delta_u f^j(t') dt',$$

where $G(t, t')$ is the Green matrix of the system (1), satisfying to the equation

$$\frac{dG_j^i(t, t')}{dt} = \frac{\partial f^i}{\partial x^k} G_j^k(t, t'),$$

and to the condition $G(t, t) = E$, where E is identity matrix.

Then variation of the functional (1) can be written in the form

$$\delta_u \Phi = \int_{t_0}^T \int_{\Omega} \frac{\partial g}{\partial x} G(T, t') \delta_u f(t, x) \varrho(t, x) dt. \quad (1)$$

Let introduce the differential form

$$\psi(t, x) = - \frac{\partial g}{\partial x} \Big|_{x=x_T} G(T, t),$$

satisfying to equation and condition

$$\frac{d\psi}{dt} = -\psi \frac{\partial f}{\partial x}, \quad \psi(T) = - \frac{\partial g}{\partial x} \Big|_{x=x_T}.$$

Then the functional variation (1) takes the form

$$\delta_u \Phi = - \int_{t_0}^T \int_{\Omega} \psi(t, x) \delta_u f(t, x) \varrho(t, x) dt.$$

Assume that u is a piecewise constant vector function

$$u = u_i, \quad t \in [t_{i-1}, t_i], \quad i = \overline{1, M}, \quad t_M = T.$$

Then functional (1) can be considered as function of rM control parameters. The derivatives on these parameters are

$$\frac{\partial \Phi}{\partial u_i^k} = - \int_{t_0}^T \int_{\Omega} \psi(t, x) \frac{\partial \delta_u f(t, x)}{\partial u_i^k} \varrho(t, x) dt. \quad (1)$$

Passing to the summation on macroparticles within the framework of the method of macroparticles, write the functional derivatives in the form

$$\frac{\partial \Phi}{\partial u_i^k} = - \int_{t_0}^T \sum_{j=1}^N \psi(t, x_{(j)}) \frac{\partial \delta_u f(t, x_{(j)})}{\partial u_i^k} dt,$$

ELECTRON GUN WITH ADIABATIC PLASMA LENS

A. Drozdovsky, A. Bogdanov, S. Drozdovsky, R. Gavrilin, A. Golubev, I. Roudskoy, S. Savin, V. Yanenko, SSC RF Institute of Theoretical and Experimental Physics, Moscow, Russia

Abstract

For researches on plasma physics has been designed and constructed the electronic gun with the cold cathode on energy to 300 кэВ. The gun have the parameters: time width of pulses -100 ns, current amplitude - 100 A. The adiabatic plasma lens is developed for transportation and compression of the received electron beam. Results of researches are presented.

INTRODUCTION

The electron beam with energy in hundreds кэВ is necessary for carrying out researches in the field of plasma physics - studying of formation of Z-pinch [1]. For these purposes the electron beam has to have the following parameters: current amplitude > 100 A, front duration ~ 10 nanoseconds, energy of electrons > 200 keV. The experimental installation is shown on fig. 1. The electron beam is entered through foil into the experimental channel with pressure ~ 1 mbar. The beam size is reduced in the adiabatic plasma and then is injected in the camera for Z-pinch formation. For creation of the required accelerating voltage form was accepted the scheme of the generator on cable lines with use of the double forming line of Blumlein (DFL) and the cable transformer of Lewis [2].

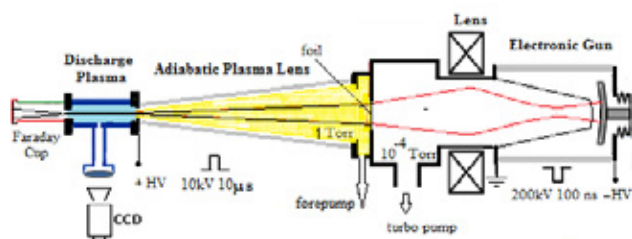


Figure 1: Set up of the adiabatic plasma lens with the ITEP electron gun.

THE GUN INSTALLATION

The gun installation (fig. 2) consists of actually electron gun with magnetic lens, surveillance camera with the scintillators located in it. Vacuum pumping of an electronic gun is made by the turbomolecular pump, and of plasma part of installation - the roughing-down pump. The appropriate volumes are separated from each other by a mylar film. The desorption emitter was used for reduction of requirements to vacuum. Such long-lasting emitter was developed in ITEP [3]. The gun emitter of an electron beam (fig. 2) is located in the center of a cathode. The desorption emitter represents a set of thin plates of mica and copper. The emitter diameter is 50mm,

* Work supported by the Russian Foundation for Basic Research (grant № 12-02-00866-a)

ISBN 978-3-95450-170-0

diameter of a cathode electrode is 110 mm. The gap width is about 50 mm.

Fig. 3 represents simulation results of the electron beam propagation from cathode (C) to adiabatic magnetic lens. Emission current of 100 A and 50 mm cathode-anode gap under voltage of 200 kV were assumed during calculation.

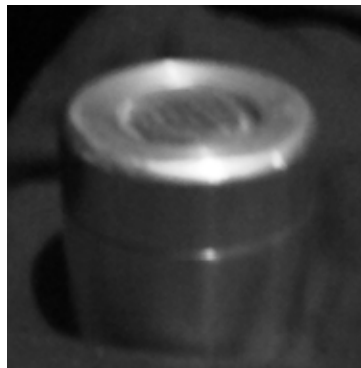


Figure 2: The cathode assemble.

The simulation was performed using numerical code PICSIS-2D [4] based on use of system of the equation of Vlasov-Boltzman with calculation of collisions of particles by Monte-Carlo method. The program enables to calculate a transportation of relativistic charged particles in arbitrary 2D electromagnetic fields taking into account its space charge and self-magnetic field.

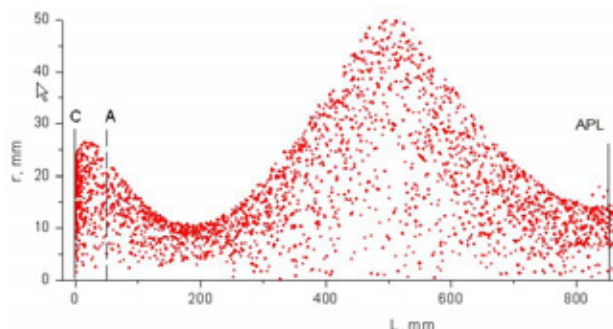


Figure 3: Electron beam propagation; I=100A, U=200kV.

PULSE MODULATOR

For creation of the accelerating voltage was accepted the scheme (fig. 4) of the generator on cable lines with use of the double forming line of Blumlein (LB) and the cable transformer of Lewis (TL). Generators of this kind were realized [5] and on them voltage about 300 kV impulses were received. For switching of the LB was used by "pseudospark switches" TPI1-10k/50. The forming line was executed from 18 couples 10-meter RC-50 cables. It is loaded from a high-voltage source through R_h resistance. To reduce communication between an exit

AXIAL INJECTION TO A COMPACT CYCLOTRON WITH HIGH MAGNETIC FIELD

V. L. Smirnov, S. B. Vorozhtsov
Joint institute for nuclear research, Dubna, Russia

Abstract

One of advantages of a compact cyclotron over other type accelerators is a small size mainly defined by the facility's bending magnetic field. In such cyclotrons an application of an external injection is required in some cases. But for high magnetic field of the cyclotrons (over 4-5 T) there appears a severe problem to make the 1st turns in the machine with external injection of accelerated particles. This paper describes a proposal of a new central region structure of a compact cyclotron that permits one to successfully solve the problem of the axial injection into such a facility using a spiral inflector.

INTRODUCTION

To reach the smallest accelerator size, application of an as high as possible magnetic field of the machine is required. In the compact cyclotron with high magnetic field its magnitude is mainly limited by the minimal focusing available. Thus, in sector structures with large spiral angles of 60-70 degrees and maximal possible deep valleys the practically reachable limit for the central field would be 4-5 T. In a cyclotron with external ion source the particle injection in the accelerator central region is one of the main problems. A design of the cyclotron central region is a key moment for such accelerators. An application of a conventional spiral inflector [1] leads to substantial particle losses on the first turns in the magnetic field.

A possible way to increase the particle transmission through the central region is the application of a higher dee voltage and increasing the number of the dees [2]. Such approach contradicts the main requirement to the modern compact accelerators – the minimum power consumption at their use. Application of higher particle injection energy also can help in solving the problem [3]. But the modern ion sources have restrictions on the maximal possible particle energy at the level of 25-30 keV for the singly charged ions. Besides, at high energies the inflector voltage also should be higher that essentially complicates development of the machine. Miniaturization of the central region structure [4] can also be a solution. This approach in the spiral inflector with minimum size implies very complicated structure of the cyclotron center.

In this report the authors propose a very different approach to the cyclotron central region configuration. In the suggested structure the trajectories of the injected particles on the first turns in the magnetic field and RF are axially separated from the inflector external surfaces [5].

CENTRAL REGION STRUCTURE

The particle trajectory curvature in the high magnetic field is smaller than the spiral inflector external dimensions. Therefore, the injected particles get lost on the inflector case during their initial turn. To prevent those particle losses it is proposed to inject them under some angle with the accelerator median plane at the inflector exit. Such particles make the first turns with some offset to the median plane excluding in this way their collision with the inflector outside surface. The further consideration deals with some hypothetic compact cyclotron having the central magnetic field of 4.5 T. Simulations were performed by the SNOP program of particle tracing [6] in three-dimensional fields of the main magnet, the spiral inflector and the accelerating dees calculated in the Tosca\Opera3D program. As a test particle H⁺ ion injected from axial line with energy 25 keV was used.

As mentioned above in the proposed method the particle trajectory radius on the first turn should not be larger than the effective inflector half-size. To provide required inclination of the particle trajectory to the median plane at the inflector exit, inflector electrodes should be cut off at its exit by some small angle defined by calculations. In our case 20 degrees was chosen to cut (Fig. 1).

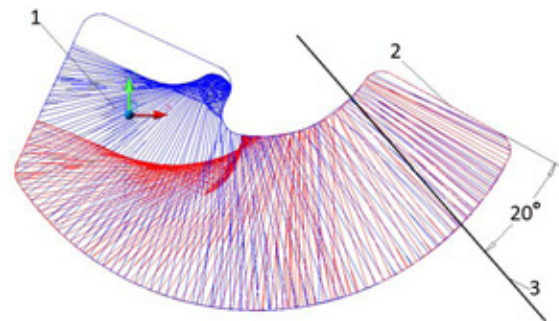


Figure 1: Spiral inflector cut: 1 – inflector entrance, 2 – inflector exit, 3 – cutting plane.

In this case the particle trajectory makes ~ 6 degree angle with the median plane, and the radius of curvature of the particle trajectory is 5.5 mm. Due to axial separation of the particle trajectory with the inflector they do not intersect despite larger effective radius of the inflector of 9 mm. To minimize the axial size of the inflector case the lower electrode is set at ground potential and connected electrically to the inflector case. The upper electrode is under the potential of +10 kV (Fig. 2).

COMPLEX SHUNT IMPEDANCE AND BEAM-RF CAVITY INTERACTION

V.G.Kurakin, Lebedev Physical Institute, Moscow, Russia

Abstract

Two approaches usually are used to describe beam-cavity interaction in accelerator based applications. The first one is electro dynamical and uses Maxwell equations to derive appropriate equations, field modes expressions being necessary to calculate field amplitudes excited by moving charges in the cavity. The other one uses LC circuit to derive appropriate equations for voltage amplitude induced in cavity by accelerated bunches, thin accelerating gap to some extent being not fully correctly defined representation in such approach. In this paper, the expressions are derived that describe beam-RF cavity interactions in terms of so called complex shunt impedance, strict electro dynamical approach being used in calculations. It is shown that complex shunt impedance module coincides completely with usual shunt impedance definition that up to now is used widely to describe rf cavity efficiency. The physical sense of its phase is given in the paper as well. Both complex shunt impedance module and its phase can be calculated or measured experimentally.

INTRODUCTION

To analyze the processes resulting from beam-cavity interaction two approaches are used mainly. The first one is based on Maxwell equations solving. Cavity eigen functions for vector potential are found that together with differential equations for fields amplitudes form the basis for following analysis. In other approach mentioned the RF cavity is replaced with the electrical circuit containing active resistance, capacitance and inductance, their values are chosen in such a way to have the resonance frequency, quality factor and shunt impedance the same for the RF cavity and for the circuit. In this approach one has an analytical representation so necessary for analysis but the questions concerning approach justification and some uncertainty arise.

In this paper we use strict field approach based on Maxwell equation to derive the equation for field amplitude that might be suitable for processes analysis in accelerator containing RF cavity. Complex shunt impedance concept have been introduced and this appeared be fruitful for beam-cavity interaction processes description in RF accelerator based applications problems.

ELECTRODYNAMICS OF RF CAVITY-BEAM INTERACTION

To find out the fields that induces moving charge in a RF cavity, we will use the method that had been developed in [1]. Vortex electrical $\vec{E}(\vec{r}, t)$ and magnetic

$\vec{H}(\vec{r}, t)$ fields are represented as derivatives of vector potential $\vec{A}(\vec{r}, t)$ on time t and space \vec{r} coordinates:

$$\vec{E}(\vec{r}, t) = -\frac{\partial \vec{A}(\vec{r}, t)}{\partial t}, \quad \vec{H}(\vec{r}, t) = \frac{1}{\mu_0} \text{rot} \vec{A}(\vec{r}, t) \quad (1)$$

where μ_0 is magnetic permeability of free space. Here and later SI units are used. Vector potential satisfies the wave equation

$$\Delta \vec{A}(\vec{r}, t) - \frac{1}{c^2} \frac{\partial^2 \vec{A}(\vec{r}, t)}{\partial t^2} = -\mu_0 \vec{j}(\vec{r}, t) \quad (2)$$

$\vec{j}(\vec{r}, t)$, c being current density and the light velocity.

To find out the expressions for vector potential we will use the most direct way. Namely, we represent vector potential as an expansion on the infinite sum of RF cavity eigen functions $\vec{A}_\lambda(\vec{r})$ with time dependent coefficients $g_\lambda(t)$:

$$\vec{A}(\vec{r}, t) = \sum_{\lambda=1}^{\infty} g_\lambda(t) \vec{A}_\lambda(\vec{r}) \quad (3)$$

with the boundary conditions $\vec{A}_\lambda|_{\Sigma} = 0$ on cavity surface.

Starting from the equation (2) and taking into account (3) one can easily obtain the equations for cavity vector eigen functions and appropriate time dependent coefficients (fields amplitudes):

$$\Delta \vec{A}_\lambda(\vec{r}) + k_\lambda^2 \vec{A}_\lambda(\vec{r}) = 0 \quad (4)$$

$$\frac{d^2 g_\lambda(t)}{dt^2} + \omega_\lambda^2 g_\lambda(t) = \int_V \vec{j}(\vec{r}, t) \vec{A}_\lambda(\vec{r}) dV \quad (5)$$

Here $k_\lambda = \omega_\lambda / c$ are eigen values of boundary values problems (4), the specific solutions for RF cavities are called cavity modes, ω_λ being the eigen angular frequencies of appropriate modes, c is light velocity. Integration in formula is assumed to be performed over cavity volume V . Last equation can be generalized up to the next one

$$\frac{d^2 g_\lambda(t)}{dt^2} + \frac{\omega_\lambda}{Q_\lambda} \frac{dg_\lambda}{dt} + \omega_\lambda^2 g_\lambda(t) = \int_V \vec{j}(\vec{r}, t) \vec{A}_\lambda(\vec{r}) dV \quad (6)$$

if losses in cavity and outside are taking into account. Here Q_λ stands for cavity quality factor:

$$Q_\lambda = \frac{\omega_\lambda W_\lambda}{P_\lambda} \quad (7)$$

OUTPUT ENERGY VARIATION IN THE SC LINAC FOR THE PROTON RADIOTHERAPY

I.A. Ashanin, S.M. Polozov, A.V. Samoshin, National Research Nuclear University MEPhI (Moscow Engineering Physics Institute), Moscow, Russia

Abstract

Current success of the superconducting linear accelerators based on independently phased SC cavities gives a seriously reason to consider such structure in proton radiotherapy. Superconductivity allow to solve at once some problems concerned with a low rate of energy gain, high length, higher capacity losses and higher cost of the proton linear accelerator subsequently. One of the traditional aims of such facilities is receiving of the beam energy about 240 MeV with possibility of fluently regulation in range from 150 to 240 MeV that responds to irradiate the tumors located at different depth. The possibility of beam energy variation by means of RF field phase in last resonators and number of the resonator turn-off becomes the major advantage of the proton SC linac.

The optimal choice of accelerator parameters and the beam dynamics simulation results with using BEAMDULAC-SCL code will presented [1]. Methods of the output energy variation with beam quality preservation in the proton SC linac will discussed.

INTRODUCTION

The very high procedure cost caused by accelerator and its engineering systems cost is main factor limiting proton therapy application and ideas to reduce the cost are very actual.

The proton beam basically receives in proton synchrotrons or cyclotrons [2]. The proton beam can be accelerated also in linac but main limitation is a low rate of the energy gain that involves increasing the accelerator length. Superconductivity allows essentially reduce the linac length, that is important by economic and technical aspects. Contemporary progress in SC linacs development allows proposing their using for medical application [3]. Such facilities satisfy to all standard demands for medical using. It's energy of the beam about 240 MeV with fluently regulation, possibility of control of beam envelope up to 6 mm, intensity of the beam not less than 10^9 p/s. Besides SC linacs have some significantly advantages. It's a very high rate of energy gain for the period of the structure that allows reducing the facilities length and low requirement in RF power feeding. Also the possibility of easily beam energy variation by means of a number of the resonator turn-off (deeply variation) or RF field phase in last resonators (slow variation).

Beam focusing can be provided with the help of SC solenoids following each cavity or with the help of RF focusing [4]. Using a solenoid into focusing period will allow to make optimal choice of main accelerator parameters and to provide the transverse and longitudinal beam motion stability.

Beam dynamics simulation directed to produce the fluently tuning of the beam energy in range 150-240 MeV with preserving beam quality will discuss. Such tuning of energy can be realized in the hardware way without use of padding filters by means of voltage change on cavities or of input phase variation in cavities.

GEOMETRIC CHARACTERISTICS

It is advisable to divide accelerator into several groups, consists of cavities having identical geometry. A slipping of the particles relative to the accelerating wave presents in such SC structure. The slipping value must not exceed an acceptable value. The number of cavities should be limited and the number of groups should be minimal. The geometrical velocity β_g of the RF wave is constant for any group of cavities and the number of such groups in linac should be minimized to reduce the accelerator cost [5].

So in our case the phase slipping factor was limited by 18 %. The accelerator will be divided into four groups of cavities with geometric velocity of cavities $\beta_g = 0.09, 0.18, 0.31$ and 0.49 respectively. The first two groups consist of cavities with two accelerating gaps and the third and the fourth would consist of three gap cavities (see Fig. 1).

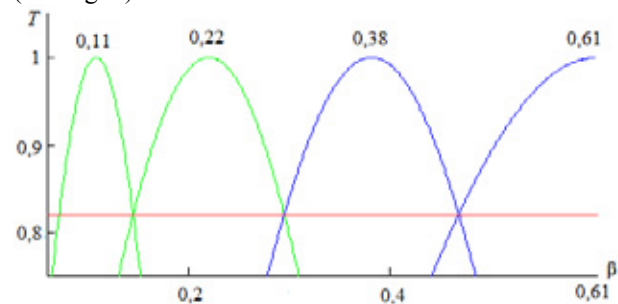


Figure 1: Slipping factor value depending on β .

BEAM DYNAMICS SIMULATION IN POLYHARMONIC FIELD

Beam dynamics simulation results for the last group having the beam energy range from 123.2 to 240 MeV will present below. The electric field amplitude for each cavity is equal 14.20 MV/m, the length of each cavity 0.386 m, the particle phase into RF field -25° and operating frequency $f = 702$ MHz, magnetic field $B = 3$ T.

Beam dynamics simulation results in polyharmonic field in the last part are shown in Figure 2.

LEPTA - THE FACILITY FOR FUNDAMENTAL AND APPLIED RESEARCH

E. Ahmanova, V. Drobin, P. Horodek, I. Meshkov, O. Orlov, A. Rudakov,
 V. Seleznev, A.A. Sidorin, S. Yakovenko, JINR, Dubna, Russia
 A. Kobets[#] JINR, Dubna and Institute of Electrophysics and Radiation Technologies,
 NAS of Ukraine
 M. Eseev JINR, Dubna and M.V. Lomonosov Pomor State University, Russia

Abstract

The project of the Low Energy Positron Toroidal Accumulator (LEPTA) is under development at JINR. The LEPTA facility is a small positron storage ring equipped with the electron cooling system. The project positron energy is of 2 – 10 keV. The main goal of the facility is to generate an intense flux of positronium atoms – the bound state of electron and positron.

Storage ring of LEPTA facility was commissioned in September 2004 and is under development up to now. The positron injector has been constructed in 2005 ÷ 2010, and beam transfer channel – in 2011. By the end of August 2011 experiments on injection into the ring of electrons and positrons stored in the trap have been started. The recent results are presented here.

LEPTA RING DEVELOPMENT

The Low Energy Particle Toroidal Accumulator (LEPTA) is designed for studies of particle beam dynamics in a storage ring with longitudinal magnetic field focusing (so called "stellatron"), application of circulating electron beam to electron cooling of antiprotons and ions and positronium in-flight generation.

For the first time a circulating electron beam was obtained in the LEPTA ring in September 2004 [1]. First experience of the LEPTA operation demonstrated main advantage of the focusing system with longitudinal magnetic field: long life-time of the circulating beam of low energy electrons. At average pressure in the ring of 10^{-8} Torr the life-time of 4 keV electron beam of about 170 ms was achieved that is by several orders of magnitude longer than in usual strong focusing system. However, experiments showed a decrease of the beam life-time at increase of electron energy. So, at the beam energy of 10 keV the life time was not longer than 12 ms. The possible reasons of this effect are the magnetic inhomogeneity and resonant behavior of the focusing system.

Diagnostic System Development

Previous PU system was connected to amplifier by using the cable of near 3 meters length. That reduced significantly sensitivity for all system. New amplifier was designed, manufactured and mounted (Fig. 1). It locates directly at connector exits from vacuum chamber. Sensitivity of new system is of 1,1 mV/ μ A.

[#]-----
 #kobets@jinr.ru

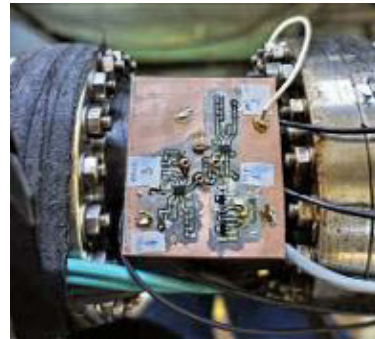


Figure 1: The new PU amplifiers.

For fine tuning of the trajectory and control of circulating positron beam aperture probe based on semiconductor gamma detector has been designed (Fig.2), fabricated, mounted and tested with positrons injected into the ring.

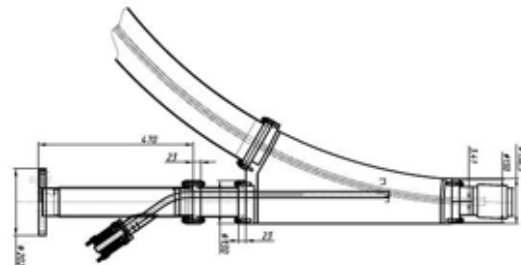


Figure 2: The circulating e⁺ beam detector.

THE POSITRON INJECTOR

In summer 2010 the slow positron source and the trap have been assembled. The first attempts of slow positron storage were performed and stored positrons were extracted to the diagnostic collector.

Vacuum System Development

New vacuum chamber for transport channel was manufactured and mounted to minimize losses during injection. Aperture was increased from 3,2 cm to 6,5 cm.

Spectrometric studies were carried out of the residual gas in the trap. As a result, it was found the presence in the vacuum volume of compounds with atomic number of 68-69 (Fig. 3).

PROJECT OF ELECTRON COOLER FOR NICA COLLIDER

E. V. Ahmanova, I. N. Meshkov, O. S. Orlov, A. Y. Rudakov, V. I. Shokin, A. A. Sidorin[#],
S. L. Yakovenko, JINR, Dubna

A. G. Kobets, Joint Institute for Nuclear Research, Russia, Institute of Electrophysics and Radiation
Technologies, NAS of Ukraine

M. P. Kokurkin, N. Y. Lysov, M. M. Pashin, All-Russian Lenin Electrotechnical Institute, Moscow

Abstract

Electron cooling system (ECS) of the NICA collider is designed to form the required parameters of the ion beam at energy of the experiment in the range of 1 - 4.5 GeV/amu that requires energy cooling electrons from 0.5 to 2.5 MeV. To achieve the required energy of the electrons all elements of ECS are placed in tanks filled with sulfur hexafluoride (SF₆) under pressure of 6 atm. For testing items ECS elements the test bench "Recuperator" is used. This paper presents the results of testing the prototype elements of the ECS and the first results of technical design of ECS.

ELECTRON COOLING SYSTEM OF THE NICA COLLIDER

High voltage elements must be placed in three tanks due to the requirements to ECS parameters (Fig. 1). ECS NICA collider has two independent electron beams. Therefore tanks 1 and 3 (Fig. 1, 2) contain a devices for generating and formation of electron beams, the acceleration of the electrons, and after passing through the cooling section, deceleration of the electrons and their energy recuperation. Tank 2 (Fig. 2) contains a high-voltage generator voltage up to 2.5 MW. Inside tanks 1 and 3 are placed solenoids of the superconducting magnetic system (the field up to 2 kGs) for transporting electron beams, so the material for these tanks could be a magnetic steel that allows using the tanks walls as magnetic shield for magnetic flux "return". All three tanks are filled with the insulating gas SF₆ («sulfur hexafluoride») under pressure of 6 atm.

Electrons of the two beams are accelerated by electrostatic voltage in a longitudinal magnetic field and when get the necessary energy transported in a longitudinal magnetic field into the cooling section (Fig. 3). In this part of the trajectory electrons and ions circulating in the collider ring, are merged.

Table 1: Parameters of ECS for NICA.

Parameter	Value
Electron energy, MeV	0,5 - 2,5
Electron beam current, A	0,1 - 1
Electron beam diameter, mm	10 - 20
Magnetic field of SC solenoids, T	0,1 - 0,2
Relative current losses at recuperation	3×10^{-4}
Elegas (FS ₆) pressure, bar	6

[#] sidorinalexsey@gmail.com

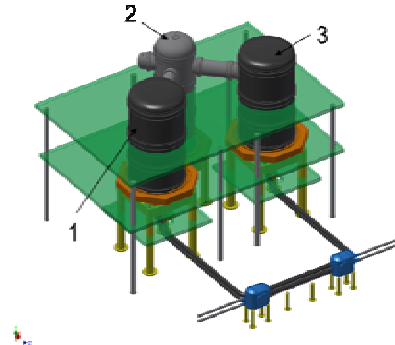


Figure 1: Scheme 1,3 - acceleration tanks, 2 - tank of the high-voltage generator.

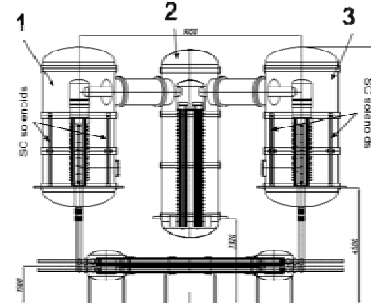


Figure 2: Tanks 1,3 - acceleration tanks, 2 - tank of the high-voltage generator.

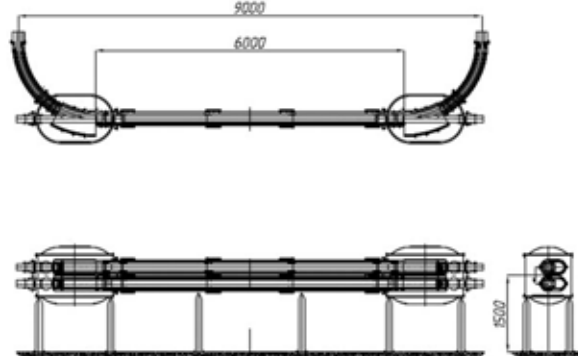


Figure 3: Transportation and cooling sections.

TEST BENCH "RECUPERATOR" AND PROTOTYPING ECS

Test bench "Recuperator" (Fig. 4, 5 and Table 2) is a model of the electron cooling system. It has linear vacuum chamber of a length of about 4 m and a diameter of 10 to 30 cm, immersed in a longitudinal magnetic field

ACCELERATION OF THE OPPOSITELY CHARGED PARTICLES IN THE SINGLE STREAM

A.S.Chikhachev, All-Russian Electrotechnical Institute, Moscow, Russia

Abstract

One of the problems arising at extraction of heavy ions from plasma is removal of electrons from a stream of particles. Therefore possibility of simultaneous acceleration in one direction as ions (electric field), and electrons (pressure gradient) is represented rather interesting. In work when using the hydrodynamic description in the accelerating interval conditions of cold ions and hot electrons are studied. Possibility of excess by ions of speed of an ionic sound is shown, and the ratio of sizes of streams of electrons and ions can be any.

INTRODUCTION

In work [1] acceleration of heavy ions in the presence of a counter flow of electrons was studied. Thus streams of charged particles were considered equal in size. We will note, however, that flows oppositely charged particles can be accelerated in one direction if electrons except force from electric field are affected by rather big force caused by pressure gradient.

MAXWELLIAN DISTRIBUTION OF THE ELECTRONS

Let at there is a source of electrons at $x = 0$ and once ionized ions, and potential $\phi(x)|_{x=0} = \phi_0$. Ions are considered cold, that is $T_i \rightarrow 0$ and them only force affects, from electric field, electrons, except a field pressure gradient ΔP works. In the stationary mode of the equation, describing system, have an appearance:

$$M \frac{v^2}{2} = -e\phi + M \frac{v_0^2}{2}, \quad (1)$$

$$mv_e \frac{dv_e}{dx} = e \frac{d\phi}{dx} - \frac{1}{n_e} \frac{dP}{dx}. \quad (2)$$

Here M - the mass of an ion, m - the mass of an electron, v_i, v_e - speeds of ions and electrons, respectively, v_0 - the initial speed of ions, P - pressure of electronic gas. In an isothermal case, $P = nT$, $T \equiv const$ - temperature of electronic gas. The equation (2) can be integrated:

$$m \frac{v_e(x)^2}{2} - e\phi(x) + T \ln \frac{n_e(x)}{n_*} = 0, \quad (3)$$

where n_* - any constant, dimensional density. We will put that there is a stream of ions Γ and a stream of electrons $\Gamma_e = g\Gamma$. Then follows from the equations of a continuity $v_e = \frac{g\Gamma}{n_e}$ and $v_i = \frac{\Gamma}{n_i}$. We will designate $\frac{e\phi}{T} = \varphi$ and will set entry conditions: at $x = 0$ $n_e = n_i = n_0$, $\varphi = \varphi_0$ Then $\Gamma = n_0 v_0$, where v_0 - the speed of ions at $x = 0$. From (3)

follows: $\varphi - \varphi_0 = \ln \left(\frac{n_e}{n_0} \right) - \frac{vg^2}{M} \frac{v_0^2}{2v_s^2} \left(1 - \frac{n_0^2}{n_e^2} \right)$. Poisson's equation has an appearance:

$$\frac{d^2 \phi}{dx^2} = 4\pi(n_i - n_e). \quad (4)$$

Using the expression for potential following from (3), we will receive from (4) equation containing only density of electrons. Passing to dimensionless variables $y = \frac{x}{\lambda}$, $\lambda^2 = \frac{T}{8\pi e^2 n_0}$, $\eta = \frac{n_e}{n_0}$ and having designated $a = \frac{m}{M} \frac{v_0^2}{v_s^2} g^2$, $S(\eta) = 1 - 2 \frac{v_s^2}{v_0^2} \left(\ln \eta + a \frac{v_s^2}{v_0^2} \right)$, we will receive:

$$2 \frac{d}{dy} \left[\frac{1}{y} \frac{d\eta}{dy} \left(1 - \frac{a}{\eta^2} \right) \right] = \eta - \frac{1}{\sqrt{S(y)}}. \quad (5)$$

Speed of a stream of ions from the above-stated expressions is defined as $v_i = v_0 \sqrt{S(\eta)}$. The equation (5) has integral of the following look:

$$\left[\frac{1}{\eta} \frac{d\eta}{dy} \left(1 - \frac{a}{\eta^2} \right) \right]^2 = C_0 + \left(\frac{a}{\eta} + \eta \right) + \frac{v_0^2}{v_s^2} \sqrt{1 - 2 \frac{v_0^2}{v_s^2} \left(\ln \eta + \frac{a}{2\eta^2} \right) + a \frac{v_0^2}{v_s^2}}. \quad (6)$$

At a zero stream of electrons (i.e. at $g = 0$) the integral (7) passes into the integral used in [2] for studying of criterion Bohms. The system of the equations describing particles a field according to definition [2], is the Hamilton, having integral system of the equations. This property remains and for more difficult case in the presence of nonzero stream of electrons. We will enter a new variable: $\eta = \exp(-z)$ also we will construct dependence

$$q(z) = a \exp(z) + \exp(-z) +$$

$$+ \frac{v_0^2}{v_s^2} \sqrt{1 - 2 \frac{v_0^2}{v_s^2} \left(-z + \frac{a}{2} \exp(2z) \right) + a \frac{v_0^2}{v_s^2}}.$$

At $a = 10^{-6}$, $v_0 = 0.1v_s$ this dependence has the appearance represented in fig. 1. The phase trajectory, the equation for which follows from (5):

$$\frac{dz}{dy} = \frac{\sqrt{C_0 + q(z)}}{|1 - 10^{-6} \exp(2z(y))|}, \quad (7)$$

at $C_0 = -0.2935$, it is represented in fig. 2. We will note that value of a constant C_0 is chosen we conceal in a way that the phase trajectory concerned an axis $\dot{z} = 0$. If $C_0 < -0.2935$, the phase trajectory breaks up to two

ELECTRODES FORM OPTIMIZATION OF RF DEFLECTING SYSTEM WOBBLER FOR FAIR PROJECT

A. Sitnikov, T. Kulevoy, S. Vysotskiy, A. Golubev, FSBI SSC RF ITEP, Moscow, Russia

Abstract

The new method for high energy density states in matter investigation, which based on irradiation of combined target by hollow high energy heavy ion beam was proposed in the Institute for theoretical and experimental physics (ITEP). The target consists of a sample of matter at the center and a hollow shell around it [1]. The experiment of high energy density states generation will be carry on at FAIR project. The RF deflecting system (Wobbler) for hollow high energy heavy ion U_{238}^{28+} beam with kinetic energy $W_k = 1$ GeV/n formation is developing at ITEP [2].

The current results of electrodes form optimization for RF deflecting system (Wobbler) which is developing at ITEP for FAIR project are shown in this paper.

INTRODUCTION

The electrodes form of RF deflecting system influence to homogeneity heavy ions U_{238}^{28+} beam with kinetic energy $W_k = 1$ GeV/n deflection was investigated. The deflecting system developed for ITEP TWAC project was taken as basis [3]. The length of deflecting cell could be defined by $D = \beta\lambda / 2$, where D – cell’s length, β – relative speed of particles, λ – wavelength of RF electromagnetic field. According to that, for particles with kinetic energy $W_k = 1$ GeV/n and resonant frequency $f_0 = 352$ MHz the cell’s length should equal to $D = 373$ mm.

RESULTS

The model of one deflecting cell for FAIR project is presented on Fig. 1. In order to increase self quality factor of the deflecting cavity the area of the electrodes stems was increased [4] as well as electrodes deflecting plates form was also changed (compared to cavity developed for ITEP TWAC project).

The method of electrodes form optimization was the same as it described in [5]. During electrodes form optimization the width of plate (EW parameter) as well as height (EH parameter) of edges were varied.

According to electrodes form optimization it was found that particles deflection homogeneity not better than 1.9% at EH = 6 mm; at EH = 10 mm and 12 mm deflection homogeneity was equal to 1.1% and 1% correspondently. The particles deflection homogeneity equaled to 0.9% was achieved at EH = 8 mm and EW = 130 mm (see Fig. 2). The cavity’s self quality factor was

also increased to $Q_0 = 20000$ which on 30% greater than Q_0 -factor of the deflecting cavity for ITEP TWAC project.

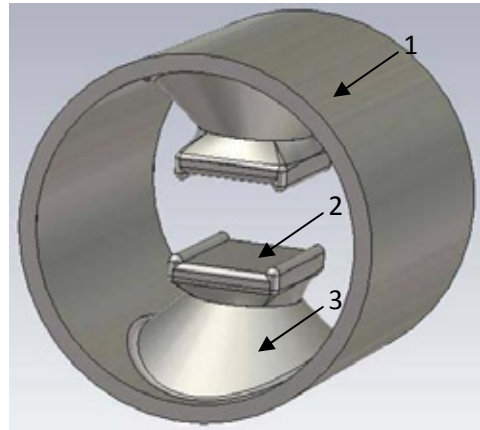


Figure 1. The model of one deflecting cell, where 1 – cavity’s shell; 2 – electrode; 3 – electrode’s stem.

The maximum intensity of the electric field on electrodes surface (E_{max}) is located on plates edges and greater than the maximum electric field intensity at axis (E_0) up to $E_{max} / E_0 \approx 3.7$ times. The typical electric field distribution on the electrodes surface is presented on Fig. 3. In order to reduce the maximum electric field intensity on the electrodes surface the electrodes edges was rounded (see Fig. 4) [6]. From Fig. 4 one can see that E_{max} / E_0 has a sharp increasing up to ≈ 4.4 at rounding radius $El_R = 5$ mm. The following increasing of El_R parameter leads to decreasing E_{max} / E_0 as well as worsening a particles homogeneity deflection (see Fig. 5). The cavity’s self quality factor Q_0 vs. El_R is presented on Fig. 6.

Copyright © 2014 CC-BY-3.0 and by the respective authors

THE FIRST DESIGN OF MEDIUM RESOLUTION MASS SPECTROMETER (MRMS) HIGH VOLTAGE PLATFORM IN A SPES PROJECT

S. Andrianov, ITEP, Moscow, Russia
M.F.Moisio, C.Roncolato, LNL, Legnaro, Italy

Abstract

A new project of 130 kV high voltage platform (HVP) is developed in a Laboratori Nazionali di Legnaro as part of SPES (Selective Production of Exotic Species) project for the production of the multiply charged rare ion beams (RIB). The HVP will be located after ECR ion source charge breeder [1]. Medium resolution mass spectrometer (MRMS) is installed at the platform to provide high purity beams with mass resolution about 1/1000. The Draft of platform design including all beamline elements is discussed. It is proposed a several way of equipment feeding on HVP, required engineering services parameters (vacuum system, cooling system, power system and etc) were defined. Some safety measures are proposed.

MRMS IN SPES FACILITY

Selective Production of Exotic Species (SPES) project is under development. The result of SPES operation should be production of the multiply charged rare ion beams (RIB) by ISOL technique which using the proton induced fission on a Direct Target of UCx. The proton driver is a Cyclotron with variable energy (15-70 MeV) and a maximum current of 0.750 mA. The RIB separate in HRMS platform and transport to charge breeder. The charge breeder is a device that accepts RIB ions coming from the Target-Ion source complex with charge state $+1$ and it transforms their charge states to $+n$. The last separator (MRMS) will be installed after the charge breeder to avoid the contamination of the selected beam by the stable contaminant introduced by the charge breeder itself [2].

The beam will transport from charge breeder to 130 kV MRMS platform, which will separate ions with mass resolution about 1/1000. The Potential of 130 kV is necessary for high mass resolution.

The beam will be transported to MRMS high voltage platform (HVP) through an 130 kV accelerate tube, ions will be focused by electrostatic lenses and after that, the ions with different mass will be selected by magnetic dipole. The beam orbit will be rotated at 90 degrees by each dipole. Separated ions will be refocused ones more in electrostatic lenses and then slows down to the initial speed (same ions speed before MRMS platform) by deaccelerating tube.

The beam line elements will be located on the platform according figure 1. MRMS platform will be enclosed in Faraday cage and will set on insulators columns.

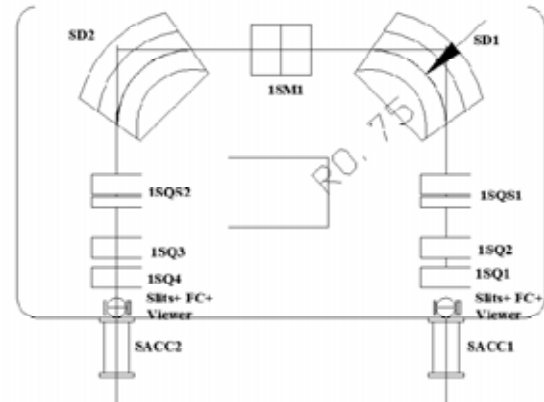


Figure 1: layout of main elements on the MRMS platform. SD1, SD2- magnetic dipoles; 1SQS1, 1SQS2 - sestupole electrostatic lenses; 1SQ1, 1SQ2, 1SQ3, 1SQ4 - quadrupole electrostatic lenses, SACC1 –accelerating tube, SACC2 – deaccelerating tube.

The platform should be located in experimental hall with sizes according figure 2 and further than 0.9 m to the nearest surface of the building. It is important to avoid electrical breakdowns. The Platform height will be 5 meters or less if for the crane movement will be free over the HVP.

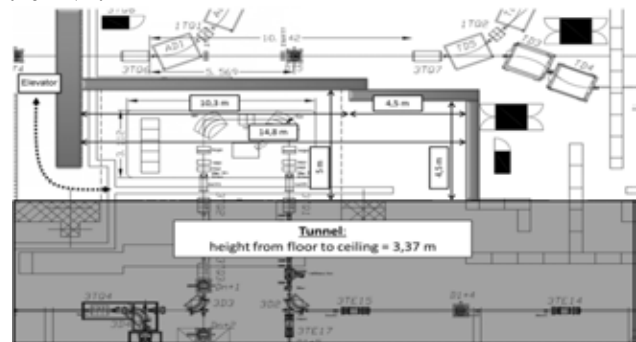


Figure 2: layout of experimental hall.

Secondary Faraday cage locating around the platform at a distance for 0.9 m.

Successful HVP design is necessary several calculations and circuits:

- power system calculations and circuit of power board;
- water cooling and ventilation system should be provided;
- radioactive and fire security should be provided;
- vacuum scheme and appropriate calculation, residual pressure should be less than 10^{-8} mbar;
- HV power supply will be defined according leakage currents;

THE ADVANCED NANOSTRUCTURE STEEL MODIFICATION BY GAS IONS BEAMS

R.P. Kuibeda, S.L. Andrianov, P.A. Fedin, B.K. Kondratiev, A.V. Kozlov, A.A. Nikitin,
B.B. Chalih, A.L. Sitnikov, S.V. Rogozhkin, T.V. Kulevoy ITEP, Moscow, Russia

Abstract

New construction materials are under developing for the nuclear energy sector. They will provide energy production, store and transportation with high efficiency and ecology safety. The nanostructures steels like a consolidation oxide dispersion strengthened (ODS) as well as ferritic-martensitic steel (for example EK-181) are the most promising materials for new generation of nuclear reactors. The experimental program for investigation of the steel nanocluster generation and growth under ion beam irradiation is ongoing in ITEP at the accelerator complex "Heavy ion prototype-1" (HIPr-1). The duoplasmatron ion source provides gas ion beams for experimental program. The source installation and its power systems development are presented. As well the results of charge state distribution measurements for nitrogen ion beam generated by the duoplasmatron and the first results of ODS materials irradiation by gas ions are described and discussed.

INTRODUCTION

The changes in chemical composition of structural steels which occur under irradiation can cause changes in their mechanical characteristics. To investigate the steel structure changes under irradiation, in ITEP experimental works for structural materials irradiation by metal ion beams are carried out since 2007 [1]. However, the investigation of materials irradiated by both gas ion beams and combination of gas and metal ion beams can significantly enlarge the experimental potential of ITEP research program.

At the accelerator "heavy ions-prototype-1" (HIPr-1) a gas ion source duoplasmatron was installed, tested, tuned and put under operation. The procedure of materials irradiation with gas ions was tested. Nitrogen ion beam with a current of 150 mA was obtained at the outlet of the injector. The results of charge state distribution measurements for nitrogen ion beam generated by the duoplasmatron as well as the first experimental data obtained for ODS steel irradiated by the nitrogen beam are presented and discussed.

EXPERIMENTAL FACILITY

Experiments on the structural steels modification are performed at the accelerator TIPr-1, which shown on figure 1. Injector system (1) consists of ion source, extraction system and accelerator tube with high voltage up to 100 kV. The beam current at the injector output is measured by beam transformer (2). The experimental chamber (3) is used for steel samples irradiation by low-

energy ion beams. Electrostatic lenses (4) provide beam matching with the input to RFQ (5). The chamber (6) has a beam detector for accelerated beam current measurements. Three magnetic quadrupoles (7) forms at the targets the beam profile needed for experiments. In chamber (8) the target assembly for material samples irradiation by the ion beam accelerated in TIPr-1 is installed. The target construction enables the irradiation experiments with samples heated to the temperature up to 700°C.

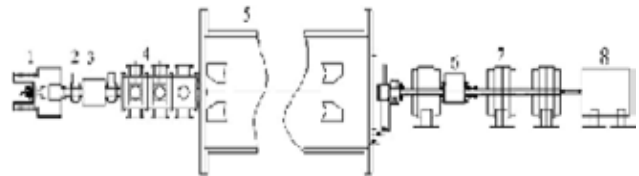


Figure 1: Scheme of accelerator TIPr-1.

Duoplasmatron, which is a regular source for proton beam generation at the injector I-2 at ITEP, was installed in TIPr-1 injector system. The pulse valve mounted at discharge chamber output significantly reduces the gas load in the injector and enables the cold cathode operation mode [2]. A system of the power supply for duoplasmatron was developed. It provides the production of an ion beam with a duration of 60 microseconds and a pulse repetition rate of 1/3 pps.

The power supply circuit of the ion source is shown at figure 2. The main elements of this circuit are a pulse discharge generator (PDG), a power supply (PSIV) for the inlet valve; power supply for duoplasmatron magnet (PSM). This circuit located on the high voltage platform.

TEST OF ION SOURCE WITH NITROGEN BEAM

Duoplasmatron was tested under operation with nitrogen ion beam. The time-of-flight method was used for charge state distribution (CSD) measurements of nitrogen ion beam generated by duoplasmatron [3]. CSD and beam current were measured for two different discharge currents: $I_{arc}=213$ A and $I_{arc}=173$ A. The CSD behavior during the beam pulse for discharge current of 173 A is shown in Figure 3. The measured distribution of different ions in total beam current are shown in Table 1.

METHOD OF BROADBAND STABILIZATION OF THE VEPP-4 MAIN FIELD

A. Pavlenko, BINP SB RAS; NSU, Novosibirsk, Russia

A. Batrakov, G. Karpov, I. Nikolaev, V.Svishchev, BINP SB RAS, Novosibirsk, Russia

Abstract

The stability of the main field has great influence on precision experiments on particle physics which are performed on VEPP-4M facility currently. A method of broadband stabilization of the VEPP-4M main field allowing us to achieve field stability better than 0.5 ppm over DC - 50Hz frequency range is presented. The method combines NMR stabilization and feedback loop using induction signal.

INTRODUCTION

It is necessary to know the beam energy of cycling accelerators in the particle physics experiments. At VEPP-4M experiment of CPT-invariance test by comparison of spin precession frequencies of electron and positron simultaneously circulating in VEPP-4M storage ring with accuracy 10^{-8} is planned [1]. The error of this experiment directly depends on stability of guiding magnetic field therefore long-term stability and field ripples are of the great importance. Long-term (hours) stability 10^{-6} allow one to find optimal parameter for the measurements. High-frequency ripples (up to 5 Hz) results in broadening of resonance spin precession frequency. This effect increases statistical error of the experiment. The frequencies more 10 Hz result to side spin resonance harmonic and could be excluded by optimal experiment parameters choice. Furthermore field instability induces beam orbit pulsation which has negative influence on count rate of Touschek polarimeter and increases the systematic error of the experiment. So, detrimental influence of field pulsation in a range from 0.01 to 10 Hz on statistic and systematic error in this experiment requires wide range stabilization system of guiding field of VEPP-4M storage ring.

THE VEPP-4M MAIN FIELD QUALITY

The VEPP-4M magnetic structure containing about 100 bending magnets are supplied by high current power supply IST. The main field varies in the range from 0.15 T at injection energy to approximately 0.55 T at maximum energy [2]. All magnets are connected in series, and current is changed from 2 kA to 5.5 kA. Long-term stability of supply current stays at 10^{-5} relative level. In series with the bending magnets, there is “out of ring” additional calibration magnet which is fully identical to bending magnets.

The precision NMR magnetometer [3] is used to measure absolute value of the VEPP-4M main field in the calibration magnet. Full measurement cycle consists a few elementary cycles. Each cycle includes only one

excitation RF pulse and one NMR response signal. Typical NMR signal duration for the VEPP-4M dipole magnet in the field range 0.15-0.2 T is ~ 5 ms. Time interval between elementary cycles T_e is defined by NMR working substance relaxation time. For VEPP-4M NMR probe $T_e \approx 0.08$ s. So, during full busy time real measurement is performed only within short interval ~ 5 ms separated with 0.08 s, where no NMR signal presents. To improve measurement accuracy the accumulation of NMR response signals is used (usually 8 – 16 elementary cycles).

To increase stability of the VEPP-4M main field, the feedback loop was implemented into the power supply control using data given by NMR magnetometer. The difference between set point and measured field is converted to an additive to be added to value measured with DCCT. That “via-DCCT” way allows correcting the power supply current. The integral term of PID controller is used with integral gain approximately equals to 0.5. Higher gain value results in feedback loop instability. The correction rate is about 1 s, providing field correction in the band from 0 Hz up to 0.1 Hz. Fig. 1. presents the NMR magnetometer data with the feedback off and on.

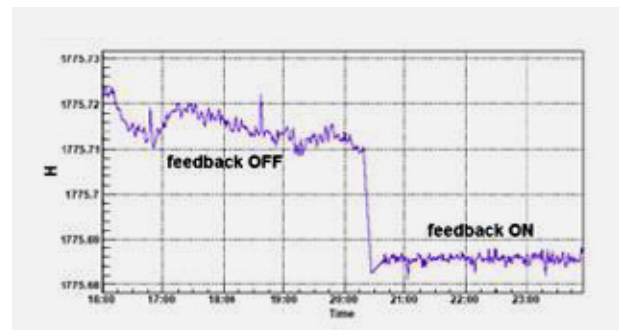


Figure 1: The NMR stabilization efficiency.

The long-term instability is about 1 ppm (RMS). However, NMR measurements don't provide information about amplitude and frequency content of field instability for frequencies higher than 1 Hz. In order to measure high frequency ripples it was used the induction sensor placed into calibration magnet. The sensor is equipped with electrostatic shield which suppresses coupling with power supply rails. The sensor has magnetic area $\omega S = 7.7 \text{ m}^2$. Its output voltage is recorded by the multimode digital integrator VsDC3 [4] and these data are processed to get Fourier transform. The spectral components are divided by $2\pi F \cdot \omega S \cdot B$ factor giving magnetic field ripple amplitude relative to mean value B at frequency F . Fig. 2 (blue plot) presents the VEPP-4M field ripple spectrum.

MAGNETIC SYSTEM OF ISOCHRONOUS CYCLOTRON F250 FOR PROTON THERAPY APPLICATIONS

Yu. G. Alenitsky[#], N.L. Zaplatin, E.V. Samsonov,
V.P. Dzhelepov Laboratory of Nuclear Problems, JINR, Dubna, Russia

Abstract

Possibility of the isochronous cyclotron F250 creation with protons energy ~ 250 MeV on the basis of magnet with pole diameter 6 m, which is used for the synchrocyclotron (Phasotron), is examined in the JINR Laboratory of Nuclear Problems (LNP). The proposed cyclotron F250 will make it possible to strongly decrease the electric power of magnet and to avoid the need of beam degradation from 680 MeV to 250 MeV.

For creating the required magnetic field of the cyclotron F250 it is necessary to change the form of steel spiral shims and disks, located inside a vacuum chamber of synchro-cyclotron. The basic parameters of the magnetic system of the cyclotron F250 with the condition of retaining the vacuum chamber and the magnet yoke of synchrocyclotron are given.

INTRODUCTION

The basis of the experimental base for JINR Laboratory of Nuclear Problems (LNP) until 1979 served the first accelerator of Dubna - synchrocyclotron. As a result of a number of improvements this accelerator for a long time remained one of the most powerful installations of this type [1].

In (1967 -1970) the project [2] of reconstruction the synchrocyclotron into a small meson factory with the energy of protons 680 MeV was developed. In (1979 - 1984) this project was realized with the maximum intensity of the internal beam of protons 7 mA and with the efficiency of extraction $\sim 50\%$. The obtained parameters of accelerator made it possible to substantially enlarge the program of physical and applied works on the accelerator [3].

At present a medico - biological complex operates in LNP for treating the oncologic sick with the use of protons at energies 160-250 MeV. For determining the required energy of protons the information about the mean free path of protons in the correspondence for the position of Bragg's peak in each case is used. Necessary energy of protons is obtained by means of degrader system providing a retarding the extracted beam of protons with 680 MeV to 250 MeV and less. In this case the utilized for medical purposes intensity of beam does not exceed 50 nA.

The successes achieved in the last decade in the proton therapy led to development and creation of the specialized accelerators for this purpose. The considerable progress in this direction is achieved in the creation of isochronous cyclotrons [4, 5].

[#]alen@jinr.ru

The considerable progress in this direction is achieved in the creation of isochronous cyclotrons [4, 5]. However, the cost of construction as well as the operating costs of such cyclotrons comprises the rather great values.

In connection with the foregoing it looks appropriate to develop a project with a partial use of magnetic, high-frequency and other systems of working accelerator for creation on their basis an isochronous cyclotron for proton therapy.

The decommissioning of the JINR Phasotron will allow in the shortest possible time with minimal capital expenditure to create an isochronous cyclotron for protons up to 250 MeV with an intensity of the extracted beam about 50 mA.

CALCULATION OF MAGNETIC FIELD

General view of F250 magnetic system, including the magnet of the working JINR Phasotron and the lids of vacuum chamber with the system of spiral shims of new configuration is shown in Figure 1. Position of the main elements of the magnetic system in the gap between poles of the electromagnet ($\varnothing=6000$ mm, $d=1540$ mm), that provide the desired field in the mid-plane is shown in Fig. 2.

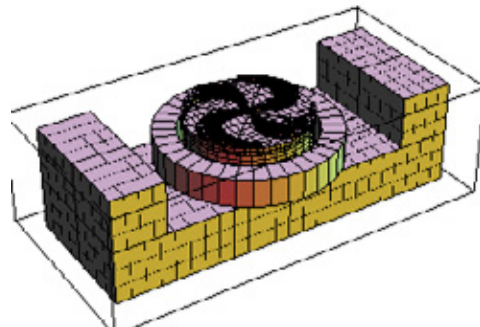


Figure 1: General view of FC250 magnetic system.

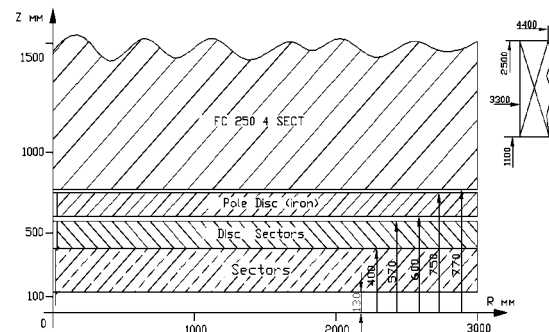


Figure 2: Scheme of the main elements location on vertical cross section.

MAGNETIC FIELD DESIGN AND CALCULATION FOR FLNR DC-280 CYCLOTRON

B.Gikal, G.Gulbekian, I.Ivanenko, J. Franko, JINR, Dubna, 141980, Russia
 T.Belyakova V.Kukhtin, E.Lamzin, S.Sytchevsky, ERIEA, St. Petersburg, 189631, Russia

Abstract

The isochronous cyclotron DC-280 is intended to accelerate the ion beams with A/Z from 4 to 7 up to the energy 8 – 4 MeV/nucleon. The wide range of the magnetic field levels from 0.64T till 1.32T allows to make a smooth variation of the beam energy over the range $\pm 50\%$ from nominal. For operational optimization of the magnetic field the 11 radial and 4 pairs of harmonic correcting coils are used. The numerical formation of the magnetic field is carried out. The problems and solutions of DC-280 magnetic field design are described.

INTRODUCTION

The new isochronous cyclotron DC-280 is now under construction in Laboratory of Nuclear Reactions (FLNR, JINR, Dubna). The cyclotron is intended for accelerating the beams of heavy ions from Carbon to Uranium of the energies from 4 to 8 MeV/nucleon [1]. The cyclotron has a H-shape main magnet with 4 meter pole diameter. The magnetic structure allows to carry out the smooth adjustment of the beam energy over the range $\pm 50\%$ from nominal by means of variation of the average magnetic field level at the range from 0.64T till 1.32T. The isochronous field is formed by 4 pair of 45-degree sectors. The operational correction of the magnetic field is realized by means of 11 radial and 4 pairs of harmonic correcting coils. The betatron frequencies lies on the range $1.005 < Q_r < 1.02$ and $0.2 < Q_z < 0.3$.

Table 1: Main parameters of the DC-280 cyclotron

Main size of the magnet, [mm]	8760×4080×4840
Weight of the magnet [t]	1100
Maximal power, [kWt]	≈ 280
Diameter of the pole, [mm]	4000
Distance between the poles, [mm]	500
Number of the sectors pairs	4
Sector angular extent (spirality)	45° (0°)
Sector height, [mm]	111
Distance between the sectors (magnet aperture), [mm]	208
Distance between the sector and pole (for correcting coils), [mm]	35
Number of radial coils	11
Number of azimuthal coils	4

NUMERICAL FORMATION OF DC-280 CYCLOTRON MAGNETIC FIELD

The numerical 3D formation of DC-280 magnetic field was made in some stages using the KOMPOT program package [2-4]. At the first stage the optimization of magnet yoke was carried out. The criteria of optimization is the magnetic field inside yoke elements should not exceed 1.5 – 1.6 T. In this case the efficiency of the magnetic system stays in linear area, figure 2.

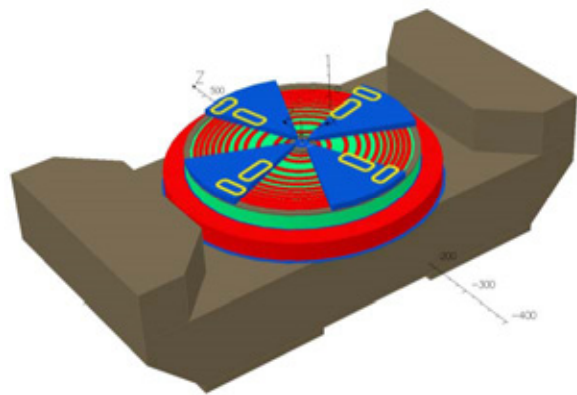


Figure 1: The model of DC-280 magnetic system.

The important problem of DC-280 magnet yoke optimization was the decreasing of the fringe field level over the magnet, where ECR ion source and axial injection line are placed. The special form of the upper (and lower for symmetry) balk of yoke and usage of the magnetic shield platform lets to decrease the fringe field down to acceptable level about 40Gs near ECR ion source and horizontal elements of beam injection line.

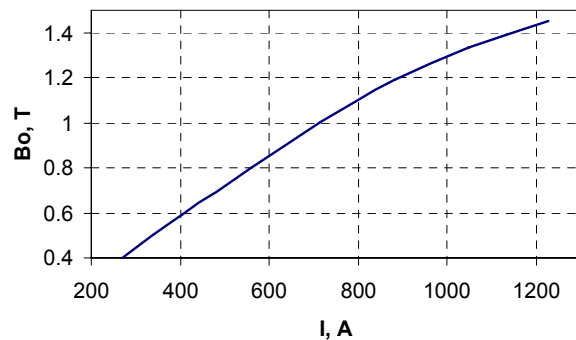


Figure 2: The current of main coil and the magnetic field level for DC-280 magnetic system.

The distance in 500-mm between poles was chosen to place the high-voltage (up to 130kV) RF system and the independent Flat-Top system. The isochronous form of the magnetic field is formed by 4 pairs of sectors. The

VIRTUAL LABORATORY OF VACUUM TECHNIQUE

G.P. Averyanov, V.V. Dmitriyeva, V.L. Shatokhin,
National Research Nuclear University (Moscow Engineering Physics Institute)
Moscow, Russia

Abstract

The report considers the interactive computer modeling of vacuum systems. Operation of real vacuum systems is modeled by simulating computer code. It is possible to assemble virtual installation, to choose the necessary pumps (from the database of low-vacuum and high-vacuum ones), to select the vacuum connecting pipes with the required parameters. The vacuum chamber volume and its internal surfaces characteristics (roughness, types of preliminary processing), defining outgassing from these surfaces are set.

INTRODUCTION

Vacuum Technique virtual laboratory is part of a complex of similar Electrophysics Laboratories, developed at the Department of Electrophysical Facilities (EF) of NRNU MEPhI. Computer modelling and simulation of individual components and entire electrophysical systems is a promising and in some cases the only possible way to replace the full-scale simulation. The creation of computer-based simulators is used in various fields of technology, including nuclear physics field (i.e. nuclear power reactors management simulators). The development of the set of laboratory exercises for Electrophysics solves the following tasks:

- acquire technology skills in assembly and maintenance of various subsystems and systems of EF (as simulator);
- to investigate the structure and the main characteristics of the EF devices and different modes of their work;
- gain experience in EF designing and master the methods of their calculation.

The vacuum system is an essential specialty of any accelerator. In this regard, the "Vacuum Technique" educational laboratory has existed since the founding of the Department of EF. Real vacuum systems of accelerators can have a very large extent, complex structure, and the procedure for their pumping (including heating of system) can take many days. Therefore, the development of computer workshop was a logical continuation of the vacuum practical work, significantly expanding its functionality.

VACUUM SYSTEMS MODELING THEORY

The simulation program algorithm is based on the following basic theoretical principles of vacuum technology [1, 2]. The number of gas molecules in the vacuum system is reducing by means of vacuum pumps, which create a volume flow Q , determined by the speed with which pressure p in the vacuum system of constant volume V decreases with time t :

$$Q = \frac{d(pV)}{dt} = V \cdot \frac{dp}{dt} \quad (1)$$

In reality, there is a lower limit of pressure below that pumping of the system is impossible - the ultimate residual pressure p_r . The amount of gas in the vacuum system depends on the ratio of gas flow entering the system - Q_{in} and pumping - Q_p : $Q = Q_p - Q_{in}$. The magnitude of the gas flow entering the system depends on the quality of manufacture of the vacuum system, that is, the values of leakage flow Q_l and outgassing flows Q_{gf} from inner surfaces. When the limit of the residual pressure in the vacuum system is reached mode is set to dynamic quasi-equilibrium: $Q_p = Q_{in}$. Pumped flow is equal $Q_p = Sp$, where S is pumping speed. Equation (1) takes the form:

$$p \cdot S - Q_l - Q_{gf} = V \cdot \frac{dp}{dt} \quad (2)$$

Thus $p_r = (Q_l + Q_{gf})/S$. The result of the solution of equation (2) for the total pressure will be the dependence:

$$p(t) = \frac{Q_{\Sigma}}{S} + \left(p_{st} - \frac{Q_{\Sigma}}{S} \right) \cdot e^{-t/\tau} \quad ,$$

where $Q_{\Sigma} = Q_{gf} + Q_l$; p_{st} - initial pressure in the vacuum system, $\tau = V/S$. Similar dependences can be obtained for each partial gas component $p_i(t)$. Furthermore, the system pressure cannot be obtained under the pump ultimate pressure. In case of the continues pumping flow $Q = S_p \cdot p_p = S_{ef} p$, where S_p and p_p - the pumping speed and the pressure at the pump inlet, S_{ef} - effective pumping speed of the vacuum chamber. The presence of the connecting pipelines leads to the fact that between the vacuum pump and the vacuum chamber arises a pressure differential: $p - p_p = Q/U$, U - the pipeline conductivity. Thus, the pumping of the vacuum chamber is carried out with some S_{ef} , lower than S_p .

Considering these equations, we come to the pumping model determined by the ordinary differential equations with initial conditions (Cauchy problem). The solution to this problem has been realized by the Runge-Kutta method of fourth order.

VACUUM ELEMENTS MODELS

Each of the pumps designed to operate over a certain pressure range with approximately constant pumping speed - S_0 . The ultimate pump pressure p_0 determined by

MEASUREMENT OF THE DOSE RATE AND THE RADIATION SPECTRUM OF THE INTERACTION OF 2 MeV PROTON BEAM WITH A VARIETY OF STRUCTURAL MATERIALS*

D. Kasatov[#], A. Makarov, S. Taskaev, I. Schudlo
BINP SB RAS, Novosibirsk, Russia,

Abstract

At the BINP, a pilot epithermal neutron source is now in use. It is based on a compact Vacuum Insulation Tandem Accelerator (VITA) and uses neutron generation from the reaction ${}^7\text{Li}(p,n){}^7\text{Be}$. Irradiation experiments using various structural materials were carried out. The results of measuring the intensity and the spectra of the γ and X-ray radiation are discussed in the present work. This work is a part of a plan to create a therapeutic beam and strategies for the use of the accelerator for clinical application.

INTRODUCTION

Presently, Boron Neutron Capture Therapy (BNCT) [1] is considered to be a promising method for the selective treatment of malignant tumors. The results of clinical tests, which were carried out using nuclear reactors as neutron sources, showed the possibility of treating brain glioblastoma and metastasizing melanoma not curable by other methods [2, 3]. The broad implementation of the BNCT in clinics requires compact inexpensive sources of epithermal neutrons. At the BINP the source of epithermal neutrons based on 2 MeV Vacuum Insulation Tandem Accelerator (VITA) and neutron generation through ${}^7\text{Li}(p,n){}^7\text{Be}$ reaction was proposed [4] and created.

General view of the accelerator is shown in Fig. 1. Negative hydrogen ions are injected and accelerated up to 1 MeV by potential applied to the electrodes, then H^- turn into protons in the stripping target and at last the protons are accelerated up to 2 MeV by the same potential. Pumping of the gaseous stripping target is carried out by cryogenic and turbomolecular pumps through the jalousies. The potential of the high-voltage and five intermediate electrodes is supplied by a high-voltage source through the insulator which has a resistive divider.

Presented work is aimed on measurement of lithium target radiation hazard and to find materials for high-energy beam transporting channel and for substrate of neutron producing target with minimum radiation emission during proton bombardment. There were studied different materials.

EXPERIMENTAL LAYOUT

Generation of γ - rays was carried out by directing the proton beam on targets made of various materials. The

* The study was performed by a grant from the Russian Science Foundation (Project No.14-32-00006) with support from the Budker Institute of Nuclear Physics.

[#] kasatovd@gmail.com

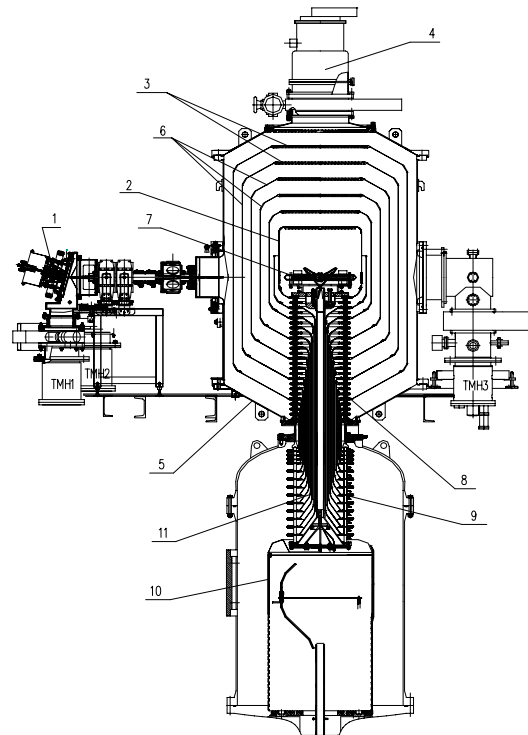


Figure 1: High-current vacuum insulation tandem accelerator: 1 – ion source (H^-); 2 – high voltage electrode; 3 – electrode shutters; 4 – cryo pump; 5 – accelerator vacuum volume; 6 – intermediate electrodes; 7 – stripping target; 8 – feedthrough insulator (vacuum part); 9 – feedthrough insulator (gas part); 10 – high voltage source; 11 – coaxial feeding tubes.

target is a disc of 100 mm diameter and thickness from 1 mm to 10 mm depending on the material mounted on a cooled copper substrate. Gamma spectra were detected by BGO spectrometer. BGO spectrometer was located at a distance of 75 cm from the target along the beam axis and was covered by a lead shielding having thickness of 50 mm with collimation hole 25 mm in diameter. The spectrometer was calibrated using the isotopes ${}^{137}\text{Cs}$ and ${}^{60}\text{Co}$ taking into account the background radiation from the accelerator [5]. After irradiation the target was extracted and induced radioactivity was measured. For this purpose we used NaI and BGO detectors.

Dose rate measurements were carried out by an automatic system based on ionization chambers. In some cases the neutron yield was registered by the lithium glass detector.

MEASUREMENT OF THE SPATIAL DISTRIBUTION OF GAMMA RADIATION AT TANDEM ACCELERATOR WITH VACUUM INSULATION *

I. Schudlo[#], D. Kasatov, A. Makarov, S. Taskaev
Budker Institute of Nuclear Physics SB RAS, Novosibirsk, Russia

Abstract

The experiments on generating 2 MeV proton beam with the current of 1.6 mA were carried out at BINP. During the experiments the spatial distribution of the bremsstrahlung dose rate was studied. According to the experimental results the suggestion of the reasons for the radiation appearance and ways to reduce it were made.

INTRODUCTION

At the BINP, the source of epithermal neutrons for boron neutron capture therapy of malignant tumors based on the tandem accelerator with vacuum insulation and a lithium target is created and put in operation [1]. The circuit source is shown at Fig. 1. The proton beam energy of 2 MeV and a current of 1.6 mA is obtained at the accelerator-tandem with vacuum insulation, marked by rapid acceleration - 25 kV/cm. Generation of neutrons occurs as a result of the threshold reaction ${}^7\text{Li}(p,n){}^7\text{Be}$ while dumping the proton beam onto the thin lithium target with intense cooling.

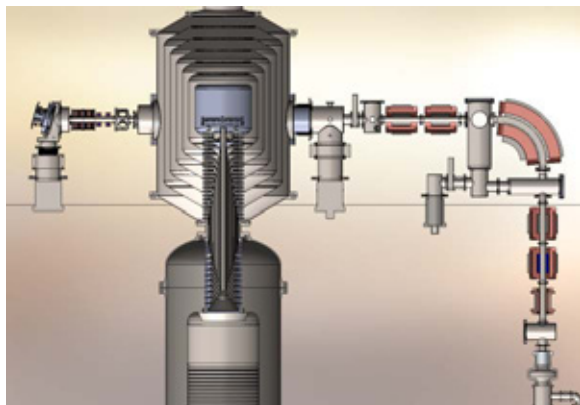


Figure 1: High-current vacuum insulation tandem accelerator.

To conduct BNCT it is required to increase the proton beam current at least up to 3 mA. But the increase in the injected current accelerator leads to unstable operation of the accelerator and requires research to ascertain the causes of the current limit. It was assumed that one of the beam current limitations is presence of accompanying electrons in the accelerator channel. The electrons are produced by the interaction of low energy beam of H^- ions with the residual gas in the input node of the accelerator. The electrons are accelerated to the full energy according the accelerator voltage and absorbed in

* The study was performed by a grant from the Russian Science Foundation (Project No.14-32-00006) with support from the Budker Institute of Nuclear Physics.
Cshudlo.i.m@gmail.com

the construction materials of the accelerator generating intense bremsstrahlung radiation. To investigate the electron current the experiment was conducted on measurement of the angular distribution of the accelerator gamma radiation.

EXPERIMENTAL LAYOUT

During the experiment, the beam of accelerated protons with a current of 0.5 mA is measured by the Faraday cup, located at the accelerator output. Measurements of gamma dose are carried out using two dosimetry detectors Berthold LB-112. One detector is placed at a distance of three meters from the center of the accelerator at a 90 degree angle to the beam axis, the measurements with the second detector were carried out at different angles to the beam axis at the same distance to the accelerator. The detectors are located at the horizontal plane with the acceleration tract.

EXPERIMENTAL RESULTS

The measured gamma dose distributions are presented at Fig. 2 and 3.

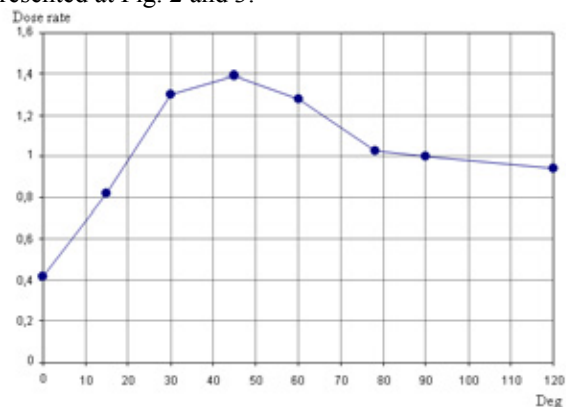


Figure 2: A gamma dose rate in dependence on the radiation emission angle. The value is normalized to the reading of the detector mounted at an angle of 90° to the beam axis.

The dose rate lowering at the angles 0°-30° is the result of gamma attenuation by the construction elements: the stripping tube and output pumping volume are located between the detector and the gamma source area. Actual trend should have higher values according to Fig. 3. Such a dose distribution having the preferred direction coinciding with the accelerated beam could be explained if the bremsstrahlung radiation is caused by the relativistic electrons.

ESTIMATION OF THE EFFICIENCY OF BIOLOGICAL SHIELDING FOR THE CIRCULAR HALL OF U-70 ACCELERATOR AT IHEP

G. Britvich, M. Kostin, V. Pikalov, O. Sumaneev, IHEP, Moscow Region, Russia

Abstract

Report presents estimation of biological shielding efficiency for annular hall of U-70 accelerator. Distribution of neutron flux in concrete shielding of proton accelerator measurements carried out by method of long-lived isotopes specific activity determination. The experimental data may be compared with Monte-Carlo simulation.

INTRODUCTION

During construction of the new medical channel for carbon ions beam extraction the side concrete shielding of the accelerator was disclosed. We have got a good opportunity to measure depth distribution of the gamma-activity of the shielding on the height of 10 cm from the beam orbit plane. Such measurement allows us to estimate efficiency of the neutron radiation attenuation in the biological shielding of accelerator.

GEOMETRY OF MEASUREMENTS AND BOUNDARY CONDITIONS

Cross-section of the U-70 side shielding is shown in Fig.1. This shielding was partly disclosed for the new channel construction. Point M corresponds to the internal target 35/1 of channel #18. This target was working during previous run of U-70 since 09 to 21.04.2012. Berillium target (with 3×3 mm² cross-section and 30 mm length) was irradiated by 5×10¹¹ protons with 50 GeV energy during every 9.7 sec cycle. Induced radioactivity was measured along lines 1-4 in the Fig. 1. Measurements were done on the surface of concrete blocks at the level of 2 m from the floor. Beam orbit is laying at the level of 2.15 m from the floor. Blocks were removed from the shielding for the measurements to improve background conditions. One can see measurement points marked, detector and its shielding.

GAMMA-SPECTROMETER

Scintillation gamma-spectrometer with NaI(Tl) crystal was used for the measurements. Crystal size is 40×40 mm², it was equipped with PMT XP 2212. Parameters were measured in operational conditions, with 50 m cable and rate ~ 103 Hz. 43 calibration sources were used.

GAMMA-ACTIVITY OF THE CONCRETE

Measurements were done in two concrete blocks along lines 1-4 (see in Fig. 1) in set of points placed in 25.4 cm from each other. Typical gamma spectrum is shown in Fig. 2. Two isotopes – ²²Na and ⁵⁴Mn – could be easily

identified. ²²Na is created by the fast neutrons with energy threshold 13 MeV in the reaction ²³Na(n, 2n)²²Na, and ⁵⁴Mn in the reactions ⁵⁵Mn(n, 2n)⁵⁴Mn with 11 MeV threshold and ⁵⁴Fe(n, p)⁵⁴Mn with 1.5 MeV threshold [1-2]. ²⁴Na is presented in cement, ⁵⁵Mn and ⁵⁴Fe are presented in cement, gravel and steel fixtures.

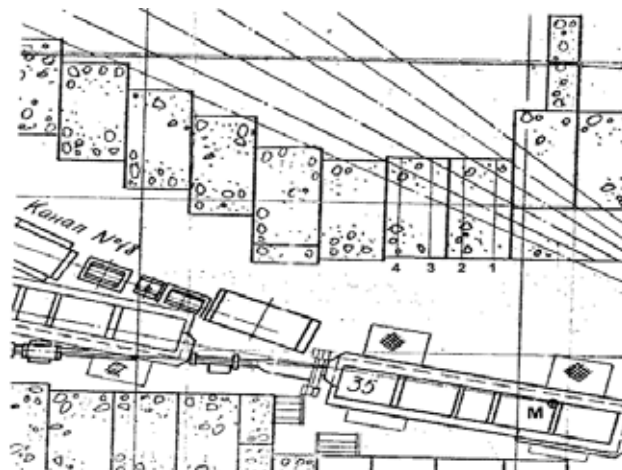


Figure 1: Accelerator equipment and shielding layout in the U-70 circular hall in the region of 34, 35 and 36th magnet blocks.

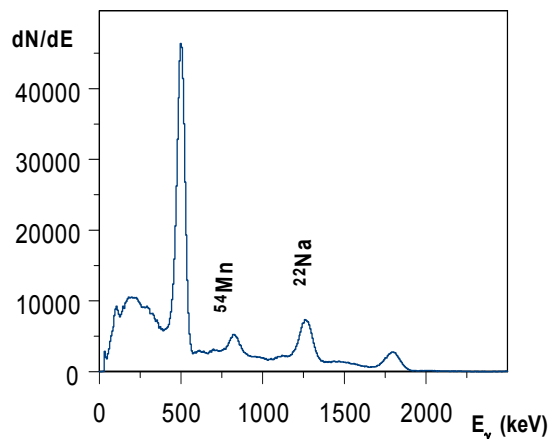


Figure 2: Gamma-spectrum measured on the concrete surface.

ABSOLUTE ACTIVITY OF ²²Na AND ⁵⁴Mn ISOTOPES IN CONCRETE

Detector is placed on the concrete surface and measure number of gamma rays (N_γ) in the point from the semi-infinite layer of concrete.

DEVELOPMENT OF ACCELERATOR FACILITIES AT SSC RF – IPPE

V.A. Romanov, S.V. Bazhal, A.I. Glotov and K.A. Rezvykh, SSC RF – IPPE, Obninsk, Russia

Abstract

Short overview of status and operation of accelerator facilities of the SSC RF – IPPE for various applications in nuclear science and technologies is given. Some results obtained as well as prospect of development of the accelerator facilities are described.

INTRODUCTION

An infrastructure for experimental research in nuclear physics based on high-voltage accelerators has been developed at the SSC RF-IPPE for more than half a century. The results obtained have made significant contribution to the solution to problems of fission physics, solid-state physics and studies of materials under radiation, as well as to the build-up of nuclear data for development of fast neutron reactors and to some other fields of basic and applied research.

At the present time scientific research on the accelerators at the SSC RF-IPPE is carried out in the following main fields:

- Low and intermediate energy nuclear physics. Nuclear data for nuclear power engineering. Closed fuel cycle. Safe handling of radioactive waste and spent fuel [1-4].
- Solid state physics. Physics of radiation damage and studies of materials under radiation [5-7].
- Nuclear microanalysis. Analysis of composition and structure of materials [8-10].
- Basic research on dusty plasma physics [11-13].
- Development of technology of membranes [14].
- Nuclear medicine [15-16].

Experimental facilities based on six electrostatic accelerators were constructed at the institute. The EGP-15 tandem accelerator (Fig. 1), the largest electrostatic accelerator in Russia, is among those six machines. This tandem accelerator was designed and manufactured at the Institute for Physics and Power Engineering in close cooperation with many Russian scientific organizations.

The accelerator facilities provide a wide spectrum of species of accelerated ions (H, He, Li, C, O, F, Al, Si, Cl, Fe, Ni, Zr) formed in the continuous or pulsed ion beams with current in the range 10^{-8} A to 10^{-3} A and energy varying from several hundred keV to tens of MeV. The main operational characteristics of the accelerators are given in Table 1.

The following factors determining interest in electrostatic accelerators can be mentioned among the others:

- high uniformity of energy of accelerated beam;
- broad range of accelerated ions;
- possibility of quick alteration of species of accelerated particles;
- intensity of ion beams produced at the accelerators of this type are in the range 10^{-8} A to 10^{-3} A;



Figure 1: The EGP-15 tandem electrostatic accelerator.

Table 1. The main operating characteristics of accelerator facilities of the SSC RF-IPPE

Model	Ion Energy, MeV	Ion species	Beam Mode	Beam Current μ A
EG-2.5	0.2÷3.1	P, D	continuous	0.1÷30
		He, N, Ar, O		0.01÷10
EG-1	0.9÷4.5	P, D	continuous	1.0÷20
			pulsed	2000
KG-2.5	0.3÷2.2	P, D	continuous	100÷2000
			pulsed	5
EGP-15	4÷12 (P)	heavy ions	continuous	400
			pulsed	0.01÷1.0
EGP-10 (temporarily closed)	3.5÷9.0	P, D	continuous	0.01÷10
			pulsed	400
KG-0.3 (temporarily closed)	0.3	P, D	continuous	10÷2000
			pulsed	5000

PRODUCTION OF ACCELERATING EQUIPMENT FOR NUCLEAR MEDICINE IN NIEFA. POTENTIALITIES AND PROSPECTS

M.F. Vorogushin[#], Yu. N. Gavrish, A. P. Strokach

JSC “D.V. Efremov Institute of Electrophysical Apparatus”, St. Petersburg, Russia

Abstract

The D.V. Efremov Institute (NIEFA) is the leader in Russia in designing and manufacturing of the accelerating equipment for medicine. About one hundred of linear accelerators for the beam therapy and more than forty cyclotrons for production of radiopharmaceuticals have been designed, manufactured and delivered to clinics of Russia and some foreign countries.

The equipment designed and manufactured in NIEFA in its technical characteristics is on a par with foreign analogs and sufficiently cheaper in expenditures for personnel training, hardware and software compatibility, warranty and post-warranty service, delivery of spare parts and updating.

In accordance with Federal Targeted Programs on the development of medical and pharmaceutical industries up to 2020, the production facilities, material and technical resources have been prepared for the organization of serial production of cyclotrons and gamma tomographs.

A leap forward in the nuclear medicine, understood as the introduction of nuclear-physical technologies into medicine, is directly connected with a broad application of charged particle accelerators. This is most distinctly manifested in diagnostics and treatment of the most dangerous and widely spread oncologic and cardiovascular diseases, which rate of mortality mainly defines an average age of human life in Russia.

A single-photon emission computer tomograph «EFATOM» [1] has been designed in NIEFA for radionuclide diagnostics. It is used to visualize images obtained by using special radiopharmaceuticals. This method allows the anatomy and functioning of various organs to be studied as well as, osteal pathologies to be diagnosed. A wide range of available radiopharmaceuticals and methods makes possible diagnostics practically of any organ. The information obtained is used in oncology, cardiology, nephrology, neurology, endocrinology, traumatology, hematology, gastroenterology, in cases of cerebrum brain diseases, etc. A package of clinical programs was developed in cooperation with the staff of the State St. Petersburg University for diagnostics of the aforementioned scope of diseases. It was tested in leading clinics of Russia and was awarded the top assessment. Radionuclide examinations with emission tomographs are one of the main diagnostic methods all over the world. In developed countries, tens of millions radionuclide examinations are carried out annually, and this number increases by 10-12% each year.

[#]vorogushin@luts.niefa.spb.su

Upon completing clinical tests, the «EFATOM» (see Fig.1) was included on the State Register of RF Medical Products, and in 2011 it was included on the List of products intended for serial production. More than 15 thousand examinations have been performed with the «EFATOM» in clinical hospital № 83, Moscow.

The main features of the «EFATOM» are as follows. Analog signals are transformed in the digital detection block at the output of each photomultiplier with a subsequent processing by a digital processor. This allows the maximum resolution to be realized. The gantry provides fixing of two detection units and their travel along radial, axial and angular coordinates. Detectors' positioning is computer-controlled. Patient's support system provides patient's fixation in the lying position and its travel in vertical and horizontal planes. Both manual and computer control is possible.

Further progress of this diagnostic method can be facilitated by application of the gamma-tomograph together with a computer tomograph, which realizes a technology combining the functional sensitivity of the single emission tomography with a high anatomic resolution of CT. Designing and construction of such a combined apparatus is a near-future aim of NIEFA in the field of diagnostics.



Figure 1: The «EFATOM» gamma-tomograph.

The accumulated clinical experience shows that nearly in 20% of cases more exact diagnostics with the positron-emission tomography (PET) using ultra-short-lived isotopes is required after the gamma-tomograph examination. PET allows the visualization of biological processes behavior in organs and tissues of a human-being on the molecular level, and both quantitative and qualitative assessments of the information obtained. For example, the accuracy of a malignant tumour detection,

ISBN 978-3-95450-170-0

RADIOBIOLOGICAL RESEARCH WITH CHARGED PARTICLES BEAMS IN ITEP

N. Markov[#], A. Kantsyrev, I. Roudskoy, ITEP, Moscow, Russia
A. Colubev, ITEP, Moscow, Russia and MEPHI, Moscow, Russia

Abstract

Radiobiological researches with heavy ions have been started at ITEP in 2006 on unique heavy ion accelerating facility ITEP-TWAC. The main purpose of these researches is study of the biological efficiency of carbon ions for different types of biological objects, such as tumor and normal cells, in the framework of the development of heavy ion therapy for cancer treatment in Russia. Another possible area of application of this research is the space radiobiology, studying stochastic and deterministic effects of ionizing radiation in the space environment on human. In this work the experimental setup for radiobiological research with heavy ions in ITEP, the dosimetry system for dose measurements and the results of the radiobiological researches with carbon ions are presented.

INTRODUCTION

In the last few decades there is a tendency in the increasing of the number of hadron (protons and heavy ions) therapy centers, that are in general hospital-based facilities in versus the previous times when the treatments were performed in nuclear physics research centers. For today, hadron therapy in Russia is only represented by proton therapy, that is carried out in three scientific research centers in ITEP (Moscow), JINR (Dubna) and PNPI (Gatchina). Research in the field of carbon ion therapy is at the very beginning and currently several projects of the new facilities construction, mainly based on the particle accelerators for nuclear physics research, are under discussion.

In 1997 the project for the reconstruction of ITEP U-10 proton synchrotron (TWAC-ITEP project) was started. The aim of this project was to create new facility for heavy-ion acceleration up to relativistic energies and ion accumulation with energies up to several hundreds of MeV/u [1]. In 2004 realization of the first stage of the TWAC-ITEP project has been completed and as one of the results a possibility to accelerate and accumulate carbon ions C^{6+} with energy suitable for therapy application was shown [2]. After several years radiobiological research program with carbon ions was initiated in ITEP. Since then in collaboration with biophysicist and radiation oncologist from JINR and Russian Cancer Research Centre various kind of radiobiological experiments (surviving of irradiated cells, chromosome aberration, mutagenic influence of heavy ions) with cancer and normal cells, as well as with other types of biological systems have been carried out.

[#]markov@itep.ru

EXPERIMENTAL SETUP

For radiobiological research at the TWAC-ITEP accelerator facility an experimental setup was organized at the end of the 511 beam-line (fast extraction beam-line from accelerator-storage ring U-10) in the building 120. Layout of the experimental setup is illustrated in Fig. 1

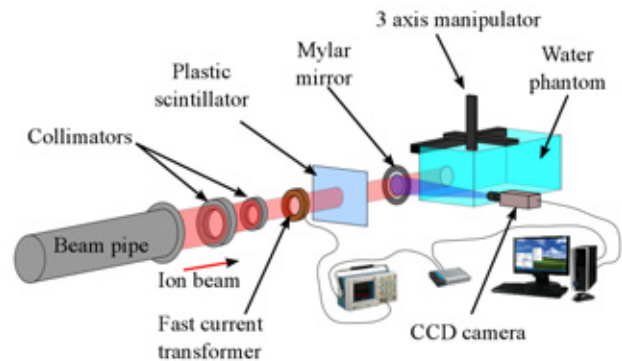


Figure 1: Layout of the experimental setup.

Formation of the dose fields with characteristic transverse dimensions of 20-100 mm was performed by system of magnetic elements, defocusing the ion beam at a considerable distance from the place of exposure and passive collimating system, located in the immediate vicinity of the irradiated target. Homogeneity of the field was controlled by the intensity of the luminescence of the plastic scintillator (Bicron BC412). The image of the beam on the scintillator was transferred to the CCD camera by means of a mirror from metalized Mylar, placed at an angle of 45 degrees to the beam axis.

For measurements of spatial distributions of the absorbed dose to water, as well as alignment of the biological targets during irradiation, was developed and produced water-phantom with the established three-axis manipulator. For readout and analysis of the signals from the detectors and instruments used in the experiment, as well as for operation of the manipulator, developed in ITEP hardware-software complex was used [3].

DOSE-FIELD MEASUREMENTS

In the study a beam of carbon ions, accelerated to energy of 215 MeV/amu in the booster synchrotron UK was used. The level of ion accumulation in a storage ring U-10 varied the number of particles per pulse. As in these experiments it was possible to use only ion beam pulses, generated in fast extraction mode, with single pulse width approximately 800 ns (FWHM), firstly questions of the carbon ions dosimetry have been considered. Due to the

ACCELERATOR HADRON THERAPY TECHNIQUE DEVELOPED AT JINR

E.M. Syresin, Joint Institute for Nuclear Research, Dubna, Russia

Abstract

Accelerator hadron therapy technique is one of applied researches realized at JINR. The JINR-IBA collaboration has developed and constructed the C235-V3 cyclotron for Dimitrovgrad hospital center of the proton therapy. Proton transmission in C235-V3 from radius 0.3m to 1.03 m is 72% without beam cutting diaphragms; the extraction efficiency is 62%. The main advantage of this cyclotron in comparison with serial commercial cyclotrons of IBA is related to higher current of the extracted beam.

The cancer treatment is realized in JINR on the phasotron proton beam. More than 1000 patients were treated there. A project of the demonstration center of the proton therapy is discussed on base of a superconducting 230 MeV synchrocyclotron. The superconducting synchrocyclotron is planned to install instead of phasotron in Medical Technical Complex of DLNP.

The project of the medical carbon synchrotron together with superconducting gantry was developed in JINR. The basis of this medical accelerator is the superconducting JINR synchrotron – Nuclotron. One important feature of this project is related to the application of superconducting gantry.

PROTON CYCLOTRON C235-V3

The JINR-IBA collaboration has developed and constructed the C235-V3 proton cyclotron (Fig.1) for Dimitrovgrad hospital proton center. The C235-V3 cyclotron, superior in its parameters to the IBA C235 medical proton cyclotron, has been designed and manufactured by the JINR-IBA collaboration. This cyclotron is a substantially modified version of the IBA C235 cyclotron.

Modification of the extraction system is the main aim of the new C235-V3 cyclotron [1-2]. The main feature of the cyclotron extraction system is a rather small gap (9 mm) between the sectors in this area. The septum surface consists of several parts of circumferences of different radii. The septum thickness is linearly increased from 0.1 mm at the entrance to 3 mm at the exit. The proton extraction losses considerably depend on the septum geometry. In the septum geometry proposed by JINR, where the minimum of the septum thickness is placed at a distance of 10 cm from the entrance, the losses were reduced from 25% to 8%. Together with the optimization of the deflector entrance and exit positions it leads to an increase in the extraction efficiency to 80%. The new extraction system was constructed and tested at the IBA C235 cyclotron. The experimentally measured extraction efficiency was improved from 60% for the old system to 77% for the new one.



Figure 1: Cyclotron C235-V3 in JINR engineering center.

Another difference in the structure of the magnetic field for the C235-V3 cyclotron compared to an IBA C235 serial cyclotron is related to the value of the radial component of magnetic field in the median plane, bump parameters, and the minimal value of the vertical betatron frequency in the central area of the cyclotron.

The bump of magnetic field B_z in the center is used in many cyclotrons for axial focusing during the first turns, when the B_z variation is low. When the decreasing field of the bump passes to the increasing isochronous one, the dip in the axial betatron frequency Q_z could appear. In the C235-V3, Q_z decreases at a radius of 10 cm down to $\sim 0.04-0.05$.

The presence in the area of the Q_z minimum of the mean radial component of the magnetic field B_r with a level of 5 G and gradient of 5 G/cm in the median plane (Fig.2) results in the transformation of coherent motion of the center of gravity of the beam in this area into the noncoherent oscillations of individual particles and coherent oscillations of the center of gravity. The simulated axial r.m.s. ($\pm 2\sigma$) size (Fig.3) is equal to 6 mm at $B_r=0$, it increases up to 12 mm at B_r corresponded to shim thickness of 2mm (Fig.2) and 8 mm at optimized shim thickness of 1.7 mm. In the C235-V3, the B_r component was optimized using the establish of shim correctors at the sectors.

In experiment, the r.m.s. vertical size of the beam (2σ) (Fig.4) at the radii of 15–20 cm is $\sim 17-18$ mm and becomes comparable with the vertical aperture of the accelerator of 20 mm determined by the interdee gap.

OPERATION AND DEVELOPMENT OF THE BINP AMS FACILITY

S.A. Rastigeev, V. V. Parkhomchuk, BINP SB RAS, Novosibirsk, and NSU, Novosibirsk, Russia
 A.R. Frolov, A.D. Goncharov, V. F. Klyuev, E.S. Konstantinov, A.V. Petrozhitskii, BINP SB RAS,
 Novosibirsk, Russia
 L. A. Kutnykova, IAE SB RAS, Novosibirsk, Russia

Abstract

The BINP AMS facility is the accelerator complex for accelerator mass spectrometry. The most distinguishing features of BINP AMS is the use of the middle energy separator of ion beams, the magnesium vapors target as a stripper and time-of-flight telescope for accurate ion selection. Present status and development of AMS complex for extension of applications are reviewed.

INTRODUCTION

The accelerator mass spectrometry is an ultra-sensitive method of isotopic analysis for archaeology, biomedical, environment science and for another field. It's based on measurements of the ratio between isotopes. The ratio between isotopes in sample can be less than 10^{-14} . So, the counting methods are used for detection of such low radiocarbon concentration [1-3]. The AMS system consists of the ion source, low energy channel, tandem accelerator and high-energy channel [4-6]. The tandem accelerator is a folded type vertical machine. The low energy beam line is used for initial isotopes selection. The tandem accelerator is applied for rejection of the molecular ions and of course for obtaining necessary beam energy for radioisotopes detector. The high-energy beam line is used for the subsequent ions selection and for radioisotopes detection.

The most distinguishing features of our AMS machine are the use of the middle energy ions separator. The middle energy electrostatic separator is located inside the tandem terminal. It can essentially decrease the ion background [7,8]. The next important distinguishing feature is the magnesium vapors stripper [9] instead of the gaseous one. The molecular destruction and ion recharging by magnesium are localized into the hot tube of the stripper. Moreover, the moment of time for ion detection can be registered with 16 μ s channel width by TOF detector [10,11]. This data is used for calculation of number of detected ions per unit time, allowing filtering the background ions from electrical breakdowns.

The accelerator mass spectrometer created at BINP SB RAS is installed at CCU "Geochronology of the Cenozoic era" for sample dating by the ^{14}C isotope and recently upgraded for biomedical applications. Over the past year have been analyzed more than 500 samples. Given the interest in using AMS in the biomedical field, the first biomedical researches are started jointly with biologists [12].

ION SOURCE

The multi-cathode (for 23 samples) sputter ion source is used for AMS analysis. The typical current of negative carbon ions is about 10 μ A for analyzed samples. The negative ions are produced by bombarding the graphite target with positive cesium ions. The vapor is formed by heating of the reservoir with cesium. Then the vapor via the pipe rises from the reservoir to the ionizer. The positive charged Cs ions are produced on a hot tantalum ionizer. The cesium ion beam is focused on the carbon sample placed on the cathode, because the working surface of ionizer is a spherical-shape cup. The copper sample holder has the inner diameter of 2 mm. The sample after AMS analysis is present at the Fig.1. As seen, the sputtering region of the sample is about 0.5 mm in diameter.

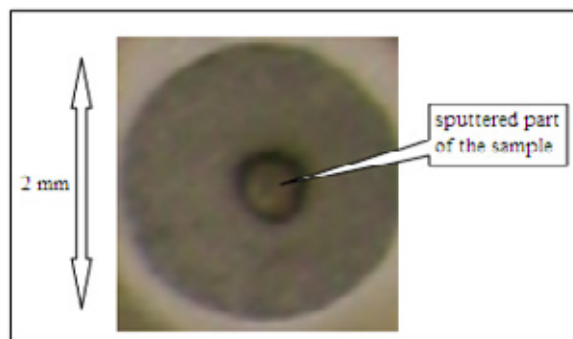


Figure 1: The sample in the ion source sputtered by cesium beam.

ION SELECTION

The sensitivity and reliability of radiocarbon measurement is limited by ion background. The nitrogen ions have the same mass as radiocarbon ones, but they are filtered by BINP AMS complex. The negative nitrogen ions are unstable, but the negative molecular NH^- ions can rich high voltage terminal. The positive nitrogen ions are produced from the breakup of NH^- ions after passing through the stripper. The energies for nitrogen from NH^- molecules are always less than the radiocarbon ions energy into tandem terminal, because nitrogen ion gets only a part of the molecule's energy. The BINP AMS complex has the electrostatic filter into tandem terminal for effective filtration of the different energy ions.

To test such selection, the NH^- molecular ions was accelerated and passed through 180° electrostatic bend which was set for ions energy 14/15 and charge state 3+

EXTENDED SCOPE OF APPLICATION OF INDUSTRIAL ELV ACCELERATOR

N.K. Kuksanov, Yu.I. Golubenko, P.I.Nemytov, R.A. Salimov, S.N. Fadeev, A.I. Korchagin, D.A. Kogut, E.V. Domarov, A.V. Lavruchin, V.G. Cherepkov, V.A. Semenov, Budker INP, Novosibirsk, Russia

Abstract

ELV accelerators are DC machines, designed and manufactured by Budker Institute of Nuclear Physics of Siberian Branch of Russian Academy of Science. These machines are well known in the world. They are operating from Germany in West to Indonesia and Malaysia in East. Main application of these accelerators is the treatment of polymers. New development of ELV accelerators is concerning the low energy range and design of self-shielded accelerators. There are the set of self-shielded accelerators. The lowest energy is 150 - 200 kV. These machines are unified with usual ELV accelerators and extend their application area. For industrial tomography based ELV4 accelerator was developed with low values of ripple current ($\leq 2\%$) and the instability of energy ($\leq 5\%$) of the electron beam.

INTRODUCTION

Radiation-chemical technology with the use of electron accelerators as the sources of ionizing radiation had been widely developed. Budker Institute of Nuclear Physics of the Siberian Branch of Russian Academy of Sciences is one of the world leaders in the development, design, production and delivery to the industry of electron accelerators of different types (i.e. continuous accelerators based on high-voltage rectifier, high frequency, pulse, etc.), covering a wide range of accelerated electrons energy and power. ELV accelerators hold a specific place in the range of equipment manufactured by the Institute. Compact dimensions and high operational qualities have allowed BINP take a leading position in the market of industrial accelerators, both in Russia and abroad. The ELV accelerators series has the range of accelerated electrons energy from 0.3 to 2.5 MeV, maximum beam power for separate machines from 20 to 100 kW and maximum beam current up to 100 mA. The special accelerator was designed and manufactured for ecological and research purposes with a beam power 400 kW.

DEVELOPMENT OF ELV ACCELERATORS FAMILY

ELV accelerators high voltage source is a generator with a cascade of parallel inductive links. HV rectifier column is installed inside the primary winding. The primary winding is powered by a frequency converter on the base of IGBT transistors. The secondary winding of the coil have the maximum induced voltage of about 20 kV. This voltage is rectified by voltage doubling circuit.

Rectifier unit connected in series or series-parallel to form the column of HV rectifier, ending with the high-voltage electrode. The injector control unit is located inside the high-voltage electrode. Accelerator tube is placed inside the rectifier column and the top of the tube is connected with the high-voltage electrode. All these elements are placed inside the pressure vessel filled with insulating gas (SF₆). This design reduces the overall dimensions of ELV accelerators and makes them the most compact among the devices of this class. The accelerator is supplied with gas system that enables to save SF₆ gas during maintenance and repair. Vacuum systems and the extraction device are attached to the bottom of the vessel. The cathode is placed at the upper end of the accelerator tube. The electrons emitted by the cathode have the full energy at the exit of the accelerator tube. They are passing through the system of scanning magnets that evenly distribute electrons on the foil window. The electron beam is scanned in 2 directions along and across the window. The material moves under the window in the transverse direction and is treated by extracted electrons. The beam position inside window is monitoring. The accelerator control is equipped with an automated system that enables not only to make the operator's job easy, but to synchronize the process equipment and the accelerator, or combine them into one complex.

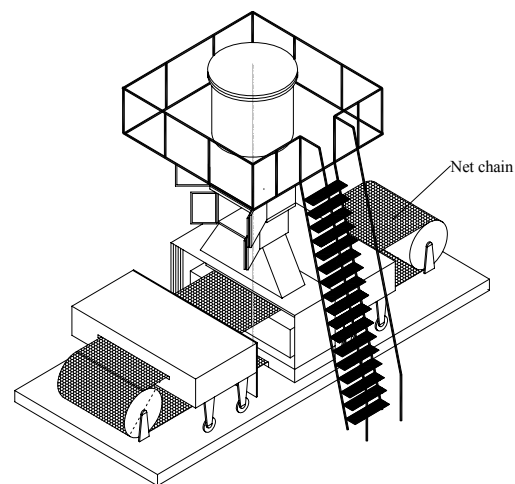


Figure1: 0.3 MeV*100 mA accelerator for tire industries.

The analysis of demands for accelerators (a market for accelerators) was made in 2011. As a result, the in-demand accelerators are distributed evenly for maximum energy from 1 MeV up to 2.5 MeV. Concerning the beam power – all queries on the boosters had 100 kW beam

LIA-2 AND BIM ACCELERATORS AS PART OF RADIOGRAPHIC COMPLEX AT RFNC-VNIITF

A. Akhmetov, S. Khrenkov, P. Kolesnikov, E. Kovalev, O. Nikitin, D. Smirnov, Russian Federal Nuclear Center — Zababakhin All-Russian Scientific Research Institute of Technical Physics (RFNC-VNIITF), Snezhinsk, Russian Federation

Abstract

The paper describes installations included in the radiographic complex at RFNC-VNIITF, their purpose, composition, and principle of operation. The paper presents the synchronizing system for the betatron complex based on BIM pulse air-cored betatrons and LIA-2 linear induction accelerator, as well as the synchronizing circuit and functioning algorithm in the mode of BIM and LIA-2 combined operation. This combined mode of operation was tested and results of this testing are also provided.

COMPOSITION OF THE RADIOGRAPHIC COMPLEX

The radiographic complex includes the betatron complex consisting of two pulse air-cored betatrons BIM (further – betatron complex) and linear induction accelerator LIA-2 (further – LIA-2). The betatron complex ensures two-direction recording of dynamic objects at 90° between directions. Each betatron in the betatron complex can generate from one to three radiation pulses in one gas-dynamic experiment. LIA-2 is placed between betatrons and can generate up to two radiation pulses.

The betatron complex and LIA-2 are independent units.

The betatron complex is intended study high-speed processes in gas-dynamic experiments using the pulse shadow X-ray diffraction technique. Main technical characteristics of the betatron complex are given in table 1 [1].

Table 1: Main technical characteristics of the betatron complex

Parameter (Units)	Value
Boundary energy of bremsstrahlung spectrum (MeV)	65
Penetrability in Pb (mm)	165
Radiation source size (mm)	2.5x6
Duration of γ -radiation pulse in the mode of one radiation peak generation (ns)	100
Max. number of successive pulses	3
Time interval between γ -radiation pulses in the mode of three radiation peaks generation (μ s)	0.5-5

Penetrability of the betatron complex was estimated based on a X-ray diffraction image of a lead test object "wedge" [2] positioned at the 4-m distance from a target. Maximum thickness of the test object was 100 mm with

the 10-mm step. Two more lead blocks with the total thickness of 100 mm were placed in front of the test object. The recording unit was immediately adjacent to the "wedge". The maximum penetrability of the betatron complex was 180 mm. The X-ray diffraction image of the "wedge" is given in Fig. 1.

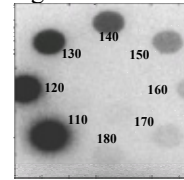


Figure 1: X-ray diffraction image of test object "wedge".

The radiation source size was estimated based on the X-ray diffraction image given by the pinhole camera positioned at the distance of 1 m from the target. The recording unit was positioned at the 3-m distance. The radiation source size was measured at 0.5 blackening density minus background. Blackening density distribution after X-raying of the pinhole camera is given in Fig. 2.

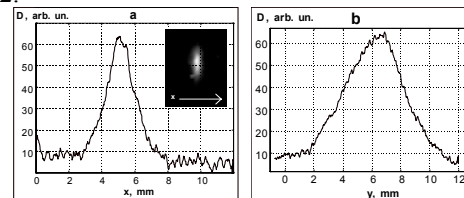


Figure 2: Blackening density distribution after X-raying of the pinhole camera.

Electrons are deflected onto the target either in one pulse or in portions with the formation of up to three X-ray pulses with a certain intensity relation between them depending on a particular task. For this purpose, installation is equipped with generators that deflect the electron beam onto the target. Usually, total energy is distributed as follows: 1-st pulse takes 10-15%, 2-nd pulse – 30%-40%, and 3-d pulse – 50%-60%.

LIA-2 is a high-quality injector of a large-scale linear induction accelerator LIA-20 intended for small-direction X-ray tomography complex. Thanks to high-quality of the formed electron beam, LIA-2 is used as an independent X-ray installation. Main technical characteristics LIA-2 are given in table 2 [3].

Table 2: Main technical characteristics of LIA-2

Parameter (Units)	Value
Max. beam energy (MeV)	2.0
Max. beam current (kA)	2.0

MAIN PARAMETERS AND OPERATIONAL EXPERIENCE WITH NEW GENERATION OF ELECTRON ACCELERATORS FOR RADIOGRAPHY AND CARGO INSPECTION

A.N. Ermakov^{a,b,#}, A.S. Alimov^{a,b}, B.S. Ishkhanov^{a,c}, I.A. Frejdovich^d, A.N. Kamanin^{a,b}, V.V. Klementiev^b, V.V. Khankin^{a,b}, S.V. Lamonov^d, L.Yu. Ovchinnikova^{b,c}, N.I. Pakhomov^{a,b}, Yu.N. Pavshenko^{b,d}, A.S. Simonov^{b,d}, I.V. Shvedunov^b, N.V. Shvedunov^{a,b}, V.I. Shvedunov^{a,b}, I.Yu. Vladimirov^{b,c}, D.S. Yurov^{a,b}

^{a)}Skobeltsyn Institute of Nuclear Physics, Lomonosov Moscow State University

^{b)}Laboratory of Electron Accelerators MSU, Ltd.

^{c)}Physics Department, Lomonosov Moscow State University
Leninskie Gory, 119992 Moscow, Russia

^{d)}"Research and Production Enterprise "Toriy", Obrucheva 52, 117393 Moscow, Russia

Abstract

We describe main parameters and operational experience with new generation of electron accelerators for radiography and cargo inspection developed with participation of scientists, engineers and technologists from Lomonosov Moscow State University and "Research and Production Enterprise "Toriy". Two accelerators are described: accelerator for radiography UELR-8-2D with beam energy regulated in the range 3-8 MeV and dose rate from 0.5 to 15 Gy/min and accelerator for cargo inspection UELR-6-1-D-4-01 with pulse to pulse energy switching between 3.5 and 6 MeV, with repetition rate 400 Hz and dose rate 4 Gy/min. Both accelerators use klystron as an RF source, which is fed by a solid state modulator.

INTRODUCTION

Main directions for perfection of electron accelerators for radiography are connected with the possibility of regulating the accelerated beam energy and dose rate of bremsstrahlung in a wide range to achieve optimum conditions for defects visualization for different thicknesses of material; with minimization of the electron beam spot size at bremsstrahlung target in order to improve spatial resolution; with extended life of the bremsstrahlung target; reduction in weight and size characteristics of the accelerator; increasing its resource; simplifying the operator work and servicing; in reducing parasitic radiation.

Electron accelerator for modern cargo inspection complex capable to recognize the effective atomic number of the contents of the container [1] in addition to the features listed above must be able to switch the energy of the accelerated beam from pulse to pulse between two or more values; must ensure high stability of the beam energy and dose rate; must have a short transient time after switching on X-rays; must be able to generate packages of closely spaced pulses of different energy [2], following with a high repetition rate.

The above requirements are the basis for the design of accelerators described in this report.

a_ermak1978@mail.ru

COMMON FEATURES

Developed accelerators for radiography and cargo inspection have several common features. In particular, the change of the energy of the accelerated beam in both cases is done by changing the level of the accelerating field. To ensure the high quality of the beam at more than twice change of the energy the standing wave on-axis coupled accelerating structure was optimized in order to produce the transverse and longitudinal beam focusing with capture efficiency more than 60% in the whole range of the accelerating field variation. The sealed-off design of the accelerating system, consisting of an accelerating structure with RF antenna, electron gun, vacuum RF window, ion and getter pumps and intensively cooled bremsstrahlung target, is used. The electron gun is attached to the accelerating structure using Conflat joint that facilitates the repair in the case of cathode filament failure. Exterior view of the accelerating system is shown in Fig. 1.



Figure 1: Accelerating system.

Accelerating structure is fed by the pulse multi-beam klystron KIU-168 [3] operating under reduced high voltage. To power klystron and electron gun solid state modulator [4] is used. The parameters of the modulator

DEDICATED DC-110 HEAVY ION CYCLOTRON FOR INDUSTRIAL PRODUCTION OF TRACK MEMBRANES

B.N.Gikal, S.N.Dmitriev, G.G.Gulbekian, P.Yu.Apel, S.L.Bogomolov, O.N.Borisov, V.A.Buzmakov, A.A.Efremov, I.A.Ivanenko, N.Yu.Kazarinov, V.I.Kazacha, I.V. Kalagin, V.N.Melnikov, V.I.Mironov, S.V.Pashchenko, O.V.Semchenkova, V.A.Sokolov, N.F.Osipov, A.V.Tikhomirov, A.A.Fateev, M.V.Khabarov, FLNR JINR, Dubna, Russia

Abstract

In the Laboratory of nuclear reactions JINR dedicated accelerator complex on the basis of the heavy ion cyclotron DC-110 for the industrial track membrane production has been developed and created. The isochronous cyclotron DC-110 accelerates the ions Ar, Kr and Xe with a fixed energy of 2.5 MeV/nucleon and intensity of 10-15 μA . The cyclotron is equipped with ECR ion source - DECRIS-5 (18 GHz) and axial injection system. The pole diameter of the magnet is 2m. Isochronous magnetic field formed by shimming sectors on the level of 1.67 T. Accelerated ions $^{40}\text{Ar}^{6+}$, $^{86}\text{Kr}^{13+}$, $^{132}\text{Xe}^{20+}$ have close mass-to-charge ratio, which allows changing particles without changing the operation mode of the cyclotron. Accelerator complex DC-110 is capable of producing up to 2 million square meters of track membranes per the year.

INTRODUCTION

A series of heavy-ion accelerators for applied purposes have been developed and created at the Laboratory of Nuclear Reactions of the Joint Institute for Nuclear Research. The IC-100 cyclotron was put into operation in 1985 and upgraded in 200-2002 [1,2]. In 2004-2006 the DC-60 cyclotron was created for the Interdisciplinary Research Center of the Gumilev Eurasian National University (Astana, Kazakhstan) [3,4]. The accelerator beams are successfully used for solid state physics research, and track membrane production. Based on the technological solutions and experience of operating the IC-100 and DC-60 accelerators there has been developed the project of the DC-110 cyclotron [5,6]. The accelerator complex produces intense Ar, Kr, and Xe ion beams with a fixed 2.5 MeV/nucleon energy, which allows the production of track membranes on the basis of up to 30 μm thick polymer films.

The accelerator complex includes:

- the DC-110 cyclotron,
- ECR ion source and axial beam injection system,
- accelerated beam transport channel equipped with technological equipment for irradiating the polymer film,
- vacuum system,
- electrical supply and control system,
- cooling system.

The accelerator is furnished with one polymer film irradiation channel. The possibility of installing a switching magnet and assembly of a second channel is provided for increasing the productivity of the equipment

by simultaneous irradiation of film on one channel and preparing for installation on the other.

The cyclotron magnet has a 2m pole diameter. The ions being accelerated are $^{40}\text{Ar}^{6+}$, $^{86}\text{Kr}^{13+}$ и $^{132}\text{Xe}^{20+}$ with close mass-to-charge ratios of 6.667, 6.615, and 6.600, which allows realizing an acceleration regime practically at a fixed frequency of the accelerating system and fixed magnetic field.

The DC-110 accelerator does not provide for ion energy variation and changes in the mass-to-charge ratio of accelerated particles. This concept is characterized by increased reliability and by simplicity of controlling the complex.

ION SOURCE

The 18 GHz DECRIS-5 ion source was developed on the basis of sources of the DECRIS-4 (14 GHz) series with copper windings created at LNR (JINR, Dubna) [7] by intensifying the magnetic structure and changing to a new type of microwave oscillator. The DECRIS-5 ion source created for industrial application is characterized by increased reliability.

To ensure the design parameters of the beams accelerated on the DC-110, the ion source should generate intensities of $^{40}\text{Ar}^{6+}$, $^{86}\text{Kr}^{13+}$ and $^{132}\text{Xe}^{20+}$ ion beams of not less than 85 μA , 150 μA and 150 μA , respectively. After assembling the ECR source and axial injection system, thorough adjustment of all systems of the source and axial injection channel was carried out. Beams of Ar, Kr, and Xe ions were produced from the source. The possibility of producing maximum Ar, Kr, and Xe ion beam intensity was investigated, the results are given in Table 1.

Table 1. Maximum ion beam intensities obtained from DECRIS-5 source in μA (Z - ion charge).

Z	8+	9+	11+	15+	18+	19+	20+
Ar	1200	750	300				
Kr				325	182	120	70
Xe							220

BEAM AXIAL INJECTION SYSTEM

For transporting the ion beam of the ECR source to the center of the cyclotron, beam axial injection system is used, which is composed of:

- 3 focusing elements, 2 correcting elements,
- analyzing magnet,
- diagnostic elements of the injected beam,

CC-189M CYCLOTRON SYSTEM

A.P. Strokach, O.L. Veresov, Yu.N. Gavrish, A.V. Galchuck, S.V. Grigorenko, V.I. Grigoriev, M.A. Emeljanov, M.L. Klopenkov, A.N. Kuzhlev, V.G. Mudroliubov, G.V. Muraviov, V.I. Nikishkin, V.I. Ponomarenko, Yu.I. Stogov, S.S. Tsygankov,
JSC “D.V. Efremov Institute of Electrophysical Apparatus”, St. Petersburg, Russia

Abstract

The CC-18/9M cyclotron system has been designed, manufactured and delivered to NIITFA, Moscow. The system consists of an updated CC-18/9M cyclotron and a targets system. The cyclotron is intended to produce accelerated proton and deuteron beams with an energy of 12-18/6-9 MeV and current up to 150/70 μ A, respectively. For this purpose, a shielding-type electromagnet and a resonance system have been afresh designed. The target system for the production of F-18 and C-11 radionuclides for PET has been designed in NIEFA for the first time.

The CC-18/9M cyclotron system was designed for the delivery to JSC «NIITFA», Moscow with a view to creating a pilot PET center. The cyclotron system consists of an updated CC-18/9M cyclotron and a target system. This cyclotron is a new version of three CC-18/9 machines manufactured previously and delivered to PET centers of the University in Turku, Finland, Russian Research Center for Radiology and Surgical Technologies, Pesochny, St. Petersburg and «VNIITF », Snezhinsk town, Chelyabinsk region, Russia. To widen the possibilities of application and increase the marketability of the CC-18/9M cyclotron, the energy of accelerated proton and deuteron beams is made variable in the range of 12-18 and 6–9 MeV, respectively. Simultaneously, the design current of protons and deuterons is increased by one and a half in comparison with the original model, i.e. up to 150 и 70 μ A, respectively.

The new version of the cyclotron keeps the continuity in the main engineering solutions proven in CC-18/9 and MCC-3015 machines [1, 2]:

- shielding-type electromagnet with a limited number of holes in the shielding,
- vertical median plane to give an easy access to in-chamber devices by moving apart the movable part of the magnet along the guides,
- the vacuum chamber of the cyclotron made as a part of the electromagnet,
- the resonance system located completely inside the vacuum chamber of the electromagnet [3],
- extraction of beams of accelerated protons and deuterons by stripping negative ions on carbon foils practically with no loss of intensity,
- an external injection system, which significantly reduces the working gas admittance from the source
- to the vacuum chamber, facilitates production of high vacuum and consequently reduces the losses of ions in the acceleration process by molecules of the residual gas [4],
- acceleration of negative ions of hydrogen and deuterium at one fixed frequency of the RF field (the 2nd and 4th harmonics, respectively),
- installation of movable shims in special recesses to correct the magnetic field topology and to ensure isochronous field when changing the type of ions to be accelerated,
- extraction of proton and deuteron beams through 3 windows made in the vacuum chamber. Two windows are intended for installation of targets directly onto the magnet (“near” targets) and the third window is used to transport the beam to remote targets,
- simultaneous extraction of beams with a max energy to one of remote and one of near targets,
- standard set of components of a beamline transporting the beam to remote targets: matching magnet, 2 correcting magnets, doublet of quadrupole lenses and switching magnet making possible the beam transport to 3 target devices,
- compete automatic control of the cyclotron system.

In the process of designing, the following principal modifications were made, which significantly improved the conditions of service and maintenance/repair compared to the original model:

- A new resonance accelerating system consisting of 2 mirror-symmetrical resonators has been designed. In CC-18/9 cyclotrons, one resonator was used, the central conductor of which consisted of two dees, two stems, which had a common part with a shorting flange. The new design allowed the loss power to be reduced from 18 to 13 kW. Due to the resonance system symmetry, was reduced the effect of thermal deformations, which in the original machine limited the beam current in the continuous mode. The operating frequency of the new resonance system of 40.68 MHz (38.2 MHz -in the original model) coincides with the operating frequency used in the MCC-3015 cyclotron., so in both models identical RF power supply systems can be used.
- The new cyclotron design allowed 2 cryogenic pumps to be installed on the vacuum chamber, which provided more uniform distribution of pressure and, as a consequence, lower losses of ions in the acceleration by molecules of the residual gas.

SEE TESTING FACILITIES AT FLNR ACCELERATORS COMPLEX: STATE OF THE ART AND FUTURE PLANS*

S. Mitrofanov, B. Gikal, G. Gulbekyan, I Kalagin, V. Skuratov, Y. Teterev, N. Osipov, S. Paschenko
JINR, Dubna, Moscow Region, Russia
V. Anashin, United Rocket and Space Corporation, Moscow, Russia

Abstract

The Russian Space Agency (Roscosmos) utilizes U400 and U400M cyclotrons at accelerator complex of the Flerov Laboratory of Nuclear Reactions (FLNR) of the Joint Institute for Nuclear Research (JINR) in Dubna for heavy ion SEE testing. The ions up to the Xe and Bi with the energy up to 40 AMeV are available for the users. The detailed overview of the facility and the features of diagnostic set-up used for ion beam parameters evaluation and control during SEE testing are discussed. The road map for the strategic development of this field in FLNR is presented.

INTRODUCTION

Since becoming discovery in 1975 [1], intensive investigations of single-event effects (SEE) in electronic devices have resulted test method and facility developments. As known, the ion energy for such experiments should be high enough as 3 MeV/nucleon. Therefore, heavy ion beams in this energy range are delivered from large accelerators. Usually they are located at basic physics research laboratories. Currently, there are several major heavy ion beam facilities in the U.S. and Europe that are available for SEE testing [2]. The Russian Space Agency (Roscosmos) utilizes U400 and U400M cyclotrons at accelerator complex of Flerov Laboratory of Nuclear Reactions (FLNR) of Joint Institute for Nuclear Research (JINR) in Dubna for heavy ion testing. U400 cyclotron has been in operation since 1978 and delivers ion beams of atomic masses $4 \div 209$ at energies of $3 \div 29$ MeV/nucleon [3]. U400M cyclotron has been in operation since 1991. This cyclotron was originally intended for acceleration of ion beams with $A/Z=3 \div 3.6$ (A - atomic weight of the accelerated ion; Z - ion charge when accelerated) at energies of 34-50 MeV/nucleon. The beam is extracted from cyclotron using stripping foil. In 2008 the U400M possibilities have been extended by addition of the ion beams with $A/Z=8 \div 10$ at energies of 4.5-9 MeV/nucleon to carry out the experiments on synthesis the new super heavy elements as well as applied researches [3]. Last few decades the SEE testing have been carried out using ion beam transport lines designed for nuclear physics experiments. However, specific requirements to ion beam parameters, like uniformity over large irradiating area, beam intensity variation from units to hundred thousands of particles per second and etc., could not be realized in full by these facilities.

To reproduce the effects of a heavy component of cosmic radiation for the SEE testing one should use the low-intensity ($10^3 - 10^6 \text{ cm}^{-2} \text{ s}^{-1}$) heavy ion beams with the LET range in silicon, typical for ion energies of 50-200 MeV/nucleon. But, keeping in mind to test the real DUT which are in metal and plastic housings, as well as ready-to-use electronic boards, the heavy ion beams with energies in the range 5 - 50 MeV/nucleon must be used in experiments.

The main purpose of this report is to describe heavy ion beam lines specialized for SEE testing at FLNR JINR accelerator complex. Originally these facilities were designed to meet demands of EIA/JESD57 and ESCC BS 25100. Since becoming operational in 2010, the low energy beam ($3 \div 6$ MeV/nucleon) facility has been available to users. The facility for the SEE testing at high energy ($20 \div 40$ MeV/nucleon) was successfully commissioned in January'14. The third line is based on U400 and after modernization of this cyclotron in 2015 there will be the possibility to make the SEE testing with the fluent energy variation for every ion [3].

ION BEAM LINE WITH ENERGIES OF 3-6 MEV PER NUCLEON AT U400M.

The ion beam line for SEE testing is a part of the U400M cyclotron. This beam line contains: ion beam transportation system, beam monitoring system, energy measurement system and user's vacuum test chamber with a mounting and positioning assembly to hold the sample in the irradiation field. The photograph of the experimental set up showing its components is given in Fig. 1. The beam leading line is separated from a bending magnet (1) by vacuum gate valve (2). The next transport element is two-coordinate beam-positioning magnet (3) guiding the beam through variable size diaphragm placed in entrance of the 50 Hz X-Y magnetic scanning system (4). Scanning system provides exposure over the target area 200×200 mm with inhomogeneity better 30% in the flux range of $1 \div 10^5$ particles/cm²s. To choose appropriate ion energy and the LET value we use a degrader with tantalum foils of 5, 9, 12.5, 14, 19, 22.5, 25 of 27 microns thickness. A driver of foils holder is designated as (5) in Fig. 1. Energy of particles passed through the foils as well as initial ion energy is measured by time-of-flight (TOF) method. Ions with $3 \div 9$ MeV/nucleon energy pass the distance between two pick up electrodes (8), 1.602 m, during 39-67 ns. These parameters were chosen to register the time of passage of one bunch according to the beam time structure at U-400M cyclotron - the duration

* This work was sponsored by the Russian Federal Space Agency by special agreement between Institute of Space Device Engineering and Joint Institute for Nuclear Research.

MODERNIZATION THE MODULATOR OF THE RF-GENERATOR ION LINEAR ACCELERATOR LU-20

A.V. Butenko, A.I. Govorov, D.E. Donets, V.V. Kobets,
V.A. Montchinsky, A.O. Sidorin, Dubna, Russia

Abstract

The report discusses the replacement of the lamp switch the modulator semiconductor. A schematic of the modulator and a semiconductor switch scheme protection against voltage surges in the generator lamp. Replacing the lamp switch it possible to increase the output power generator.

INTRODUCTION

Modulator frequency generator ion linac LU-20 was commissioned at the beginning of 70th years. Currently modulator lamps GMI-34B used in this modulator, taken out of production and the existing stock has long worn out and due to the increase of the internal resistance of these lamps, the anode voltage on the generator lamps significantly decreased and the generator does not produce RF-power required to normal operation of the accelerator. It was therefore decided to replace the modulator lamps solid state switch HTS 501-80-LC2 firm "BEHLKE" Germany. This decision was implemented.

THE MODULATOR

RF-generator supplying linear accelerator LU-20 was



Figure 1: Modulator of the RF-generator.

launched in 1970. It provides a nominal power level in the cavity of the accelerator. Eventually all aging occurred generator elements. In the 90 years has stopped the release of modulator tubes GMI-34B used as a key modulator of the generator. I had to work on finding a used lamps. To ensure the total anodic current generator tubes 220 A key is a four connected in parallel modulator tubes GMI-34B (Fig. 1). Since the lamp old internal resistance from them several times the rated and thereon a high voltage drop is applied to the anodes generator tubes. As a result, the output power of the generator is insufficient to provide desired accelerating voltage in the resonator of the accelerator.

It was decided to replace the modulator tubes semiconductor switches. The switches were ordered us "BEHLKE" Germany. The first experience of replacement bulbs semiconductor switches proved unsuccessful. After working the switches was breakdown.

SIMULATION OF THE MODULATOR

After analyzing the causes of the breakdown of the switch modeling work was conducted modulator using Micro-cap 9. The modeling was made for the lamp and the semiconductor switch. Several schemes have been analyzed with a semiconductor switch. The modeling was assembled circuit protection semiconductor switch and then on the simulator breakdowns in generator lamps were tested semiconductor switch and perfected the technique of working as part of a key generator in normal mode and circuit protection from breakdowns in key generator lamps and from spontaneous elongation of the anode pulse. Fig.2 is a schematic diagram of the

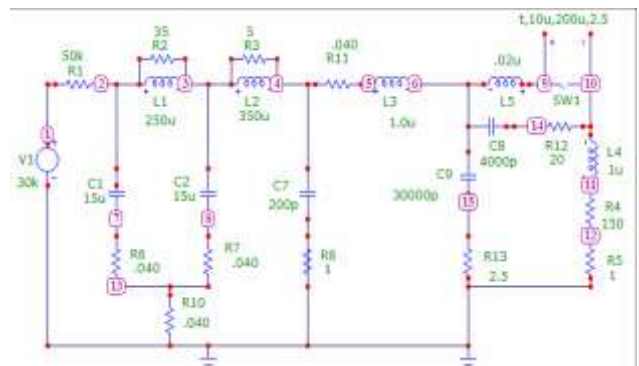


Figure 2: Scheme of the modulator.

modulator on which to carry out simulation of the modulator. Figure 3 shows the simulation results.

Copyright © 2014 CC-BY-3.0 and by the respective authors

MODERNIZATION THE MODULATORS KLYSTRONS ACCELERATING STAND OF THE ELECTRON LINEAR ACCELERATOR LINAK-800

V.V. Kobets, N.I. Balalykin, P.P. Zhuravlyv, A.G. Kobets, V.G. Shabratov, G.D. Shirkov, A.G. Sorokin, JINR, Dubna, Russia

Abstract

The report presents the work on the modernization of the modulator klystron second accelerating station of the acceleration stand on the basis of electron linear accelerator LINAC-800. The analysis of the modulator first accelerating station and made suggestions for improving the management system modulator. The functional circuit blocks control the modulator.

INTRODUCTION

Equipment for control of the modulator klystron 1-st accelerator accelerating station of the acceleration stand on the basis of a linear electron accelerator LINAC-800 was based on the so-called "hard" logic and provides a fixed control algorithm modulator.[1] Operational management of the klystron power level produced a local manual closing desired number of sections modulator (PFN modules). Also carried out manually switching frequency modulator battery life and modulator switching trigger from an external clock source. In the operation of the modulator identified the need provide both local manual control modulator and local indication of the state of the modulator, and the potential control modulator using computational tools and providing top-level to the top level of operational information section operation modulators.

To implement the requirements set forth above new algorithms have been developed management of the modulators klystrons of the accelerating stations the linear electron accelerator of the acceleration stand and new hardware requirements. They are as follows.

Instead, the pulse generator to the "hard" logic was applied management controller specifically designed for this task. Due to the need to develop specific requirements regarding management of the modulator, the implementation of the user interface and the input and output channels of information.

Instead, the control unit on the PFN "hard logic" used block-based 8-bit microcontroller.

To increase the reliability of electronic components and diminishing the amount of electronic components instead of discrete active components and chips low degree of integration applied chips with medium and high level of integration, applied to surface mounting technology instead of mounting holes. This reduced the size of the nodes, which reduced the level of interference from the pulse amplifier and improve noise immunity of the whole device.

To organize the cable connections between control units PFN and PFN modules was introduced patch panel,

allowing to increase the reliability of connections and reduce errors when connecting modules.

For communication with the top management level was selected RS-485 interface. Selection of the interface due to the fact that the requirements on the speed of information exchange with the upper level is initially low (not more than several packets per second) on the one hand and on the other - to the requirements of simplicity and reliability of the interface RS-485 fully satisfies.

FUNCTIONAL BLOCK DIAGRAM OF THE CONTROL MODULATOR

As a result, the control circuit is a modulator of a multiprocessor system with one master controller and several slave controllers (Fig. 1).

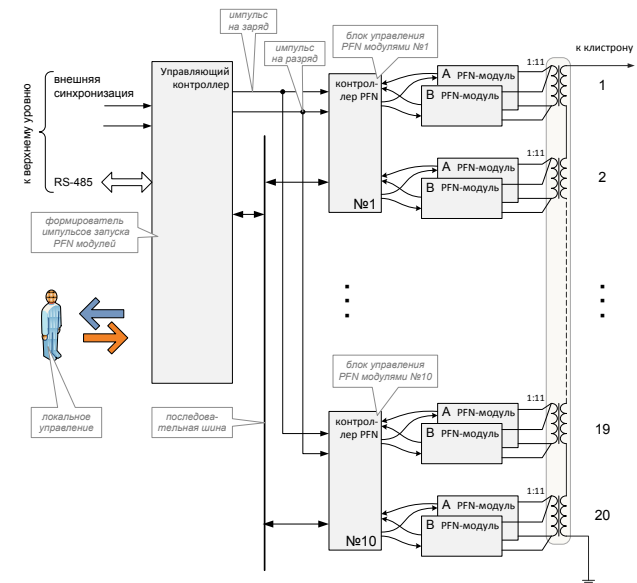


Figure 1: Functional diagram of the control unit modulator.

The control unit by a modulator consists of the control controller which generates pulses start modules PFN, and ten controllers PFN, which form the charge and discharge pulses modules PFN, PFN modules include team-master controller and the controller sends control information on the charging and discharging storage modules PFN. Operator on the master controller is set startup frequency modulator with local work or run mode from the external clock. Is defined as the number of units involved PFN to obtain the required RF power. Next, the master controller generates control pulses to the general charge and discharge of storage modules PFN and sends serial

SYSTEM POWER MICROWAVE IMPULSE COMPRESSION BASED ON DOUBLE FORMING LINE

G.O. Buyanov, A.P. Klachkov, A.A. Osipov, A.G. Ponomarenko, National Research Nuclear University «MEPhI», Moscow, 115409 Russia

Abstract

In this article presents the results of an electrodynamic modeling and optimization of the design of the compressor based on double forming line (DFL), proposed new structure to effectively accumulate and output energy from a multimode resonator with working mode H_{01}^{\square} .

THE PRINCIPLE OF OPERATION OF THE COMPRESSOR BASED ON DFL

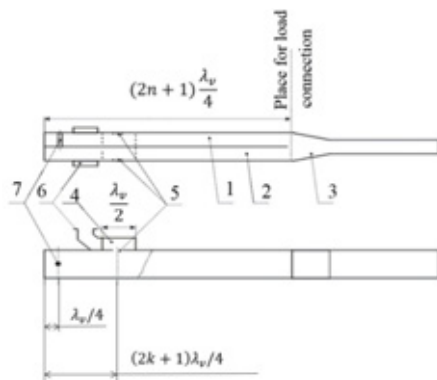


Figure 1: Compressor based on DFL.

In the compressor which bases of the double forming line (DFL) resonator-energy accumulator (see Fig. 1) consists of two waveguides 1, 2 long odd number of quarter-wave [1,2]. On the one hand, these waveguides are shorted, and with the opposite side waveguide 3 is connected to these waveguides, whose height in this location is twice the height of the waveguide drive. A standing wave is excited in the drive so that throughout the process of accumulation of the field in the two waveguides are strictly antiphase. Due to this fact and because of the special choice of the length of the waveguide cross-sectional load connection antinode of the electric field is realized. The waveguide load is excited at the same time load the fields of the two waveguides drive in opposite to the load and the energy does not go (see. Fig. 2 a).

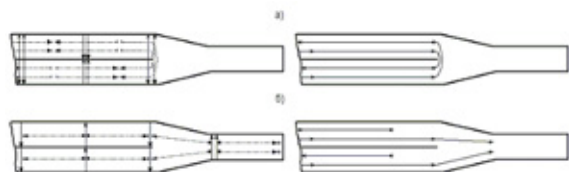


Figure 2: The field structure and scheme of wave propagation in a compressor with DFL. a-accumulation, b-output after $t=l/v_{gr}$.

Switchboard (position 7 in Fig. 1) is placed inside of any waveguides spaced at the distance $\lambda_g/4$ from the shorted end. Its inclusion leads to the fact that the phase of the wave reflected from the left end, changes to π . After a time, l/v_g (see Fig. 2, b), this wave reaches the section connecting the load, radically changes the conditions for the excitation of the waveguide 3, now the waveguide load is exciting in phase by two waves arriving here on the left, both of them rush to the load without reflection. So, the reflected waves in waveguides formed by the trailing edge of the drive, which section returns to the load after a time $2l/v_g$. At this moment all the electromagnetic energy originally stored in two sections of the resonator drive is transmitted to the load.

COMPRESSOR DFL BASED ON MULTIMODE WAVEGUIDES.

Previously worked on the design of single-mode waveguides [3,4,5,6]. The aim of this work is to study the compressor to work with oversized waveguides mode H_{01}^{\square} . Compressor design built on the single-mode waveguides have large losses, low dielectric strength, which significantly limits the maximum compression ratio and power of the compressed pulse. The performance parameters of the compressor can be improve by using multimode waveguides with a working mode H_{01n}^{\square} . For example, cross-section waveguides increases from $28,5 \times 12,6$ mm to 72×34 mm allows you to raise the compression ratio in 2.65 times and the maximum output power in 6.3 times.

The device power output (see Fig. 3) is H-tee matched two inductive pins.

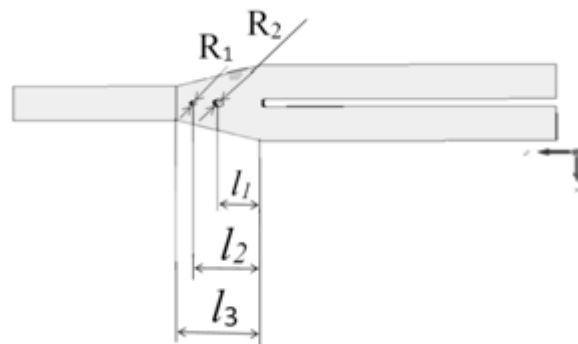


Figure 3: Sketch of the microwave - compressor $l_1=53.4$ mm; $l_2=42.5$ mm; $l_3=27$ mm; $R_1=2$ mm; $R_2=3.2$ mm

It is known that in the output device power have to use nonstandard waveguide section $72 \times 28,5$ mm at the

FIELD OPTIMIZATION TECHNIQUE OF THE MULTIGAP H-MODE RESONATORS

A.B. Buleyko, M.V. Lalayan, S.E. Toporkov, National Research Nuclear University MEPhI
(Moscow Engineering Physics Institute), Moscow, Russia

Abstract

High frequency optimization of multigap IH-/CH-resonators involves the number of problems to be solved. It is important to obtain high values of effective shunt impedance and uniform accelerating field distribution along the axis. To reach both of these goals design of H-mode resonators contains flat vanes (pylons). This article presents the results of electrodynamic modelling of CH- and IH-resonators in case of zero gap between end walls of the vanes and resonator sidewall [1]. The values of the optimized shunt impedances, Q-factor and field flatness for IH- and CH-designs are presented.

INTRODUCTION

Investigated IH- and CH- cavities were designed for the beam velocities $\beta = 0.1$. The operating frequency of the inter-digital structures is equal to 162MHz. Whereas, CH-resonators operate in 324 MHz band since they are excited at higher operating mode H_{210} . Each cavity type works on π -mode. Cavity design in either case features constant period D along axis and acceleration gap between drift tubes $t = D/2$. Whole structure consists of 9 RF gaps with beam aperture diameter $D_a = 15mm$.

To estimate the field flatness following factor was used:

$$K = \frac{E_{min}}{E_{max}} \cdot 100\%,$$

where E_{min} and E_{max} – on-axis minimal and maximal accelerating field strengths.

ELECTRODYNAMIC MODEL

CH-resonator

As it was mentioned the CH-cavity design includes flat vanes (see fig.1.). Each pylon has one rectangular hole cut out at the last drift tube end. The opposite pylon part is flat but its position is variable and defined by parameter L_{gap} .

First step of the field flatness optimization consists in selection of correct start length of holding rods l_{stem} and correct vane height h_{vane} . It should be mentioned that each l_{stem} value (e.g. $l_{stem} = 35, 40, 45, 50$ mm) could be associated with different pylon geometries defined by h_{vane} . Almost all of these combinations could be tuned to the operating frequency by appropriate geometry of the pylon hole choice. But during selection the necessary geometry from all possible designs the field flatness also needs to be considered: in our case initial K values should lie in the range from 85% to 95%. Dimensions of possible holes could be different: for long rods ($l_{stem} =$

45,50mm) the longitudinal length reaches 110mm (which is quite large regarding $D = 46.3$ mm), for short rod length ($l_{stem} = 35$ mm) they become compact (as it shown at fig.1.). Maximum value of shunt impedance among all l_{stem} values stays unchanged. Thus there was chosen the geometry with short holding rods $l_{stem} = 35mm$, large vane $h_{vane} \sim 100$ mm and compact holes in it.

At the fig.2 the dependence of the field flatness during parametric sweep of L_{gap} is presented. All another geometric dimensions stay fixed.

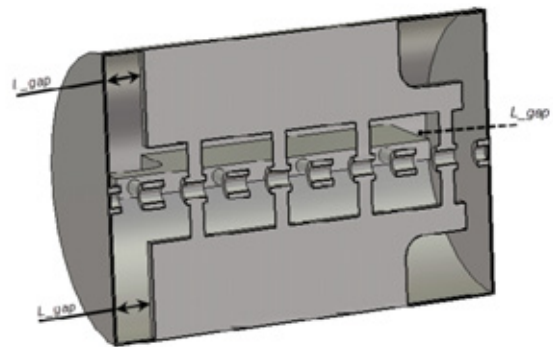


Figure 1: The designed layout. Each vane contains 1 rectangular hole and 1 movable sidewall (positioned by L_{gap}).

From the graph it could be found out that the best field flatness is observed in case of zero gap $L_{gap} = 0$ mm. According to the magnetic field distribution inside such geometry four separated magnetic fluxes around each vane combine in one common flux. Absolute value of magnetic field distribution is presented at fig. 3: the flux turns around the vane at point A, then goes through plane B to point C, makes another turn around vane and then continues the propagation to the point D in similar way.

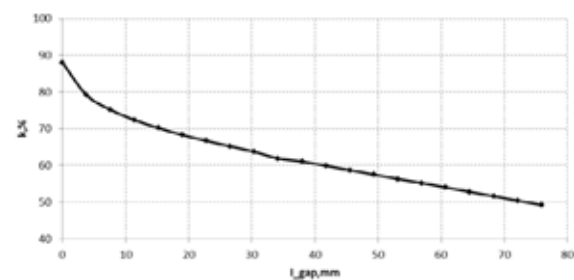


Figure 2: Dependence of the field flatness vs. distance L_{gap} .

Also it should be noted that during parametric sweep resonant frequency and shunt impedance had negligible changes: frequency was shifted from 324MHz

OPTIMIZATION OF ELECTRIC FIELD DISTRIBUTION INSIDE MULTI-GAP CH-RESONATOR

S.E. Toporkov, National Research Nuclear University MEPhI (Moscow Engineering Physics Institute), Moscow, Russia

Abstract

RF H-mode resonators are frequently used in the most modern proton accelerators. For instance crossbar H-mode (CH) [1] resonators could be mentioned. For this cavity type the task of accelerating field flatness tuning is quite important. This paper presents the results of the electric field adjustment on the beam axis for different CH-geometries.

INTRODUCTION

The main goal during investigation was to achieve the even accelerating field distribution for the different geometries of CH-resonator. Main variable parameters are presented at table 1.

Table 1: The designed parameters

Number of periods	7; 9; 11;
Aperture diameter, mm	15; 20; 30
Beam velocity $\beta=v/c$	0,07; 0,08; 0,09; 0,10

The layout of the 7 and 9-gap CH- cavities is presented in Fig. 1-2. All CH-cavity designs considered operate at 324MHz and have a constant period $D=\beta\lambda/2$. Acceleration gap between drift tubes $t=D/2$.

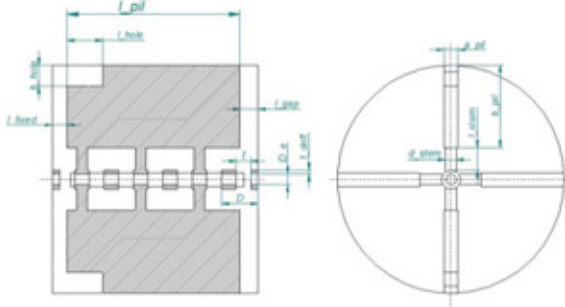


Figure 1: The designed layout.

To estimate the field flatness the uniformity factor was used:

$$k = \frac{E_{\min}}{E_{\max}} \cdot 100\%,$$

where E_{\min} - minimal accelerating field amplitude, E_{\max} - maximal accelerating field amplitude.

FIELD FLATNESS TUNING TECHNIQUE

To optimize both electric field distribution and effective shunt impedance geometry includes flat vanes (see Figs.1, 2.). Each vane (pylon) has one rectangular hole made on downstream pylon side. The opposite pylon part is flat but its position is variable and defined by parameter L_{gap} .

The tuning task consists of several steps. First the optimal start value of holding rod length l_{stem} and its optimal relation with the pylon height ($b_{\text{pil}} / l_{\text{stem}}$ see Fig.1.) should be chosen for specified beam velocity, aperture diameter and number of periods. It determines initial values of field flatness (it should be better than 15-20%) and optimal values of effective shunt impedance

Then the most significant improvement on the field distribution is introduced by the length L_{gap} (see Fig.2.) between end walls of the tank and the pylon. Dependence of the field uniformity vs. this length is presented in the Fig.3. It could be mentioned that the best field flatness was obtained in case of zero gap ($L_{\text{gap}}=0$ mm). For such cavity geometry magnetic field distribution differs from the classical CH – resonator, it transforms in one common magnetic flux like in split-coaxial cavities [2]. According to the magnetic field distribution inside such geometry four separated magnetic fluxes around each vane combine in one common flux.

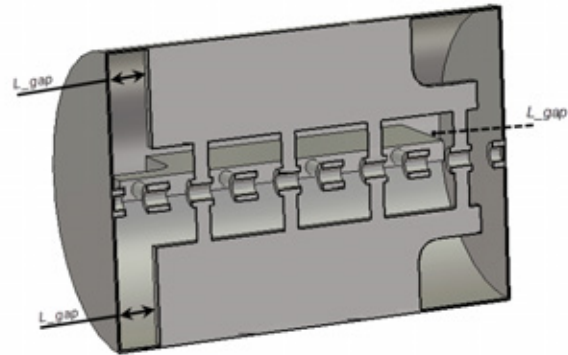


Figure 2: 3D-view of the CH-resonator. Each vane contains 1 rectangular hole and 1 movable sidewall (position defined with L_{gap} value).

It should be noted that resonant frequency and effective shunt impedance have some changes with L_{gap} variation: frequency shifts to 1-3% and effective shunt impedance changes to 5-15% depending on aperture diameter, number of periods etc.

THE OPTIMIZATION OF THE BUNCHER AT 145.2 MHZ TO REDUCE MULTIPACTOR EFFECT

M.A. Gusarova, I.I. Petrushina, S.M. Polozov, National Research Nuclear University «MEPhI»,
Moscow, Russia

A.S. Plastun, T.V. Kulevoy, FSBI «SSC RF ITEP», Moscow, Russia

Abstract

The results of the 145.2 MHz single gap buncher cavity in order to reduce multipacting discharge influence are presented in this paper. Resonant voltages, impact energies and corresponding particle trajectories are obtained. The ways of cavity design modifications to reduce multipacting discharge effects are considered.

INTRODUCTION

The proposed cavity is a single gap buncher of medium energy beam transport system (MEBT) for linear injector of Nuclotron-NICA project (JINR) [1-2]. The cavity shape is a modified E_{010} pillbox. The modifications are performed in order to decrease the cavity size and to place MEBT quadrupoles near the cavity, according to the general layout. 3D model of the buncher cavity before the optimization is presented in Figure 1.

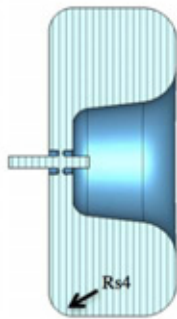


Figure 1: Side-view of the buncher cavity.

Computer simulations of the multipacting discharge were performed using MultP-M [3] and CST PS [4] software. The possibility of multipacting discharge was concluded from the percentage growth rate of secondary electrons number inside the cavity, the shapes of resonant electron trajectories and the energy of impact with the cavity surface. Secondary emission coefficients for copper surface that were used in simulation are taken from [5].

MULTIPACTING DISCHARGE SIMULATIONS OF THE NON- OPTIMIZED CAVITY

Electric field and voltage values presented in this paper are normalized to 1 J of energy stored in the cavity. Initial

computer simulation with MultP-M code was performed in order to identify the most dangerous levels of normalized voltage in the range $U_N = 0 - 5$, which can induce the progress of multipacting. The operating voltage of 150 kV corresponds to the normalized voltage of $U_N = 0.45$, and the operating voltage of 337 kV corresponds to $U_N = 1.0$. Figure 2 illustrates the number of particles percentage growth rate after 10 RF periods for U_N levels from 0 to 5.

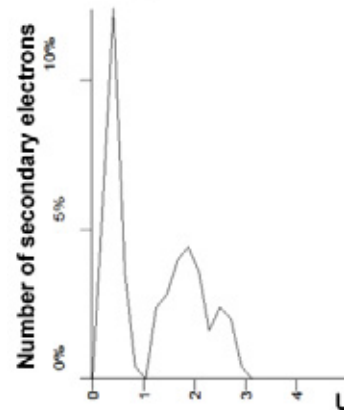


Figure 2: Number of particles percentage growth rate of after 10 RF periods for U_N levels from 0 to 5.

Figure 2 shows the possibility of multipacting at U_N voltage levels from 0 to 3 with two or three peaks, which correspond to several different multipacting spatial domains. The detailed analysis has detected these three spatial domains of multipacting discharge, which are presented in Figure 3 along with particle trajectories. In the range of $U_N = 0.001 - 0.018$ (Figure 3a), the number of particles growth rate peak is observed at $U_N = 0.015$. Multipacting discharge shifts outside from accelerating gap and totally attenuates after 40 RF periods.

The trajectories in the range of $U_N = 0.063 - 0.461$ is shown in Figure 3b. Secondary electrons return to the cavity surface every single RF period, so this discharge is of the 1st order. Simulation has shown stable electron trajectories in the whole range of $U_N = 0.063 - 0.461$ during 50 - 200 RF periods. The number of particles growth rate peak is observed at $U_N = 0.417$, which is close to the operating value. In this case, the discharge remains stable for more than 200 RF periods. The impact energy is 800 eV at $U_N = 0.14$, while at $U_N = 0.424$ it is 1400 eV. Analysis of secondary emission coefficient variation has shown that the surface quality and polishing are very important for discharge attenuation.

MULTP-M CODE GEOMETRY IMPORT MODULE PERFORMANCE OPTIMISATION

S.A. Khudyakov, M.A. Gusarova, M.V.Lalayan, National research nuclear university MEPhI, Moscow, Russia

Abstract

Introduces the new features of the module import geometry for three-dimensional modeling program multipactor MultP-M. On an example, consider an increase in the speed and accuracy of the calculation using a new algorithm for calculating the use of loading geometry format STL.

INTRODUCTION

Earlier [1] new module of geometry import for multipactor discharge simulation code MultP-M implementation and testing results were presented. This upgrade allows device under investigation geometry to be directly imported as STL file. Previously device under simulation shape was described using Boolean operations on basic geometry primitives like brick, torus, sphere etc. Results obtained using this code were compared and found coincident with known numeric, analytical and experimental data. Figure 1 shows geometry import module interface developed.

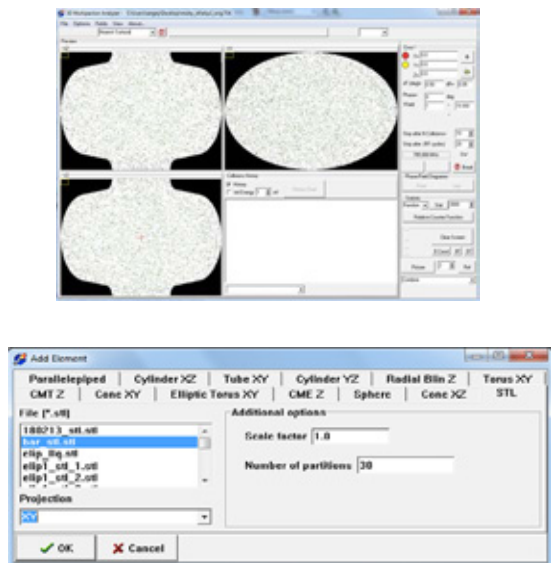


Figure 1: STL import module interface.

Tests showed [1] that new module operates correctly and could be used instead of preceding one with practically the same accuracy as it is illustrated in Figure 2. However despite of pretty effective algorithms and numeric models implementation it was found that computation time significantly grows for fine mesh models. This paper reports the simulation algorithm

optimization solutions developed for MultP-M code that allow it to operate faster without detriment to accuracy.

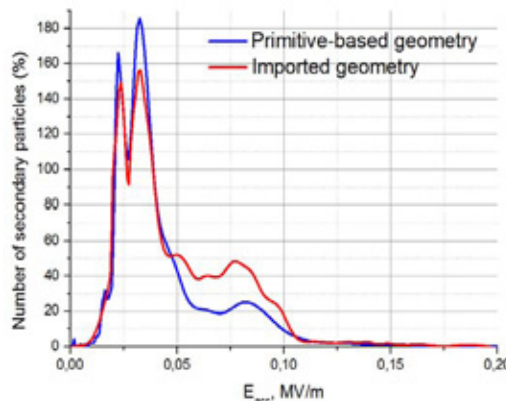


Figure 2: Simulation accuracy test.

MULTP-M AND STL FILE

While MultP-M multipactor discharge simulation code runs the main task to be solved is to determine each electron location with respect to model confines, i.e. to decide whether particle is inside the model boundaries or not. In case of boundaries defined as set of geometric primitives this task could easily solved using simple math. STL file describes 3D objects by their facets thus making this math much more complicated.

Geometry import module developed incorporates ray tracing algorithm [2] in order to get point position with coordinates (x, y, z) relative to facets specified 3D body.

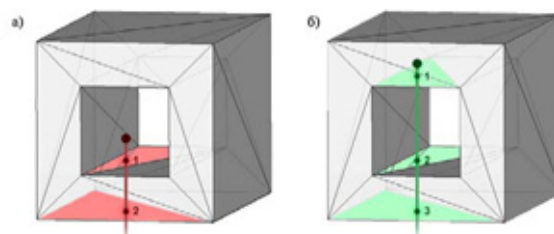


Figure 3: Different point and body collocation: a – point is outside body, ray has even number of boundary crosses; b – point is inside body, odd crosses number.

This algorithm demands 3D body under consideration to be closed. STL standard also sets the same requirement to all objects described.

So one has to develop algorithm that calculates number of ray and boundary crossings. This algorithm is

ISBN 978-3-95450-170-0

COMPARISON OF HIGHER ORDER MODES DAMPING TECHNIQUES FOR AN ARRAY OF SINGLE CELL CAVITIES

Ya.V. Shashkov, N.P. Sobenin, National Research Nuclear University MEPhI (Moscow Engineering Physics Institute), Moscow, Russia
M.M. Zobov, LNF-INFN, Frascati (Rome), Italy

Abstract

The LHC High Luminosity upgrade program considers an option of using additional cavities, operating at multiples of the main RF system frequency of 400 MHz. Such harmonic cavities should provide a possibility to vary the length of colliding bunches. In order to supply the required harmonic voltage several single cell superconducting cavities are to be used. It is desirable to house more cavities in a single cryostat to reduce the number of transitions between "warm" and "cold" parts of the cryogenic system. In this paper we study electromagnetic characteristics of a chain of the single cell superconducting cavities coupled by drift tubes. In order to reduce the influence of Higher order modes (HOM) excited in the structure on the beam stability and to minimize eventual power losses we analyze the HOM parameters and calculate the wake potential decay rates due to application of different HOM damping devices. In particular, the methods of HOM damping with rectangular waveguides connected to the drift tubes, the loads placed in the fluted and ridged drift tubes, as well as combinations of these methods are compared.

INTRODUCTION

In the frameworks of High Luminosity LHC upgrade [1] an application of additional second harmonic cavities with the operating frequency of 800 MHz is currently under discussion. It is desired to combine more such cavities in a single cryostat in order to avoid multiple transitions between cryogenic and warm areas. However, connecting several cavities in a chain can create parasitic higher order modes (HOM) that may affect the stability of circulating beams and lead to excessive power loss. In order to reduce the influence of HOM excited in the structure by passing beams their electromagnetic characteristics were calculated and the decay rates of the induced wake potential in the chain of cavities with different HOM damping devices were analyzed. In particular, the methods of HOM damping with rectangular and ridged waveguides attached to the beam pipes, usage of fluted and ridged beam pipes, as well as combinations of these methods were considered and compared.

ARRAY OF TWO CELLS

HOM extraction from superconducting cavities could be realised in different ways. The most common HOM

damping technique is the HOM extraction with couplers. These devices are effective but they also have some disadvantages. They break the cylindrical symmetry of operating mode leading to appearance of the transverse potential (kick-factor); they are subjects to all kinds of pollutions and multipactor discharge [2]. Another method implies HOM extraction to the load placed outside of a cryogenic system. The load can be made of ferrites or in a form of resistive material on an inner surface of the drift tube. In this case, it is necessary to have frequencies of these HOM higher than cut-off frequencies of drift tube in order to provide conditions for HOM propagation toward the load.

In [3, 4] HOM damping technique for the structure with fluted beam pipe was considered. Such beam pipe provides conditions for HOM propagation toward the load. In this structure a high speed of wake field decay was observed that is why it was decided to consider the option of a chain of two such resonators (Fig 1a).

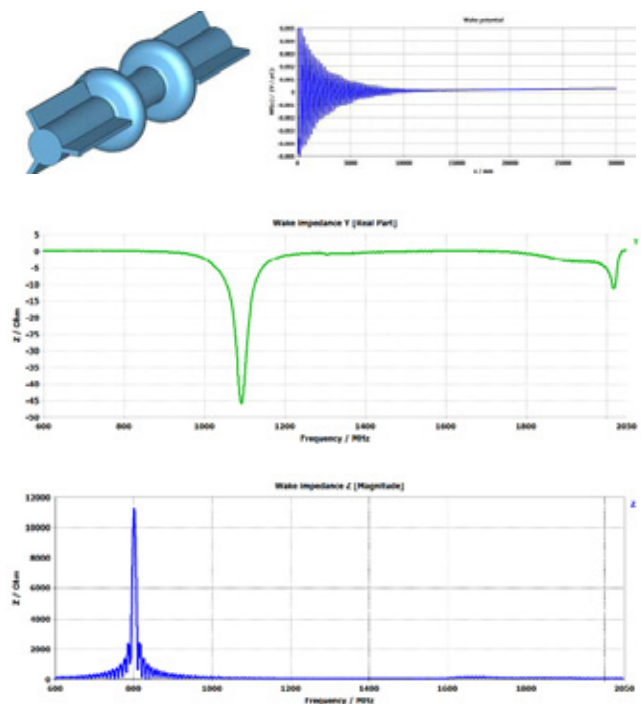


Figure 1: a). Array of 2 cells with fluted beam pipe; b). Dipole wakefield; c). Transverse impedance; d). Longitudinal impedance.

Fig 1b shows that the wake potential falls almost to zero at a distance comparable to the bunch separation in LHC. The high decay rate could be achieved due to the

*Work supported by RFBR grant 13-02-00562/14 and by the EU FP7 HiLumi LHC - Grant Agreement 284404

TEST RESULTS OF 433 MHZ DEUTRON LINAC (RFQ)

O.L. Veresov, S.V. Grigorenko, Yu.V. Zuev, A.N. Kuzhlev, A.K. Liverovskij,
I.I. Mezhov, A.A. Ryaskov, Yu.A. Svistunov, A.P. Strokach, V.F. Tsvetkov,
JSC "NIEFA", 196641 Saint-Petersburg, Russia

Abstract

The results of bench tests of an RF-frequency deuteron accelerator (RFQ) with an output energy of 1 MeV and operating frequency of 433 MHz are presented. The paper describes specific features of the RFQ construction and assembly, RF power supply system and test procedures. Parameters of the facility when operating with a beam energy analyzer and Be target are given.

INTRODUCTION

Starting from 2005, JSC "NIEFA" carried out R&D works on the creation of compact accelerating structures with RFQ and APF. These structures can be used in contraband detection systems, ADS, medical facilities for BNCT, or carbon therapy [1]-[3]. In the paper we consider an RFQ structure designed for use as a part of a small-scale facility for neutron production. The main design parameters of the structure are shown in Table 1. Specificity of operation at a frequency of 433 MHz and problems in the manufacturing of an RFQ with a precise channel for the beam acceleration are discussed in [4].

FEATURES OF DESIGN AND ASSEMBLY

Four massive parts with space-modulated vanes made of oxygen-free copper serve as a base of the RFQ construction, Fig.1. When assembling, the components are joined together in pairs like a sandwich, and adjusting copper spacers are set between the parts. The rigidity of the construction is provided by bolting the parts with numerous connecting rods placed along the vanes from the outer side. Bolting power is used for additional tuning of operating frequency. The longitudinal alignment of modulated vanes consists in a small shifting of supporting parts and control of their mutual position. In case of the vane-tip damage, a 10-20 μ m layer can be removed from the tip surface with a corresponding decrease in spacers height to remain unchanged the operating frequency.

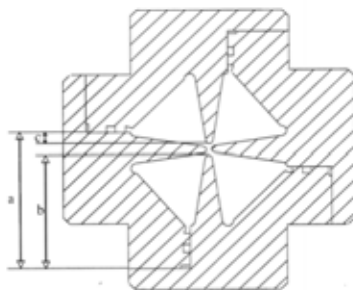


Figure 1: Structure cross-section.

Table 1: RFQ Design Parameters

Parameter	Value
Type of resonator	4-vane
Accelerated particles	D [±]
Operating frequency, MHz	433
Beam injection energy, keV	25
Beam output energy, MeV	1
Current pulse length, μ s	100
Pulse repetition rate, Hz	10
Intervane voltage, kV	50
Average channel radius, mm	1.8
Minimal channel radius, mm	1.18
Peak surface electric field, Kilpatrick	≤ 2
Input beam synchronous phase, degrees	-90
Output beam synchronous phase, degrees	-23
RFQ acceptance (norm.), π -mm · mrad	0.89
Vane length, mm	1090
RFQ resonator length, mm	1300

The modulation of each vane was checked in twenty points with a precision calibrated ruler of black granite and a linear encoder for sub-micron measurements. The results have shown that deviations in the modulation amplitude were not more than 8 μ m. A difference in the distance between neighboring vanes, which disturbs the channel quadrupole symmetry, was not more than 10 μ m. High quality of the RFQ manufacturing and assembly made unnecessary special tuners reserved for the equalization of the RF field along the resonator length.

ELECTRODYNAMIC CHARACTERISTICS OF RFQ RESONATOR

The measured Q-factor of the resonator was 6800. The results of measuring the magnetic field distribution along the resonator are shown in Fig.2. Fig.3 demonstrates the intervane voltage as a function of measured RF power. The RFQ intervane voltage corresponding to different levels of RF power was determined from the endpoint of the bremsstrahlung spectrum [5]. To make the spectral analysis, a measuring system [6] with a scintillation detector was used. The results of the detector calibration by reference to Am-241 are shown in Fig.4. The FWHM-to-maximum position ratio is 21keV/59.5keV, consequently, the detector energy resolution is 0.35.

CASCADE INTERFERENCE SWITCHES IN ACTIVE MICROWAVE COMPRESSORS*

S.Gorev, S.Artemenko, V.Avgustinovich, V.Igumnov, V.Kaminsky, S.Novikov, Yu.Yushkov[#],
Tomsk Polytechnic University, Tomsk, 634050, Russia

Abstract

The switching element is usually located in the area of maximum electric field strength and the desire to put it in the area of lower field strength, but keeping the same efficiency and steadiness, of operation is quite understood. Presumably a cascade switch might provide the required way of operation. Two designs of cascade switches were examined. The first one was formed by waveguide tees connected in a way when a direct input arm of a next tee is connected to a side arm of a preceding tee. The second was a set of tees connected in series through their direct arms. It was shown that the considerable decrease of the switched power value and the increase of the output power and stability of the output pulse parameters can be provided.

INTRODUCTION

Requirements applicable to high power microwave sources are diverse. The sources in particle accelerator technique should have high efficiency, beside high pulse power values, steady phase and oscillation frequency and also rectangular envelope of output pulses. The possibility of meeting most of requirements in resonant microwave compressors [1] is strongly influenced by operating quality of the switch controlling the coupling between a cavity and a load and being, factually, a device of energy extraction. Precisely this device determines the output power level, repetition rate and steadiness of output pulse parameters. Taking strict requirements for switch operation into account it is one of the most troubled elements of a compressor. The trigatron type of a gas-filled microwave switch is usually used as the energy extraction device. Its electric strength is normally lower than one of the cavity volume as it is located in an area of high electric field strength. Therefore the electric strength of the switch determines the compressor limiting output power and steadiness of output pulse power.

The way of a power increase and output pulse steadiness improvement when the energy is extracted through the H-tee waveguide interference switch is considered in the report. The main idea of the element operation is that the switched power is distributed between several switches connected by a certain manner [2,3]. The cascade of tees connected as "side arm – direct arm" and series connection "direct arm – direct arm" may serve as main designs. Conditions enabling the considerable electric field strength decrease in arms of the

switching tees along keeping field strength in the volume of the storage cavity are considered as well.

CASCADE OF TEES IN SIDE ARM

In the cascade of tees in the side arm of the switch a direct arm at each sequential tee is connected with a side arm of the proceeding one. Other direct arms of tees are short circuited. The switching arm is the side short circuited arm of the last tee. In this arm the microwave switching gap is located at quarter of the waveguide wavelength from the short circuiting end plate. Input direct arms of the tees have lengths equal to half wavelength in a waveguide and output short circuited ones – quarter of the wavelength. This configuration of tees provides mode "closed" to the switch. The tees are opened in sequence starting with the last tee. Once the microwave switch gap for the last tee is closed this tee is getting opened and the half wavelength of its input arm changes into the quarter wavelength of the total section of input direct arms. This results in sequential opening of all tees.

The power decrease is obtained due to matching each tee from the side arm. It is well known the power in the side arm in tees of this type is half as much as the power fed by the direct arm [4]. This means the switched power is decreased by the factor of 2^3 , which is equal to eight times, when three tees are used in the circuit design.

The main switch characteristic – the transition attenuation in storage and extraction modes of operation and the wave amplitude amplification in the cavity volume and the side tee arm of the storage mode – can be easily obtained by using of scattering matrix method. The results of calculation are presented as plots on Fig.1.

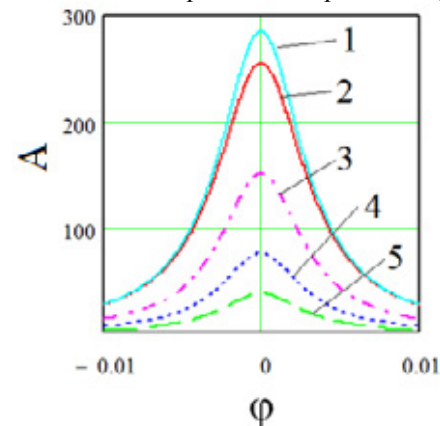


Figure 1: wave amplitude amplification A in the cavity volume and side arms of tees against the phase shift at discharge gap operation.

* The work was supported by The Ministry of Education and Science of Russian Federation within the program "Nauka", project N 1814.
#yuyu@tpu.ru

OVERSIZED INTERFERENCE SWITCHES IN MICROWAVE PULSE COMPRESSORS*

S.Artemenko, V.Avgustinovich, S.Gorev, V.Igumnov, V.Kaminsky, S.Novikov, Yu.Yushkov[#]
Tomsk Polytechnic University, Tomsk, 634050, Russia

Abstract

Oversized interference switches in resonant microwave compressors have high electrical strength. The switches of two types with a gaseous discharge gap were studied experimentally. The first type was developed on basis of the oversized rectangular waveguide H-tee with the H_{01} operation mode. The output pulse power of 2.8MW and pulse width of 3.5ns were obtained. The second type was a compact packet of common single mode switches incorporating the five identical waveguide tees. Synchronous operation of the switches was provided by the gas discharge plasma formed in the mutual side arm of the packet.

INTRODUCTION

Microwave resonant compressors (MRC) produce pulses by accumulating energy in a resonant cavity during a relatively long time and subsequent rapid extraction of the energy into a load. The ultimate output power of a MRC is equal to a power of the travelling wave component in a resonant volume. The coupling between a cavity and a load is controlled by the phase shift between the waves radiating from the cavity and from the side arm of the tee. The phase is inverted by the gaseous microwave switch having the trigatron type triggering. The limited cross section of a single waveguide limits the electrical strength of the elements and the output power value. An increase of gas pressure leads to big energy losses in the discharge plasma and a decrease of efficiency. For example the output pulse power for switches located in S-band waveguides of the cross section $72 \times 34 \text{ mm}^2$ does not usually exceed 200 MW [1] and the efficiency is within the range of 0.2-0.3 at the losses value in the switch of 2-3dB. The switching in oversized cavities involving mode transformation increases the limiting output power [2,3]. This report presents the study of switch designs based on oversized waveguides but intended for fast energy extraction and keeping high values of amplification.

OVERSIZED INTERFERENCE SWITCH

It was assumed the strong coupling between the output line and the switching resonator and the necessary frequency change are enough for developing an effective interference switch no matter what operational wave mode is used.

Switching resonators made of single mode waveguides

were connected to storage volumes by T-junctions or bridge junctions and demonstrated high switching efficiency. Although the cross section limited by the cut-off frequency value limits the electric strength and the output power.

One possible solution of increasing a waveguide cross section is the use of rectangular waveguides with H_{01} operational wave mode [4]. Corresponding elements in a tee or bridge manner keep the switching parameters of single mode analogs, does not require the special mode transformation into the primary mode of an output waveguide and make the maximum output peak power greater by several-fold. These oversized switches, besides usual requirements to the level of multimode transformation, raise some specific conditions to be provided for effective operation of the switch and the compressor. In order to provide switching over to extraction the phase of wave reflected from the tee should be changed by about 180° along with the change of the frequency beyond the resonance curve by value of $\delta f \approx nf / Q_a$, where $n \geq 3$ and Q_a - quality factor of the tee arm. Although it was found the dimensions of switching arm should be less some value determined by the ratio of the volume parameter transient time to the time of two ways wave travelling along the storage cavity.

The expression for the limit of the oversized waveguide wall size at the given arm length of $L_{arm} \approx \lambda_w / 2$ was derived:

$$b_{max} < \frac{z_0 Q_{arm} l^3}{90naL_{arm} \lg\left(\frac{2l}{r}\right)} = \frac{z_0 Q_{arm} (0.2Lv_{pl}/v_g)^3}{90naL_{arm} \lg\left(\frac{0.4Lv_{pl}/v_g}{r}\right)} \quad (1)$$

where v_g – wave group velocity, v_{pl} – plasma propagation velocity, $L_{arm} \approx Tv_g / 2$, l – length of the plasma spark channel, r – cross section radius of the plasma channel. As is clear from (1) the size is proportional to $f^{1.5}$. This means the switches are more efficient for higher frequencies of the microwave band when the relative increase of the wall size is higher at given T .

Experimental study was made in X-band and the tee waveguides had the cross section of $58 \times 25 \text{ mm}^2$. External view of the tee is shown in Fig.1. The longitudinal section of the tee is identical to the single mode one. So when dimensions are precise and operational mode H_{01} is not converted the switch of this type operates similarly to the common switch as there are no physical causes impeding that. It was proved by measuring the transition attenuation in the switch close state. The attenuation was $41 \pm 2 \text{ dB}$ in

*The work was partially supported by the state order "Nauka" of RF Education and Science Ministry, project 1814.
[#] uyuy@tpu.ru

THE UTILIZATION OF STANDARD DC ACCELERATOR ELV FOR THE TOMOGRAPHY

N.K. Kuksanov, R.A. Salimov, P.I. Nemytov, S.N. Fadeev, E.V. Domarov, K.A. Bryazgin, D.A. Kogut, Budker INP, Novosibirsk, Russia

Abstract

ELV accelerators have been developed at the Institute of Nuclear Physics, Siberian Branch of the Russian Academy of Sciences and occupy a special place in the spectrum of the equipment produced by the Institute. These machines are widely used for radiation modification of polymers and worked well in a variety of processes in many countries of the Eurasian continent. Using serial ELV accelerators for industrial tomography opens up new possibilities for industrial technologies. This increases the requirements on the stability parameters of the injected electron beam.

The article formulates the requirements for electron accelerator ELV for tomographic studies, pulsation energy and beam current. Described Schottky effect affects to the shape and size of the ripple current, and the method for increasing the stability of the beam parameters. These machines are unified with conventional accelerators ELV and expand the scope of their utilization.

INTRODUCTION

Budker Institute of Nuclear Physics of the Siberian Branch of Russian Academy of Sciences is one of the world leaders in the development, design, production and delivery to the industry of electron accelerators based on high-voltage rectifier, covering the energy range from 0.3 to 2.5 MeV, maximum beam power for separate machines from 20 to 100 kW and maximum beam current up to 100 mA. These properties, as well as compact dimensions and high operational qualities have allowed BINP take a leading position in the market of industrial accelerators, both in Russia and abroad. But if the application of ELV accelerators for radiation modification of materials is related with ensuring the required level of uniformity of the radiation dose [1], the use of ELV accelerators for the tasks of industrial tomography is associated with the need to fulfill the following requirements on the parameters of the injected beam:

- energy pulsing at the level $E = 1,0 \text{ MeV} \leq \pm 5\%$;
- current ripple at the level $I_{\text{beam}} = 100 \text{ mA} \leq \pm 2\%$.

These conditions were formulated as a result of a number of experiments on the industrial 100-kW accelerator of the ELV type, whose special features are the high electron energy (1.4 MeV) and the possibility of extracting the focused electron beam directly into atmosphere.

The Design of the Accelerator

To conform to these requirements and to take to account specific requirements of design, ELV4-based accelerator has been developed (Figure 1).

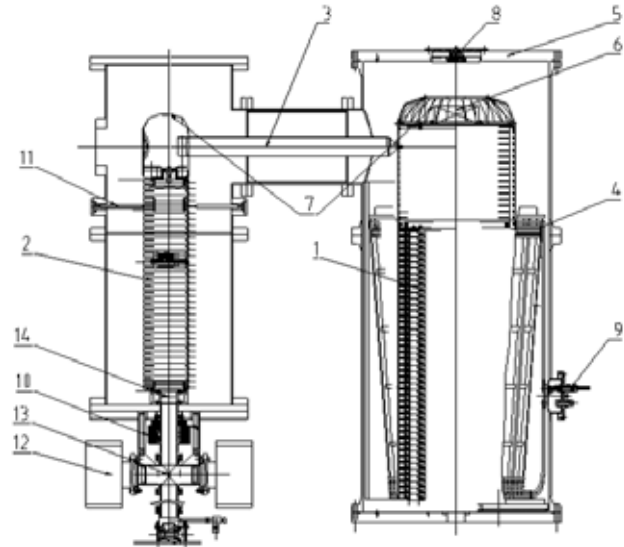


Figure 1: Common design of accelerator: Common design of accelerator: 1 - column rectifying sections; 2 - accelerating tube; 3 - gas feeder; 4 - the primary winding; 5 - the case of the pressure vessel; 6 - block injector control; 7, high voltage electrodes; 8 - the optical elements of the beam current control system; 9 entries of the primary winding; 10 - lens; 11 - supports to support tube; 12 - ion pump vacuum system; 13 - docking port of the vacuum system; 14 - bellows for fixing the accelerating tube.

Energy Pulsing

To reduce the energy pulsing, the series of experiments was carried out on a standard accelerator ELV-4. Energy was measured by the sensor circuit shown on Figure 2.

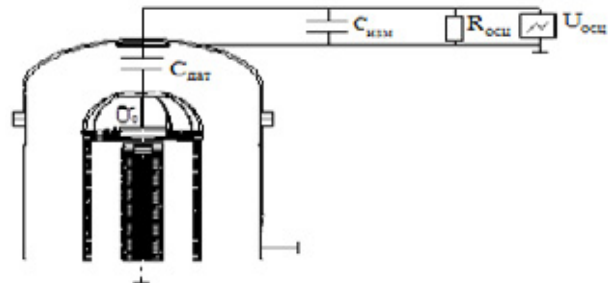


Figure 2: Sensor circuit for measuring pulsation energy.

The pulsing of energy measured by this sensor and the spectral decomposition of the signal is shown in Figure 3.

It shows three distinct peaks:

STUDYING OF THE ACCOMPANYING CHARGED PARTICLES IN THE TANDEM ACCELERATOR WITH VACUUM INSULATION*

D. Kasatov, A. Makarov[#], I. Shchudlo, S. Taskaev,
Budker Institute of Nuclear Physics, Novosibirsk, Russia

Abstract

On the tandem accelerator with vacuum insulation in a steady long mode it was obtained 1.6 mA current of protons with 2 MeV energy. It was studied the one of the possible reasons of current limitation – the appearance of accompanying charged particles during acceleration of the ion beam.

The paper presents and discusses the results of the accompanying beam measurement using a special detector. The detector registered an opposite positive current in the range of 80-170 μA , which is directly dependent on vacuum conditions in the accelerator. Also it was measured the dependence of the dose rate on the total current in the accelerating gap. These measurements confirmed that injected H^- beam ionizes residual and stripping gas mainly in the area before the first electrode and two proposals were made to minimize the accompanying current.

INTRODUCTION

Presently, Boron Neutron Capture Therapy (BNCT) is considered to be a promising method for the selective treatment of malignant tumours [1]. The results of clinical trials, which were carried out using nuclear reactors as neutron sources, showed the possibility of treating brain glioblastoma and metastasizing melanoma incurable by other methods. The broad implementation of the BNCT in clinics requires compact inexpensive sources of epithermal neutrons. At BINP the source of epithermal neutrons based on Vacuum Insulation Tandem Accelerator (VITA) and neutron generation through ${}^7\text{Li}(p,n){}^7\text{Be}$ reaction was proposed [2] and launched [3,4].

For providing BNCT it is required a high flux of epithermal neutrons which is dependent on proton current and energy. Now on VITA it is obtained 1.6 mA current of protons with 2 MeV energy in a steady long mode [5]. These parameters are sufficient for *in vitro* [6] and *in vivo* studies, but not enough for treating people. In this work it was investigated the one of the possible reasons of current limitation – the appearance of accompanying charged particles in the accelerating channel. There were proposed several origins of these spurious particles: ionization of the residual gas, ionization of the stripping gas in the accelerating channel and positive argon ions coming out of the charge-exchange target.

* Work is financially supported by the Russia through the Ministry of Education and Science of Russia (project RFMEF160414X0066)
A.N.Makarov@inp.nsk.su

EXPERIMENTAL SETUP

In order to register and measure the accompanying current the special detector was constructed and installed in the input flange of the accelerator tank. It is mounted in such a way that H^- particles can not reach it, and only positive particles that are going from the opposite direction to H^- beam can hit the detector (Fig. 1).

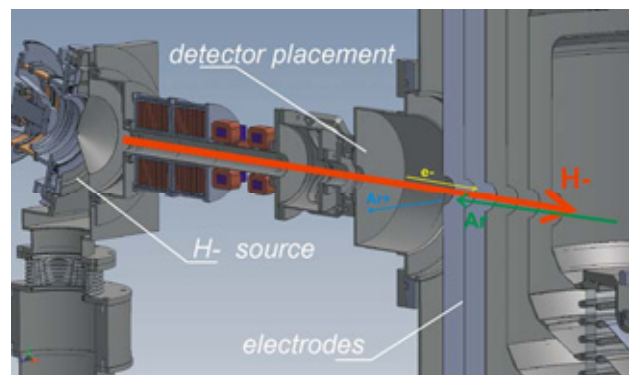


Figure 1: Placement of the argon detector.

The choice of this location for the detector is made due to previously registered modification of the surface of rotating diaphragm, which was mounted in the input flange of the accelerator tank. During the planned disassembly of the accelerator it was found the distinct imprint on the diaphragm presumably left by outgoing positive beam. Surface modification of the imprint was confirmed by scanning electron microscope Jeol JCM-5700 and energy dispersive X-ray analyzer of elemental composition IncaEnergy.

The detector consists of two insulated rings (with diameters 52 – 90 mm and 92 – 138 mm) surrounding the beam transporting channel and covered with suppressing grid under -40 V potential (Fig. 2). For convenience the square of the inner disk is twice as much as the aperture square; the square of the outer disk is twice as much as the inner disk square.

MEASUREMENTS

Fig. 3 shows that the positive current in the range of 80-170 μA measured by the detector is a direct function of the vacuum conditions in the accelerator. It can be seen that once the gate of the cryogenic pump was opened (1400 s) – the positive argon current has immediately decreased by 5 times and no breakdowns happened after that. In the same time the output proton current stayed almost unchanged. It can also be seen that argon current

DEVELOPMENT OF THE INJECTOR FOR VACUUM INSULATED TANDEM ACCELERATOR

A. Kuznetsov, A. Ivanov, A. Koshkarev, D. Kasatov, M. Tiunov, BINP SB RAS,
Novosibirsk, Russia

Abstract

The new beam injector of negative hydrogen ions was designed for modernization of the epithermal neutron source based on the tandem accelerator with vacuum insulation. The parameters of the ion source used in the injector construction allow one to increase the H^- current from 5 mA to 15 mA. Preliminary acceleration of the injecting beam can provide more reliable operation of the facility when changing the parameters of the injecting beam or the tandem accelerator voltage. Realization of this injector will make the next step towards the creation of a compact source of epithermal neutrons for boron neutron capture therapy of malignant tumors in clinics. The paper presents the injector design and computer simulations of the beam transportation.

INTRODUCTION

The tandem accelerator with vacuum insulation of electrodes (VITA) [1, 2] built at BINP is designed specifically for the development of the AB-BNCT concept [3]. The epithermal neutrons generation reaction is ${}^7\text{Li}(p,n){}^6\text{Be}$, and the estimated proton current for minimal therapeutic neutron flux should be higher than 3 mA @ 2.5 MeV energy [4] meanwhile about 10 mA required for comfortable BNCT treatment.

The VITA facility design is shown at Fig. 1. The particles acceleration takes place in two stages in a tandem accelerator. At the first stage the negative hydrogen ions are accelerated by the high voltage electrode potential to the half of required energy, and then the ions meet the gas stripping target to be converted into protons and accelerated again by the same potential to the full beam energy. Several innovative ideas were realized in the accelerator design to allow for stable acceleration of intense beam in a compact facility.

The initial ion beam is produced by the injector composed of the ion source, low energy beam line and magnetic elements providing focusing and correction of the beam. Series of investigations have revealed the limitations of injecting current. The main problems are the ions loss due to high residual gas concentration and the ability of the stripping gas to rich the injector and corrupt the stability of the ion source [4]. To provide a reliable H^- beam for clinical application of the facility the new injector is designed. The paper presents the design scheme of the injector and the results of calculations performed.

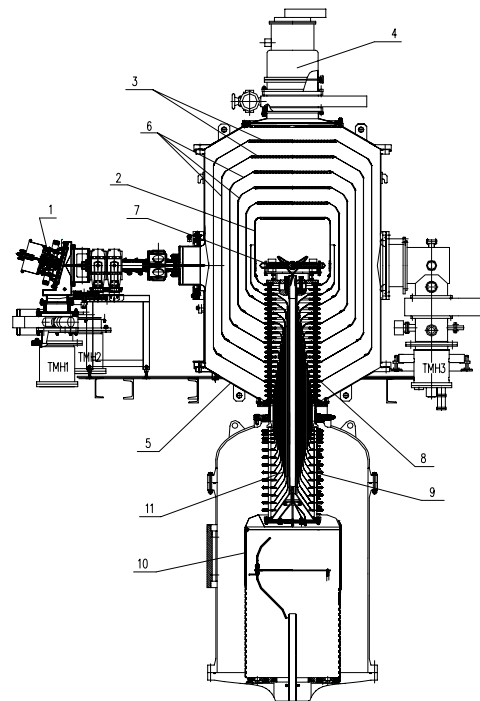


Figure 1: Scheme of the VITA facility. 1—ion source (H^-); 2 – high voltage electrode; 3 – electrode shutters; 4 – cryo pump; 5 – accelerator vacuum volume; 6 – intermediate electrodes; 7 – stripping target; 8 – feedthrough insulator (vacuum part); 9 – feedthrough insulator (gas part); 10 – high voltage source; 11 – coaxial feeding tubes.

EXISTING INJECTOR CONSTRUCTION

The scheme of the existing injector is shown at Fig. 2. The surface-plasma ion source with Penning discharge and with hollow cathode is used to generate the beam of negative hydrogen ions with the energy of 21 keV and the current up to 5 mA. The output aperture of the ion source has the diameter of 3 mm and the beam angular divergence is about ± 100 mrad. The magnet required for Penning discharge turns the beam to the angle of 15° , and the cone diaphragm passes the axial part of the beam into the transport channel through the aperture with 28 mm diameter. Then the beam is focused by two magnetic solenoids and directed to the accelerator through the beam diagnostics chamber. The beam transport channel is a long tube with 50 mm diameter that limits the pumping speed significantly and does not provide the appropriate vacuum level resulting in up to 50% of generated ions loss due to interaction with the residual gas.

MODIFICATION OF THE ARGON STRIPPING TARGET OF THE TANDEM ACCELERATOR

A. Makarov, S. Taskaev, P. Vobly, Budker Institute of Nuclear Physics, Novosibirsk, Russia
Yu. Ostreynov, Novosibirsk State Technical University, Russia

Abstract

Presented work is aimed on modernization of the gas stripping target that is used in the Vacuum Insulated Tandem Accelerator (VITA) to recharge negative hydrogen ions into protons. The target construction was modernized to get higher efficiency of the beam transportation, suppressing gas flow into the acceleration channel, and to raise the current of the accelerated proton beam. The design of the modernized stripping target, the calculated data on the magnetic fields and particle trajectories are presented.

INTRODUCTION

The Vacuum Insulated Tandem Accelerator (VITA) was developed in the Budker Institute of Nuclear Physics [1] to produce epithermal neutrons for boron neutron capture therapy in the ${}^7\text{Li}(p,n){}^7\text{Be}$ reaction. The parameters of the generated radiation allow us to carry out in vitro and in vivo investigations of BNCT. In present moment the modernization of the facility elements is carrying out to meet the parameters required for clinical usage.

The design of the VITA facility is shown at figure 1. The principle of the tandem accelerating scheme is accelerating of the negative hydrogen ions to the 1 MeV energy determined by the high voltage electrode potential, recharging the ions into protons in the gas stripping target and then accelerating to the 2 MeV energy by the same accelerating potential. Stripping target is made as a tube 16 mm in diameter and 400 mm long with the supply of the stripping gas (argon) in the middle (figure.2).

When studying the dependence of beam stripping on the argon pressure we have found an effect that can be explained by the appearance of the additional flow of positively charged ions of the stripping gas in accelerating channels. The interaction of the injected ion beam with the gas in the stripping target leads to ionization of the argon and to appearance of a low-ionized plasma with a positive potential. Under the influence of this potential part of positive argon ions comes out of the stripping target, enters into the acceleration channel where it is accelerated. This effect causes an additional load of power source, deterioration of the high-voltage strength in the vacuum gap and limiting of the proton beam current.

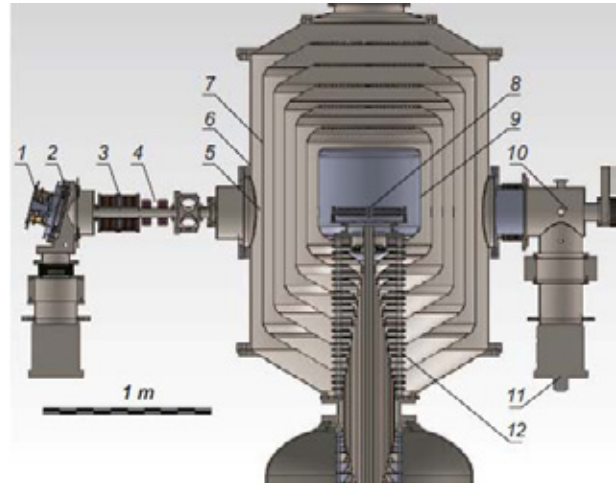


Figure 1: High-current vacuum insulated tandem accelerator. 1—H ion source, 2—diaphragm, 3—magnetic lenses, 4—corrector, 5—a temporary location of the beam detector, 6—accelerator, 7—electrodes, 8—stripper, 9—high voltage electrode, 10—high energy beam transport, 11—turbo molecular pumps, 12—insulator.

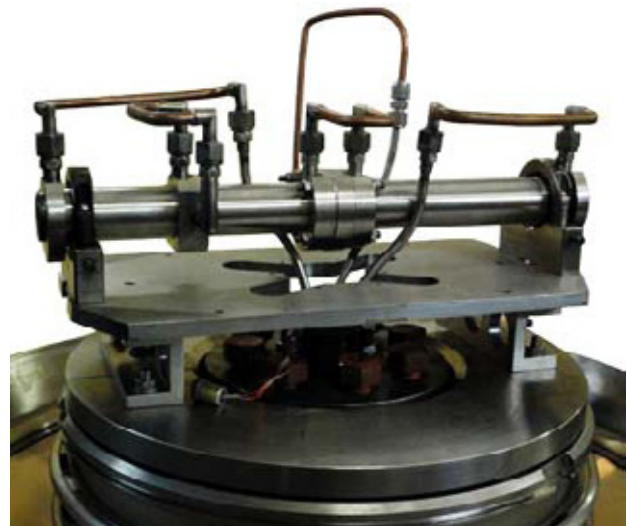


Figure 2: Ø16-mm stripping target placed on the feedthrough insulator.

FIRST RESULTS OF EXPERIMENTS WITH THE EXTRACTED CARBON BEAM AT THE U-70 ACCELERATOR

G. Britvich, S. Gorokhov, N. Ivanova, V. Kalinin, M. Kostin, A. Koshelev, A. Lukyantsev, S. Makonin, A. Matyushin, A. Maximov, V. Milyutkin, A. Ostankov, V. Pikalov, M. Polkovnikov, V. Seleznev, A. Sotnikov, IHEP, Moscow Region, Russia
E. Beketov, S. Koryakin, A. Lychagin, M. Troshina, S. Ulyanenko, MRRC, Obninsk, Russia

Abstract

The scheme of the C ions beam production with energy 455 MeV/nucleon from the U-70 accelerator was described briefly. The equipment facilities for the radiobiology experiments were shown. Experimental parameters of the carbon beam were described. The first experimental results were shown.

INTRODUCTION

Carbon beam program at IHEP has been started at 2001. The goal is to create an Ion beam therapy Center.

Project state. For today we have finished:

- Laser based carbon ions source;
- Acceleration of carbon ions in the I-100 linac;
- Transfer line between I-100 and U-1.5 booster;
- Modernization of U-1.5 and U-70 equipment;
- Stable acceleration of carbon ions in U-1.5 and U-70;
- Slow extraction of the carbon beam from U-70 with parameters appropriate for the medical practice;
- U-70 biological shielding was modified to build radiobiological extraction line (Channel #25) in the experimental hall;
- Magnetic elements for the head part of the Channel #25 mounting (four dipoles and four quadrupoles);
- Slow extraction of the carbon beam with 450 MeV/A energy into the temporary radiobiological setup (VRBS) at the Channel #25;
- Three runs of the VRBS with the carbon beam at 450 MeV/A.

Carbon ions are accelerated up to the 450 MeV/A in U-1.5 booster, and then are transferred into the U-70 synchrotron. Carbon beam is not accelerated in the U-70. Carbon ions are collected in the U-70 and then are transferred by means of slow extraction scheme into the VRBS region.

Parameters of the extracted carbon beam and background conditions were measured, and VRBS was qualified for the radiobiological studies.

EXPERIMENTS WITH EXTRACTED CARBON BEAM

Experimental studies with extracted carbon beam at VRBS were done during three last runs of U-70. Water phantom with 3D system of detector movement. This phantom is installed in the VRBS zone. It has 15 mm thick side walls and 30 mm front wall made from polycarbonate.

Bragg peak position was measured in this phantom by means of:

- Clinical dosimeter with natural diamond detector;
- Clinical dosimeter with TM-30013 ionization chamber with graphite walls;
- Radiochromic film Gafchromic EBT3.

Thin ionization chambers were used to measure intensity of the extracted carbon beam. These chambers were designed and produced at IHEP. Chamber with 200x200 mm² cross-section was used for general beam intensity measurements. To measure transversal distribution of the extracted beam density 2D multicellular chamber was used. One cell has 1x1 cm² size, number of cells is 64 (8x8) wall.

Ionization chambers were calibrated with activation detectors data. Pure carbon discs 40 mm in diameter and 5 mm thickness were used as activation detectors. Detectors were placed on the flange of OM-1 magnet in between OM-1 and OM2 magnets. Measurements data are shown in Table 1.

Table 1: Activation detectors calibration

Date	Particles	Cycling	Intensity by cycle
30.03.2014	Proton E=1,3 GeV	7	$1,9 \times 10^{10}$
04.04.2014	Proton E=1,3 GeV	7	$1,3 \times 10^{10}$
04.04.2014	Carbon E=455 MeV/nucleon	7	$4,5 \times 10^8$
21.04.2014	Carbon E=455 MeV/nucleon	7	$1,5 \times 10^9$

Extracted beam composition was studied. For this goal detecting setup was combined from three 1 mm thick and 1 cm² square scintillation detectors, dE/dx ion-implanted Si detector with 450 um thickness and 1 cm² square, and full absorption BGO detector. Time-of-flight, amplitude analysis and 2D amplitude analysis methods were used. As a result of measurements it was found that extracted carbon beam at VRBS has 11% of admixtures, which corresponds to the amount of matter crossed by beam upstream of the VRBS.

EXPERIMENTAL STUDY OF THE TIME DEPENDENCE OF THE ACTIVITY OF DELAYED NEUTRONS IN THE FISSION OF ^{235}U BY NEUTRONS FROM THE REACTION $^7\text{Li}(p, n)$ ON THE ELECTROSTATIC ACCELERATOR EG-1

K.V. Mitrofanov, V.M. Piksaikin, A.S. Egorov, V.F. Mitrofanov, D.E. Gremyachkin, B.F. Samylin,
State Scientific Center of Russian Federation Institute of Physics and Power Engineering,
Obninsk, Russia

Abstract

In the present work the installation created on the basis of the accelerator EG-1 (IPPE) for the experimental studies of the time dependence of delayed neutron activity from neutron induced fission of ^{235}U is described. Measurements were carried out with neutron beam generated with the help of the $^7\text{Li}(p,n)$ reaction. The lower limit of the investigated time range was governed by the proton beam switching system that was 20 ms. It was shown that the temporary characteristics of delayed neutrons from the fission of ^{235}U by epithermal neutrons is consistent with the time dependence which at present is recommended as a standard. In case of the fast neutron induced fission of ^{235}U the measured decay curve of delayed neutrons shows excess of counting rate in the time interval 0.01–0.2 s as compared with the decay curve corresponding to the recommended data.

Experiment was carried out at the accelerator IPPE EG-1. Block scheme of the experimental setup is shown in Figure 1.

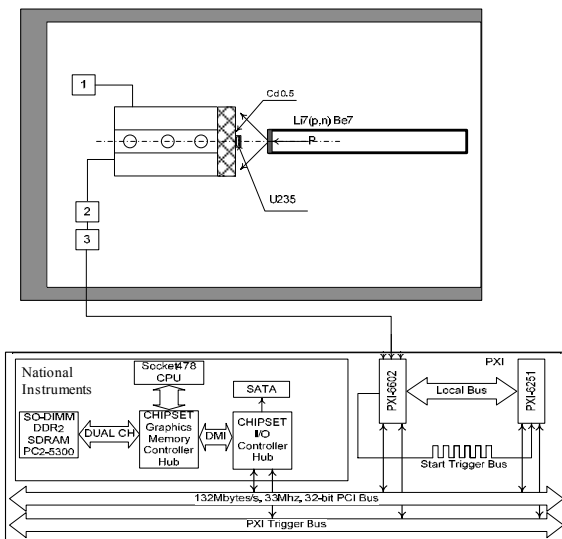


Figure 1: Block scheme of the experimental setup is performed on the basis of the system of accumulation of National Instruments. 1 – high voltage source; 2 – preamplifiers of signals from the counters SNM-18; 3 – summator of signals from the preamplifier of detector counters.

The neutron detector is an assembly of three counters SNM-18 (working gas: a mixture of 97% He-3 + 3% Ar. The pressure of 405 kPa) mounted in a polyethylene box. Signals from the counters SNM-18 received consistently to preamplifiers, amplifiers and conditioners. TTL signals received on the adder were formed at the output of the last, combined into a single digital stream of information transmitted by electronic analysis system and accumulation.

In this work, the neutron detector was set up, in which the effect of the distortion of the counting characteristics was absent at the initial time after irradiation session. In addition, the counting characteristics of the detector is not distorted even during irradiation intense beam of neutrons generated in the lithium target under the action of protons. The neutron source was a lithium target irradiated by a proton beam. The current in the experiment was 10 μA . The proton energy was 2.6 MeV.

There were two types of experiments. In the first experiment, the irradiated sample was placed on a side surface of a neutron detector. In a second experiment, a ^{235}U sample was placed in cadmium cover and a lead shield was placed between the detector and the sample. Obviously, in the first experiment, the neutron spectrum is significantly softer than the case of experiment №2, because the direct beam of the neutrons from the target is added the neutrons scattered by the material of the neutron detector. In the second experiment, a sample of ^{235}U is at a distance of 5 cm from the detector, and the scattered neutron at the detector are intensity absorbed by cadmium filter. Lead filter is designed to shield the detector from the possible detection of delayed gamma rays from the sample ^{235}U . A sample of ^{235}U is a metal disk of 3 mm thickness and 41 mm in diameter, located in a metal shell. Measurements in the experiments were carried out for two different irradiation times – 180 s and 15 s. The experimental method used in this experiment based on the cyclic irradiation of fissile samples in a neutron flux of Li(p,n) reaction and the measurement of the time dependence of the delayed neutron activity [2].

THE FIRST EXPERIMENT

To verify the correct operation of all the experimental equipment (neutron detector with a registration tract, the electronic data storage system) the obtained data were processed to evaluate the time parameters of the delayed neutron. The estimation of parameters of the delayed

REGISTRATION OF GAMMA RAYS FROM THE REACTION $^{16}\text{O}(\text{n,p})^{16}\text{N}$ ON THE DIRECT NEUTRON BEAM OF CASCADE GENERATOR KG-2.5

K.V. Mitrofanov, V.M. Piksaikin, A.S. Egorov, B.F. Samylin,
 State Scientific Center of Russian Federation Institute of Physics and Power Engineering,
 Obninsk, Russia

Abstract

In the present work the results of analysis of the oxygen content in the water with the help of gamma-rays registration from the reaction $^{16}\text{O}(\text{n,p})^{16}\text{N}$ is described. The samples were installed permanently on the direct beam of neutrons generated by the reaction $^7\text{Li}(\text{d,n})$ in the cascade generator KG-2.5 (IPPE). A comparison was carried out with experimental data obtained by the activation method in similar experimental conditions.

The method of determination of oxygen in the samples is based on the reaction $^{16}\text{O}(\text{n,p})^{16}\text{N}(\beta^-)$. A beam of neutrons generated in the reaction $^7\text{Li}(\text{d,n})$ on the cascade generator KG-2.5 was used for irradiation of the sample. The energy distribution of neutrons from the target in the case of deuterons with an energy of 0.7 MeV is shown in Figure 1. There is a homogeneous group of neutrons in the region of 14 MeV (the channel of reaction $^7\text{Li}(\text{d,n})^8\text{Be}$) and a continuous spectrum of neutrons with energies ranging from very small up to 14 MeV. The total neutron yield from this reaction for deuterons with an energy of 1 MeV and a thick target is about $3 \cdot 10^7$ neutrons/ $\mu\text{A}/\text{sr}$.

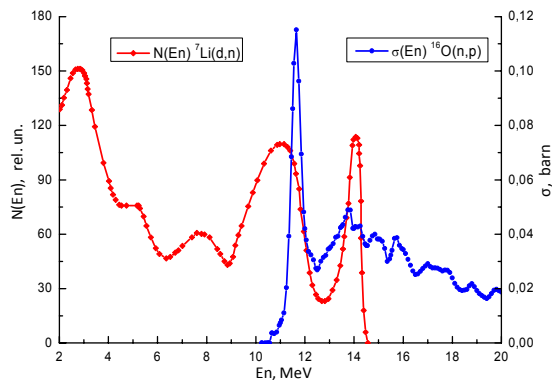


Figure 1: The energy spectrum of neutrons in the $^7\text{Li}(\text{d,n})$ at an angle $\theta=0^\circ$ at $E_d=0,7$ MeV and a cross section of reaction $^{16}\text{O}(\text{n,p})^{16}\text{N}$.

The same figure shows a cross section of the reaction $^{16}\text{O}(\text{n,p})^{16}\text{N}$. It is seen that only a small fraction of the total neutron spectrum is effective for generating reaction $^{16}\text{O}(\text{n,p})$ (~ 15%). The rest of the neutrons generates the background component of the resulting gamma-spectra, which is caused by the reactions (n,γ) , $(\text{n},2\text{n})$, (n,α) , (n,p)

of setup constructional materials (including detector materials), which generate a spectrum of gamma rays in the range of 0-3 MeV. There is an opportunity to distinctly register gamma rays with energies 7.12 and 6.13 MeV produced by beta decay of ^{16}N . [1]

Methodical difficulty of this experiment is the intensity of gamma background caused by the above reactions. These gamma rays produce a large load electronic path of the spectrometer. It leads to a distortion of the response function of the spectrometer and bandwidth of gamma spectroscopy system.

One of the consequences of high load detector is, for example, blocking the registration of high-energy gamma rays. The parameters of the electron spectrometric channel and of the detector shielding was optimized to solve this problem (choosing the correct amplifier and its mode of operation, the choice of parameters for the formation and registration of signals). There was also selected the optimum exposure time mode irradiation of samples and recording the spectra of gamma-ray induced activity.

The water was selected as a sample. The permanently installed water sample was irradiated for 10 s. Time of measurement of the induced activity was 100 s. The experimental scheme for the case of a stationary target is presented in Figure 2.

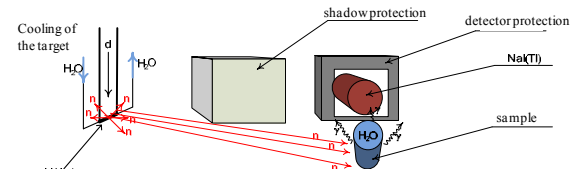


Figure 2: The experimental scheme for the identification of oxygen on the direct beam accelerator. NaI(Tl) - 100x100.

A similar experiment was carried out in the absence of the sample (background measurement). The results are shown in Figure 3.

CONDITIONING AND MONITORING OF CLEANNESS OF HIGH VOLTAGE SYSTEM WITH GASEOUS INSULATION

K.A. Rezvykh and V.A. Romanov, SSC RF – IPPE, Obninsk, Russia

Abstract

New effective technique of conditioning of gaseous insulation of electrostatic accelerator is described. To achieve stable breakdown voltage, accelerator conditioning procedure would take 7-8 hours (volume of pressure tank is 9 m^3). Three methods of monitoring cleanness of gaseous insulation are proposed.

HIGH UNSTABLE VOLTAGE

The paper is devoted to preliminary tests of accelerator without tubes. Cleanness of the system is usually achieved by step-like increasing of gas pressure (“from low to high pressure” method). Breakdowns are repeated until the breakdown voltage rise stops. The method is ineffective since it disregards the second source of instability of breakdown voltage, namely: presence of free solid particles in the vessel space.

Influence of particles was evidently found when testing the EG-2.5 and the EG-3 accelerators without tubes with positive voltage polarity. N_2/CO_2 gas mixture always contained 20% of CO_2 . Tests were carried out by step-like decreasing of gas pressure (“from high to low pressure” method). High unstable breakdown voltage first appeared under gas pressure of 1 MPa during fourth breakdown after the start of the experiment. Then the breakdown voltage gradually decreased down to about 0.8 of high unstable value and increased again up to 1.09 of this value in the thirteenth breakdown.

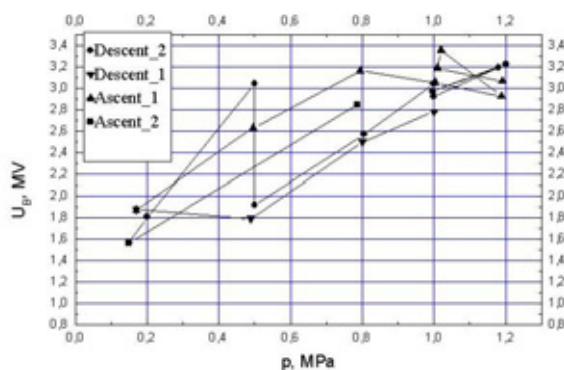


Figure 1: Breakdown voltage of the EG-2.5 accelerator before conditioning versus vessel pressure measured in descending and ascending series of tests. Descent_1 curve corresponds to “low unstable breakdown voltage” mode, Descent_2 curve corresponds to “stable” and “high unstable voltage” modes. Ascent_1 and Ascent_2 curves correspond to “high unstable breakdown voltage” modes.

After that we replaced the whole amount of insulation gas and obtained “four parallel lines” picture (Fig. 1), i.e. four voltage values corresponding to the same pressure. No special gas conditioning was conducted. The first descending series of tests started with 1 MPa pressure in “low unstable voltage” mode and it was converted into “high unstable voltage” mode upon pressure decrease down to 0.17 MPa. In the first ascending series of tests, “high unstable voltage” mode was stopped upon reaching 1.0 MPa pressure and it was converted into “the low unstable voltage” mode starting from 1.2 MPa pressure.

The abrupt change of the average stable breakdown voltage to high unstable value was observed in the second descending series of tests under 0.5 MPa pressure (after the fifth breakdown) with multiplicity of 1.9 relative to its value. It should be noted that high unstable breakdown voltage naturally arose under constant N_2/CO_2 gas pressure maintained within 0.1–1 MPa operating range and it was kept during the second ascending series of tests.

“High unstable voltage” mode is slightly mentioned in [2].

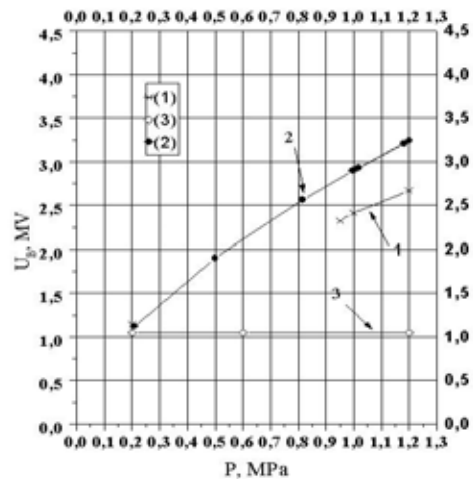


Figure 2: Breakdown voltage of the EG-2.5 accelerator versus vessel pressure before and after “from high to low pressure” conditioning. Curves 1 and 2 correspond to “low unstable” and “stable” modes, and curve 3 corresponds to “conditioning without breakdowns” technique (to remove light particles from the vessel).

NEW CONDITIONING TECHNIQUE

It is experimentally found that polished electrodes have the most relative increase of breakdown voltage, i.e. the highest conditioning effect [3]. Therefore one can consider free solid particles as the main cause of insulation deterioration. The particles arise and start

SET-UP FOR MEASUREMENTS OF DELAYED NEUTRON CHARACTERISTICS IN INTERACTION OF HEAVY NUCLEI WITH RELATIVISTIC PROTONS OF THE SYNCHROCYCLOTRON PINP GATCHINA

A.S. Egorov, V.M. Piksaikin, V.F. Mitrofanov, B.F. Samylin, State Scientific Center of Russian Federation Institute of Physics and Power Engineering, Obninsk, Russia

Abstracts

In present paper the method and set-up for measurements of delayed neutron characteristics in interaction of heavy nuclei with relativistic protons are described. On the basis of this method the time dependence of delayed neutron activity has been measured from interaction of ^{238}U sample with 1 GeV pulsed proton beam of the synchrocyclotron of the Petersburg Institute of Nuclear Physics, Gatchina. The measured data was analyzed in frame of 8-group precursor's model with a consistent set of half-lives. Obtained results on the fractional yields of delayed neutron precursors are compared with an appropriate data from the fast neutron induced fission of ^{238}U .

EXPERIMENTAL METHOD AND SET-UP

The measurements of delayed neutron decay from the fission of ^{238}U induced by relativistic protons were carried out on the set-up installed at the synchrocyclotron of the Petersburg Institute of Nuclear Physics, Gatchina. The synchrocyclotron is a pulsed accelerator with a 1 GeV proton beam intensity of about 10^{10} protons/cm²·s in the location of sample. The width of proton pulses in the ^{238}U experiment was 0.008 s with the repetition time of 0.02 s.

The experimental method employed in the measurements of delayed neutron decay curves is based on cyclic irradiations of the ^{238}U samples by protons followed by the registration of the time dependence of accumulated delayed neutron activity.[1]

Block diagram of the experimental setup is presented on figure 1.

The detector is shielded against the neutron background by borated polyethylene and cadmium sheets. The amplifier (A) and pulse discriminator (D) were used for two sets of counters – outer and inner as related to incident neutrons. The output signals from these electronic channels are fed to a mixing module (Σ) coupled with DAQ electronic system. The dead time of neutron detector is 2.3 ± 0.2 μs .

The pneumatic transfer system is capable to transport the sample for the time short enough to measure the delayed neutron yields with the shortest half-lives. Two electromagnetic valves are responsible for the sample transportation route. The stainless steel tube with inner diameter of 12 mm and wall thickness of 1 mm serves as a pneumatic flight guide (3). The positions of the sample in the neutron detector and irradiation location are fixed by the plugs with adjustable central hole which provides

the excessive pressure in front of the moving sample and smoothes the contact between the sample and the plug. The information on the sample location is obtained from sample position detector (6). Time of flight of the sample is about 150 ms.

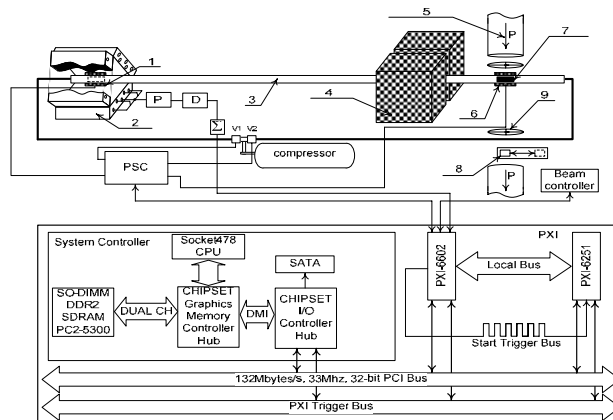


Figure 1: Block diagram of the experimental setup: 1,6-sample position detector; 2-neutron detector; 3-pneumatic transfer system; 4-neutron detector shield; 5-beam line; 7-sample of ^{238}U ; 8,9 Laser positioning device; (P) preamplifier, (D) pulse discriminator; (Σ) summator; (PSC) Pneumatic System Controller; In the bottom of the fig.1 is presented Data Acquisition system by National Instruments based on Labview.

RESULTS AND DISCUSSION

Composite decay curves which were measured in interaction of 1 GeV pulsed beam of protons with ^{238}U with irradiation times 15 and 180 s is presented on fig.2. The original scale of time analyzer (0.0001 s/channel) were transformed in scale of 0.1 s/channel. The obtained data were also corrected for the degradation effect of counting response of neutron detector placed in a high intensity fields of neutrons and gamma rays during irradiation time [2].

The accumulated decay curves were analyzed in the 8-group model approximation [3] with the help of the iterative least-squares method [4]. The relative abundances for ^{238}U were obtained on the basis of experimental data which were measured with different irradiation times. In the analysis of the delayed neutron time-dependence the data with irradiation time of 180 s were used to obtain the group constants for the first, second and third group of delayed neutrons. Group constants for the fourth to the eighth groups were

COMPARISON OF BIOLOGICAL IMPACT OF PROTON AND ION BEAMS IN RADIATION TREATMENT

Mark Kats, ITEP, 25, B.Cheremushkinskaya, Moscow, Russia

Abstract

The work contains the comparison of biological doses' distribution calculated for treatment of the same targets by proton and ion beams. Advantages of the ion beam are shown for targets with different sizes and with different depths.

We made an attempt to compare the distribution of the biological dose for treating same targets with proton and ion beams. The research [1] based on the calculations performed with TRIM program [2] contained the evaluation of the integral distribution of the physical dose D and biological dose $BD = D * RBE$ in water environment with a single-direction irradiation using the target scan with the thin beam for different target sizes (a cylinder with the diameter d and the size along the beam d) and with varying depth within the body L . The number of layers for the scanning was determined by the allowance for the consistency of irradiation ($\pm 5\%$). It was assumed for the calculation purposes that the beam has impulses' discrepancy of $dP/P = \pm 0.5\%$ (where P is the particle's impulse), the initial angle divergence (± 2 mrad), the lateral dimensions equal to the size of the target (in accordance with the target's scan) and that it is directed at a patient with such variable energy that Bragg's peak would be at a depth of the layer required for the irradiation. The calculations included the particles' diminution caused by the nuclear interaction, the impact of repeated Coulomb's dispersion, the statistical dispersal of range's size and the dependency of relative biological efficiency RBE of particles with the given energy at the current depth within the body.

This dependency is not known authentically. The amount of RBE strongly depends on dE/dx [KeV/mkm], from the type of cells, from the organ that is being irradiated, from the method of measurement and from the size of a single dose. The curve shown on Figure 1, taken from the source [3] and from Figures 1.2, 4.1, 4.2 and from source [4] was used to evaluate the amount of RBE, depending on dE/dx .

The calculations were made for the target sizes d from 1cm to 16cm with the depth of target's deposition from $L \geq 1$ cm to $(L+d)=30$ cm. The research [1] shows that the basic distribution of the integral BD in relation to depth can be approximately (with the accuracy of $\pm 10\%$) described as a constant in the target ($BD = 1.0$) and as a plateau until the target with $BD=K$, with the transitional zone of 3 cm (see table 1 and Fig. 2). Tailings in the zone's distribution, which appear during ions' fragmentation, were not accounted for.

Additionally, there are zones of irradiation on the side of the target, related to the secondary particles' dispersion in the body, and beyond the target, related to

particles' scattering within the beam with impulses dP/P and with the statistical dispersion of ranges. The sizes of these zones depend on the depth and can be estimated through the calculations utilizing the THRIM program.

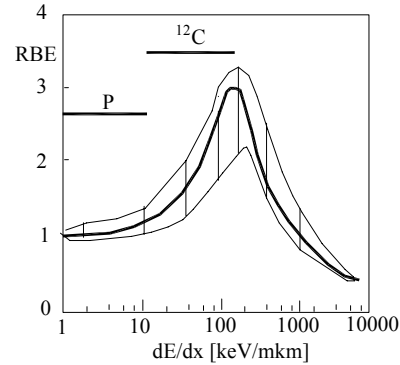


Figure 1: Dependence of RBE from dE/dx .

Table 1. The evaluation of K (the relation of BD on the plateau until the target to BD in the target), depending on the target's size, during target's irradiation in the water environment, using the single-direction scanning with ion and proton beams.

Target cylinder, diameter d [cm]; its size d in depth	1	2	4	8	16
Protons K	0.55 ± 0.10	0.60 ± 0.10	0.70 ± 0.08	0.80 ± 0.07	0.95 ± 0.05
Carbon ions K	0.28 ± 0.05	0.38 ± 0.05	0.51 ± 0.05	0.70 ± 0.05	0.95 ± 0.05

Ion beams additionally irradiate the healthy tissues behind the target. This is related to potential nuclear interactions and with the possible disintegration of ions into charged particles and neutrons (fragmentation). Newly created particles have varying directions and energies, which is why they don't have the maximum energy release at the same place, where the initial ions have Bragg's peak. The distribution of the physical dose beyond Bragg's peak was calculated and measured multiple times (Fig. 2 [5]). The lower the depth of the target is, the smaller are the ranges of the ions, the less nuclear interactions take place. For the depth of 30 cm, the level of the physical does immediately beyond the target's volume is 15% of the does within the target, lowering with the depth. This means that the level of the biological dose beyond the target is always below 8% from BD within the target, due to fragmentation.

PRIOR PROTON MICROSCOPE

A.V. Kantsyrev, A.A. Golubev, A.V. Bakhmutova, A.V. Bogdanov, V.A. Panyushkin,
 VI.S. Skachkov, N.V. Markov, A. Semennikov, ITEP, 117218, Moscow, Russia
 D. Varentsov, P. Lang, M. Rodionova, L. Shestov, K. Weyrich, GSI, 64291, Darmstadt, Germany
 S. Udrea, TUD, 64277, Darmstadt, Germany
 C. Barnes, F. Mariam, F. Marrill, C. Wilde, LANL, NM 87545, Los Alamos, USA
 S. Efimov, Y. Krasik, O. Antonov, Technion, 3200003, Haifa, Israel

Abstract

The new proton radiography facility PRIOR[2] (Proton microscope for FAIR) was developed at SIS-18 accelerator at GSI (Darmstadt, Germany). PRIOR setup is designed for measurement, with high spatial resolution up to 10 μm , of density distribution of static and dynamic objects by using a proton beam with energy up to 4.5 GeV. In the first experiments with static objects with 3.6 GeV proton, was demonstrated a spatial resolution of 30 μm . Dynamic commissioning was performed with target based on underwater electrical wires explosion with electrical pulse with current amplitude of ~ 200 kA and rise time ~ 1 μs .

INTRODUCTION

The study of high-energy-density (HED) matter generated by the impact of intense heavy ion beams dense targets is one of the most challenging and interesting topics in modern physics [1]. Measurement of density distribution, with good spatial and temporal resolution, of matter is important task for fundamental understanding of dynamic material properties in extreme states. High-energy proton radiography exceeds X-Ray diagnostic method in many ways, because it has more transmission ability and high spatial and density resolution. The best spatial resolution was obtained by means of high-energy proton microscopy technique [2]. Novel high-energy proton microscope called PRIOR (Proton Microscope for FAIR)[3] will be the key diagnostic instrument for HED research program of HEDgeHOB collaboration at FAIR. (HIHEX and LAPLAS experiments)

EXPERIMENTAL SETUP

The magnetic system of the PRIOR beam-line consists of two sections (fig. 1). The first, matching section, contains electromagnetic-quadrupole lenses and provides formation of a proton beam for the objects imaging task (beam size, angular distribution). The second section is a magnification section ($K \sim 4$) that consists of four Permanent Magnet Quadrupoles (PMQ) lenses. Length of the two PMQ lenses 144 mm and 288 mm the other two, magnetic field on pole is 1.83T, aperture 30 mm, magnetic material NdFeB. Tungsten collimators (with elliptical hole), installed at central plane of magnification section, provide regulation of contrast of the proton-radiographic images.

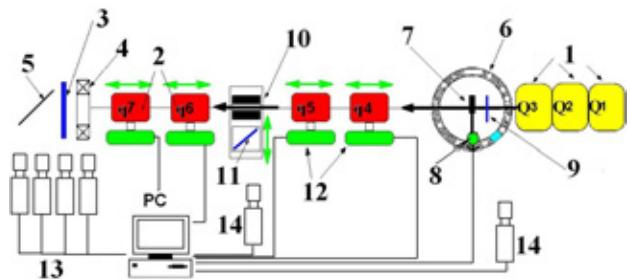


Figure 1: Photo and scheme of PRIOR proton microscope. 1- electromagnetic quadrupoles (matching section), 2- quadrupole lenses on permanent magnets PMQ (magnification section), 3-scintillator, 4- fast current transformer, 5- mylar foil mirror, 6- vacuum or water target chamber, 7- target, 8- target manipulator, 9- beam position/profile monitor (Bicron scintillator), 10- collimators, 11- beam position monitor, 12- linear actuators, 13- fast CCD cameras, 14- CCD cameras for beam tune

Investigated object installed in vacuum chamber between first and second section. The registration system for static experiments consists of CsI scintillator and plastic scintillator (Bicron BC-412) for dynamic one with two types of intensified CCD cameras PCO DiMAX and PCO DicamPro.

STATIC COMMISSIONING

The aim of first experiments at PRIOR was an adjustment of matching and magnification sections of ion optical scheme of setup to achieve best spatial resolution of proton-radiography images. Static objects were used to measure spatial and density resolutions and to estimate chromatic aberration. Primarily the setup was expected to run with 4,5 GeV proton beam. However due to radiation damage of the magnetic material of PMQ lenses (falling gradient and an increase the amplitude of the high-order harmonics of magnetic field) static commissioning of

STUDY OF POSSIBILITY OF INDUSTRIAL APPLICATION OF ION INJECTOR I-3

P. N. Alekseev, ITEP, Moscow, Russia

Abstract

Ion injector I-3 of the ITEP-TWAC accelerator complex consists of a buncher, two-gap accelerating cavity and a beam transport line. Laser ion source is used to generate ions for the injector. Possibility of application of the injector to dope semiconductor materials with variable energy ions is considered. Results of beam parameters optimization by numerical simulation to produce uniform distribution of particles density and required energy spread on the target are presented.

and base slice of 57 ± 2 mm and thickness of 120 ± 700 μm . Deviation of irradiation dose over the surface should not exceed 20%.

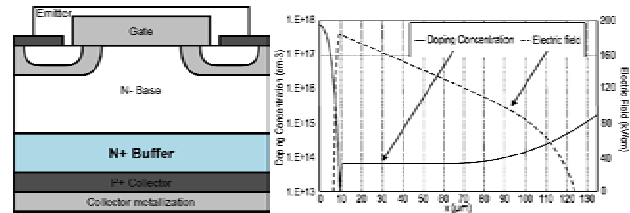


Figure 2: Structure of SPT IGBT.

INTRODUCTION

Layout of the ion injector [1] is shown on Fig. 1. A solid-state target is placed at the target chamber of Laser Ion Source (LIS). The chamber is under potential of 50 kV. Laser pulse focused on the target produces plasma. The ion beam is formed at the extractor then is focused by means of electrostatic lenses, passes through the buncher and accelerated in the two gap resonator at the voltage of up to 2 MV per gap. Resulting beam energy is up to 4 MV per charge. It is possible to accelerate ions with A/Z from 2 to 5. The injector is able to produce ions of carbon, aluminium, silicon, iron and silver with intensity up to 5×10^{11} particles per pulse and repetition rate of 1 Hz.

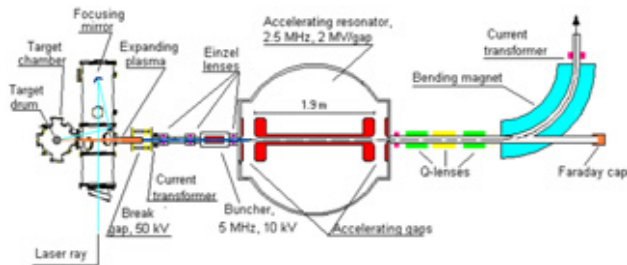


Figure 1: Layout of I-3.

Parameters of the accelerator allow considering it for industrial application in the area of doping of semiconductor materials [2]. Energies of ions in range of hundreds keV to units of MeV allows to provide a deep or a mid-deep ion implantation.

One of the possibilities of such application is production of buffer zone of Soft Punch Through (SPT) IGBT [3]. Fig. 2 shows the cross section of such SPT IGBT and concentration of the doping which should be produced to provide required electric field distribution inside the wafer [4]. Different technologies require different thickness of the buffer layer. To create the buffer layer some n-type particles, such as Phosphorus, should be implanted with a dose higher than 5×10^{12} cm^{-2} . Required particles energy is up to 2-4 MeV per nucleus, or even more. Silicon wafers have diameter of 150 ± 1 mm

SOURCE OF IONS

LIS generates ions of different charge states at the same time. These ions are presented in the accelerated beam in different concentrations depending on configuration of the ion source and the accelerator.

An experiment on production of phosphorus ions on LIS is in the beginning stage. Fig. 3 shows structure of silicon beam on the outlet of the accelerator that was produced by LIS with L-100 laser in 2011 [5].

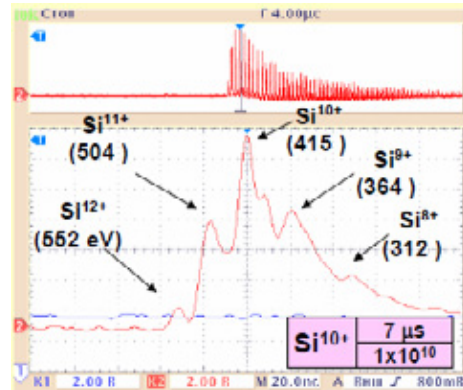


Figure 3: Structure of Si-beam produced by L-100.

Closeness of silicon and phosphorus atoms and similarity of their ionization potentials [6] allows assuming that the structure of phosphorus beam produced by L-100 will include ions of charge 8, 9, 10 and even 11, produced by L-20 - from 4 to 8.

By means of laser's power tuning and positioning of the target it is possible to achieve domination of the particles with required value of ion charge in the beam.

THE SIMULATION

While the accelerator is used as an injector of synchrotron it typically operates at maximum possible energy of ions. But in case of doping of semiconductor

DESIGN OF MULTIFUNCTIONAL FACILITY BASED ON ECR ION SOURCE FOR MATERIAL SCIENCE

S. Andrianov, B. Chalykh, M. Comunian, G. Kropachev, R. Kuybeda, T. Kulevoy, A. Ziatdinova, ITEP, Moscow, Russia; LNL-INFN, Legnaro (PD), Italy; NRNU "MEPhI", Moscow, Russia

Abstract

The traditional experimental method for new materials radiation resistance investigation is a reactor irradiation. However, there are some difficulties during steel exposure in reactor. Simulation method based on ion irradiation allows accelerating the defect generation in the material under investigation. Also a modification of materials by ion beams represents the great practical interest for modern material science. The design of the test-bench based on ECR ion source and electrostatic acceleration is presented. This paper describes the results of beam dynamics simulation in the transport channels of the test-bench. Simulation was carried out in the "real" fields. Continuous ion beam achievable at the test-bench enables beam fluence on the target up to 10^{16} p/m².

INTRODUCTION

The creation of new high-tech energy systems is associated with the use of new radiation-resistant materials. A necessity emerges to study and test the new materials. Neutron flux irradiation of samples occurs in the reactor. Certain difficulties arise when steel is exposed to radiation in the reactor. These problems are primarily associated with the time it takes to reach required doses. Even in fast reactors the exposure to the required doses may take years. There is a need to take into account the complexity and high cost of reactor-based systems and, consequently, of the tests themselves. High level of induced radioactivity of the materials is another factor which complicates their study. It emerges in the course of long-term irradiation in the reactor core and makes it difficult to further study the irradiated samples. Low-energy ions can be used to model the process of kicking out atoms formed in the course of neutron irradiation. Ion beams irradiation is an express analysis method which was offered in the 80-s[1]. This method allows to accelerate the process of defect emergence in irradiated materials due to the speeding up of dose accumulation. It must be taken into account that the speeding up of the dose accumulation during the simulation may lead to discrepancies in the results as compared to the real condition that exist in the reactor. Hence, it is considered necessary to reproduce the conditions of the reactor as closely as possible. The process of defect formation depends on the temperature, so the irradiated target will be specially heated. Now, experiments are carried out using a pulse beam on HIP-1 RFQ [2]. Oscillation of samples temperature must not exceed 1-3 degrees Celsius. This criterion is very hard to achieve when using a pulse beam.

In order to be able to reproduce the processes in the reactor with greater accuracy our target will not only be heated but defect containing area will be implanted with ions of hydrogen and helium. This will be done with the intention to model the accumulation of He and H in the reactor wall under the influence of the neutron flux.

Besides radiation-resistant material research, modification of materials by high energy ion beams is of great practical interest. Vanadium, chromium, tungsten ions beams can be used for this purpose. A great increase in durability and surface strength can be achieved by irradiation with powerful beams[3].

TEST-BENCH SET-UP

It is planned that apart from material science related tests experiments to study the interaction of the ion beam with plasma and metal vapor targets will be carried out as well. For plasma target and material modification experiments ion beams of 1-2 MeV are necessary. In order to achieve this installation of electrostatic accelerating tube has been planned.

ITEP is developing a multifunctional facility which will make possible the ion beam experiments that will allow to investigate materials by means of express analysis based on imitation of damages materials sustain in the reactor.

The test-bench is designed to have four experimental channels:

1. For experiments simulating of damage caused by neutrons
2. For both modifications of material surfaces and simulation experiments
3. For plasma target experiments
4. For injection of ion beam into accelerating structure

Experimental channels will exit the bending magnet at 90°, 60°, 30°, 0° angles correspondingly.

Specifications of the last two channels are still being discussed. So modeling of their beam dynamics will be carried out at a later date.

Geometry and tract elements of the test-bench were chosen on the basis of beam dynamics modeling.

It had two stages:

1. Modeling of beam dynamics in approximation to "ideal" fields[4].
2. Modeling of beam dynamics in approximation to "real" fields.

Modeling for Fe¹⁰⁺, H⁺, He⁺ ions was done in both channels.

In order to minimize the possible effects of chemical reactions on the experiment it is best to use the ions of the same element of which the target is built. In this case the Fe ions are going to be used as it is the main constituent of construction steel. A modern ECR ion source can

THE INDUCTION SYNCHROTRON WITH A CONSTANT MAGNETIC FIELD

G.V. Dolbilov[#], Joint Institute for Nuclear Research, Dubna, 141980, Russia

Abstract

In this paper the possibility of accelerating charged particles in a "nearly constant" orbit in a constant magnetic field is discussed.

The trajectories of the accelerated particles are formed by set azimuthally short bending magnets in which the deflection angle is independent of the particle energy.

Focusing of the beam is carried out by the alternating field bending magnets and quadrupole lenses.

The particles are accelerated by the electric field induction sections. Stability of longitudinal oscillations is determined by the shape of the top of the accelerating pulse.

INTRODUCTION

- Features Traditional cyclic accelerators:
 1. Accelerators with a constant magnetic field.
 - High ranges of change in orbital radius.
 - Heavy weight of magnets.
 2. Accelerators with a constant radius of an equilibrium orbit
 - Magnetic strengths depends on energy of ions.
 - Resonant frequencies of the HF-field depends on energy of particles (cyclic frequency).
- The Induction Synchrotron with Constant Magnetic Field
 1. The Magnetic field is constant in time.
 - The Orbital radius $r \sim r_{max}$
 - Particle trajectories – arc chords.
 - $\Delta r = r_{max} - r \leq r_{max}(\pi/N)^2$, N - arc chord number.
 2. The Induction accelerating electric field:
 - Isn't present resonant systems with a variable frequency.
 - Synchronization is carried out by sync pulses.

Scheme accelerator with a constant magnetic field is shown in Fig. 1.

MAGNETIC SYSTEM OF THE SYNCHROTRON

1. Special sections of magnetic dipoles form the near-circular orbit with $r \approx r_{max}$ radius.
 - Each dipole of section (Fig.2) deflects the accelerated beam on $\Delta\Theta/2$ angle.
 - This angle doesn't depend on energy of particles if the internal border of dipoles corresponds to equality

$$x = \pm \left[(r_{max} - r) \sin \frac{\Delta\Theta}{2} + x_0 \right]$$

x - distance of internal border of dipoles to bisector of angle $\Delta\Theta$

x_0 - the size determined by a concrete design of section
 r , r_{max} - the current and maximum radiuses determined by energy of a particle.

2. The focusing forces of magnetic section.
 - Magnetic fields of section focus the accelerated particles in the horizontal plane.

- Magnetic forces of section defocus the accelerated particles in the vertical plane.
- Additional lenses on an entrance and an exit of magnetic section are required.

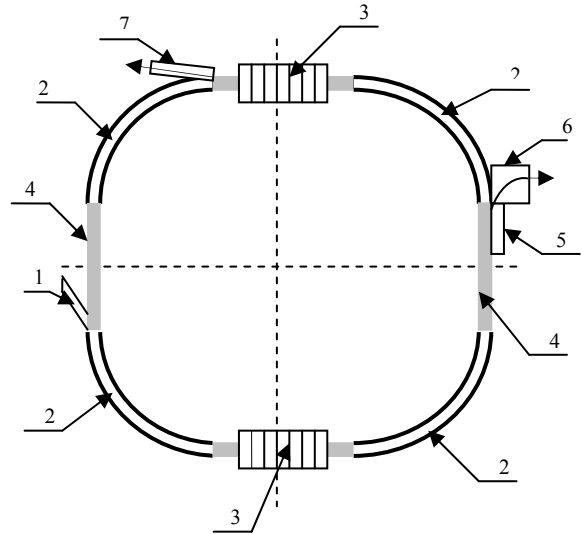


Figure 1: Scheme accelerator with a constant magnetic field. 1 - Injector; 2 - Set of special sections of magnetic dipoles; 3 - Induction accelerating sections; 4 - Straight-line segments; 5-7 - System of fast and slow beam extraction.

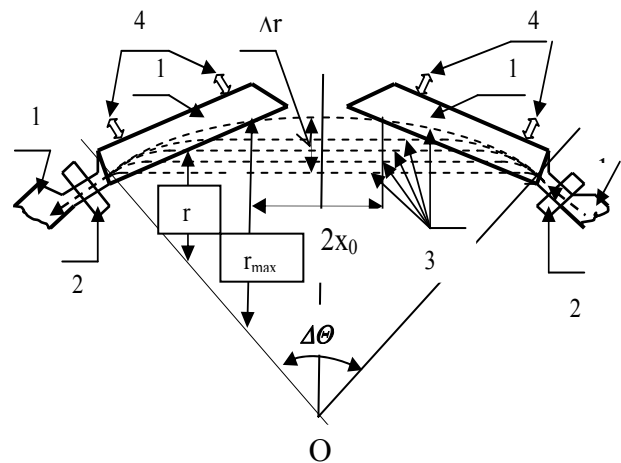


Figure 2: The warrant of the bending magnetic section using dipoles with a uniform field. 1 - Dipoles with a uniform field; 2 - Additional focusing lenses; 3 - Beam trajectories; 4 - System tuning the beam trajectory, 5 - $\Delta\Theta$ - The center angle of a beam deflection.

Copyright © 2014 CC-BY-3.0 and by the respective authors

THE COMPACT INDUCTION ACCELERATOR OF ELECTRONS FOR RADIATION TECHNOLOGIES

G.V. Dolbilov[#], Joint Institute for Nuclear Research, Dubna, 141980, Russia

Abstract

The electron accelerator with energy <10 MEV uses a rectangular pulse of the accelerating induction voltage and a trapezoidal pulse of a leading magnetic field. To preserve the equilibrium orbit radius constant special relationship between the amplitude and temporal characteristics of the magnetic induction and the accelerating voltage inductors are made. It is possible to maintain an orbit close to constant in a constant magnetic field in time. The accelerator contains alternating-sign focusing in dipole magnets and rectilinear accelerator parts.

INTRODUCTION

For receiving electron beams with energy of 0.5-10 MeV the cyclic accelerator in which particles are accelerated by linear induction section can be used [1,2].

For formation of the closed equilibrium orbit of electrons two methods can be used:

1 - a method with the magnetic field growing at acceleration;

2 - a method with a magnetic field, constant on time;

In a both cases the accelerator contains alternating-sign focusing in magnets and rectilinear accelerator parts.

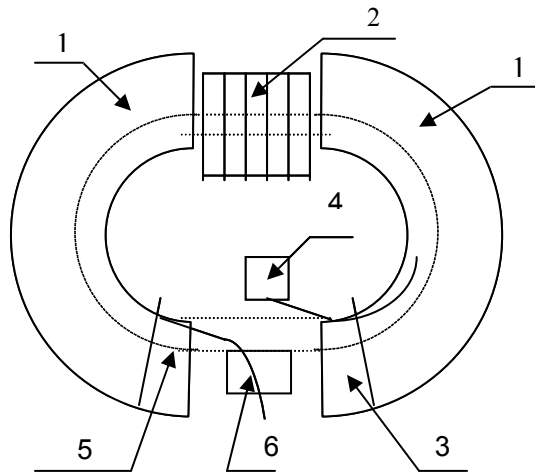


Figure 1: The scheme of the accelerator. 1 - the magnetic system with alternating focusing; 2 - the linear induction accelerating system; 3-6 - systems of input and output of electrons.

THE ELECTRON ACCELERATOR WITH A VARIABLE MAGNETIC FIELD [3]

For $R(t) = R_0 = \text{Const}$, the following condition has to be carried out

$$\frac{dB}{dt} = \frac{nU_{ind}}{LR_0}$$

where n – number of inductors; U_{ind} – inductor voltage; L – orbit perimeter.

Energy of electrons 0.5-10MeV can be reached for one pulse T_1 - duration

$$T_1 = 10^{-4} - 10^{-6} \text{ s}$$

To this end total cross-section of inductors of accelerating section is equal to

$$S = \frac{WL}{\Delta Bc}$$

where W - energy of electrons, L - perimeter of an orbit, $\Delta B \leq 2B_s$, B_s - induction of saturation of inductors, c - velocity of light.

Diagram of magnetic induction, $B(t)$, and the accelerating pulse of induction section, $U(t)$, shown in Fig. 2.

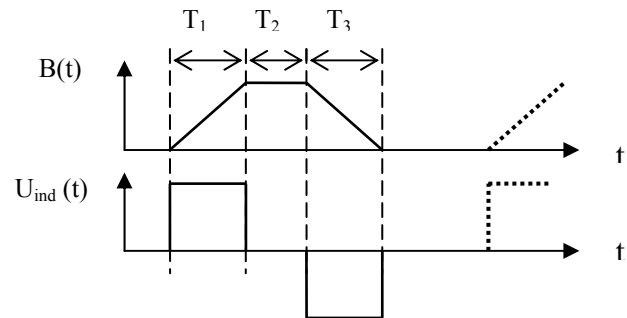


Figure 2: Diagram of magnetic induction and the accelerating pulse of induction section. T_1 – Time of acceleration of electrons, T_2 - Beam extraction time, T_3 - Time of magnetic reversal of inductors of section.

THE ELECTRON ACCELERATOR WITH A CONSTANT MAGNETIC FIELD

The magnetic system of the accelerator is a set of special sections of magnets (Fig.3). The section contains two dipoles. Each dipole deflects the beam at the predetermined angle of $\Delta\Theta/2$ which doesn't depend on energy of the accelerated particles.

- The beam trajectory with the maximum energy is r_{\max} radius circle;
- The beam trajectory with energy of injection is $\Delta\Theta$ angle chord.

$$\Delta r = r_{\max} - r_{\min} = r_{\max} \left(1 - \cos \frac{\Delta\Theta}{2}\right)$$

$$\Delta r \approx R_{\max} \frac{1}{2} \left(\frac{\Delta\Theta}{2}\right)^2$$

PROJECT OF DEMONSTRATION CENTER OF THE PROTON THERAPY AT DLNP JINR

E.M. Syresin, G.A. Karamysheva, M.Y. Kazarinov, N.A. Morozov, G.V. Mytzin, N.G. Shakun
Joint Institute for Nuclear Research, Dubna, Russia

J. Bokor, Faculty of Electrical Engineering and Information Technology, Slovak University of Technology, Bratislava, Slovakia

Abstract

JINR is one of the leading proton therapy research centers of the Russia. The modern technique of 3D conformal proton radiotherapy was first effectuated in Russia in this center, and now it is effectively used in regular treatment sessions. A special Medico-Technical Complex was created at JINR on the basis of the phasotron used for proton treatment. About 100 patients undergo a course of fractionated treatment here every year. During last 14 years were treated by proton beams more than 1000 patients.

A project of the demonstration center of the proton therapy is discussed on base of a superconducting 230 MeV synchrocyclotron. The superconducting synchrocyclotron is planned to install instead of phasotron in Medical Technical Complex of DLNP. The new transport channel is designed for beam delivery to the JINR medical cabin.

PROJECT OF DEMONSTRATION CENTER OF PROTON THERAPY

The pioneering proton therapy researches began at JINR in 1967 [1]. The phasotron with the proton energy of 660 MeV and current of 2 μA is used for medical applications [1-3]. More than 1000 patients were treated at JINR by the proton beams. During the last years around 100 patients per year got the proton treatment there.

The superconducting synchrocyclotron is planned to install instead of phasotron in Medical Technical Complex of DLNP. The new transport channel is designed for beam delivery to the JINR medical cabin. The equipment of the demonstration center of the proton therapy and realized here technologies will be lay in the base of the future Dubna hospital center of the proton therapy. The final stage of the project is creation of the Dubna hospital center of the proton therapy on basis of the superconducting synchrocyclotron and the rotating gantry (Fig.1). The first stage of this project is related to the construction of the demonstration center of the proton therapy on base of a superconducting 230 MeV synchrocyclotron.

High magnetic field of 5T is used in the superconducting synchrocyclotron where the requirement of isochronism is unnecessary and weak focusing is obtained from the negative gradient of the rotationally symmetric magnetic field. The synchrocyclotron has

following peculiarities in comparison with the isochronous cyclotron: the RF frequency is periodically modulated and the beam is pulsed; the longitudinal dynamics becomes a major aspect of the beam physics with energy-phase oscillations bound by a separatrix; the beam is captured at injection only during a limited time window; the regenerative extraction is needed to recover the beam which has a very small turn separation at extraction; the extracted beam has a relatively low intensity of 20 nA; the central region is strongly reduced in size compared to an equivalent isochronous cyclotron.

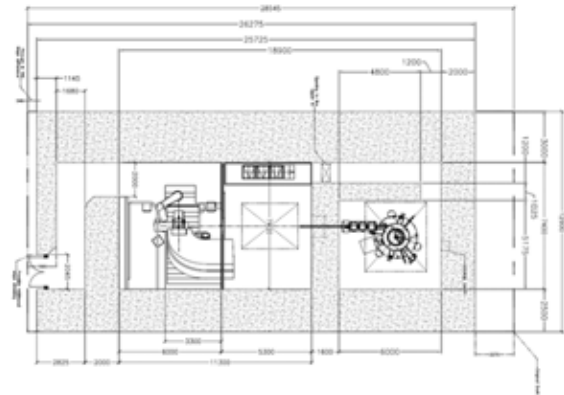


Figure 1: Scheme of Dubna hospital center of proton therapy.



Figure 2: Scheme of synchrocyclotron with beam delivery channel and modernized medical cabin in demonstration center of proton therapy.

POSITRON ANNIHILATION SPECTROSCOPY AT LEPTA FACILITY

P. Horodek, Institute of Nuclear Physics PAN, Krakow, Poland

A.G. Kobets, Institute of Electrophysics and Radiation Technologies NAS, Kharkov, Ukraine

I. N. Meshkov, O.S. Orlov, A.A. Sidorin, JINR, Dubna, Russia

Abstract

Positron Annihilation Spectroscopy (PAS) is a sensitive method dedicated to detection of open-volume type of defects in materials. Nowadays, this technique is of a great interest due to the practical character of obtained results. New devices using monoenergetic positron beams are built. The poster presents progress in this field at LEPTA project at Joint Institute for Nuclear Research in Dubna, present and future directions of works.

INTRODUCTION

Positron Annihilation Spectroscopy (PAS) is a great method for detection open-volume defects on the atomic level. It is applied in the field of solid body physics as well as in the material research. It gives interesting results as the independent method or the complementary technique for other methods such as Rutherford Back Scattering (RBS) or Mossbauer Spectroscopy.

PAS is based on the special properties of positron – electron annihilation process. Positron annihilates with its antiparticle – electron and as a result in 99.8 % cases two gamma quanta with energy of about 511 keV are emitted. [1] The annihilation process does not take place immediately, but positron spends some time in the matter on the thermalization and diffusion stages. [2] This time depends on the electron concentration in the structure. If the lattice includes defects the electron density is lower in comparison to a non-defected area and in this was positron life time will be longer. The positron life time means the time between positron emission eg. from the ²²Na isotope and annihilation. Because the electron momenta inside traps are also lower in comparison to the bulk, it also finds a reflect in the annihilation characteristics. In this way the energy of gamma quanta will be changed as a result of Doppler effect according to formula

$$E_{\gamma} \cong mc^2 + E_b \pm \frac{p_{\parallel}c}{2} \tag{1}$$

where E_b is the energy of positron-electron pair coupling and p_{\parallel} is a perpendicular component of the positron-electron pair's momentum. This effect is observed as the broadening of annihilation line 511 keV. The broadening always appears in this case but for positrons trapped in the defects will be smaller considering the lower electron momenta. It should be noticed that the momentum of thermalized positron can be negligible. Thus the registration 511 keV line gives information about momentum state of electrons taking part in annihilation process. It is the role of Doppler Broadening of Annihilation Gamma Line (DB) technique.

DOPPLER BROADENING OF ANNIHILATION GAMMA LINE TECHNIQUE (DB)

The formula describing the changing of gamma energy can be also expressed as following

$$E_{\gamma} \cong mc^2 \pm \sqrt{\frac{1}{2}mc^2 E} \tag{2}$$

If the energy of an annihilating positron equals e.g. 7eV (Fermi energy for copper), then a change of energy of annihilating gamma quantum, according to the above formula, will equal 1,34 keV. Thus, the total broadening of annihilation line will equal 2,68 keV.

Observation of such broadening requires using detectors of a high energetic resolution. Currently available germanium detectors allow to take measurements with resolution equal to 1-2 keV around 511 keV energy.

Doppler broadening of annihilation line technique is used to detect concentrations of defects such as vacancies and their accumulations. A signal from annihilation of a trapped positron gives broadening of the 511 keV line accordingly smaller than the one that would occur in case of annihilation with nucleus electrons. In other words, less defected sample gives smaller broadening of the 511 keV line.

In practice, the broadening of 511 keV line is not calculated but the analysis is limited to evaluating of two characteristic parameters, the so-called S- and W-parameters (see Fig. 1). [3,4]

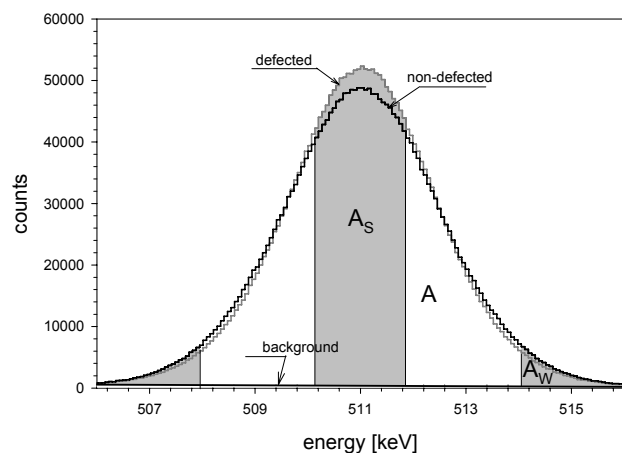


Figure 1: 511 keV lines for defected and nondefected samples.

S parameter defines proportion of annihilation of positrons with low-momentum electrons. It is closely related to concentration of defects in a material. It is

DEVELOPMENT OF THE EQUIPMENT FOR THE PROTOTYPE OF A COMPLEX OF RADIOTHERAPY AT THE NUCLOTRON-M

I.P. Yudin*, A.M. Makankin, V.A. Panacik, S.I. Tyutyunnikov, S.E. Vasilev, A.V. Vishnevskiy,
Joint Institute for Nuclear Research, Dubna, Russia
K.K. Laktionov, D.I. Yudin, Russian Cancer Research Center them. Blokhin, Moscow, Russia

Abstract

The report deals with the construction of the carbon beam transport line for biomedical research at the Nuclotron accelerator complex, JINR, Dubna. We have studied the scheme and modes of magneto-optical elements of the channel. Used electronics described. We are discussed the compilation and realization of the plan of treating a tumor located at a depth up to 30 cm. Choice of beam scanning schemes and their optimization are shown.

INTRODUCTION

One direction in the development of the Joint Institute for Nuclear Research (JINR) accelerator complex is the design of a test bench for medicobiological research based on the JINR Nuclotron [1].

While designing the test bench, the general technique for manufacturing the hadronic therapy complex is tested.

In this work we present a calculation procedure for the optics of the charge particle transport channel of the hadronic therapy complex. This channel is intended for the transportation of the $^{12}\text{C}^{+6}$ carbon ions with an intensity of $\sim 2 \times 10^9$ and an energy of 100–550 MeV/nucleon.

Figure 1 shows the circuit of the primary transport channel from the Nuclotron to experimental hall 205. An additional channel starts near the F3 focus of the primary channel.

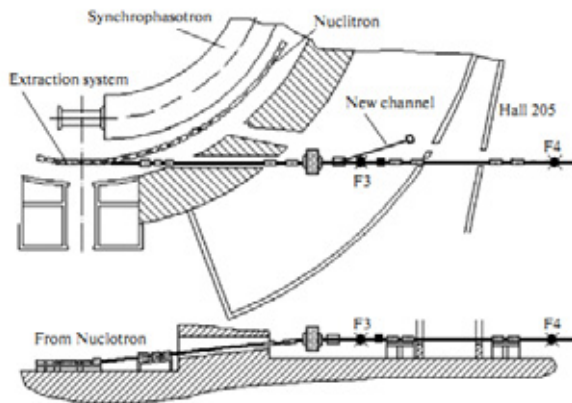


Figure 1: Layout of the primary transport channel from the Nuclotron. Top and side view. A branch of the designed channel before the F3 focus is shown.

*yudin@jinr.ru

PROBLEM STATEMENT

Mathematical Statement

To describe an envelope during beam transportation, one can use the matrix formalism:

$$X_{out} = M_N \dots M_2 \cdot M_1 \cdot X_{in}, \quad (1)$$

where X_{out} and X_{in} are the column vectors ($X = (\beta, \alpha, \gamma)^T$) of the terminal and initial conditions (consisting of the parameters of Twiss matrix) describing the beam; M_1, \dots, M_N are the transformation matrices of channel elements, i.e., drift gaps and quadrupole lenses. The thick lens approximation is used for the quadrupole elements. All transformation matrices are nonlinear with respect to the channel parameters, i.e., geometrical sizes of the elements and lens gradients.

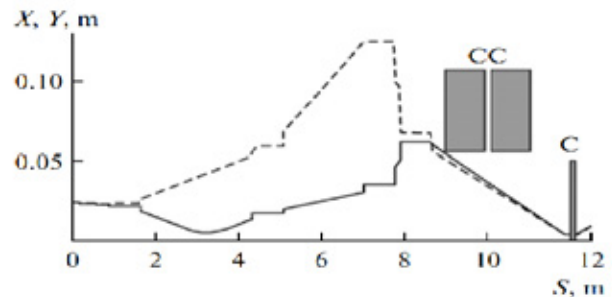


Figure 2: Position of the scanning system of magnets on a beam (CC). The scanning region in the beam focus (C).

The initial conditions for beam transport in the additional channel are taken as current values of the beam parameters from the Nuclotron primary channel. They should satisfy the conditions

$$M_{drift} \cdot X_{in} = X_{F3}, \quad (2)$$

where X_{in} is the initial conditions from Eq. (1), X_{F3} is the beam parameters in the F3 focus of the primary channel, and M_{drift} is the matrix of transformation from the additional channel branching point to the F3 focus.

The output transport values X_{out} should satisfy the focus conditions, i.e., the zero derivative of the beam envelope with respect to the transport coordinate:

$$\alpha_{x,out} = \alpha_{y,out} = 0, \quad (3)$$

where $\alpha_{x,out}$ and $\alpha_{y,out}$ are the α components of the Twiss matrix in the focus of the additional channel.

The size of the beam envelope in the focus F_k of the additional channel is close to the possible minimum satisfying the geometrical limits of the setup. The envelope minimum is considered known and determined

THERMAL SIMULATIONS OF THE BIPERIODICAL ACCELERATING STRUCTURE WITH THE OPERATING FREQUENCY 27 GHz

Yu.D. Kliuchevskaia, S.M. Polozov National Research Nuclear University MEPhI (Moscow Engineering Physics Institute), Moscow, Russia

Abstract

Biperiodical accelerating structure (BAS) represents a system based on disk loaded waveguide (DLW) with $\pi/2$ operation mode. The 1 cm band structure will have very compact transverse size. Such characteristics give it perspective to use in medical accelerators. The results of beam dynamics simulation and electrodynamic study was discussed early [1]. It will important to study the BAS electrodynamic taking into account thermal processes in structure and to design the cooling system. It is important because of the high pulse RF power (about 1.5 MW) necessary for the beam acceleration. The simulation results which are defined using CST code will presented in report. Calculation and definition of the thermal coefficient depending on speed, temperature and the water flow direction will make.

INTRODUCTION

Many medical applications need to design a compact electron accelerator. Compactness of accelerating structure can be reached by increase of the accelerating RF field frequency (frequency ranges of 6, 10 GHz are widely used and 17 and 30 GHz are also possible). Besides these accelerating structures demand lesser RF-power due to smaller internal volume and surface area. The effective medical accelerators operating on S- and H-bands are well-known [2-4]. The design of 17 GHz linear accelerator was offered [5]. BAS represents a modified structure on the $\pi/2$ mode in which case the accelerating cells length increase and coupling cells length decrease. The main aim of simulation was geometry definition providing the operating frequency 27 GHz. General view of the accelerating structure is shown in Figure 1. As a result of tuning the cell geometry with optimal characteristics was defined and they are presented in Table 1.

Table 1: Optimal parameters values of the BAS

Parameter	Value
Operating mode	$\pi/2$
Length of accelerating cell, mm	4.5
Length of accelerating system, mm	55
Frequency, GHz	27
Length of wave, mm	10
Radius of the drift tube, mm	4.5
Radius windows coupling, mm	0.8
Radius of the accelerating cell, R_{cell} , mm	8.8
Radius of blending sidewall, R_{lc} , mm	1
Radius of coupling cell, mm	3.8
Length of coupler, mm	50

High power pulse gyrotrons are one of possible power sources types in 30 GHz band. The power system of proposed linac will differ from conventional C-band medical linac therefore gyrotrons can produce the long pulses (hundreds of μs) with low repetition rate. High-efficiency pulse and CW gyrotrons of frequency range 27–30 GHz have been developed at the Institute of Applied Physics of Russian Academy of Sciences. Pulse power reaches to 15 MW at the efficiency of 50 % in gyrotrons with the high operating voltage 500 kV [6]. Accordingly to preliminary estimations based on the gyrotron theory and experimental results pulse and average power of the order the gyrotron is capable of producing 2 MW peak RF power in pulses with pulse duration 400 μs and a repetition rate of 10 Hz.

The combination of high electromagnetic fields and long RF pulse in resonators on operating frequency leads to temperature increase on the surface, to thermal deformations and to noticeable change the resonator characteristics during the RF pulse [7]. The thermal analysis was performed for such structure due to. Thermal calculations to define the frequency shift depending on temperature of cooling liquid were done.

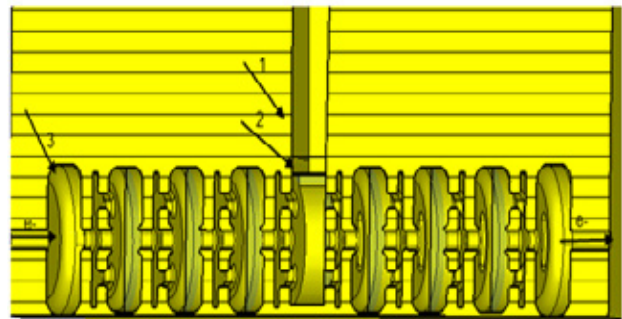


Figure 1: General view of the accelerating structure, 1 – coupler, 2 – power feeding waveguide, 3 – regular accelerating cell.

COOLING SYSTEM FOR BIPERIODICAL STRUCTURE AT 27 GHz

The simulation of BAS thermal characteristics was done using the model consisting of one accelerating cell and one coupling cell operating on frequency of 27 GHz. The geometry of the BAS cell is shown in Figure 2. The copper BAS based on the DLW with magnetic coupling was studied, it operates on the standing wave. The high operating frequency 27 GHz is the feature of this structure

A PROTOTYPE OF A PHASED ARRAY FOR DEEP THERMORADIOTHERAPY

S.M. Polozov, A.M. Fadeev, A.A Blinnikov, S.M. Ivanov, National Research Nuclear University MPhI (Moscow Engineering Physics Institute), Moscow, Russia

Abstract

It is proven that hyperthermia increases radiation and chemotherapy efficiency. In oncology, the generation of a higher temperature at a tumor-involved region of the body is called hyperthermia. The thermoradiotherapy is widely and effective uses. A phased array of eight dipoles for the hyperthermia treatment of deep-seated tumors is proposed earlier. The power and phase coherently delivered to the radiating elements can be varied, so that the electromagnetic field is increased at the tumor location and decreased in the normal tissues. The prototype of the phased array of two dipoles and the RF power scheme are presented and results of experiments are discussed. Measured and simulated temperature distributions along the line connecting two dipoles are discussed in this paper.

INTRODUCTION

Hyperthermia is an efficient adjuvant for the common modalities such as surgery, radiation and chemotherapy. Many researches have shown that hyperthermia temperature can damage and kill tumor cells, thus reduces tumor size. However the main advantage is that hyperthermia is a promising approach to increase efficiency of chemotherapy or radiation therapy. Under hyperthermia temperature some tumor cells become more sensitive to the radiation and anticancer drugs. The effect on surviving fraction depends both on the temperature increase and on the duration of the expose [1, 2]. Treatment requires that temperatures within tumor remain above 43 °C during 30-60 min, while maximum temperature in normal tissues have to be lower than 42°C.

In previous papers the phased array for deep hyperthermia was suggested [3, 4]. This phased array consists of eight dipole antennas arranged on an inner side of a cylindrical dielectric tank. Dipoles are surrounding the patient body and the amplitudes and phases of each antenna are under control of the operator as shown in Figure 1. Necessary distribution of E-field can be reached by means of independent feeding of each dipole that permits us to vary amplitudes and phases of electromagnetic field. In other words we can concentrate absorption energy of E-field and deliver therapeutic heat in tumor and at the same time prevent extra heating of normal tissues.

Deionized water filling space between patient and array is for cooling outer side of body and for better matching. The E-field energy is extremely concentrated in the inner side of a shell due to the electric field energy density inside the shell is higher by a factor ϵ (the relative dielectric constant of the medium) than outside the shell.

ISBN 978-3-95450-170-0

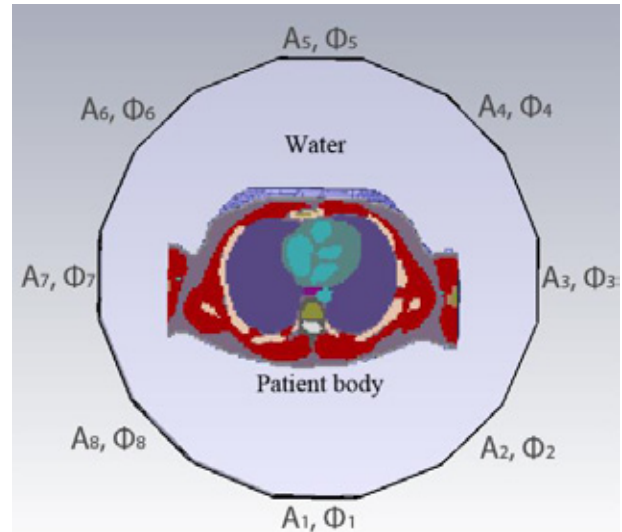


Figure 1: Patient body surrounded by phased dipoles array. Dipole antennas have amplitudes $A_1...A_8$ and phases $\Phi_1... \Phi_8$ respectively.

EXPERIMENTAL SETUP

In this paper the prototype of the phased array of two dipoles is presented. The RF power system schematic layout of this prototype is shown in Figure 2, where 1 – driving generator Agilent N5181A, 2 – preamplifier Analog Device 5545 (fixed gain 25 dB, 30 MHz-6 GHz, 5 V), 3 – Wilkinson power divider, 4 – phaseshifter Mini-Circuit JSPHS-150 (100-150 MHz, 0-12 V), 5 – amplifier Toshiba S-AV32A (134-174 MHz, 12.5 V, 60 W), 6 – matching circuit. Single phaseshifter is enough to produce any phase lag between two dipoles. The operating principle of such layout is the following. The RF signal at 150 MHz from signal source splits into two channels by microstrip power divider. Then by means of controlled one phase shifters and two solid state amplifiers we can adjust phase and amplitude of every signal. Due to these adjustments peak temperature moving is available. Solid state RF amplifier Toshiba S-AV32A is simple and stable in operation but it needs intensive cooling system.

For impedance measurements a commercial network analyzer system Agilent Technologies E5061A was used. Impedance matching is provided with short circuit stub. The stub is positioned a distance from the load. This distance is chosen so that at that point the resistive part of the load impedance is made equal to the resistive part of the characteristic impedance by impedance transformer action of the length of the main line. The length of the stub is chosen so that it exactly cancels the reactive part of the presented impedance. Return loss plot for one

INTERDISCIPLINARY GLOSSARY — PARTICLE ACCELERATORS AND MEDICINE

V.V. Dmitrieva*, V.S. Dyubkov†, V.G. Nikitaev, S.E. Ulin,
National Research Nuclear University “MEPhI”, Moscow, Russian Federation

Abstract

A general concept of a new interdisciplinary glossary, which includes particle accelerator terminology used in medicine, as well as relevant medical concepts, are presented. Its structure and usage rules are described. An example, illustrating the quickly searching technique of relevant information in this Glossary, is considered. A website address, where one can get an access to the Glossary, is specified. Glossary can be refined and supplemented.

INTRODUCTION

Number of fields of science as well as its applications are founded and evolved swiftly today. It results in new concepts, professional terminology, which can significantly complicate an understanding and information perception by specialists in the interdisciplinary fields. In particular this situation takes place in the case of specialist cooperation from medicine and particle accelerator fields. Particle accelerators, in that case, are effectively used for disease diagnostics and therapy.

Special problems appear when students and post-graduates study special medicine and particle accelerator courses at Universities, in which rather difficult, and often impossible, to teach courses simultaneously on physics and medicine at the highest level [1].

Interdisciplinary Glossary was made up with the aim of improving the knowledge in the field of particle accelerators and medicine. We hope that Interdisciplinary Glossary will be useful for students, technologists, scientists & users of key facilities.

GLOSSARY STRUCTURE

High-tech nuclear medicine centres are built up for the provision of high quality medical diagnostics and therapy in Russia today, where experts in various scientific fields and application areas work together with doctors.

Interdisciplinary Glossary, which includes a set of hard and electronic copies as well as database of Glossary and contains terminology and explanation in genetics, biology, radio-biology, radiochemistry, radiation safety, radio-pharmaceutical, oncology, information technology, particle accelerators, physical methods and means of radiation for medical imaging, is required to provide communication between all members on issues concerning common activity in the field of application of methods and tools for nuclear medicine and radiation therapy for cancer diagnostics and treatment.

* vvdmitrieva@mephi.ru

† vsdyubkov@mephi.ru

In particular, particle accelerators are used for radioactive isotope production as well as radio-diagnostics and oncological diseases therapy, sterilization of medical instruments and transplant tissues.

Particle accelerators for medicine are classified into linear and cyclic on the one hand and into electron and proton/ion on the other hand. Generally, electron linear and cyclic accelerators are used for radiotherapy, whereas proton and ion accelerators are mainly used for nuclear medicine purposes [2, 3]. It is well known that different types of ionizing radiation (photons, electrons, protons, ions, neutrons, π -mesons) are used in radiation therapy. The type and energy of ionizing radiation in complex treatment are determined by a stage and malignant neoplasm prevalence [4].

Interdisciplinary Glossary includes about 1000 terms and explanations, namely:

- 180 on particle accelerators,
- 200 on oncology,
- 200 on computing,

and other terms and explanations that concern radio-biology, radiochemistry, radiation safety, radio-pharmaceutical etc.

Glossary content has been edited by experts of the corresponding fields of knowledge. Glossary content is sorted by subject and alphabet.

Glossary is based on relational database management system (DBMS) MySQL platform. Operation principle of the DBMS MySQL is similar to any other DBMS operation principle that uses SQL as the command language for creating/deleting databases, tables, replenishing the tables with a data, sampling data [5].

phpMyAdmin was installed for easy data management. phpMyAdmin is a LAMP (Linux, Apache, MySQL, and PHP) application specifically written for administering MySQL servers. phpMyAdmin has tools for visual table creation, and also allows one to create, modify and delete tables by means of the SQL toolkit.

Flowchart of the developed application is shown in Fig. 1.

An *administrator* interface consists of:

- category management that allows one to create, delete, and modify Glossary categories/subcategories;
- article management that allows one to create, delete, and edit articles included in all Glossary categories/subcategories;
- user management that allows one to assign/remove user rights to certain categories.

A *moderator* interface consists of:

- category management that allows one to create, delete, and modify Glossary categories/subcategories, which is assigned with administrator rights;

MULTIFUNCTIONAL EXTRACTION CHANNEL DEVELOPMENT HEAVY ION RFQ (RADIO FREQUENCY QUADRUPOLE)*

E.Khabibullina[#], R.Gavrilin, B. Chalykh, G. Kropachev, R. Kuibeda, S.Visotski, T. Kulevoy, A.Golubev, ITEP, Moscow, Russia

M. Comunian, LNL-INFN, Legnaro (PD), Italy

E.Khabibullina[#], T. Kulevoy, NRNU "MEPhI", Moscow, Russia

Abstract

In the ITEP the Heavy Ion RFQ HIP-1 (heavy Ion Prototype) has to provide ion beams for two different experimental programs. The first one, aimed to irradiation resistance investigation of reactor construction materials, is successfully ongoing. Samples of new materials for reactors were irradiated by beams of iron, vanadium and titanium ions accelerated by the RFQ. The irradiated materials were investigated by both transmission electron microscope and atom-probe tomography. The second one is under development and it is aimed to investigation of ion beam interaction with plasma and metal vapour targets. For this program a wide range of beams (both gas ions and metal ones) accelerated in the RFQ can be used. Based on beam dynamics simulation the design of new RFQ output beam line enabling both experiments realization was developed. Details of beam dynamics simulation and output line design are presented and discussed in this paper.

INTRODUCTION

In the ITEP the Heavy Ion RFQ (Fig.1) provides irradiation resistance investigation of reactor construction materials. The HIP-1 is a heavy ion RFQ linac accelerating ion beams generated by either MEVVA ion source or duoplasmatron. It provides accelerated beam of ions from C^+ to U^{4+} with energy of 101keV/n and several mA of current[1].

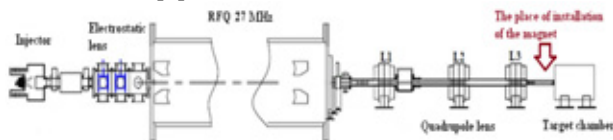


Figure 1: The Heavy Ion Prototype.

For project realization the special target chamber providing sample heating up to desired temperature from range of 20°C to 700°C was developed. A set of experimental works for reactor material resistance investigation were carried out already [2].

The experiments of heavy ion beam interaction with plasma and metal vapor target can't be carried out simultaneously with ones for reactor resistance investigation at the existing RFQ output beam line. The existing output beam channel of TIPr-1 can't be used for both targets, for reactor materials investigation and for

plasma-beam interaction. The target for imitation experiments with reactor materials is nontransparent. The target for plasma and metal vapor interaction with ion beam is transpired but a considerable amount of intensity (more than 90%) is lost during beam passage through plasma target diaphragms.

According to theoretical models the plasma (ionized gas) has a higher stopping power for ion beam with energy of about 100 keV/n compare to both gas target and even metal one [3]. The design of new beam line is under development now. The results of simulation are presented and discussed.

PLASMA TARGET

The plasma target device generates plasma by an electric discharge igniting in two collinear quartz tubes, each of 5 mm in diameter and 78 mm long. The capacitor bank of $\sim 3 \mu F$ provides the discharge at voltage up to 5 kV and produces the electrical current flowing in two opposite directions in both quartz tubes. Such a design for the plasma target enables suppression the well-known effect of the plasma lens caused by the magnetic field of the discharge current. The focusing effect of the first discharge tube is compensated for the defocusing effect of the second one. Symmetry of the discharge ensures by special inductivity coils, included into the discharge circuit, with two wires for the two current branches wind in the opposite directions (Fig.2).

An ultimate vacuum obtained in the target is $1.6 \cdot 10^{-7}$ mbar. During experiments the target pressure may be varied by inlet valve in the range from 1 to 10 mbar. It allows plasma production with variation of both an electron density and a of ionization rate [4].

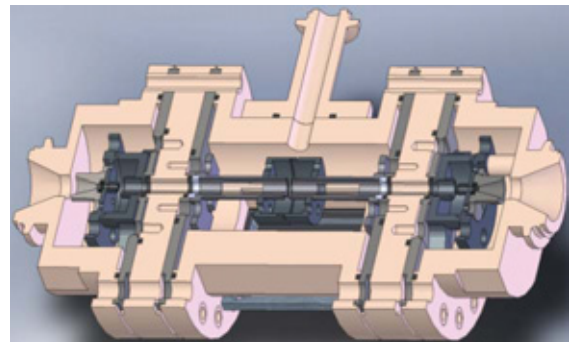


Figure 2: Cross-section view of the plasma target device.

INDUSTRIAL PROTOTYPE OF COMPACT CW LINAC*

D.S. Yurov, A.S. Alimov, B.S. Ishkhanov, N.I. Pakhomov, V.P. Sakharov, V.I. Shvedunov,
Skobeltsyn Institute of Nuclear Physics, Lomonosov Moscow State University, 119992 Moscow,
Russia

Abstract

A compact continuous-wave linear accelerator for industrial applications with an output electron energy of 1 MeV and design average beam current of 25 mA is described. The results of beam dynamics, accelerating structure, and RF system simulation are presented, accelerator construction and first results of its commissioning are described.

INTRODUCTION

1 MeV RF CW electron accelerator [1] with a maximum beam current of 25 mA for radiation technologies is being developed at SINP MSU. Accelerator commissioning started in the falls, 2013. At present accelerator is being operated for testing radiation influence at the materials properties and for investigating the radiation degradation of solar cells and circuit boards properties, designed for space operation.

ACCELERATOR DESCRIPTION

The accelerator scheme is shown in Fig. 1.

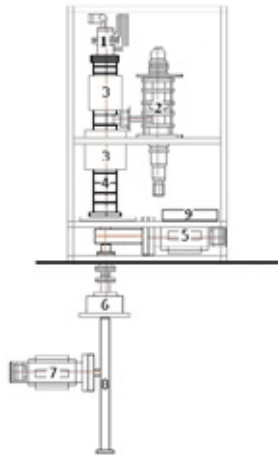


Fig. 1. The accelerator scheme.

An electron gun (1 in Fig. 1) with two focusing electrodes and an operating cathode voltage of -15 kV is located directly at the input flange of the accelerating structure (4). Focusing electrode voltage controls an output gun current from 0 to 250 mA. On-axis coupled biperiodic accelerating structure operates at a frequency of 2450 MHz. A klystron with a maximum output power of 50 kW [2] supplies the accelerating structure with RF power through the central accelerating cavity. Similar high voltage allows to use a common power supply for the klystron and the electron gun. The klystron operates in a self-oscillating mode provided by a low-power RF system (9) which fixes out a positive feedback loop

between the klystron and accelerating structure. Magnetic shielding (3) is installed above the structure. Steering coils and solenoidal lens are located in between the structure and magnetic shielding. The accelerator vacuum is provided by an ion pump (5) and a sputter-ion pump of the electron gun. Depending on beam applications different systems can be installed at the output of the accelerating structure. To measure high power beam parameters a Faraday cup with water cooling is placed at the output, provided with vacuum system comprising a rough pump and a turbomolecular pump. The beam scanning system, consisting of a beam divergence camera (8), bending magnet (6) and an ion pump (7) is used for materials irradiation. The bending magnet is powered by the voltage with an amplitude and shape required for the formation of a uniform radiation field over the entire surface of the output window with 5x70 cm² dimensions. Accelerator operating volume is separated from atmosphere by 50 microns titanium foil fixed at the beam divergence camera output flange. The accelerating structure and the klystron are cooled with distilled water. A total water consumption of accelerator cooling system is 120 l/min.

The accelerator operation is managed by the control system based on programmable microcontrollers (PMC). The system provides control of all accelerator systems via the remote terminal and information on their operation status. The control system is equipped with a set of emergency – red buttons, and operational interlocks - accelerator hall open door, poor ventilation level, bad vacuum, insufficient structure and klystron water flow, unlocked accelerator case, as well as klystron beam and body overcurrents.

Accelerator photo with the beam scanning system is shown in Fig. 2.



Fig. 2. Photo of the accelerator with the beam scanning system.

DESIGN OF A LINEAR ACCELERATOR WITH A MAGNETIC MIRROR ON THE BEAM ENERGY OF 45 MeV

A.N. Ermakov, B.S. Ishkhanov, A.N. Kamanin, V.V. Khankin, L.Yu. Ovchinnikova[#],
 N.I. Pakhomov, I.V. Shvedunov, N.V. Shvedunov, V.I. Shvedunov, I.Yu. Vladimirov, D.S. Yurov,
 Skobeltsyn Institute of Nuclear Physics, Moscow State University, Leninskie Gory 1, 119992
 Moscow, Russia

A.I. Karev, V.G. Raevsky, P.N. Lebedev Physical Institute, RAS, Leninsky prospect 53, 117924
 Moscow, Russia

Abstract

The results of calculation and optimization of pulsed linear accelerator with magnetic mirror on the beam energy, adjustable in the range of 20 - 45 MeV, designed for explosives detection and other applications are presented. The accelerator consists of an electron gun with an off-axis placed cathode with a beam hole on axis; of about 1.6 m long section of standing wave bi-periodic accelerating structure, operating at 2856 MHz, which is optimized to achieve the capture coefficient of more than 50% and of the energy spectrum width of about 2%; of a movable dispersion free magnetic mirror made with rare earth permanent magnet material. Accelerator provides acceleration of the beam with a pulse current of 100 mA to an energy of 45 MeV with RF power consumption less than 10 MW.

INTRODUCTION

Electron accelerators with energies of the accelerated beam in the range of 20-30 MeV to 100 MeV can be used for medical isotope production, activation analysis, radiation therapy, as the injector for the storage rings, used for basic research in nuclear physics.

One of the promising and new applications of electron accelerators in this energy range is the detection of explosives by photonuclear reactions [1-3]. For the practical implementation of this technique a compact, easy to operate accelerator generating pulses of accelerated beam with an energy of about 45 - 50 MeV, with a charge per pulse of about 1 μC with a repetition rate of 50 -100 Hz is required. Sufficiently high charge per pulse is necessary to provide high sensitivity of the detection method.

Previously, as such an accelerator - pulsed race-track microtrons (RTMs) with energy of 70 MeV [4] and 55 MeV [5] were considered. Advantages of the RTM as compared with linac for the energy range above 20-30 MeV are compactness and low cost. However, operating experience with these RTMs showed that practically attainable accelerated pulse current is limited to about 10 mA, besides there is serious problem associated with the high level of beam losses during acceleration, resulting in high level of induced activity in the elements of the accelerator.

As a compromise, in this paper we consider a single-section standing wave linac with a magnetic mirror. A linac with magnetic mirror – linotron - was proposed in [6]. The practical implementation of the accelerator based on this principle with maximum beam energy of 25 MeV – reflexotron - was described in [7].

Here we present a design of the electron linear accelerator with a magnetic mirror for maximum beam energy of 45 MeV.

ACCELERATOR SCHEME

A schematic view of the accelerator is shown in Fig. 1, its main parameters are listed in Table 1. Electron beam from an electron gun (1) is injected into an accelerating structure (2) and is accelerated up to energy 22.5 MeV. Then the beam is reflected back by a magnetic mirror (6) and accelerated once more to the final energy 45 MeV. To provide beam passage through the accelerating structure with minimal losses steering coils (3) and a quadrupole lens (5) are used. An accelerating field in the accelerating structure of a required level is produced by an RF system (8), which is fed by a high voltage modulator (9). A cooling system (10) is used to remove heat from the RF system, the modulator, the accelerating structure, the magnetic mirror. The steering coils and quadrupole lens are fed by current sources (11). Parts of accelerator are also: a gun power supply (7), vacuum system (12), mirror position control (13). Beam current at different points is measured by beam current monitors (4). Accelerator operation is controlled by a control system (14).

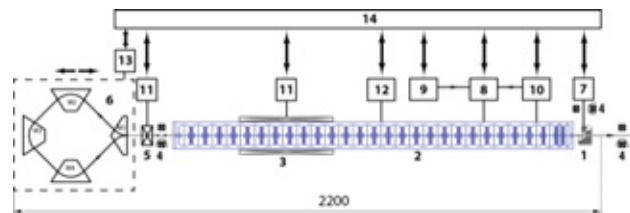


Figure 1: Accelerator scheme.

Table 1: Accelerator parameters

Parameter	Value
Max. beam energy	45 MeV
Max. pulse current	100 mA
Pulse duration	10 μs
Max. repetition rate	100 Hz
Operating frequency	2856 MHz
Max. pulsed RF power	10 MW

[#] lub.ovch@yandex.ru

THE X-RAY SYSTEM WITH SUB-SYSTEM OF SHAPING OF FAN-SHAPED BEAM AND ITS APPLICATION IN THE CUSTOMS INSPECTION SYSTEMS

A.M. Fialkovskiy, Y.N. Gavrish, P.O. Klinovskiy, K.V. Kotenko, V.P. Malyshev,
D.A. Solnyshkov,
JSC “D.V. Efremov Institute of Electrophysical Apparatus”, St Petersburg, Russia

Abstract

The analytical survey of X-ray sources based on linear electron accelerators applied in the customs inspection systems (IDK) was carried out on the grounds of requirements to customs inspection systems.

The test results of the linear electron accelerator IDK-6/9 MeV which allows to generate the X-ray mode with energies of 6 and 9 MeV are given in this article.

The questions of unification of linear electron accelerators for different IDK are also studied.

It is proved that the D.V. Efremov Institute of Electrophysical Apparatus (JSC “NIIEFA”) has the necessary scientific and technical potential and is ready to work out and to produce the X-ray sources for Automobile, Sea and Railway Inspection Systems (IDK). In addition to that the JSC “NIIEFA” is ready to organize the serial production of X-ray sources for inspection systems.

INTRODUCTION

Integration of the Russian Federation into the world economic processes leads to the significant increasing of cargo traffic through its territory. The work-load of the Customs has also increased greatly. The most serious problem is an inspection of large-sized cargos; air, sea and railway containers; vehicles and refrigerators

The effective solution is possible with using of the customs inspection systems (IDK). The operating principle of the IDK is based on scanning of monitored objects by a narrow fan-shaped beam of bremsstrahlung with the following recording of a received shadow image and its computer reconstruction by a special software.

ANALYSIS OF REQUIREMENTS

As a result of analysis of different IDK types and taking into account the customs problems the Customs of the Russian Federation formed technical requirements for different IDK types: stationary (with energy 8-9 MeV), easy-to-build (relocated) (with energy 5-6 MeV) and mobile (with energy 2,5-4 MeV). This conception was fulfilled within the framework of the Federal target program “The State border of the Russian Federation (2003-2010)”.

The experience of creating of IDK in «Ilek» as well as the analysis of development tendencies of IDK of leading world manufacture allow to form new uniformed requirements for IDK and X-ray sources. The main characteristic of IDK are given in Table 1.

Table 1: IDK main characteristics

Parameter	Mobile	Relocated	Stationary
Penetration capability for steel	260 mm	400 mm	410 mm
Detection of steel wire without a barrier, diameter not more than	2,0 mm	0,7 mm	0,5 mm
Detection of steel wire behind a 100 mm steel barrier, diameter not more than	5 mm	1.5 mm	1,5mm
Detection of steel wire behind a 250 mm barrier, diameter not more than	-	7 mm	6 mm
Contrast sensation	3%	1%	1%
Carrying capacity, pcs	80 pcs	25 pcs	25 pcs
«Dual energy» mode	+	+	+

The realisation of the parameters given in Table 1 (especially Penetration capability and «dual energy» mode) [1]) requires the accelerators with energy up to 9-10 MeV with a possibility of energy changing. The parameters are given in Table 2.

THE LINEAR ELECTRON ACCELERATOR IDK-6/9 MEV

The linear electron accelerator IDK-6/9 MeV is used as a source of the X-ray bremsstrahlung. It was developed for using in customs control systems of large-sized cargos and vehicles [2].

The base operating mode of the accelerator is 6 MeV of the bremsstrahlung which provides penetration capability for steel more than 300 mm. If necessary the accelerator can be switched to an operating mode with energy 9 MeV of the bremsstrahlung. It provides the possibility to divide studied objects in accordance with a criterion organics/non-organics using the method of “two

HISTOGRAM BASED BREMSSTRAHLUNG RADIATION SOURCE MODEL FOR THE CYBERKNIFE MEDICAL LINEAR ACCELERATOR

G.E. Gorlachey, Burdenko Neurosurgery Institute, Moscow, Russia

A.V. Dalechina, A.I. Ksenofontov, National Research Nuclear University MEPhI (Moscow Engineering Physics Institute), Moscow, Russia

Abstract

The accuracy of dose calculations is of fundamental importance in treatment planning of radiation therapy. The dose distributions must be calculated and verified by an accurate algorithm. The Monte Carlo simulation (statistical method, based on random sampling) of radiation transport is the only method that makes it possible to perform high-precision dose calculations in the case of a complex geometry. The main bottleneck for the application of this method in practical planning of radiation therapy is the lack of a general virtual source model of the accelerator radiation source. There are several approaches that have been described in the literature [1].

The goal of this work is to build a source model, based on histogram distributions, to represent the 6 MV photon beams from the CyberKnife stereotactic radiosurgery system [2] for Monte Carlo treatment planning dose calculations. The transport of particles in treatment head of CyberKnife was simulated. Energy, radial and angular distributions were calculated. Source model was created on the base of the cumulative histograms. This approach provides producing an unlimited number of particles for the next dosimetric planning. Results of source modelling were verified in comparison with full-scale simulation without model. Good agreement was shown with calculations using the source model of the linear accelerator treatment head.

INTRODUCTION

The human body consists of tissues and cavities with different physical and radiological properties. Conventional, deterministic dose algorithms cannot provide accurate calculation dose distributions in some difficult cases, particularly in heterogeneous patient tissues. The method Monte Carlo is the most accurate method for patient dose calculations in radiotherapy. This method allows to simulate processes of material-radiation interaction inside the radiotherapy units and in the patient body [1]. The MC method, as applied to radiation transport problems, has been described by Rogers and Bielajew as follows: "The Monte Carlo technique for the simulation of the transport of electrons and photons though bulk media consists of using knowledge of the probability distributions governing the individual interactions of electrons and photons in materials to simulate the random trajectories of individual particles" [1]. The one of the drawbacks of Monte Carlo simulation as applied to radiation transport has been long calculation times. However, the development computer technologies

has significantly reduced calculation times. MC treatment planning algorithms become widespread in the radiotherapy community. The other aspect, which has great influence on using MC method in routine clinical practice, is the general virtual model of the linear accelerator treatment head. The general virtual model has to permit to apply algorithm of dose calculations for any accelerator and substantially improve accuracy. In addition, beam modelling can effect considerable savings in computing time and disk space [3]. A beam model is any algorithm that delivers the location, direction, and energy of particles to the patient dose-calculating algorithm [1]. Accurate source model is an essential requirement for accurate dose calculation within the patient's body. There are three possible approaches, described by different authors: direct use of phase space information from the accelerator treatment head simulation, development of multiple-source models, particles are grouped by the location of their last interaction and then scored at the phase-space plane leading to subsources [1]. Fluence distributions for each subsurface may be reconstructed from the phase-space data in the form of correlated histogram distributions. Other approach is measurement-driven models. Information for the model can be deconvolved from measured data. The goal of this work is to characterize the 6 MV photon beams from the Cyber Knife treatment head and develop the source model to accurately represent and reconstruct the beam. We have developed source model based on a phase space data, which contains histogram distributions.

MATERIALS AND METHODS

CyberKnife

The CyberKnife system used a flatterer-filter-free 6MV Linac accelerator mounted on robotic arm (Kuka, Augsburg, Germany) with 6 degrees of freedom (rotation and translation). The CyberKnife has been used to treat prostate, lung, brain, spinal cord, liver or pancreas with millimetric conformity [4]. Circular treatment fields, ranging from 60 to 5 mm field size in diameter at source detector distance (SSD) of 80 sm. are created using either 12 fixed collimators or an Iris variable aperture collimator. In this work, the 800 MU/min version installed in Department of Radiology and Radiosurgery of N.N. Burdenko Neurosurgical Institute, mounted with fixed collimators was studied.

MAGNETIC BUNCHER ACCELERATOR UELV-10-10-T-1 FOR STUDYING FLUORESCENCE AND RADIATION-PHYSICAL RESEARCHES

Yu.S. Pavlov, B.B. Dobrohotov, B.A. Pavlov, O.N. Nepomnyaschy, V.A. Danilichev, IPCE RAS, Moscow, Russia

Abstract

Accelerator UELV-10-10-T-1 is equipped with special system of injection and magnetic buncher with the purpose of generation picoseconds the beam duration 50 ps with the current 150 A at energy 10 MeV for studying fluorescence and radiation-physical researches. For maintenance of the magnetic bunching the accelerator works in the mode of the reserved energy when duration of the pulse of injection (2,5 nanoseconds) is much less than time of filling of a wave guide energy (100 nanoseconds). At a pulse microwave of capacity 10 MW the energy which has been saved up in the wave guide, makes about 2 J. It provides an opportunity of a cutting collimator separately chosen bunch after scan of "package" by a rotary magnet. After an output from the accelerator the package electrons from 3-5 bunches acts in magnetic buncher consisting of two electromagnets. In buncher the beam is scanning as "fan", and then focused. At a current of the beam 30 A in the pulse duration 2,5 nanoseconds distinction on energy between the adjacent bunches makes of 300 keV, that provides an opportunity of the cutting collimator the separate chosen bunch after space scanning with a rotary magnet. At a magnetic bunching electrons in "head" of a bunch have the big energy and are transported on trajectories with the big radius than "tail" electrons. Thus "compression" of the bunch on time is attained and accordingly the charge of a bunch increases.

purpose of generation picoseconds beam for studying fluorescence and radiation-physical researches [1-7]. The basic connections between the equipment of system of formation of accelerator UELV-10-10-T-1 are submitted on a function chart (see Fig. 1).

MAGNETIC BUNCHER TECHNOLOGY

Appearance of system of formation is shown in Fig. 2. The principle of action of system of formation is based on features of work of the accelerator electrons in a mode of use of the reserved energy. In such accelerator at sufficient loading the current arises significant reduction of energy electrons between the next bunches, as is used for allocation of a separate clot from an initial pulse with the help of a dividing electromagnet.

Duration of bunch makes approximately 0,1 periods of the microwave of fluctuations of the generator of the accelerator (~ 50 ps).

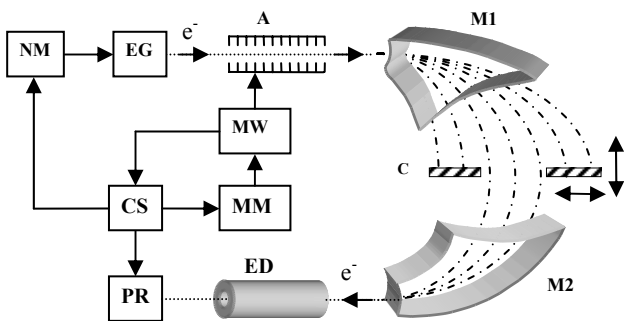


Fig. 1: A function chart of system of formation picoseconds pulses on accelerator UELV-10-10-T-1. NM - nanosecond modulator; EG - an electronic gun; A - the accelerator; M1 - a rejecting magnet; M2 - a focusing magnet; C - collimator; ED - the electro-optical detector of parameters of the beam; PR the pulse registrar; CS - the circuit of synchronization; MM - the modulator magnetron; MW - magnetron.

Accelerator UELV-10-10-T-1 is equipped with special system of injection and magnetic buncher with the



Fig. 2: Appearance of system of formation picoseconds pulses on accelerator UELV-10-10-T-1.

For maintenance of a magnetic grouping the accelerator works in a mode of the reserved energy when duration of a pulse of injection (2,5 ns) is much less than time of filling of a wave guide energy (100 ns). At pulse power of the microwave 10 MW the energy which has been saved up in a wave guide, made about 2 J. At a pulse current more than 10 A distinction energy the next clots makes about 200 keV. It provides an opportunity of a cutting collimator separately chosen clot after scanning of "package" by a rotary magnet. After an output from the accelerator the bunch electrons as a package from 3-5 clots acts in magnetic buncher consisting of two electromagnets. In buncher the beam is scanning as "fan", and then focused.

Magnetron with capacity 10 MW in a pulse allow "to reserve" in the wave guide energy up to 2 J and to spend her for small time of injection electrons (2,5 ns) in

NEUTRON RADIATION MONITORING OF THE THERAPEUTIC PROTON BEAM TRANSPORTATION

V. Skorkin, INR RAS, Moscow, Russia

Abstract

A monitoring system online controls a therapeutic proton beam by measuring a secondary neutron radiation from the beam losses. The system consists of neutron detectors in the transport path passage from Linac to the facility of proton therapy and terminal controller connected to the computer. The neutron detectors measure a level of the secondary neutron radiation in real time along of the transport channel, near the formative elements.

INTRODUCTION

A result of the proton beam loss is formed neutron secondary radiation. The neutrons in the transport channels can be registered with help of fast neutron detectors. A level of secondary neutron radiation in the transport path of the proton beam is proportional to the average beam current and beam losses [1]. Fig. 1 shows the neutron radiation in the transporting channel at the average beam current of 0.7 mA to 35 mA.

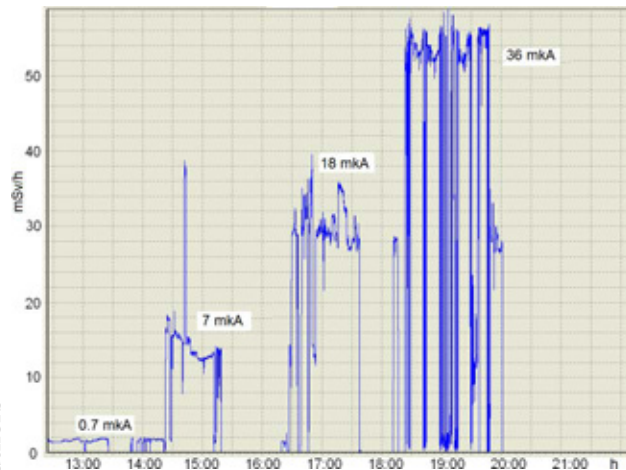


Figure 1: Diagram of the neutron radiation dose power measured in the beam transport channel.

The information about the neutron radiation intensity allows you to determine beam loss in different parts of the transport channel. The neutron monitor of the proton beam transport allows you to measure the temporal variations of the beam intensity in local areas transporting channels. These changes arise are due to changes in operating mode of the channels or instability of the elements forming the beam transport channels.

MONITORING THERAPEUTIC BEAM

The system monitoring the beam transport includes a terminal controller, which is connected to the computer. The neutron detectors are located along the ion guide, near the formative elements of the transport channels and

ISBN 978-3-95450-170-0

the target of the proton therapy facility. The layout of neutron detectors of the system monitoring the proton beam transportation in Complex of proton therapy is illustrated in Fig. 2.

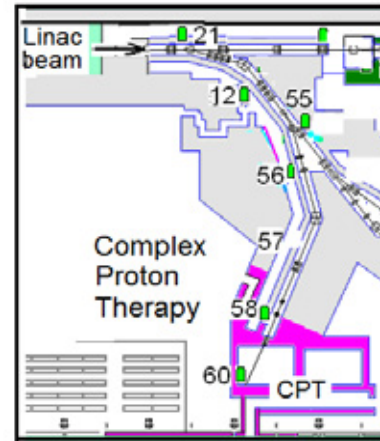


Figure 2: Complex of proton therapy.

The detectors in the transport channels are used for the beam loss measurements. Software module monitoring system determines and shows the dose power of the secondary neutron radiation in real time. The changing of the intensity of the beam of protons due to the unstable form of the elements in the medical channel caused by blocking is shown in Fig. 3.

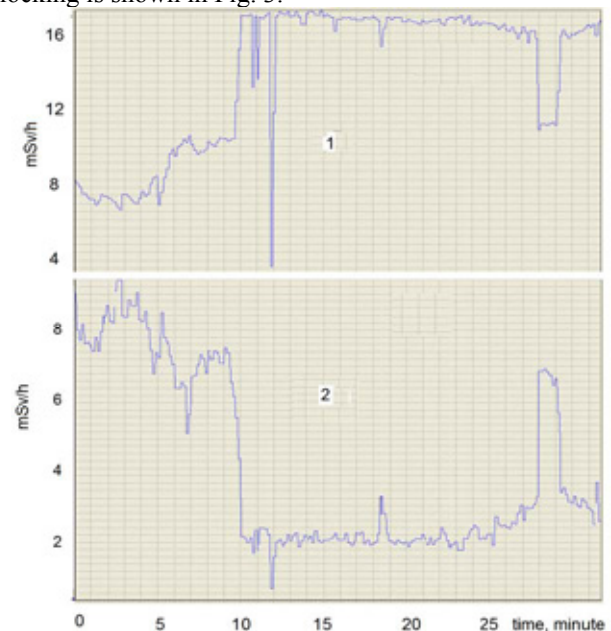


Figure 3: Diagram of the neutron radiation intensity in the beam transport channel. 1 – neutron background near the bending magnet; 2 - neutron background in front of the collimator.

SMALL-SIZE HIGH-PERFORMANCE ARSA ACCELERATORS FOR ON-LINE TESTING FOR ECB RADIATION HARDNESS

S.L.Elyash, S.P.Pukhov, A.V.Rodigin, A.L.Yuryev, RFNC-VNIIEF, Sarov, Russia

Abstract

At present an extent of electrical engineering item tests for pulsed ionizing radiation (IR) hardness has abruptly increased. Solving of such problems with the help of only powerful simulators seems impossible due to significant time and material costs. Results of studies, performed in RFNC-VNIIEF, RISI and other organizations [1], have shown that optimal combination of small-size high-performance accelerators ARSA and powerful simulators allows a significant reduction of terms and costs for radiation tests, an increase of fidelity and self-descriptiveness of the results obtained.

As opposed to IC test simulation methods using laser radiation, ARSA accelerator employment allows approaching of the process inspection conditions to the real-life environment [2].

BRIEF DESCRIPTION OF ARSA ACCELERATOR

ARSA is a small-size pulsed electron direct-action accelerator with oil insulation [3, 4], see fig. 1. It consists of a high-volt unit 1 with accelerating tube 4, located in the sealed container, charger 2 and a control board 3. A specific feature of a ten-cascade Marx generator used in the accelerator is a pulsed charging of reservoir capacitors. Cascade current is switched with the aid of metal-ceramic pressurized spark gaps [5].

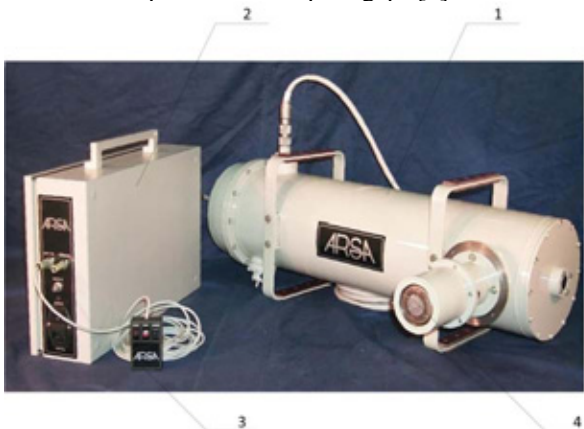


Figure 1: Small-size pulsed accelerator ARSA.

A sealed-off accelerating tube with a through target represents a vacuum diode with an explosive-emission cathode and titanium anode. Anode of 50 μm thickness is an output window for electron beam. To generate bremsstrahlung radiation onto the outer tube window surface there is mounted a target made of 50 μm thick tantalum foil and 2 mm thick aluminum filter for absorption of electrons passed through the window and target. Edge type cathode of diameter 10 mm supplies a homogeneous radiation spot.

A PULSED FIBER-OPTIC MONITOR-DOSIMETER WITH A DETECTOR CHANNEL FOR RADIATION PULSE SHAPE MONITORING

For the purposes of on-line monitoring of small-size pulsed ARSA accelerators' dose a fiber-optic monitor-dosimeter (MD) [6] has been developed, see fig. 2. It is structurally unified and used together with the accelerator's control panel. For MD one foresees also a possibility for autonomous operation in the mode of dose monitoring.



Figure 2: Fiber-optic monitor-dosimeter, combined with ARSA control panel.

MD represents a combination instrument, comprising:

- fiber-optic pulsed X-ray dose meter;
- pulse counter with nonvolatile memory for control over the facility life;
- storage device for each pulse dose values;
- pulse dose adder in a series;
- blocking device upon a specified dose is reached;
- port for reading of accumulated data into the computer.

Fiber-optic pulse dosimeter has a number of advantages:

- instant obtaining of measurement result as compared to the thermoluminescent dosimeter;
- high noise immunity, low detector's degradation as compared to meters based on semiconductor diodes;
- availability of new service-feature features (counter, adder, nonvolatile memory, port), due to employment of modern micro-processor.

A radiation detector in the device is scintillator CsI(Tl). The light is transferred from the detector to a photodetector through plastic fiber-optics of 1 mm diameter. A pin-photodiode is used as a photodetector. A peculiar feature of MD structure is a one-piece assembly

DEPTH DOSE DISTRIBUTION OF THE BREMSSTRAHLUNG GENERATED BY THE BETATRON OB-4 IN DIFFERENT ENVIRONMENTS

I. Miloichikova, V. Ruchyeva, E. Shuvalov, S. Stuchebrov, TPU, Tomsk, Russia

Abstract

In the paper the dosimetric parameters measurement technique of the bremsstrahlung generated by betatron OB-4 is described. The radiation dose measurement results from the bremsstrahlung generated by betatron are shown. The depth dose distributions of the bremsstrahlung generated by betatron obtained with the help of the solid thermoluminescent detectors DTL-02 and the dosimeter UNIDOS E equipped with a PTW Farmer cylindrical ionization chamber type 30013 in the different environments (in the air, in the water and in the lead) are illustrated.

INTRODUCTION

Within a research framework of the development of the new methods to reduce radiation doses for the objects under radiographic analysis, it was proposed to use the pulsed irradiation source synchronized with the detecting device. Such X-ray visualization setups based on the pulsed X-ray generator RAP-160-5 were created in the Department of Applied Physics of the Tomsk Polytechnic University. The previous tests showed a significant radiation dose decline to the objects in comparison with conventional techniques [1, 2]. For estimation of the suitability of using the portable betatron OB-4 as a source of bremsstrahlung for visualization purposes it is necessary to investigate the dosimetric parameters of the device.

The research objectives are:

- to obtain the depth dose distribution in the air, lead and water of the pulsed bremsstrahlung generated by the betatron OB-4;
- to analyse the suitability of using the compact pulse betatron OB-4 as a source of bremsstrahlung for visualization purposes.

MATERIALS AND METHODS

Emitting source

The portable betatron OB-4 was used as a source of emission. This betatron is used as a pulsed source of bremsstrahlung. The material of the target is tungsten (0.6 cm thick). The maximum kinetic energy of the electrons is 4.0 MeV.

The general quantities of the portable betatron OB-4 are: the frequency of radiation impulse is 400 Hz; the duration of one pulse is about 15 μ s [3].

Dosimetric equipment

The main problem associated with the dosimetry of the pulsed radiation is the response rate of the dosimeters.

This problem can be solved by using the storage type of the detectors. The solid thermoluminescent dosimeters DTL-02 were used as dosimetric equipment for initial estimation of the radiation doses. The thermoluminescent material of the detectors is LiF: Mg, Ti. The dosimetric complex based on the thermoluminescent dosimeters DTL-02 is designed for the personal dosimetry. The dosimeters DTL-02 can work in the energy range of gamma radiation from 15 keV to 10 MeV, the dose range varies from 20 μ Sv to 10 Sv [4].

The dosimetry protocol for megavoltage photon beams (with nominal energies between 1.25 and 50 MeV) adopted by the AAPM is recommended to use the ionization chambers as the basis for measurements [5]. The universal dosimeter for radiation therapy and diagnostic radiology UNIDOS E equipped with a PTW Farmer chamber type 30013 was used in the experiments [6, 7].

The PTW Farmer cylindrical ionization chamber type 30013 is used for absolute photon and electron dosimetry. This chamber is waterproof and can be used in water phantoms. The main parameters of the cylindrical ionization chamber type 30013 are: the nominal photon energy range is from 30 keV to 50 MeV; the electron energy range is from 10 MeV to 45 MeV; the dose range varies from 0.1 mGy to 1 Gy; the sensitive volume is 0.6 cm³ [7].

Experimental setup

The irradiation scheme is shown in the figure 1. The irradiation source (1) was placed in lead dome (2) with the output window. The detector (3) was positioned on the radiation axis opposite the output window.

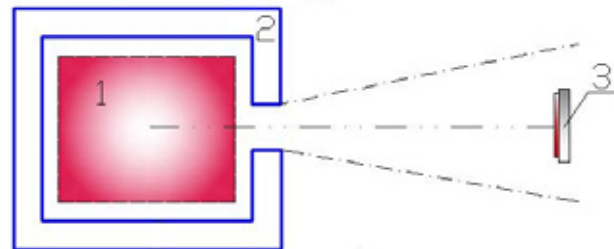


Fig. 1. The irradiation scheme: 1 – the portable betatron OB-4; 2 – the lead dome; 3 – the plane-parallel ionization chamber type 23342

For obtain the depth dose distribution in the lead of the bremsstrahlung generated by the betatron OB-4 the lead plates with the different thickness (0.3, 0.6, 0.8, 5.0 cm) was used.

For obtain the depth dose distribution in the water of the bremsstrahlung generated by the betatron OB-4 the

STATUS OF EXPERIMENTS ON SURFACE MODIFICATION OF MATERIALS ON THE ACCELERATOR HIP-1

B.B. Chalykh, A.V. Kozlov, R.P. Kuibeda, S.V. Andrianov, D.A. Aparin, P.A. Fedin, N.N. Orlov, A.A. Nikitin, A.A. Bogachev, A.A. Aleev, A.A. Andreev, G.N. Kropachev, N.A. Iskandarov, A.A. Golubev, NRC KI SSC of RF ITEP, Moscow, Russia
S.V. Rogozhkin, T.V. Kulevoy, NRC KI SSC of RF ITEP, Moscow, Russia; NRNU MEPhI, Moscow, Russia

Abstract

Ion implantation is an effective method for materials surface modification for various technological applications. The most common examples of its use are an increase of the durability, corrosion resistance, heat resistance for various industrial steels and special alloys for applications in biology and medicine, strengthening and changes in the morphology of the surface layers of polymers. Work in this direction is underway at the accelerator HIP-1 in ITEP. To provide the experiments, the beams of iron, vanadium and titanium generated by vacuum-arc metal ion source, as well as ion beams of nitrogen generated by duoplasmatron ion source are used. Several sets of experiments for the modification of the surface features were carried out. The transmission electron microscopy (TEM) and tomographic atom-probe microscopy (TAP) were used for samples analysis after ion beam treatment.

of carbon (about 8×10^{17} ions / cm^2) allows achieving a significant increase in durability by forming a carbon layer on the product surface [5]. Improvement of the corrosion resistance can be obtained by implantation of chromium and rare earth metals ions [6]. Since the implantation of different chemical element ions into material can significantly modify the properties of their structure in sub-surface layers, the use of composite beams may be the best technology in the preparation of materials for specialized applications.

To provide experimental activity, the beams of iron, vanadium and titanium generated by vacuum-arc metal ion source, and beams of nitrogen generated duoplasmatron were accelerated in the heavy ion HIP-1 (Heavy Ion Prototype). Several sets of experiments for the modification of the surface features were carried out. The results of the first experiments of surface modification by ion beams are presented.

INTRODUCTION

Ion implantation is widely used as a method for modification of materials in order to improve their physical and chemical parameters. The ions used can be divided into light ones (typically nitrogen, carbon, oxygen and boron) and heavy ones (chrome, titanium, and tungsten). For biomedical applications, it is effective to use silver ions, copper and other elements to improve the bactericidal properties of steels, titanium alloys, CoCr alloys without losing their strength and corrosion resistance [1]. To improve the wear resistance and durability of industrial steels, implantation of nitrogen ions is used widespread [2, 3]. It is shown that the hardening depends not only on the dose of implanted nitrogen, but also on the chemical composition of the material to be modified and formed as a result of nitride complexes [4]. Furthermore, implantation of high doses

FACILITY AND EXPERIMENT

The scheme of RFQ HIP-1 is shown on Fig.1. The accelerator assembly consists of the 100 kV terminal (1), low energy beam transport (LEBT) line with two electrostatic Einzel lenses (3) and diagnostic chamber (2), 27 MHz RFQ section and channel with 3 magnetic quadruple lenses (L1,L2,L3) and diagnostic station (5) at the output of the accelerator.

The accelerator allows the two types of experiments: at "low energy" when the irradiation of samples is carried out at the output of the injector inside the diagnostic chamber A (fig.1. pos.2) for further study by transmission electron microscopy (TEM) and tomographic atomprobe microscopy (TAP). Another type is the samples irradiation by "high energy" beams at the output of the accelerator (fig.1. pos. 5) for the further samples testing by transmission electron microscopy [7].

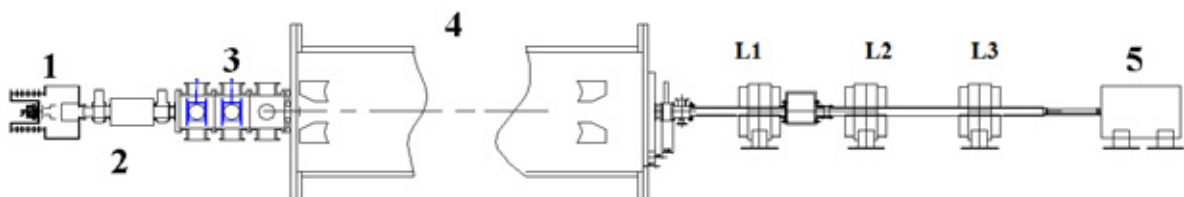


Figure 1: ITEP RFQ HIP-1. 1 - injector, 2 - diagnostic chamber A, 3 - electrostatic lens, 4 - RFQ, 5-diagnostic chamber B, L1,L2, L3 –quadruple lenses.

METHOD OF MEASURING FAST NEUTRON FLUENCE USING THE PLANAR SILICON DETECTORS

A.I. Shafronovskaia, N.I. Zamyatin, A.E. Cheremukhin, LHEP JINR, Dubna, Russia
(on behalf of the QUINTA Collaboration)

Abstract

The technique reported of fast neutron fluence measurements using silicon detectors. One of the main macroscopic effects at radiation damage of silicon detectors by fast neutrons is increase of the reverse current. The increment of the reverse current detector is a linear dependence on fast neutron fluence and is determined by the formula (Eq. 1):

$$\Delta I = \alpha_I \times F \times V, \quad (1)$$

where $\Delta I = (I_{\text{irrad.}} - I_{\text{nonirrad.}})$ (A) – the measured increment of the reverse dark current after irradiation of the detector normalized to temperature of +20°C, $\alpha_I = (5 \pm 0.5) \times 10^{-17}$ (A/cm) – current constant radiation damage of silicon for neutrons with energy 1 MeV, F (cm²) – equivalent fluence of fast neutrons with energy 1 MeV, $V = d \times S$ (cm³) – the volume of the detector at the full depletion voltage. The experimental results of measurements of fast neutron fluence with silicon detectors are obtained on the pulsed fast neutrons reactor (IBR-2, channel #3) and on the experimental facility QUINTA JINR, Dubna.

MECHANISM OF RADIATION DAMAGES BY FAST NEUTRONS OF SILICON (SI-DETECTORS)

Fast neutrons with energy of $E_n > 100$ keV are create in volume of silicon radiation damages in the form of violations of a crystal lattice (knocking-out by a neutron of primary atom from lattice site and then created a cascade of defects already beaten out atoms).

Reverse thermogeneration current of the detector grows linearly [1] with increasing fast neutron fluence (see Eq. 1).

The physical meaning of the constant α_I are following: when irradiated silicon detector volume 1cm³ neutrons with an energy of 1 MeV and a fluence value of 1 n/cm² current of the detector is increased due to radiation damage to 5×10^{-17} A at +20°.

RADIATION DAMAGE OF SILICON DETECTORS UNDER IRRADIATION WITH FAST NEUTRONS ($E_N > 100$ KEV)

What Happens in Irradiated Silicon

Knocking-out of atom of Si from a crystalline grid with formation of vacancy (V) and interstitial atom Si (I).

V and I to form - electrically active deep centers (VV, VO, VP, IC, I VP, etc.).

Effects of Deep Centres (see Fig. 1)

- Thermal generation / recombination of carriers in volume leads to an increase in reverse (dark) current of the detector, leading to increased noise and power dissipation on the detector.
- Capture (e-h)-pair reduces the primary ionizing charge collection efficiency and, consequently, to reduce the signal from the ionizing particles.
- Compensation impurity results in a change of volume resistivity values of the detector and to change the operating voltage (voltage of full depletion of the detector), respectively.

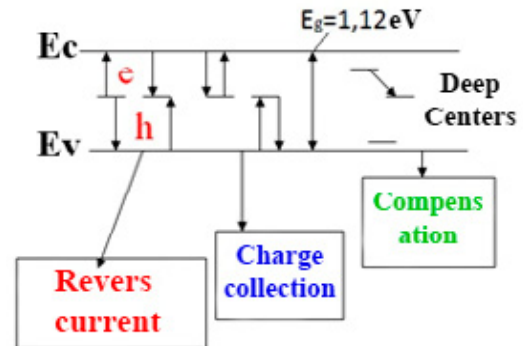


Figure 1: Effects of deep centers.

Fig. 2 shows function of defect formation of $D(E)$ in $\text{MeV} \times \text{mb}$, (Ougouag) and the function NIEL-FN-522 in $\text{keV} \times \text{cm}^2/\text{g}$, (van Ginneken) [2].

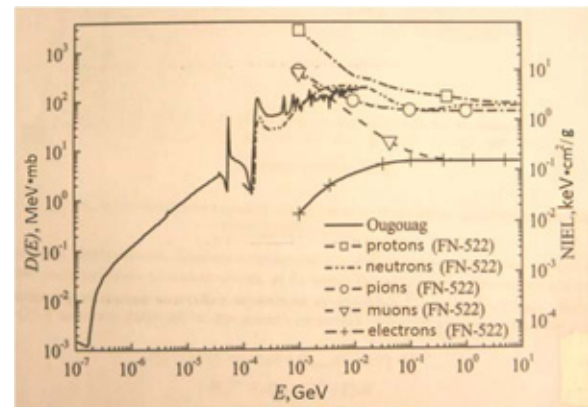


Figure 2: Function of defect formation of $D(E)$ and the function NIEL-FN-522.

RESULTS OF LIA-2 OPERATION

P. Logachev, A. Akimov, P. Bak, M. Batazova, A. Batrakov, D. Bolkhovityanov, A. Eliseev, G. Fatkin, A. Korepanov, Ya. Kulenko, G. Kuznetsov, A. Pachkov, A. Panov, A. Starostenko, D. Starostenko, BINP SB RAS, Novosibirsk, Russia
 A. Akhmetov, S. Hrenkov, P. Kolesnikov, E. Kovalev, O. Nikitin, D. Smirnov, RFNC-VNIITF, Snezhinsk, Russia

Abstract

Recent results of LIA-2 operation are presented. High quality of intense electron beam has been achieved in design intervals of energy and current. All key elements of accelerator based on domestic technology successfully passed through long term operational tests.

INTRODUCTION

Linear induction accelerators are widely used now for x-ray flash radiography of high optical density objects [1]. This particular application of linear induction accelerators is very exigent to high current electron beam quality. The value of electron beam emittance determines the minimum electron beam spot size on the target, and thus the space resolution of this method. The first experimental results of LIA-2 operation at BINP were presented three years ago [2]. Now this accelerator is successfully used for X-ray flash radiography in RFNC VNIITF [3]. High quality electron beam produced by LIA-2 together with proved reliability of new technical solutions [4], [5], [6] make a good base for full scale 20 MeV radiographic LIA project.

FEATURES OF LIA-2 OPERATION IN RADIOGRAPHIC REGIME

The radiographic regime of LIA-2 operation restricts unfortunately the maximum electron beam energy and current. This phenomenon connected with X-ray conversion target explosion and ballistic penetration of small tantalum drops into accelerating bit-slice HV insulator and LIA-2 diode. This leads to significant breakdown strength reduction both in accelerating tube and diode (see Fig. 2). Thus reliable LIA-2 operation with X-ray conversion target explosion can be held up to 1.6 MeV and 1.5 kA of electron beam energy and current. The maximum energy and current for reliable operation without target explosion were obtained at the level of 2 MeV and 2 kA. It corresponds to design values. X-ray conversion target is placed at 3.9 m from the cathode. Electron beam energy deposition in 0.5 mm thick tantalum target for 1.6 MeV, 1.5 kA, 200 ns can be calculated as 230 J (1 MeV of energy loss per electron). It corresponds to 5000 K of melted target part on Fig.1 and about 1 bar of saturated vapor pressure of tantalum. There is a maximum size of hole in the target for fixed beam energy, current and pulse duration (in the case of increasing of the beam diameter on the target, the hole does not appear). For this particular case the maximum diameter of the hole is equal to 6 mm (see Fig. 1 and 4).



Figure 1: Maximum hole diameter in 0.5 mm thick tantalum target for 1.6 MeV, 1.5 kA, 200 ns electron beam.

In the case of the best focusing of electron beam on the target the minimum hole diameter is 1 mm (see Fig. 4) and peak tantalum temperature is about 200000 K. This is target explosion.

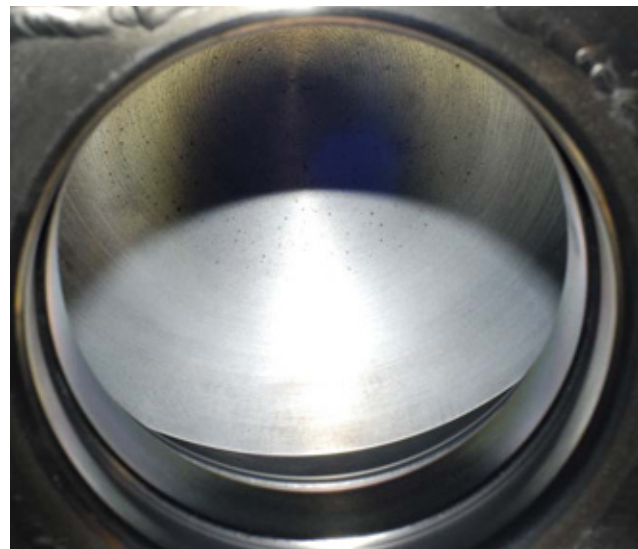


Figure 2: Damage of the central part of LIA-2 cathode by tantalum drops from the target. View on the cathode through the anode aperture.

The damage of the cathode central part due to target explosion (see Fig. 2) leads to emission degradation from

EXPERIENCE IN RESEARCH, DEVELOPMENT, CONSTRUCTION AND COMMISSIONING OF NORMALLY CONDUCTING ACCELERATING STRUCTURES

L.V. Kravchuk, V.V. Paramonov *, INR of the RAS, Moscow, 117312, Russia

Abstract

The experience and results of research, development, construction and start of normally conducting accelerating structures for high intensity hadron linear accelerators at medium and high energies is summarized. Created methods and obtained results provided construction and start of operation of accelerating system in INR H- linac with designed energy 600 MeV. The research results allow generalize the properties of high energy structures and develop methods and criteria for improvements. Basing on research results, the high energy accelerating structure, which surpasses analogues in the total list of parameters, is proposed and tested.

INTRODUCTION

Instead of progress in development of superconducting structures for high energies, the normal conducting structures have the high value for high energy intense hadron linacs. The report presents briefly the main steps and INR results in this activity.

DAW CONSTRUCTION FOR INR LINAC

INR activity in accelerating structures originates from construction of accelerating system for high energy part of INR linac, Fig. 1. This system consists of 27 four-tanks cavities, operating at $f_a = 991$ MHz. DAW tanks contain from $N_m = 18$ to $N_m = 27$ DAW modules, see Fig. 3a. The total number of DAW modules in the system is ~ 2400 and the system length is $\approx 300m$.

DAW structure, invented by V.G. Andreev, [1], for INR



Figure 1: DAW accelerating structure in the INR linac.

linac was developed and tested in RTI AS USSR and the framework technology was established. The first three steps – hot sludge to $\approx 500mm$ blanks from 170mm OFC rods, pre-forming with stamping and draft pre-turn were performed in industry under INR and RTI monitoring. Another steps of construction, starting from accurate processing and continuing through RF tuning, brazing of DAW tanks and finishing with system commissioning, were performed by INR in-house. For mass production, all steps in construction, such as reasonable and motivated tolerances for DAW modules treatment, fast and precise RF tuning of DAW tanks, HOM displacement and so on, were optimized and improved. In the DAW construction there were no DAW modules lost due to non-compliance.

Individual RF tuning for frequencies of operating f_a and coupling f_c modes for DAW modules is not required, due to coupling coefficient $k_c \sim 40\%$ of the structure. DAW tanks were tuned in assembly of N_m modules. Coupling mode can not be excited in DAW tanks and to close the stop band non direct methods for stop band width $\delta f = f_c - f_a$ definition are required. Due to large k_c , DAW dispersion curve in the f_a vicinity is essentially not linear and linear approximation from nearest modes $\delta f = f_u^{(1)} + f_d^{(1)} - 2f_a$, tolerable for structures with $k_c \sim 5\%$, Side Coupled Structure (SCS) and Annular Coupled Structure (ACS), results in $\delta f \sim 1MHz$. High order approximations for δf definition were developed for DAW tanks tuning, [2], resulting in $\delta f \leq 100kHz$. Basing on DAW particularities, the optimized procedure for tanks tuning was developed, [3], minimizing number of tuning operations.

The High Order Modes (HOM) with field variations on

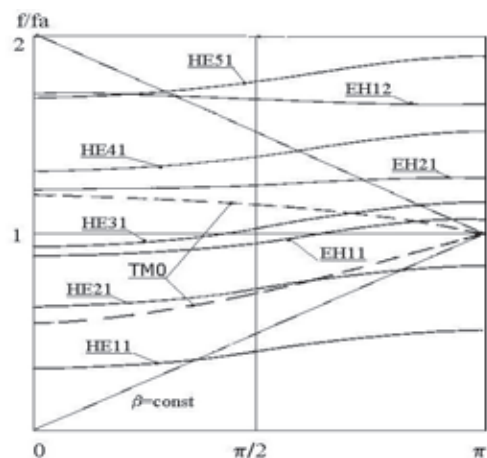


Figure 2: HOM dispersion diagram for the DAW, $\beta = 0.43$.

STATUS OF THE NUCLOTRON

A. Sidorin, N. Agapov, A. Alfeev, V. Andreev, V. Batin, O. Brovko, A. Butenko, D.E. Donets, E.D. Donets, E.E. Donets, A. Eliseev, A. Galimov, E. Gorbachev, A. Govorov, E. Ivanov, V. Karpinsky, H. Khodzhbagiyani, A. Kirichenko, V. Kobets, A. Kovalenko, O. Kozlov, K. Levterov, V. Mikhailov, V. Monchinsky, A. Nesterov, A. Philippov, S. Romanov, N. Shurkhnov, G. Sedykh, I. Slepnev, V. Slepnev, A. Smirnov, G. Trubnikov, A. Tuzikov, B. Vasilishin, V. Volkov, JINR, Dubna, Moscow Region, Russia.

Abstract

Since last RuPAC five runs of the Nuclotron operation were performed. Diagnostic and control systems were improved. Commissioning of new quench detection system was completed. Deuteron beam was accelerated up to maximum design energy corresponding to 2 T of the dipole magnetic field. Stochastic cooling of coasting deuteron, coasting and bunched carbon beams was obtained. First run with new heavy ion source was performed. Results of these and other works are presented.

INTRODUCTION

The Nuclotron is used presently for fixed target experiments on extracted beams and experiments with internal target. The program includes experimental studies on relativistic nuclear physics, spin physics in few body nuclear systems (with polarized deuterons) and physics of flavours. At the same time, the Nuclotron beams are used for research in radiobiology and applied research.

Five Nuclotron runs (#46 ÷ #50) at total duration of about 4000 h were performed in the period from November 2012 till June 2014. About 70% of the runs were spending for experiments with accelerated beams (cooling down and preparation of the machine required about 25%). For more efficient usage of the beam time, during the run #49 the regime with two parallel users was realized routinely: experiment with internal target at the first plateau and beam extraction at the second one.

Improvement of the cryogenic complex performance, better cooling conditions of the magnetic system, modernization of quench detection system permitted gradual increase of the beam energy. As result during the run #48 (December 2013) the carbon beam was accelerated and extracted at maximum design energy corresponding to dipole magnetic field of 2 T.

Deuteron, lithium, carbon and argon beams were delivered for the experiments. Increase of the beam intensity and widening of the ion species are related with construction of three new ion sources: SPI (Source of Polarized Ions), LIS (Laser Ion Source), Krion-6T (ESIS type heavy ion source) [1]. New powerful laser was tested for the carbon beam generation during the run #48. For the first time Krion-6T was operated at the Nuclotron during the run #50.

Development of slow extraction system resulted in realization of acceptable quality of the extracted beam in the interval of the spill duration from 60 ms to 20 s.

In addition to the implementation of the current physics program the Nuclotron having the same magnetic rigidity as the future NICA collider [2] and based on the same type of the magnetic system is the best facility for testing of the collider equipment and operational regimes. Development works for NICA performed during recent Nuclotron runs include the testing of elements and prototypes for the MPD (Multy Purpose Detector which will be operated at the collider) using extracted deuteron beams; operational tests of the automatic control system based on the Tango platform, which has been chosen for the NICA facility; tests of diagnostic equipment for the Booster – small superconducting synchrotron constructing in the frames of the NICA project to improve the Nuclotron performance.

Simulation of the collider magnetic system operational conditions was performed at the Nuclotron during runs #45-47 (in years 2012-2013). This presumed test of the Nuclotron systems in the operational mode with long plateau of the magnetic field. In the run #45 the circulation of accelerated up to 3.5 GeV/u deuteron beam during 1000 seconds was demonstrated. During the runs #46 and #47 such a regime was used for test of stochastic cooling at the Nuclotron, which is an important phase of the NICA collider cooling system design.

In this report we are concentrated on the most important results of these works.

DEVELOPMENT OF THE ION SOURCES

The new LIS is based on commercially available Nd-YAG laser LPY 7864-2 providing output energy of 2.8 J at wave length of 1064 nm [3]. The new laser was investigated at test bench (Fig. 1) during outman 2013 and thereafter it was used at the Nuclotron run.

During the run the source and the LU-20 (linac using for injection into the Nuclotron) operation was optimized at acceleration of C^{5+} and C^{6+} ions. The current of C^{6+} beam reach to about 1.5 mA at the linac output. The pulse duration was of about 3 μ s. Routinely the injector was operated in C^{5+} mode because of larger output beam current (up to 3 mA) and slightly longer the pulse duration - about 4 μ s (the beam revolution period in the Nuclotron is about 8 s at injection energy). The carbon

ACCELERATOR COMPLEX BASED ON DC-60 CYCLOTRON

M. Zdorovets[#], I. Ivanov, M. Koloberdin, S. Kozin, V. Alexandrenko, E. Sambaev, A. Kurakhmedov, A. Ryskulov, Institute of Nuclear Physics, Astana, Kazakhstan

Abstract

DC-60 heavy ion accelerator [1], put into operation in 2006, according to its specifications - spectrum, charge and energy of accelerated ions, has the high scientific, technological and educational potential. The highest possible universality both by spectrum of accelerated ions and acceleration energy and regimes was built in DC-60 heavy ion accelerator designing. The new interdisciplinary research complex based on DC-60 cyclotron makes it possible to create a highly-developed scientific-technological and educational environment in the new capital of Kazakhstan. This article is a review of the DC-60 heavy ion accelerator and the works carried out based on the cyclotron.

INTRODUCTION

DC-60 accelerator is a dual cyclotron, which is capable of charged particles acceleration up to kinetic energies in MeV/nucleon, expressed in the following relation: $E = 60(z_i/A)^2$, where z_i - accelerated ion charge, A - atomic weight of ion. Relation (z_i/A) in formula must be within the following limits: $(z_i/A) = (1/6 \div 1/12)$, that impose constraints on charge of accelerated ions.

Prototypes ECR heavy-ion source are sources DECRIS-2 and DECRIS-3 [2] which is used in the DC-60 accelerator. On the "ECR - surface" is used magnetic field configuration «minimum B» for the plasma confinement and electronic heating. This configuration is obtained as a result of the superposition of an axial field of magnetic mirror and a radial field of a sextupole magnet. Two single coils with an iron yoke form an axial magnetic field, and the radial magnetic field is created by an NdFeB permanent sextupole of a magnet.

The operating frequency of UHF the ECR generator is 14 GHz. The flash chamber of source is insulation meant for a voltage up to 25 kV. The extraction of ions is performed two elements Plasma electrode and the mobile extraction electrode.

For the beam transport from the ECR ion source to the cyclotron created a powerful system of axial injection of beam, which is consisting of:

- focusing element;
- energy-analysing magnet;
- detecting of elements;
- bunchers;
- vacuum pumps;
- electrostatic deflectors.

The entrapment of phase to accelerate in the center of the cyclotron is $30^\circ \div 35^\circ$. This means that no more than 10% of ion of the desired charge will be involved in the

acceleration process. To increase efficiency the entrapment of the beam by axial injection systems is installed the buncher with a sine wave, which includes the beam particles in the desired range of phases and increases the capture coefficient to 30÷50 %. Turn of the beam from the vertical axial injection channel in the median plane of the cyclotron using the electrostatic spiral of inflector.

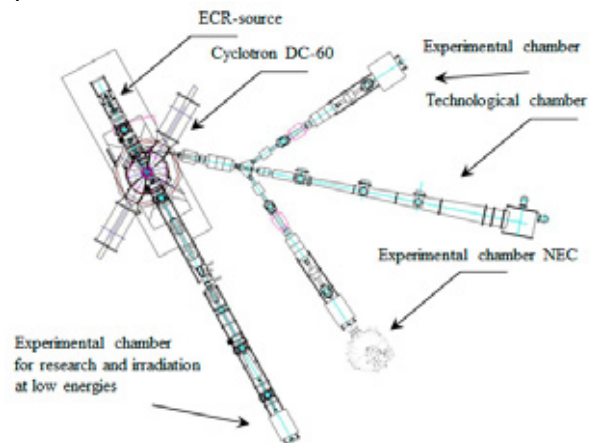


Figure 1: The scheme of the DC-60 accelerator complex.

The upper energy of the accelerated ions is 1.75 MeV/nucleon. The variation of the energy of ions in the range from 0.35 to 1.75 MeV/nucleon is provided by changes in the charge of the accelerated particles and magnetic field of the cyclotron.

High frequency system has a variation of the frequency in the band 12 - 18 MHz and provides the acceleration of ions on harmonics 4 and 6.

The electrostatic deflector with the electric field strength of 75 kV/cm is used for the beam extraction from the cyclotron which located in the cavity of the magnet. The beam transport channels from the cyclotron to the target chamber include the standard system focusing and rotation of the accelerated ions. Thus, range of ions accelerated on DC-60 cyclotron is ${}^6\text{Li}$ to ${}^{132}\text{Xe}$, variation of ion energy is over the range 0.35 to 1.75 MeV/nucleon.

CYCLOTRON OPERATION

Since 2006 to 2014 many experimental works in the domain of nuclear and atomic physics, radiation physics of solid and nanotechnology have been carried out at the DC-60 cyclotron. The data of beam time in a period of 2006 - 2014 of operation of the accelerator is shown in Fig. 2.

[#]mzdorovets@gmail.com

THE STATUS OF THE FACILITIES OF KURCHATOV'S SYNCHROTRON RADIATION SOURCE

V. Korchuganov, A. Belkov, Y. Fomin, E. Kaportsev, M. Kovalchuk, Yu. Krylov, I. Kuzmin, V. Moiseev, K. Moseev, N. Moseiko, D. Odintsov, S. Pesterev, A. Smygacheva, A. Stirin, S. Tomin, V. Ushakov, V. Ushkov, A. Valentinov, A. Vernov, NRC Kurchatov Institute, Moscow, 123182 Russia

Abstract

The first electron beam had been received 20 years ago in a storage ring SIBERIA-2 - a dedicated synchrotron radiation source in the Kurchatov Institute and, also, the official opening of the SR source for the experiments marks 15th anniversary in year 2014. The report focuses on the development of the SR source accelerator complex systems in 2014.

INTRODUCTION

The electron accelerators complex of the Kurchatov's SR source includes: a for-injector - the 80 MeV linear accelerator; the 450 MeV storage ring Siberia-1 with the natural emittance 800 nm-rad; the 2.5 GeV storage ring Siberia-2 with the natural emittance 78-100 nm-rad; two electron-optical channels – EOC-1 and EOC-2. Official opening of the Kurchatov SR source took place 1.09.1999.

KSRS FACILITIES WORK

The work of Siberia-2 on experiments is mainly carried out using SR from bending magnets in photons energy range (4-40) keV and spectral flux (10^{13} - 10^{11}) ph/s/mrad/0.1%BW during the week runs in a round-the-clock mode. Within one week 9 working 12-hour shifts are presented.

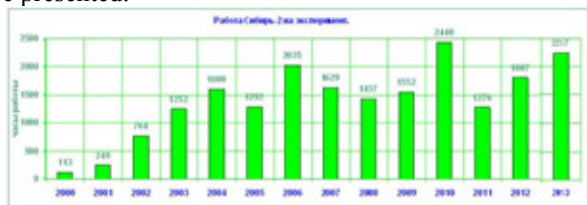


Figure 1: Experimental time at Siberia-2 in 2000-2013.

Diagram in Fig.1 shows the integral time devoted for SR experimental work at Siberia-2 in 2000 – 2013 years. Table 1 presents a statistics of SR source Siberia-2 work at SR experiment in 2013 and on June 2014. Note that in 2014 the SR source spent relatively much time in standby and adjustment mode due to stops for the works of firms according contracts (opening shielding walls, new beam lines installation, etc).

The purpose of works on 2013-2014 is both modernization of the existing equipment and introduction of new diagnostics systems mainly on Siberia-2 storage ring.

Table 1: Statistics of Siberia-2 on 2013-June 2014.

Period	2013	Jan.-June 2014
Max. electron current	112 mA	128 mA
Life time (100mA)	41.8 hrs	38.5 hrs
Operation time	3480 hrs	2371 hrs
Experiment	2257 hrs / 50%	1074 hrs / 38%
Injection	10%	11%
Tuning / Other works	17% / 23%	16% / 35%

DEVELOPMENT OF KSRS ON 2014

Siberia-2 New High Voltage Generators

The important aim was to replace old generators of the injection kickers based on the HV gas-filled electric discharge devices and the HV forming lines (20 ns, <55 kV) on the new compact LV generators (≤ 3 kA, 25 kV) working only with solid electrical components and without SF₆ gas using.

After the testing in 2011-2012 of the prototype two new generators based on pseudo-spark switches (a thyatron TPI1-10k/50) and RLC resonant circuits with a semi-sinusoidal form of currents were produced on "Pulse Systems" Ltd. (Ryasan). The final scheme of new generators is shown in Fig.2.

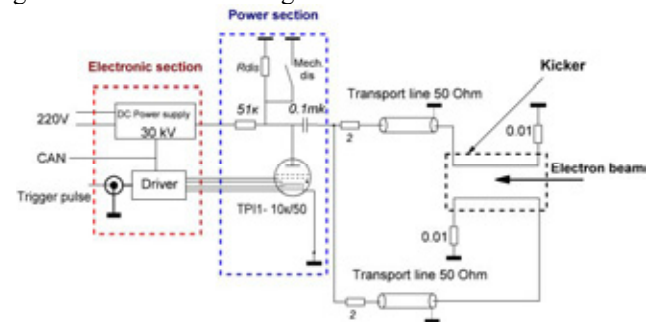


Figure 2: The scheme of new generators.

To guarantee a stable operation of the generators we have increased the working pulse duration till 1 μ sec making 2.5 times longer than revolution period and have reduced the voltage on capacitance.

The calculation without taking into account any collective excitations showed that in the case long pulse shouldn't affect the injection efficiency [2], see Fig.3.

THE NSLS-II BOOSTER DEVELOPMENT AND COMMISSIONING

V. Kiselev for the BINP and BNL teams [1]
 BINP, Novosibirsk 630090, Russia

Abstract

National Synchrotron Light Source II is a third generation light source constructed at Brookhaven National Laboratory. The project includes highly optimized 3 GeV electron storage ring, linac pre-injector and full-energy injector-synchrotron. Budker Institute of Nuclear Physics has built a turnkey booster for NSLS-II. The main parameters of the booster, its characteristics and the results of commissioning are described in this paper.

INTRODUCTION

The tender on the designing, production and commissioning of the NSLS-II booster was started in January 2010. Budker Institute of Nuclear Physics won this tender in May 2010. The booster was designed, produced and delivered in full to BNL by September 2012. During 2013 the booster was assembled and all equipment was tested. The authorization to start the commissioning of the injector was received in November 2013. The BNL and BINP teams started beam injection into the Booster on December 8. The first turn was closed soon by tuning the LTB and BR orbit correctors. The beam was accelerated to 3 GeV by the end of 2013. The commissioning of the booster was successfully completed in February 2014.

BOOSTER DESIGN

The conceptual design of the booster has been done by BNL [2].

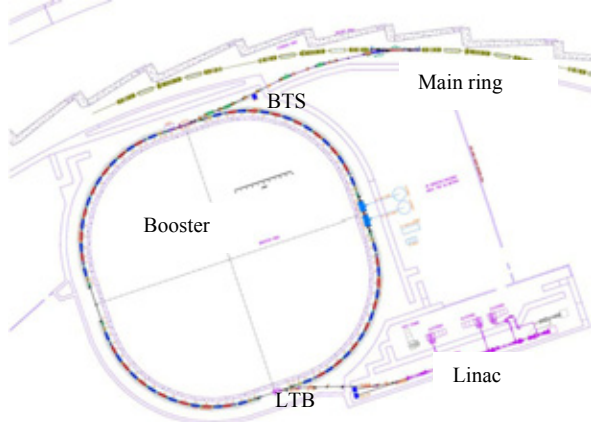


Figure 1: Schematic layout of the full energy booster.

The booster should accelerate the electron beam continuously and reliably from minimal 170 MeV injection energy to a maximal energy of 3.15 GeV and average beam current of 20 mA. The booster shall be capable of multi-bunch and single bunch operation. The main parameters of the designed booster are summarized

in Table 1. The lattice provides rather low horizontal emittance of 37.4 nm-rad at the energy of extraction.

Table 1: NSLS-II Booster Main Parameters.

Energy, MeV	200	3000
Circumference, m	158.4	
Number of periods	4	
Repetition rate, Hz	1 Hz / 2 Hz	
Bunch number	1; 80-150	
RF frequency, MHz	499.68	
Betatron tunes: ν_x/ν_y	9.646 / 3.411	
Natural chromaticity: ξ_x/ξ_y	-9.5/-13.5	
Corrected chromaticity: ξ_x/ξ_y	1.25 / 2.05	
Momentum comp. factor, α	0.00882	
Hor. Emittance: ϵ_x , nm rad	0.17	37.4
Energy spread, σ_E/E	$0.55 \cdot 10^{-4}$	$8.31 \cdot 10^{-4}$
Energy loss per turn, U_0 , keV	0.0135	685.8
Damping times: (τ_x, τ_y) , s	15.6; 7.8	0.0046; 0.0023

Lattice

The optical structure of the booster synchrotron consists of four quadrants. Two opposite straight sections of the ring contain elements for injection and extraction of the beam. Other two sections are intended for RF resonators and diagnostics. 60 magnets with combined functions magnetic field are set in the ring. The core of dipoles is a sector with parallel edges. For compensation of natural chromaticity of the structure the dipole magnets create sextupole component of a field. Separate quadrupole lenses provide adjustment of betatron working point during acceleration of particles and optimum acceptance of the structure. For correction of lattice chromaticity the separate sextupole lenses are inserted. Optical functions are shown in Figure 2.

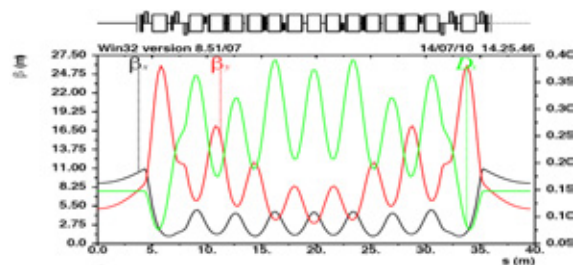


Figure 2. The betatron and dispersion functions for the lattice quadrant.

SUPERCONDUCTING MULTIPOLE WIGGLERS FOR GENERATION OF SYNCHROTRON RADIATION

N. Mezentsev, Budker INP, Russia

Abstract

Superconducting (SC) multipole wigglers are very powerful instruments for generation of synchrotron radiation of high intensity. Use of a superconducting wire for creation of a sign alternating lateral magnetic field has the big advantages in comparison of permanent magnets and conventional electromagnets. Superconductivity use allows to create much higher magnetic field at the same field period and the vertical aperture for a beam. The high magnetic field allows not only to increase intensity, but also to expand spectrum of synchrotron radiations.

The first superconducting wiggler has been made and installed on the VEPP-3 electron storage ring as a generator of synchrotron radiation in 1979. Nowadays tens of the wigglers are successfully working in the various synchrotron radiation centers and more than 10 of them were developed and made in Budker INP.

The description of magnetic properties of the wigglers, parameters of both cryogenic and vacuum systems and their technical decisions are resulted in the report.

INTRODUCTION

Multipole superconducting wigglers are installing on synchrotron radiation (SR) sources to improve user properties of radiation by increasing of rigidity and intensity of SR. The magnetic system of multipole wiggler represents an array of superconducting dipole magnets creating sign alternate lateral magnetic field. Electron beam passing through this array generates SR in each magnet which the radiation intensity is summarised from all magnets practically in the same solid angle. Use of such magnetic systems is rather effective and cheap enough way of increase in intensity and rigidity of radiation. Spectral properties of radiation from such magnetic structure depend on parameter $K = 0.934 \cdot B[T] \cdot \lambda[\text{cm}]$, where B and λ - amplitude and magnetic field period. For $K \sim 1$ - the radiation spectrum has undulator property, for $K \gg 1$ - the radiation spectrum transits to spectrum of synchrotron radiation. To expand opportunities for carrying out of experimental works and thus to prolong a life, expensive installations as electron storage rings superconducting insertion devices (SC ID) may be installed into straight sections of the storage rings to change spectral, angular, and polarizing properties of SR. These devices, as a rule, have zero first and second magnetic field integrals along electron orbit, and, therefore, they are not basic elements of the electron storage rings, and their status does not affect working reliability of all ring.

The magnetic system using superconducting magnets with NbTi/Cu or Nb₃Sn/Cu wires creates much higher field in comparison with use of conventional or

permanent magnets. However use of superconductors demands use of a cryostat for maintenance of low temperatures of magnetic system.

MAGNETIC SYSTEM OF SC WIGGLERS

Magnetic Field Distribution and Field Integrals

Magnetic field of a superconducting multipole wiggler represents a periodic, sign-variable field (1) which begins and ends by special compensating end magnets.

$$\begin{aligned} B_z &= B_0 \cos(k_0 \sigma) \cos(k_x \chi) \cosh(k_z z) \\ B_\chi &= -\frac{k_x}{k_z} B_0 \cos(k_0 \sigma) \sin(k_x \chi) \sinh(k_z z) \\ B_\sigma &= -\frac{k_0}{k_z} B_0 \sin(k_0 \sigma) \cos(k_x \chi) \sinh(k_z z) \end{aligned} \quad (1)$$

Where: $k_0 = 2\pi / \lambda_0$, $k_x = 2\pi / \lambda_x$, $k_z = 2\pi / \lambda_z$ - characteristic magnetic field variation in longitudinal and lateral directions.

The end magnets are used for creation of the first and second field integrals of the wigglers equal to zero for indemnification of a beam orbit distortion which is created by the basic wiggler field.

$$I_1 = \frac{1}{B\rho} \int_{-L/2}^{L/2} B_z(s) ds = 0 \quad I_2 = \int_{-L/2}^{L/2} ds' \int_{-L/2}^{s'} \frac{B_z(s'')}{B\rho} ds'' = 0 \quad (2)$$

Field integrals of the wiggler with odd pole number can be compensated by two end magnets with a field of 1/2 of the main field or four end magnets with the fields, equal 1/4 and 3/4 of the main field..

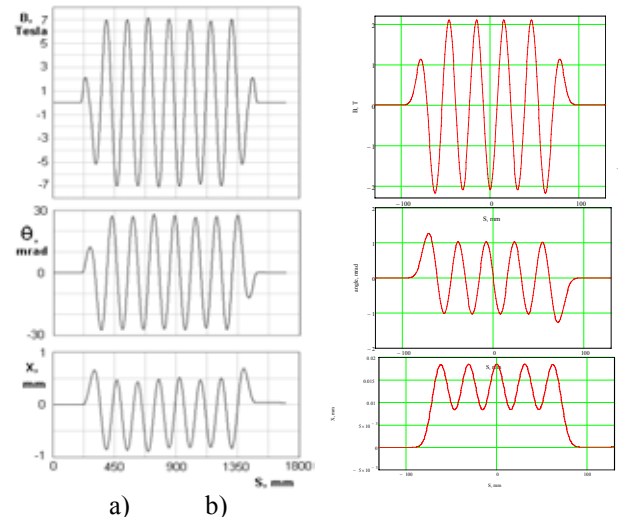


Figure 1: Magnetic field distribution and behaviour of the first and second field integrals with the end magnets of a) 1/4 and 3/4 and the end magnets of 1/2 of the main field.

PRODUCTION OF SUPERCONDUCTING EQUIPMENT AT IHEP

S. Kozub, A. Ageyev, I. Bogdanov, E. Kashtanov, P. Slabodchikov, V. Sytnik,
P. Shcherbakov, L. Shirshov, L. Tkachenko, S. Zinchenko, IHEP, Protvino, Russia

Abstract

The report overviews the recent SC-related R&D and production activity at IHEP. The scope of the paper extends over the items to follow. Two superconducting magnetic systems of Electron Lens for the Tevatron collider were developed, manufactured and successfully brought into operation. 42 cryogenic electrical feed boxes of various types for the Large Hadron Collider were developed, produced and commissioned. Results of development of fast-cycling SC magnets for the FAIR project are discussed. Operational experience acquired with the largest in Russia cryogenic system for cooling with a superfluid helium of SC RF separator for the beam transfer line #21 from the U-70 machine is presented. Test-and-trial results with HTS current leads and dipole magnet employing Bi2223 as well as racetrack coils made of second-generation HTS are reviewed.

LOW TEMPERATURE SC MAGNETS

New generation of high energy proton accelerators is based on superconducting (SC) magnets. Cooperation with international scientific accelerator centers was developed in last 15 years. In 1999 – 2000 and 2002 – 2003 two SC magnetic systems of Tevatron Electron Lens for Fermilab, USA were developed and produced. These systems were placed in the TEVATRON accelerator (Fig.1) and operated up to now.

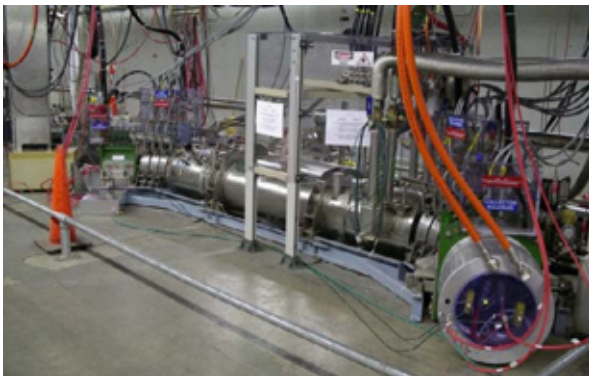


Figure 1: SC magnetic system of Tevatron Electron Lens.

The system consists of seven SC and ten copper magnets [1]. The main SC solenoid has 6.5 T nominal magnetic field, 2.5m length, 152 mm coil inner diameter. The solenoid coil was wound by the Rutherford type cable from 10 SC wires of 0.85 mm diameter. A turn number of the solenoid is 7238 and the nominal current is 1800 A. Six SC steering dipoles were placed over the solenoid. Two dipoles of 1840 mm length were arranged in the centre and four dipoles of 250 mm length in the end parts of the solenoid. The central dipole created 0.2 T magnetic field at 50 A current and the end dipole had

0.8 T at 200 A. All dipoles were wound by a cable, transposed from 8 SC wires of 0.3 mm diameter.

The system has gun and collector solenoids with 250 mm inner diameter, 474 mm outer diameter, 300 mm length, which create 0.4 T magnetic field in the aperture. Copper corrector coils are placed inside these solenoids. Three bending electron beam solenoids with 390 mm inner diameter, 500 mm outer diameter, 72 mm length are set between the cryostat and the gun solenoid as well as the same between the cryostat and the collector solenoid. A turn number of the solenoid is 48 at the nominal current 357 A. The gun, collector and bending coils of the solenoids are wound from copper cable with $8.25 \times 8.25 \text{ mm}^2$ cross section having 5.5 mm diameter hole for cooling.

From 2002 IHEP collaborated with GSI, Darmstadt, Germany. SC fast cycling magnets were developed and produced for the SIS300 accelerator of the FAIR project (Facility for Ions and Antiprotons Research) [2]. The high field fast cycling dipole model is shown in Fig. 2 and its parameters are presented in Table 1.



Figure 2: SIS300 high field fast cycling dipole model.

Table 1: Parameters of the SIS300 SC fast cycling dipole

Magnetic field, T	6
Operating current, kA	6.72
Field ramp rate, T/s	1
Number of layers	2
Strand number in cable	36
AC losses (calc.), W/m	4.7
In the coil	3.4
In the iron yoke	1.3
Stored energy, kJ	260
Inductance, mH	11.7
Coil inner diameter, mm	100
Length of SC coil, m	1
Mass of magnet, ton	1.8

INR RAS LINAC PROTON INJECTOR 100 Hz PRR OPERATION MODE

E.S. Nikulin[#], A.S. Belov, O.T. Frolov, L.P. Nechaeva, A.V. Turbabin, V.N. Zubets,
Institute for Nuclear Research of RAS, Moscow, 117312, Russia

Abstract

The injector provides linac by 400 keV protons with energy stability $\pm 0.1\%$, pulsed ion current – up to 100 mA, 50 Hz pulse repetition rate (PRR) with 200 μs duration. PRR of the injector has been doubling with goal of linac average beam current increasing [1, 2]. Main stages and results of the injector modernization are presented.

Tests conducted earlier [3] have shown that pulse shape of the accelerating voltage produced by the high-voltage pulse generator (HVPG) at 100 Hz PRR has been distorted (Fig. 1).

It is seen that the high voltage (HV) value change in last forty microseconds of pulse duration is approximately 3% of the total pulse amplitude. This is unacceptable because the specified voltage change during pulse for the proton injector is $\pm 0.1\%$.

Besides achieving a desired shape of HV pulse at 100 Hz PRR we have revealed two additional problems to be solved: first - instability of pulse amplitude and shape, associated with presence of a second 50 Hz series of pulses ("doubling of pulses") and second - overheating of the HVPG individual components and elements. This report contains, basically, the information relating to achievement of desired HV pulse shape. The HVPG circuit diagram is shown in Fig. 2.

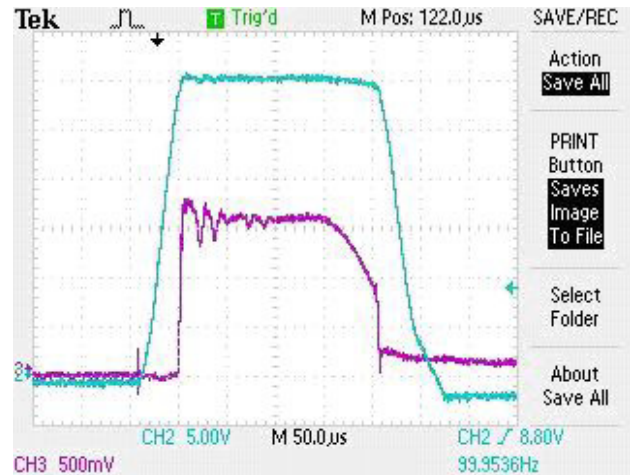


Figure 1: Oscillogram of the HVPG pulse at 100 Hz PRR (the pulse with smaller amplitude is the top of the HV pulse on a larger scale).

The HVPG consists of: 400 kV pulse transformer (PT-400), multi-cascade discriminator (MD) which stabilizes amplitude of HV pulses, sub-modulator that provides pulses with amplitude up to 20 kV to the PT-400 primary winding. The HVPG structure also includes three-phase 0 ÷ 380 V, 100 kVA auto transformer; step-up 380 V / 22 kV, 100 kVA transformer; the stabilization system of accelerating voltage which is intended to compensate the HVPG power supply slow changes, and the pulse top tilt compensation system.

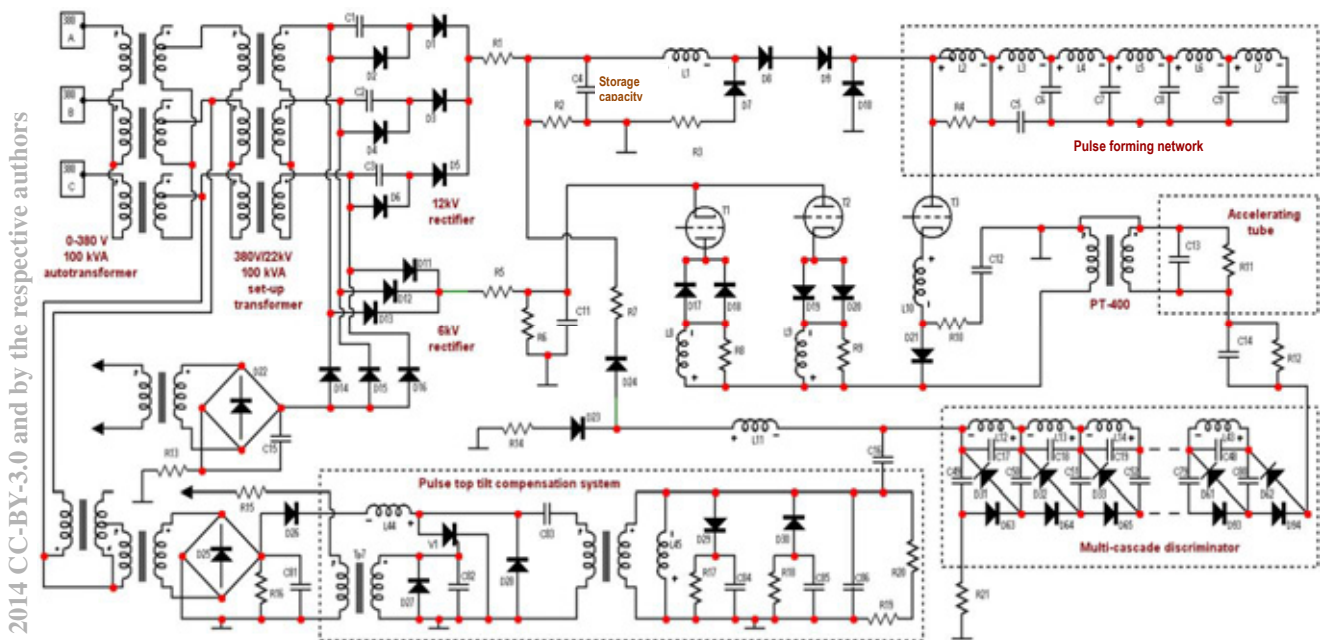


Figure 2: The proton injector HVPG electrical circuit.

CW 100 keV ELECTRON RF INJECTOR FOR 40 mA AVERAGE BEAM CURRENT

V.N. Volkov, V.S. Arbuzov, K.N. Chernov, E.I. Kolobanov, S.A. Krutikhin, G.Ya. Kurkin, E.A. Kuper, I.V. Kuptsov, S.V. Motygin, V.N. Osipov, V.K. Ovchar, V.V. Repkov, V.M. Petrov, I.K. Sedlyarov, G.V. Serdobintzev, S.S. Serednjakov, M.A. Scheglov, S.V. Tararyshkin, A.G. Tribendis, I.A. Zapryagaev, BINP SB RAS, Novosibirsk, Russia
I.V. Shorikov, A.V. Telnov, N.V. Zavyalov, RFNC-VNIIEF, Sarov, Russia

Abstract

CW 100 keV electron RF gun for 40 mA average beam current was developed, built, and commissioned at BINP SB RAS. The RF gun consists of normal conducting 100 MHz RF cavity with a gridded thermo cathode unit, CW 16 kW generator with GU-92A tetrode in the output stage, and a set of LLRF electronics. The gun was tested up to the design specifications at a test bench that includes a diagnostics beam line.

The design features of different components of the gun are presented. Preparation and commissioning experience is discussed. The beam test results are summarized.

INTRODUCTION

A 100 MHz RF electron injector was designed and manufactured at BINP for continuous wave (CW) powerful accelerator in RFNC-VNIIEF [1]. This compact accelerator, similar to the type of «RHODOTRON» [2], is designed for continuous production of short electron bunches with energy of $1.5 \div 7.5$ MeV with power of 300 kW and higher.

Each bunch passes through a single accelerating cavity of the accelerator several times. After each pass, the beam is turned in the bending magnets. In order to preserve the transverse dimensions of the electron bunches within the aperture after passing through the bends, the bunches should have small enough energy spread ($<1\%$) and be quite short (<0.2 ns).

An advantage of RF guns compared with static guns is the absence of cathode back bombardment with accelerated ions of residual gas ionized by an electron beam. This allows having a long lifetime of the cathodes and operating the gun continuously in the vacuum of $10^{-6} \div 10^{-7}$ Torr. Also, this enables raising the gun voltage and thus increasing the energy of the electron beam from 30-40 keV to 100 keV proportionally to the beam current to the power of $2/3$, in accordance with the Poisson law.

Furthermore, calculations showed that the increased voltage in the RF injector in combination with the effect of the longitudinal beam bunching therein provides a reduction in the energy spread of up to 0.3% (rms) in the first passage of the accelerator and the bunch shortening by up to 18 times.

RF INJECTOR

A grid-controlled thermo-cathode RF gun is based on high frequency quarter wave coaxial 100 MHz cavity shortened by a capacitance. The cavity is fed through an

inductive input RF power coupler from 16 kW RF generator (based on tetrode GU-92A with a 500 W transistor preamplifier). The generator is powered by high DC voltage (8 kV) source situated in a separate rack. The control system consists of two parts: i) the control system for the cathode-grid unit consisting of a block inserted into the cavity and the blocks in the control rack, ii) control units for the cavity RF system located in the same rack. Detailed description of similar RF systems is given in [3].

The average beam current is regulated by the bunch repetition frequency and bunch charge adjustment. Bunch length is determined by the bunching effect. Maximum surface RF electric field (4 MV/m at 100 kV) is concentrated at the edges of the focusing electrode (see Fig.1), so field emission dark current from these places does not get into the beam line. Main characteristics of the RF injector are in Table 1.

Table 1: Main characteristics of the RF injector

Average current of the RF injector, mA	>40
Electron energy, keV	$50 \div 100$
Bunch duration (FWHM), ns	$0.5 \div 2$
Maximum repetition rate, MHz	100
Generator RF power, kW	<16
Operating vacuum, Torr	$<10^{-6}$

RF cavity (see Fig.1) has a bimetallic cylindrical body (1) with a diameter of 500 mm and a length of 550 mm. There is a water-cooled cylindrical electrode (2) inside the cavity with the gridded thermo-cathode unit (3) mounted on its end. The space between the focusing electrode (4) and the end wall of the cavity (5) is the accelerating gap.

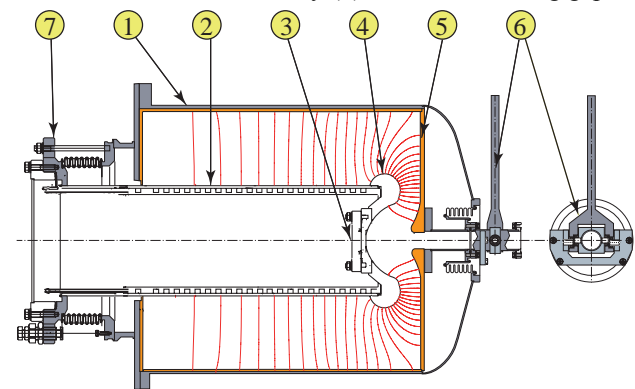


Figure 1: Sketch of the cavity RF gun with the force lines of the accelerating RF field.

STATUS OF LINACS WITH HIGH-FREQUENCY QUADRUPOLE FOCUSING LU-30 AND LU-30M IN IHEP

O.K.Belyaev, J.A.Budanov, V.P.Golubkov, A.J.Evstifeev, S.E.Zavjalov,
I.D. Kuzmin, E.V.Mazurov, S.A.Strekalovskikh, N.A.Chyornyj, IHEP, Protvino, Russia

Abstract

There are two RFQ DT proton linacs, named the LU-30 and LU-30M, in the SRC IHEP of NRC “Kurchatov Institute” that are presently in operation. Both are the unique machines employing radio-frequency quadrupole focusing up to 30 MeV at exit. The LU-30 machine now runs as a proton injector to the booster RC PS U-1.5 that feeds the main PS U-70 ultimately. The LU-30M is now run in a stand-alone test operation mode. Such a parallel functioning of these two accelerators allows to use the LU-30M as an experimental facility enabling R&D on new technical decisions and upgrades for the ageing LU-30. On the other hand, the routine operation of the workhorse LU-30 allows for testing of the technical decisions proposed under a heavy non-stop operation during the U-70 runs for fixed-target physics.

INTRODUCTION

The IHEP proton linacs, LU-30 and LU-30M, are the unique machines with Radio-Frequency Quadrupole (RFQ) focusing up to 30 MeV at exit [1, 2]. LU-30 was made as an experimental model. Since 1985 LU-30 has been operating as a proton injector to the booster RC PS U-1.5 on the packet-pulse mode, about 2500 hours per year with downtime (5÷7) %.

The LU-30M was developed from an experience of creation and operation of the LU-30. Emittance of the LU-30M beam reduced to a tenth and the beam transport along the LU-30M is higher then in the LU-30 as figure 1 shows.

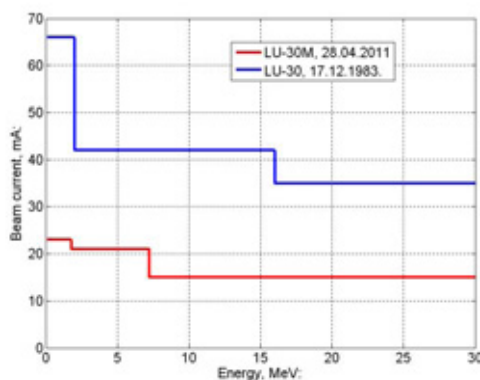


Figure 1: Beam transport in the LU-30 and LU-30M.

The other beam parameters of LU-30M are the same as the LU-30 parameters, except for the beam intensity, which is lower the project level yet. There are substantial differences in design of the accelerators:

- a modification of the electrodes of the initial part (RFQ) LU-30M allowed to halve the RFQ length;
- using the sector H-cavities in the main part LU-30M (RFQ DTL, [2]) some compensation of the decrease in accelerating rate was achieved by realizing the growth in the accelerating voltage along the accelerator;
- a modular design of the anode HV power supplies was developed for higher reliability of the RF-system [3].

Now accelerator LU-30M runs in a stand-alone test operation mode. This mode allows of using LU-30M as an experimental facility enabling R&D on new technical decisions and upgrades for increasing reliability and quality of ageing LU-30.

VACUUM BREAKDOWNS

During LU-30 operation it was noted that the breakdown frequencies for initial and main parts (RFQ, RFQ DTL) LU-30 are almost identical, but the field strength at the surface of the electrodes of this parts differs sufficiently (225 kV/cm and 380 kV/cm). Analytical treatment of the experimental dependence of the relative quality factor on the field strength at the electrodes for RFQ and RFQ DTL showed pronounced distinction between coefficients of local field enhancement for RFQ and RFQ DTL (1100 and 93 accordingly) [4]. This distinction may testify to the various factors that lead to breakdowns. According to paper [5], the values more than 200 can be explained by the presence of films and nonmetallic inclusions on the electrode surface and the smaller values – by the micro irregularities. As a result, we conclude that the products of the ion gun operation may be responsible for the pollution of the RFQ electrodes and the reduced breakdown strength.

BEAM CONDITONING

An injection system with collimators avoiding pollution of the RFQ electrodes by the ion source impurities has been developed. The optics not only effectively separates the impurities but also matches the proton beam to the RFQ in transversal motion. Figure 2 shows it schematically. A diaphragm with a hole of 3 mm in diameter is installed between two magnetic lenses (solenoids), nearby the proton beam crossover. A cylinder of 3.5 mm in diameter is placed in the middle of the second lens to separate the part of the impurity flow coming through the diaphragm hole. In addition the optics filters the transversal phase volume of the proton beam by

GEOMETRY OF QUADRUPOLE MAGNET FOR THE U-3.5 ACCELERATOR IN THE OMEGA PROJECT

L. Tkachenko, S. Kozub, P. Shcherbakov,
Institute for High Energy Physics, Protvino, Moscow region, Russia

Abstract

Accelerating complex of intensive beams of charged particles (project Omega) is being developed at IHEP. The main part of this complex is 3.5 GeV ring accelerator. The basic parameters of the quadrupole magnet for this ring are: 5.564 T/m central gradient in the 102.9 mm radius of the “good field”; the injection gradient is 1.222 T/m; the gradient ramp rate is 334 T/m/s. Different profiles of the poles were considered for the purpose of selecting the most optimal 2D and 3D geometries of the magnet. The basic parameters of the optimal geometries are presented.

INTRODUCTION

IHEP (Protvino, Russia) is developing an accelerating complex of charged particles of high intensity (project OMEGA [1]). This complex is designed to create megawatt power beams. The OMEGA project consists of a new cascade of high-intensity accelerators, which includes a linear accelerator of H⁺ ions and protons with energy of 400 MeV, followed by a rapid cycling synchrotron with energy of 3.5 GeV. Basic parameters and preliminary optimization of the geometry of the main dipole were presented in [2]. Further the 2D and 3D geometry optimization for the main quadrupole in the 3.5 GeV ring is considered.

THE OMEGA PROJECT

The OMEGA project involves the construction of Accelerator Complex for Intense Hadron Beams. This multi-purpose mega-project is being discussed at IHEP [1, 3] and is shown in Fig. 1. The proposal outlines a long-term plan to develop the accelerator and experimental facilities on the IHEP grounds for fixed-target research within and beyond the scopes of elementary particle physics. The base-line design foresees construction of a pulsed facility that will exceed 1 MW of proton beam average power, will have a pulse rate of 25 Hz, pulse width $\leq 1.5 \mu\text{s}$, clear staging, site-specific integration and upgraded plans, and reduced technical risk (through use of proven technologies). The facility comprises of a non-superconducting 400 MeV linear accelerator LU-400 followed by a 3.5 GeV rapid cycled proton synchrotron (RC PS) U-3.5. At a later stage, the U-3.5 is engaged as a new injector to the existing U-70 PS, or its updated successor. A particular stage of the project addresses either applied or fundamental science (Fig. 1). Stage-1 assumes construction of a short-pulse accelerator-driven 1 MW neutron source for applied research (material and life sciences).

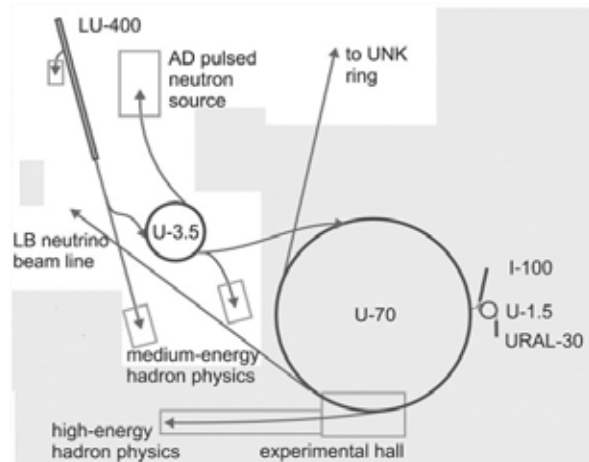


Figure 1: Tentative layout of the OMEGA facility.

Table 1: Specifications of U-3.5 (Project).

Specification	Value
Energy (kinetic), E , GeV:	0.4–3.5
Orbit length, L , m:	445.11
Magnetic rigidity, $B\rho$, T·m:	3.18–14.47
Compaction factor, α :	0.0173
Transition gamma, γ_t :	7.60
Intensity, N , ppp:	$7.5 \cdot 10^{13}$
Ramping time, t_R , s:	0.020
Cycle period, T , s:	0.040
Average beam current, μA :	300
Beam power, P , MW:	>1
RF harmonic, h :	9
Radio frequency, f_{RF} , MHz:	4.322–5.925
Net RF voltage, V_{RF} , kV/turn:	720
Lattice period:	FODO (90°)
No. of periods:	36
No. of super periods:	6
Betatron tune (H/V):	9.15/7.20

The goal for the next stage-2 is to develop the second direction of fast extraction from the U-3.5 to feed a new experimental zone dedicated to intense-beam medium-energy hadron physics. At a later stage the U-3.5 is engaged as a new injector to the existing U-70 PS, or its updated successor. To this end, the orbit length and RF harmonic number of the U-3.5 amount to 3/10 of those in the U-70. It facilitates, at most, a 3-train bunch-to-bucket transfer from U-3.5 to the U-70 ring thus yielding a beam pattern $3 \times (9 \text{ filled} + 1 \text{ empty})$ bunches there. Apart from the lower-energy mode of a 3.5 GeV proton beam stretcher delivering slow spills, the U-70 will accelerate

STUDY OF SUPERCONDUCTING ACCELERATING STRUCTURES FOR MEGAWATT PROTON DRIVER LINAC

K.A. Aliev, M.A. Gusarova, A.M. Fadeev, M.V. Lalayan, S.M. Polozov, N.P. Sobenin, O.L. Verbitskiy National Research Nuclear University MEPhI (Moscow Engineering Physics Institute), Moscow, Russia

T.V. Kulevoy, National Research Nuclear University MEPhI (Moscow Engineering Physics Institute) and Institute of Theoretical and Experimental Physics, Moscow, Russia

Abstract

The preliminary design of megawatt level proton accelerator-driver is carrying out by collaboration between Russian scientific centers MEPhI, ITEP, Kurchatov Institute. This project was supported in 2013 by the Ministry of Science and Education of Russia. The linac general layout includes SC Spoke-cavities at middle energy range and elliptical cavity at high energy one. The usage of QWR and/or HWR at 10-30 MeV was also discussed. Due to electrodynamic models of all structures types were designed and the electrodynamic characteristics were studied. QWR, HWQ and Spoke-cavities were proposed to operate on 324 MHz and elliptical cavities on 972 MHz. The main electrodynamic simulation results will present in report. The multipactor study results will also discussed.

INTRODUCTION

The study of high-power proton linac for 1.0 GeV was performed by collaboration of MEPhI, ITEP and Kurchatov institute researchers in 2013. Such linac was developed to understand the possibility of accelerator driven system (ADS) design in Russia.

The linac will consist of an RFQ, RF focusing sections and SC modular configuration sections. A number of QWR and HWR were also studied for 20-50 MeV energy range as an alternative of RF focusing sections. The SC part of developed linac can include QWR, HWR, Spoke-cavities and elliptical cavities due to. Medium energy cavities will operate on 324 MHz and elliptical one on 972 MHz [1, 2].

The results of noted above structures models design will discuss bellow. All simulations have been performed using CST Microwave Studio [3].

QWR AND HWR CAVITIES

The aim of the QWR and HWR optimization is to increase the beam energy gain and to have optimal power consumption at the same time. The beam energy gain is defined by the time-factor and the accelerating gradient. As it follows from the time-factor T definition, its maximum value is gained when the gap length is minimized. But the gap length decrease leads to higher gap capacity and, therefore, to lower shunt impedance, which is another important optimization target. The optimal value of the accelerating gap length g to the period length d equal to $1/3$ could be taken [4], since its

further decrease slightly improves the time-factor and the optimal particle velocity is only by 3 % higher than the optimal geometrical velocity β_g . Another QWR feature that affects the beam energy gain is the accelerating gradient. The accelerating gradient is estimated by the ratio B_p/E_a , where B_p is the magnetic field pick value and E_a is the accelerating field amplitude. Therefore, the ratio must be minimized for higher gradients. B_p/E_a depends on the inner and outer QWR conductor radii ratio R_i/R_o . The solution of the equation $\ln(R_o/R_i)=1$ gives the optimal value of R_i/R_o [4] and it is equal to 0.36. The QWR effective shunt impedance R_s/Q_o defines how effectively RF field energy converts to the accelerating gradient. According to the "sphere in cylinder" approach offered in [5] the ratio $R_i/R_o=0.12$ yields the maximum shunt impedance (see Fig. 1). High shunt impedance and relatively low accelerating gradient results in a resonator with optimal power consumption, while a low B_p/E_a parameter resonator has an extreme accelerating gradient. When simulating a 324MHz QWR the value $R_i/R_o=0.3$ is chosen in favour of a higher accelerating gradient. Geometrical and RF characteristics of the QWR are presented in Table 1.

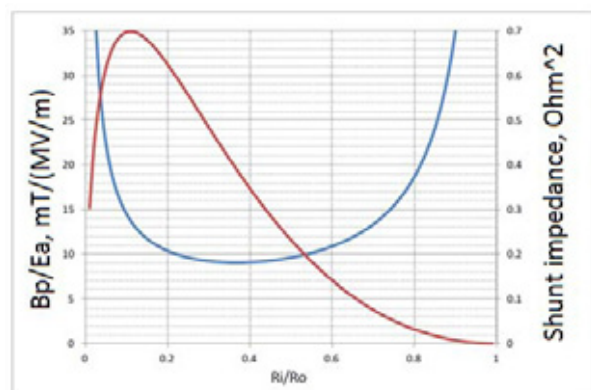


Figure 1: B_p/E_a and shunt impedance in QWR versus R_i/R_o .

The same analysis was performed for HWR also. To develop the electrodynamic model and determine the approximate geometric parameters of the HWR we assume the average value of the relative phase velocity $\beta=0.25$. The shape of the resonator should be optimized to minimize ratios B_p/E_a and E_p/E_a and get the maximum value of R_s/Q_o . Characteristics of the HWR are also presented in Table 1.

STUDY OF NORMAL CONDUCTING ACCELERATING STRUCTURES FOR MEGAWATT PROTON DRIVER LINAC

A.E. Aksentyev, A.A. Kalashnikova, M.V. Lalayan, S.M. Polozov, S.E. Toporkov, National Research Nuclear University MEPhI (Moscow Engineering Physics Institute), Moscow, Russia
T.V. Kulevoy, National Research Nuclear University MEPhI (Moscow Engineering Physics Institute) and Institute of Theoretical and Experimental Physics, Moscow, Russia

Abstract

The preliminary design of a megawatt level proton accelerator-driver is carried out by collaboration between Russian scientific centers MEPhI, ITEP, Kurchatov Institute. This project was supported in 2013 by the Ministry of Science and Education of Russia. The linac general layout includes an RFQ section and section(s) with radiofrequency focusing. The different types of RF focusing were studied due to this project: RF crossed lenses, modified electrodes RFQ, axi-symmetrical RF focusing. All such focusing can be realized by IH-type cavities. The design of a segmented vane RFQ (SVRFQ) with coupling windows and IH- and CH-type normal conducting cavities is discussed in this report. All cavities operate at 162 MHz. The main results of the electrodynamic simulation are presented.

INTRODUCTION

The study of a high-power proton linac for 1.0 GeV was performed by a collaboration of MEPhI, ITEP and Kurchatov institute researchers in 2013. Such a linac was developed to understand the possibility of design an accelerator driven system (ADS) in Russia.

The linac will consist of an RFQ, RF focusing sections and SC modular configuration sections [1, 2]. The segmented vane RFQ (SVRFQ) with coupling windows was designed for beam bunching and low energy acceleration. Original design of elliptical coupling windows was proposed. IH- and CH- cavities were simulated and its electrodynamic characteristics were optimized.

The results of the modeling of the aforementioned structures are discussed below.

SVRFQ CAVITY

A 4-vane RFQ [3] with magnetic coupling windows is considered. The windows decrease the resonant frequency, minimize mode coupling in the RFQ and result in a smaller and more easily tuned accelerator. Specifically the following characteristics are being tuned: 1) separation of quadrupole and dipole modes' frequencies (Δf), 2) ratio of the maximal surface electric field in the resonator to the accelerating field on axis (overvoltage). The accelerating potential between the RFQ electrodes is limited by 1.2-1.5 of Kilpatrick limit units for the CW mode (~130-150 kV). The tuning is performed by variation of 1) the radius of the accelerating channel aperture (a), 2) electrode tip blend radius (VR_b)

and 3) the distance between the end of a vane and the tank back wall – back end length (BBL). The parameters are shown in Figure 1.

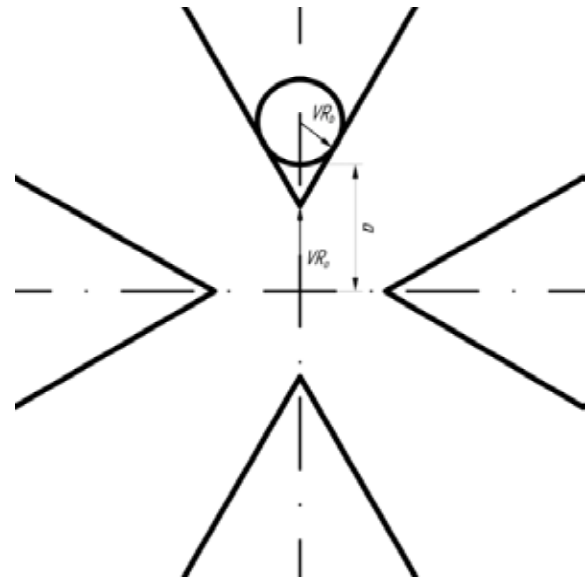


Figure 1: The SVRFQ channel geometrical characteristics.

Base parameters of the optimized and tuned SVRFQ channel were discussed in [4]. Let us discuss, now, the influence of each of channel characteristics to the ratio of the surface electric field to the accelerating field and separation of the quadrupole and dipole modes' frequencies.

Aperture Radius, VR_o

The dependence of mode separation and the overvoltage (in Kilpatrick limit units, Kp [5]) against channel aperture radius variation is presented in Figures 2 and 3 respectively. These pictures show that mode separation is proportional to the overvoltage.

Blend Radius, VR_b

From Figure 4 one sees that variation of blend radius VR_b affects channel aperture: increase of VR_b is equivalent to that in VR_o . Expectedly, the mode separation plots in both cases are similar; yet it is clear that direct variation of electrode offset VR_o has greater effect on mode separation.

STUDY OF POSSIBILITY OF 600-1000 MeV AND 1 MW PROTON DRIVER LINAC DEVELOPMENT IN RUSSIA

A.E. Aksentyev, K.A. Aliev, I.A. Ashanin, Yu.A. Bashmakov, A.A. Blinnikov, T.V. Bondarenko, M.A. Gusarova, A.N. Didenko, M.S. Dmitriyev, V.V. Dmitriyeva, V.S. Dyubkov, A.M. Fadeev, A.D. Fertman, A.A. Kalashnikova, V.I. Kaminsky, E.R. Khabibullina, Yu.D. Kliuchevskaia, A.D. Kolyaskin, M.V. Lalayan, S.V. Matsievskiy, S.M. Polozov, V.I. Rashchikov, E.A. Savin, A.V. Samoshin, Ya.V. Shashkov, A.Yu. Smirnov, N.P. Sobenin, S.E. Toporkov, O.L. Verjbitskiy, V.L. Zvyagintsev, A.V. Ziatdinova, National Research Nuclear University MEPhI (Moscow Engineering Physics Institute), Moscow, Russia

T.V. Kulevoy, S.V. Rogozhkin, National Research Nuclear University MEPhI (Moscow Engineering Physics Institute), Moscow, Russia and Institute of Theoretical and Experimental Physics, Moscow, Russia

V.F. Batyaev, G.N. Kropachev, D.A. Liakin, Yu.E. Titarenko, Institute of Theoretical and Experimental Physics, Moscow, Russia

P.N. Alekseev, V.A. Nevinitza, National Research Center "Kurchatov Institute", Moscow, Russia
S.Yu. Stark, LNL INFN, Legnaro, Italy

Abstract

Alternative nuclear energetic's technologies as fast reactors and accelerating driven systems (ADS) are necessary to solve a number of problems as U-238 or thorium fuel reactor and nuclear wastes transmutation. ADS subcritical system should consist of megawatt-power proton accelerator, neutron producing target and breeder. A number of ADS projects are under development in EU, Japan, USA, China, S.Korea at present. Superconducting linacs or their complexes with high energy storage synchrotron are under design in main projects as a megawatt power proton beam driver. In Russian Federation the complex design for accelerator-driver was carried down more than ten years ago.

INTRODUCTION

A number of ADS projects are under development in EU (EUROTRANS including MYRRHA, EFIT, AT-ADS, Trasco ets. [1-2]; MERIT [3]; ThorEA [4]), Japan (OMEGA, KART, [5]), PRC [6], S.Korea (HYPER [7]), India [8], USA [9-10]. The review of main projects was done in [11].

It should be noted that complex study of driver linac in Russia was carried down more than ten years ago in cooperation of ITAP, IHEP and Moscow Radiotechnical Institute [12-14]. Blanket studies are carried now in IPPI. The new OMEGA project at IHEP which includes a high power 400 MeV proton linac should be also noted.

The new approach to the ADS complex is now under development in framework of the project carried out by collaboration between Russian scientific centers MEPhI, ITEP, Kurchatov Institute. This project was supported in 2013 by the Ministry of Science and Education of Russia. A brief results observation for accelerator part of the project is presented in this paper. It includes accelerator-driver general layout, beam dynamics simulation,

electrodynamics simulations of accelerating cavities and analysis of technological background in Russia.

ACCELERATOR-DRIVER GENERAL LAYOUT

The conceptual design of the linac is presented in Figure 1. The linac will consist of an RFQ for beam bunching and low energy acceleration (up to 2 MeV), RF focusing section(-s) for medium energies (up to 30-50 MeV) and SC modular configuration sections for higher energies. SC QWR and HWR were also discussed for 20-50 MeV range. Several different types of RF focusing linacs were discussed for the medium energies. They are RF crossed lenses [15], modified electrode profile RFQ [16], axi-symmetrical RF focusing (ARF) [17]. The conventional modular configuration linac [18] based on spoke-cavities and 5-cell elliptical cavities were designed for high energies. The linac layout has three intermediate energy output beam lines which can be used already during the linac construction to different experiments with neutron production targets or for radiation testing of reactor construction materials.

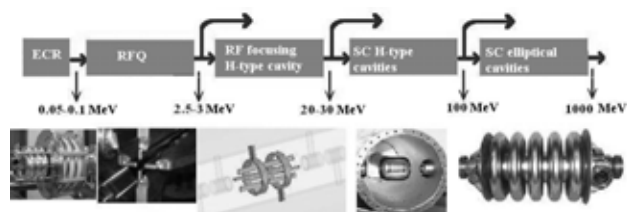


Figure 1: The linac general layout.

Note that such driver linac layout is now conventional and similar designs are proposed in main ADS projects as [1, 2, 6, 7]. The idea to use RF focusing sections for medium energy range is the main difference of our scheme.

DEVELOPMENT AND TESTING OF POWERFUL HIGH-VOLTAGE ELECTRON ACCELERATOR FOR ENERGY-INTENSIVE INDUSTRIES

N.G. Tolstun, A.V. Efremov, A.S. Ivanov, A.N. Kuzhlev, V.P. Maznev, A.I. Machecha,
V.P. Ovchinnikov, D.E. Pavluhov, M.P. Svinin, D.A. Solnyshkov,
JSC "D.V. Efremov Institute of Electrophysical Apparatus", St. Petersburg, Russia

Abstract

The report describes the results of the development and testing of the Electron-23 high-voltage high-power accelerator rated for an accelerating voltage of 1 MV and beam power up to 500 kW at the "NIIIEFA" testing facilities.

The accelerator is intended for industrial processing of flue gases from thermal power stations with the aim to reduce concentrations of nitrogen and sulfur oxides. It may also be used for other energy-consuming processes, such as treatment of wastewaters for their decontamination or processing of natural gases for their conversion into engine fuel. [1]

BRIEF DESCRIPTION OF THE ACCELERATOR

General view of the accelerator with the beam forming and extraction device is schematically shown in Fig.1.

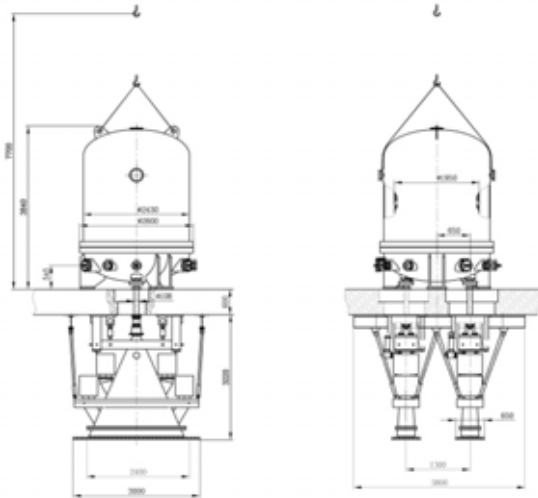


Figure1: General view and main parameters of the «Electron-23» accelerator.

The high-voltage (HV) generator, electron source and accelerating tube (AT) are placed inside a metal vessel filled with a pressurized insulating gas. A three-phase transformer-rectifier with a closed magnetic core and parallel feeding of cascades is used as a HV generator of the accelerator «Electron-23». Such a high-voltage source has a wall-plug-efficiency higher than 90% and practically no restrictions on power. The magnetic core of the HV generator is a construction symmetrical in space and consisting of 3 vertical rods and 2 horizontal annular yokes closing the magnetic flux. Three primary windings

are located on the core rods, encircled with electrostatic screens and are star-connected with a power supply. Three secondary windings consist of separate coils located coaxially with primary windings. Each three coils of the secondary winding are located at one level on different magnetic core rods. They are star-connected and together with 6 diodes form a 3-phase bridge rectifying cascade [2, 3]. In the DC voltage, all twenty seven cascades are connected in series.

The majority of the accelerator components facing the HV gap is made of insulating materials with a high-resistive conducting coating. As a rule, these elements are made of stainless steel to prevent short-circuiting around the magnetic core of the HV generator; for this reason their construction is technologically complicated. The use of insulating materials with a high-resistive coating allows us to simplify the construction and considerably reduce the manufacturing cost of these elements.

A diode-type electron source with a lanthanum hexaboride emitter of 13 mm diameter is used in the accelerator. Emitter holders are made of anisotropic pyrolytic graphite that prevents chemical interaction of the emitter with emitter-holders and provides reduction of the filament power of the electron source down to 100 W [4]. The 1st electrode of the AT serves as the electron source anode. The source filament is fed from a special winding located on the magnetic core of the HV generator. The electron beam current is controlled and stabilized from the low voltage side.

The AT consists of alternating ceramic insulators and metal electrodes forming a vacuum-tight connection. A resistive voltage divider is placed outside the tube on its electrodes. A distinctive feature of the accelerator' design is location of the AT in parallel with rods of the HV generator magnetic core inside a common vessel. Such an engineering solution allows overall dimensions to be decreased, but, requires shielding of the AT against stray magnetic fields produced by the HV generator. To achieve this, electrodes of the AT are made of permalloy, and a distance between them is rather small (12, 5 mm), resulting in the reduction of the stray magnetic field on the AT axis approximately by a factor of 100 [5].

General view of the AT installed in the accelerator is shown in Fig. 2. The accelerator design also enables installation of one more AT in the same high-pressure vessel. Tests of the machine were carried out with a single tube.

The irradiation field forming system consists of an electromagnetic lens, beam scanning device and device for the beam extraction to the atmosphere. The beam scanning device comprises longitudinal and transverse

SINGLE FREQUENCY HIGH INTENSITY HIGH ENERGY NORMAL CONDUCTING HADRON LINAC*

V.V. Paramonov[#], V. N. Leontiev, INR of the RAS, Moscow,
A.P. Durkin, MRTI, Moscow, A.A. Kolomiets, ITEP, Moscow

Abstract

Considering both the beam quality and the possibility of practical realization, the scheme and parameters for 400 MeV H- linac are discussed. The concepts for beam emittance preservation, both transverse and longitudinal, starting from RFQ, following with PMQ focusing DTL and finishing with high energy CCL part are realized. Several focusing schemes are analyzed for DTL and CCL parts. The pulse beam current is limited to the safe value 40 mA and the average current up to 2 mA is supposed by Duty Factor (DF) of 5%. The operating frequency 352 MHz for all linac parts provides the full unification for RF system of the whole. Expected beam parameters are summarized.

INTRODUCTION

From the beam dynamics issue the smooth continuous acceleration with the minimal number of simple transitions between linac parts is the best case. There is no accelerating structure for effective H- ions acceleration in the total energy range from ~ 100 keV to ~ 400 MeV and different structures are used in different linac parts, operating at different frequencies. The matching of longitudinal motion is rather complicated. matching for transverse motion is still required. It can be strongly simplified [1] for the single operating frequency f_0 in the whole linac. The scheme of proposed linac includes well known structures. RFQ is an inevitable part in the linac front end and Coupled Cell Linac (CCL) is mostly effective for high energy part. The mostly developed and effective structure for intermediate part is the Drift Tube Linac (DTL). The recent progress demonstrates both RFQ operating $f_0 \sim (300-400)$ MHz and developed CCL for the same frequency range. CERN Linac4 realizes single frequency concept up to H- energy 160 MeV. Below parameters of such linac are estimated for higher output energy. Much more details of this consideration are given in [2]. All simulations for beam dynamics are performed by using LIDOS and TRANSIT codes [3].

LINAC FRONT END

For high power high energy linac the problem of particle losses is of primary importance. The care for emittance growth preservation should be paid starting from ion source and low energy beam transport to RFQ. For RFQ essential parameters are the transverse emittance growth and output longitudinal emittance. The output beam should be bunched without tails in the phase space,

which will be transformed further in the beam halo.

To have the initial beam formation, RFQ with $f_0=352,2$ MHz and output energy $W_1=3.0$ MeV was estimated [2] assuming voltage 95.0 kV and the maximal electric field $E_{smax}=1.85 E_k$ with the cavity length 3.65 m. For the beam current $I_b=40$ mA simulations shows transverse emittance growth $\sim 10\%$ and total longitudinal emittance as 0.914π MeV-deg. For output beam the phase space portraits are shown in Fig. 1. Comparison with the recently achieved results for the J-PARC RFQ, $f_0=324$ MHz [4], and for SNS RFQ $f_0=402.5$ MHz, [5] shows the accepted parameters as reliable and RFQ cavity construction for DF=5% as realistic.

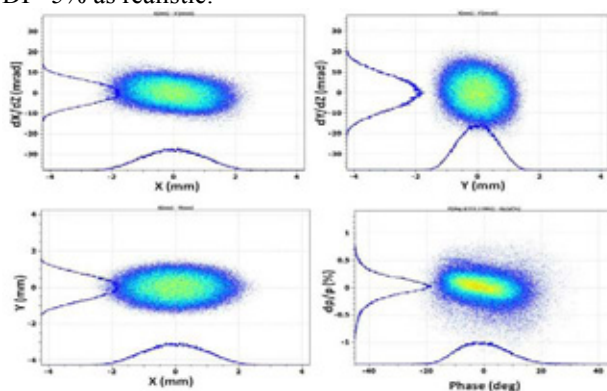


Figure 1: The phase space distributions of particles at the RFQ exit.

MEBT1

The transport line MEBT1 has the length ~ 2.31 m and is required for matching between RFQ and DTL, placement of chopper and beam diagnostic hardware. The line consists from eleven quads, chopper and beam absorber. To reduce the bunch lengthening along axis, line is equipped with two bunching cavities. The design parameters for MEBT1 elements are quite conservative [2]. Simulations show the transverse emittance growth as $\sim 30\%$ and longitudinal one as $\sim 6\%$. It is in good coincidence with similar parameters in the existing linacs – SNS, J-PARC and Linac4. The phase space portraits for beam at the MEBT1 exit are shown in Fig. 2.

DTL PART

For DTL with $f_0=352,2$ MHz application of Permanent Magnet Quads (PMQ) is motivated by higher RF efficiency. RF parameters of DTL cells were studied [2] in the wide range of dimensions. To provide the higher RF efficiency and the safe E_{smax} value $< 1.3 E_k$, one should start with small aperture diameter $2a$ and drift tube cone angle θ in the DTL beginning and increase it to the DTL

*Work supported by IHEP Contract № 0348100096313000178

[#]paramono@inr.ru

THE PROJECT OF THE HV AXIAL INJECTION FOR THE DC-280 CYCLOTRON AT THE FLNR JINR

G.G.Gulbekian, B.N.Gikal, V.V.Bekhterev, S.L.Bogomolov, A.A.Efremov, I.A.Ivanenko, N.Yu.Kazarinov, I.V.Kalagin*, V.N.Melnikov, N.F.Osipov, S.V.Prokhorov, A.V.Tikhomirov, M.V.Khabarov, Flerov Laboratory of Nuclear Reaction, Joint Institute for Nuclear Research, Dubna, Moscow reg., 141980 Russia

Abstract

The project of the high-voltage (HV) axial injection for the DC-280 cyclotron which is being created at the FLNR JINR is presented. The injection system will consist of a Permanent Magnet ECR ion source and a Superconducting ECR ion source, beam analyzing magnets, focusing solenoids, beam choppers, a polyharmonic buncher, 75 kV DC accelerating tubes, a commutating electrostatic deflector and a spiral inflector. One part of the injection system is situated on the HV platform, another part is on the grounded yoke of the DC-280 magnet. The injection system will allow one to inject efficiently ions of elements from Helium to Uranium with the atomic mass to charge ratio in the range of 4÷7.5 providing acceleration of ion currents with intensity more than 10 μ A.

INTRODUCTION

At present time the project of Super Heavy Element Factory is being realized at the FLNR JINR [1]. The project implies design and creation of the DC-280 cyclotron (Figure 1) which has to provide intensities of ion beams with middle atomic masses ($A \sim 50$) up to 10 μ A. The DC-280 will be equipped with high voltage injection system. The injection system has to provide ion transportation from the ECR-ion source to the cyclotron centre and capture into acceleration not less than 50% of ions with the atomic mass to charge ratio of $A/Z=4\div 7.5$. Our experience in modernization of U-400 cyclotron [2] and creation of the DC-110 cyclotron [3] demonstrates that at ion energies of $E_{inj}=15\div 20$ keV/Z (energy per single ion charge) the injection efficiency essentially depends on the ion beam current. At the ion beam currents of 80÷150 μ A the efficiency of capture into acceleration reaches 30÷35%, but for the ion currents less than 10 μ A increasing of the efficiency to 50÷60 % has been observed. The reason of it may be lowering influence of the ion beam space charge and decreasing the beam emittance, especially at low level of the microwave power in the ECR source. To improve the injection efficiency we will increase the injection energy up to $E_{inj}=100$ keV/Z, since the emittance and the space charge effects have to be decreased. The similar problem has been decided at Ganil, France by means of using the high voltage platform (HVP) equipped with the ECR-4 ion source [4]. Besides, we would like to create the injection

with low electrical power consumption. In the last decade some of HVP in the world were equipped with the ECR with low power consumption, for example 300 kV HVP with the superconducting PK-ISIS ECR at "Pantechnik", (France) [5], 320 kV HVP with the permanent magnet ECR at IMP, Lanzhou, China [6].

LAYOUT OF THE AXIAL INJECTION

The high-voltage axial injection of the DC-280 will consist of two HVP. Every HVP will be equipped with an ECR ion source, a focusing solenoid, Einzel lenses and a magnet for ion separation and analyzing. The high voltage accelerating tube will be installed at the edge of the HVP to increase the ion energy up to 100 keV/Z. Both HVP will be placed on standoff insulators above the DC-280 magnet. The insulators will be fastened to the grounded metal platform which leans on the DC-280 magnet yoke (Figure 1).

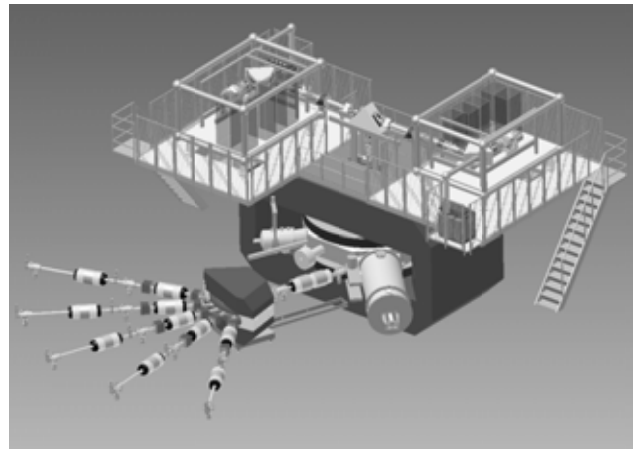


Figure 1: Layout of the DC-280 assembling.

HIGH VOLTAGE PLATFORM

We plan to limit the HVP power consumption to 50 kW to minimize maintenance charges and sizes of isolating transformers. The maximal HV on the HVP will be 75 kV. Every platform will have peripheral tube railings for equalization of the electrical potentials. Water cooling of the magnetic elements will be provided through water tube coils (head, drain) having the maximal total current leakage of 1 mA. When the HV is switched off the service personal can walk around the HVP for maintenance. The scheme allows us to work with every ECR source independently.

* kalagin@nrmil.jinr.ru

THE PROJECT OF BEAM TRANSPORTATION LINES FOR THE DC-280 CYCLOTRON AT THE FLNR JINR

G.G.Gulbekyan, B.N.Gikal, G.N. Ivanov, I.V.Kalagin*, V.I. Kazacha, N.Yu. Kazarinov, M.V. Khabarov, V.N. Melnikov, N.F. Osipov, A.V. Tikhomirov, Y.G. Teterev,
Joint Institute for Nuclear Research, FLNR, Dubna, Moscow region, Russia

Abstract

The project of beam lines for carrying out physical experiments at the DC-280 cyclotron which is being created at the FLNR JINR is presented. The commutating magnet with variable magnetic field induction up to 1.5 T gives us possibility to bend ion beams in five directions providing ion transportation through beam lines to five experimental setups. The beam focusing in the beam lines is provided by set of quadrupole lenses having the gradients up to 7.7 T/m. The beam lines are intended for the efficient ion transportation of elements from Helium to Uranium with the atomic mass to charge ratio in the range of 4-7.5 at energies from 4 up to 8 MeV/amu. The ion beam power will reach the value about 3 kW. The water cooled current aperture diaphragms will be installed into all beam lines to prevent the tube damage. The beam diagnostics consists of the Faraday caps (FC), slit collimators, sector aperture diaphragms and ionization beam profile monitors.

INTRODUCTION

DC-280 cyclotron designed at the Flerov Laboratory of Nuclear Reaction (JINR, Dubna) is intended for carrying out fundamental and applied investigations with ions from He to U (masses from $A = 2$ up to 238) produced by the ECR-source. The energy of the ions extracted from the cyclotron may vary from 4 up to 8 MeV/amu. The main parameters of the DC-280 cyclotron are given in [1].

Utilization efficiency of the accelerator is determined in many respects by quality of the transportation system for the extracted ions. Widely branched system of the beam lines allows one to carry out numerous investigations. This work is devoted to the design of the beam lines for transportation of the extracted heavy ions from the cyclotron to physical targets. Lay-out of the beam lines for heavy ion transportation is shown in Fig. 1.

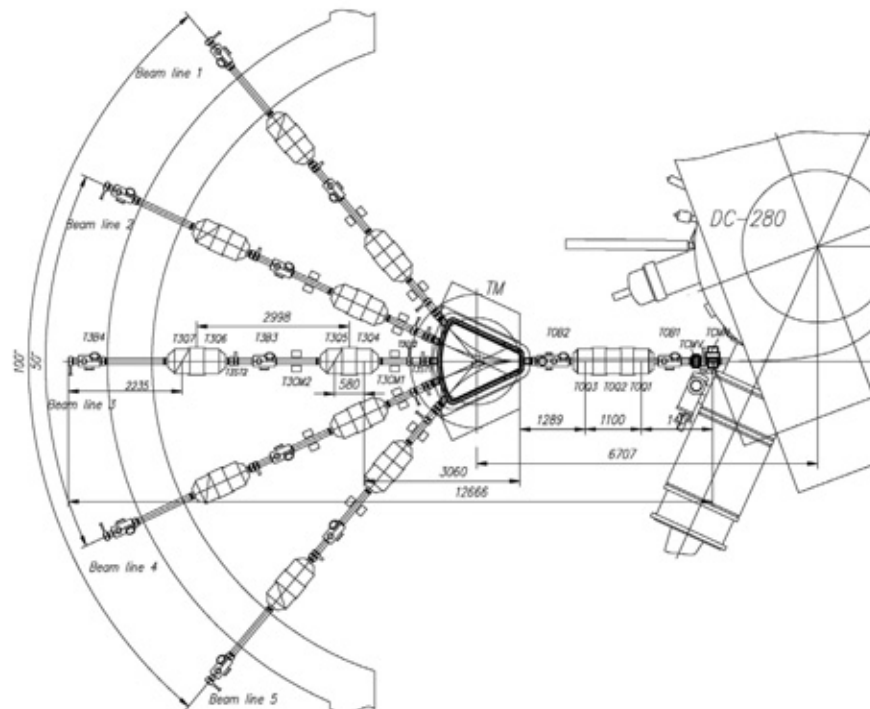


Figure 1: Lay-out of the beam lines for heavy ion transportation.

Where: **TM** is the bending magnet ($\pm 50^\circ$), **TCMH**, **TCMV** are the horizontal and vertical steering magnets at DC-280 extraction, **TxQy** are the magnetic quadrupoles, **TxCMy** are the two-plane dipole steering magnets, **TxBy** are the diagnostics boxes, **TxSTy** are the beam stoppers, **TxGVy** are the vacuum gate valves (where: x is the beam line number, y is the element number).

kalagin@nrmil.jinr.ru

ISBN 978-3-95450-170-0

MAGNETS OF INJECTION AND EXTRACTION SYSTEMS OF CYCLOTRON DC280

N.Kazarinov[#], I.Ivanenko, JINR, Dubna, Russia

Abstract

The design of two magnets of the cyclotron DC280 is presented. The magnets are the parts of injection and extraction systems the cyclotron. The design is based on three-dimensional calculation of the magnet field carried out by using OPERA 3D program code. The influence of the magnetic fields nonlinearities on ion beam dynamics is analyzed.

INTRODUCTION

The isochronous heavy-ion cyclotron DC-280 is a basic part of the Super Heavy Element Facility – the new accelerator complex of Joint Institute for Nuclear Research [1]. The DC-280 cyclotron will produce high-intensity beam of accelerated ions in the range from helium to uranium. The maximum design value of a current of ion beams will be 10 pmcA and the maximum kinetic energy will be 8 MeV/u.

In this report the design of two magnets IM90 and TM50 of SHEF is presented. The analyzing magnet IM90 is a part of high voltage injection system of DC-280 cyclotron [2]. The switching magnet TM50 is placed in extraction beam lines [3] of the facility. Depending on the magnitude of the magnetic field in magnet, the particles move on five orbits corresponding to different bending angles (0, ±25 and ±50 degrees) of the ion beam. The design is based on three-dimensional calculation of the magnet field carried out by using OPERA 3D program code [4]. The 3D computational models of the magnets are shown in Fig. 1.

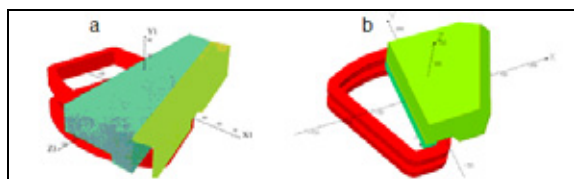


Figure 1: 3D models of IM90 (a) and TM50 (b) magnets

The 3D macro-particle beam dynamic simulation in the magnets was done in the curvilinear coordinates system connected with reference orbit, defined for computational field map. This simulation was carried out by using MCIB04 program code [5].

Inhomogeneities of the magnetic field distribution in the vicinity of the reference orbit were evaluated by Fourier analysis of the magnetic field map.

The optimum value of the basic geometrical characteristics of the magnets influencing on the form of the field distribution are found.

[#]nyk@lnr.jinr.ru

REFERENCE ORBITS OF THE MAGNETS

The reference orbits of the magnets are shown in Fig.2,3. In the case of IM90 magnet the initial approximation for the angular width of the magnet pole (84.75 degrees) found by using the results of [6] gave a good agreement of the effective bending radius (497.4 mm) and its design value (500 mm).

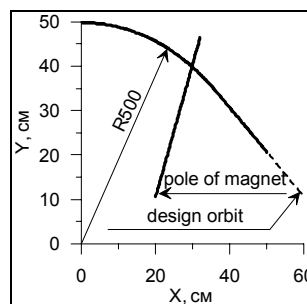


Figure 2: Reference orbit of IM90 magnet

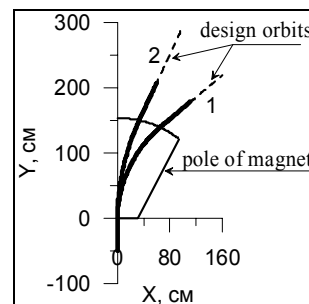


Figure 3: Reference orbits of TM50 magnet

The magnetic fields distributions at reference orbits are shown in Fig. 4-6.

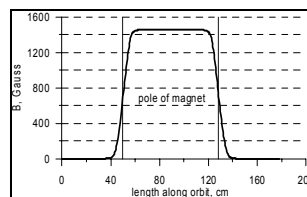


Figure 4: Bz field along reference orbit of IM90 magnet

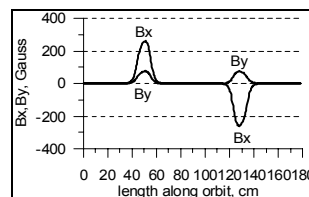


Figure 5: Bx,y field at 2 cm higher reference orbit of IM90 magnet

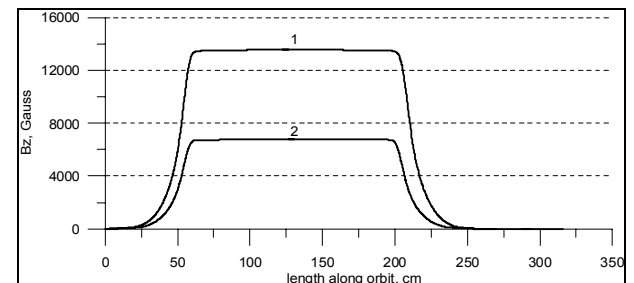


Figure 6: Bz field along reference orbits of TM50 magnet

MAGNETIC FIELD INHOMOGENEITIES

Inhomogeneities of the magnetic field distribution in the vicinity of the reference orbit were evaluated by Fourier analysis of the magnetic field map:

NLSLS-II BOOSTER VACUUM SYSTEM

V.A. Kiselev, V.V. Anashin, S.M. Gurov, A.M. Semenov*, Budker Institute of Nuclear Physics SB RAS, Novosibirsk, Russia
 A.A. Krasnov, Budker Institute of Nuclear Physics SB RAS, Novosibirsk, Russia and Novosibirsk State University, Novosibirsk, Russia

Abstract

NLSLS-II - one of the latest third-generation SR sources - is currently under commissioning at the Brookhaven National Laboratory. In order to improve the operation efficiency in a continuous mode with maximum brightness, the injectors of these SR sources are operated continuously at the energy of up to the energy of the main ring (linac or synchrotron booster) [1]. The full injection energy allows adding electrons to the travelling electrons in a storage ring rather than to regulate a magnet system. This operating mode is often named "Top-Up". NLSLS-II consists of a linear accelerator with the electron energy of up to 200 MeV, a synchrotron booster with the energy of 3 GeV, and a main storage ring. The status and review of the NLSLS-II Booster vacuum system are presented in this paper.

INTRODUCTION

Since 1992, the first specialized storage rings (3rd generation SR sources) with a large number of straight sections of a sufficient length for installation of undulators (or wigglers) and more perfect systems of the storage ring parameter stabilization have been built.

In the first specialized SR sources, electrons were injected into the storage ring at a low energy, then the energy was increased, stabilized, and experiments were carried out. The beam current decreased with time, SR intensity dropped. The cycle with energy decrease, electron storage and energy increase was repeated in 1-2 hours. This was the mode of NLSLS-I operation. NLSLS-I booster was designed for acceleration of electrons from the energy of 120 MeV up to 700 MeV, the energy of storage rings was 800 MeV (vacuum ultra-violet spectrum) and 2.8 GeV (hard X-rays).

For today, mostly 3rd-generation SR sources are in operation and under construction in the world. One of latest sources scheduled for starting-up in 2015 is NLSLS-II (Brookhaven National Laboratory, USA). Main parameters of the NLSLS-II Synchrotron are presented in [1].

VACUUM SYSTEM DESCRIPTION

The perimeter of the booster vacuum chamber is 158.4 meters. 8 all-metal electropneumatical gate valves (actuation time ~ 2-3 sec) are installed in the ring for isolation of certain sections of the booster vacuum

chamber. The booster consists of 4 arc sections (about 31 m each) and 4 straight sections (8 m each). All vacuum chambers are made of 316 L stainless steel, with Conflat flanges. The vacuum chamber aperture in arc sections is an ellipse of 41x24 mm (molecular conductivity of the chamber is about 3.2 l·m/sec); and the aperture of the majority of the chambers in straight sections is an ellipse of 62x22 mm (molecular conductivity of the chamber is about 4 l·m/sec). After manufacturing all vacuum chambers were exposed to special chemical treatment to reduce the outgassing rate [2].

For smoothness of the vacuum chamber and reduction of electron beam losses, special transitions from elliptical cross-section (24x41 mm) to circular cross-section (46 mm diameter) were produced, places for pumping were made from a one-piece tube with cut-out slots for pumping, besides, some bellows in straight sections were supplied with RF contacts having the shape of the vacuum chamber.

Residual gas pressure after accumulation of current integral of an order of 1 A·h should be not worse than 1E-7 Torr. Vacuum is provided with Gamma Vacuum ion-pumps (71 pieces) with pumping speed of 45 l/sec, placed at an average distance of 2.3 meters from each other. Two inverted-magnetron cold cathode gauges are installed in each section for vacuum measurements, and convection-enhanced Pirani gauges (MKS) are planned for forevacuum measurements. Detection of residual gas spectrum and of micro-leaks is carried out by means of MKS mass-spectrometers. Fig.1 shows the arrangement of the main components of the booster vacuum system.

RESULTS OF THE WORK PERFORMED

A rather strong synchrotron radiation results in an additional radiation-induced desorption of the residual gas molecules from the vacuum chamber walls and can cause a significant mechanical stress in vacuum chamber due to a non-uniform heating.

Despite a pulse operation mode of the booster (SR intensity duty ratio is 1/7 at a 2Hz repetition frequency), gas desorption under the influence of photons on vacuum chamber walls will exceed thermal desorption.

A relatively low SR power (maximum power is 44 W/m in BD bending magnets) does not require any special radiation absorbers. However, such radiation can cause mechanical stresses in vacuum chamber.

*A.M.Semenov@inp.nsk.su

EFFECT OF THE VERTICAL VELOCITY COMPONENT ON PROPERTIES OF SYNCHROTRON RADIATION

O.E. Shishanin, Moscow State Industrial University, Moscow, Russia

Abstract

This subject determines more precisely characteristics of synchrotron radiation when the charge particle moves on the spiral in physical devices and a space. For this purpose the Bessel functions of a high order are approximated to within the second approach. It is discussed that the vertical component of velocity in alternating magnetic fields of accelerators significantly changes the spectral and angular distributions of the radiation intensity.

Theory of synchrotron radiation when the electron has a spiral trajectory considered by many authors (see, for example, [1]). In this paper we find a more accurate synchrotron radiation formulas for the spiral and circular motion of electron in a constant and homogeneous magnetic field. For this purpose, first of all we define the asymptotic representation of the Bessel functions. Previously, several asymptotic expressions for the Bessel functions with large index were obtained [1] - [3]. Based on these methods we have extended the calculations up to the second order of accuracy [4].

However, we can take the integral representation of the Bessel functions

$$J_\nu(y) = \frac{1}{2\pi} \int_{-\pi}^{\pi} e^{i\nu\varphi - iy \sin \varphi} d\varphi.$$

When the circular motion, it will $y = \nu\beta \sin \theta$, where $\beta = v/c$ (v is the electron velocity) and θ is the spherical angle of radiation. Following Schwinger [5], we assume φ as a small parameter because the radiation is removed from the small part of the orbit in a certain direction.

To study the problem with a spiral trajectory there is a need to replace β by

$$\beta_0 = \sqrt{(\beta^2 - \beta_3^2)/(1 - \beta_3^2)}$$

and $\sin \theta$ by

$$\sin \theta_0 = (\sqrt{1 - \beta_3^2} \sin \theta)/(1 - \beta_3 \cos \theta);$$

$c\beta_3$ here is the velocity component along the magnetic field. Thus, we have

$$J_\nu(\nu\beta_0 \sin \theta_0) = \frac{1}{2\pi} \int_{-\pi}^{\pi} e^{i\nu(\varphi - \beta_0 \sin \theta_0 \sin \varphi)} d\varphi.$$

Expanding the right-hand side in terms of φ and introducing a new variable as $\varphi = pt$, where

$$p = \sqrt[3]{6/(\nu\beta_0 \sin \theta_0)} \cdot t,$$

we get

$$J_\nu(\nu\beta_0 \sin \theta_0) = \frac{p}{2\pi} \int_{-\infty}^{\infty} dt e^{i(xt+t^3)} [1 - i \frac{\nu}{120} (\frac{6}{\nu})^{5/3} t^5]$$

with $x = p(1 - \beta_0 \sin \theta_0)\nu$. Here the integral limits were extended to infinity because φ is small.

Then we use the following expressions:

$$\int_0^{\infty} \cos(t^3 + xt) dt = \frac{\sqrt{x}}{3} K_{1/3}(x_1),$$

$$\int_0^{\infty} t^5 \sin(t^3 + xt) dt = \frac{x^3}{27\sqrt{3}} K_{2/3}(x_1) - \frac{4}{27} x^{3/2} K_{1/3}(x_1),$$

where $x_1 = 2(x/3)^{3/2}$. In the first equality we took into account the terms of order

$$\varepsilon = 1 - \beta_0^2 \sin^2 \theta_0.$$

Finally for asymptotics of the Bessel function and its derivative, we obtain

$$J_\nu(\nu\beta_0 \sin \theta_0) \approx \frac{\sqrt{\varepsilon}}{\pi\sqrt{3}} [K_{1/3} + \frac{1}{10}\varepsilon(K_{1/3} - 2\mu K_{2/3})], \tag{1}$$

$$J'_\nu(\nu\beta_0 \sin \theta_0) \approx \frac{\varepsilon}{\pi\sqrt{3}} [K_{2/3} + \frac{1}{5}\varepsilon(2K_{2/3} - (\frac{1}{\mu} + \mu)K_{1/3})], \tag{2}$$

where $\mu = \nu\varepsilon^{3/2}$ and $\mu/3$ is an argument of functions K_i . The neglected terms are of the order ε with respect to the main term.

Formulas for spectral and angular distributions in the case of the spiral motion we can get a direct calculation or by the Lorentz transformations. Then for the components of the linear polarization of the radiation intensity (in the orbital plane and perpendicular to it, respectively) we get

$$dW_\sigma(\nu, \theta_0) = W_1 \beta_0^2 J_\nu'^2(\beta_0 \nu \sin \theta_0) \sin \theta_0 d\theta_0, \tag{3}$$

$$dW_\pi(\nu, \theta_0) = W_1 \cot^2 \theta_0 J_\nu^2(\beta_0 \nu \sin \theta_0) \sin \theta_0 d\theta_0, \tag{4}$$

where

$$W_1 = \frac{3}{2} W_0 \nu^2 \varepsilon_0 (1 + \beta_3 \cos \theta_0), W_0 = \frac{2}{3} \frac{e_0^4 H^2}{m_0^2 c^3}, \varepsilon_0 = 1 - \beta_0^2.$$

Radiation frequency ω will be

$$\frac{e_0 H}{mc} \cdot \frac{\nu}{1 - \beta_3 \cos \theta_0},$$

where H is the magnetic field strength. Using asymptotics, right-hand sides of (3) and (4) can be written as

$$\frac{1}{3\pi^2} W_1 \beta_0^2 \varepsilon^2 K_{2/3}^2 [1 + \frac{2}{5}\varepsilon(2 - (\frac{1}{\mu} + \mu)K_{1/3}/K_{2/3})] \sin \theta_0 d\theta_0, \tag{5}$$

HORIZONTAL EMITTANCE REGULATION AT SIBERIA-2

A.G.Valentinov, V.N.Korchuganov, Yu.V.Krylov, Yu.L.Yupinov, NRC Kurchatov Institute, Moscow, Russia

Abstract

Synchrotron radiation (SR) brightness is the most valuable parameter of every SR light source. It depends greatly on horizontal emittance of an electron beam. That's why all modern SR light sources have designed emittance of several nanometers. A horizontal emittance of SIBERIA-2 now equals to 98 nm [1]. It can be decreased by two ways. First way is to find another working point (betatron tunes) with lower emittance. Maximal possible current values of existing power supplies must be taken into account. Injection efficiency may become worse because of smaller dynamic aperture (DA) due to stronger sextupoles. Second way is to rebuild magnetic structure keeping the same betatron tunes. Advantages of this method are good injection efficiency and proved energy ramping process. Modification of the magnetic structure may be done at high energy with more stable electron beam. But the second way is not allowed to reach as lower emittance level as in the first way.

Theoretical and practical aspects of these two ways are described in the report. Magnetic structures with dispersion-free straight sections and smooth horizontal dispersion function are presented. Also structure with higher emittance is described in order to reach higher injection efficiency.

INTRODUCTION

Brightness of synchrotron radiation from dedicated SR sources depends strongly on horizontal emittance ϵ_x of an electron beam. Modern 3rd generation storage rings have ϵ_x value of about several nanometers. Today SIBERIA-2 storage ring operates with $\epsilon_x = 98$ nm at 2.5 GeV, so minimization of its value is very actual.

It may be performed by two ways. First way is to find new working point and to change magnetic structure at injection energy 0.45 GeV. Limitations imposed by power supplies (after energy ramping) must be taken into account in this case. Another problem is smaller DA in structures with smaller emittance, so injection efficiency may be decreased. Second way to minimize ϵ_x consists in reorganization of magnetic structure in old working point at 2.5 GeV after energy ramping. Established processes of injection and energy ramping are advantages of this way. Adjustment of magnetic structure takes place at high energy where stability of electron beam is much higher. But resulting emittance in the second way cannot be so small like in the first one.

NEW WORKING POINTS

ϵ_x minimization leads to stronger focusing, natural chromaticity growth and as a consequence stronger sextupoles for chromaticity compensation. Nonlinear magnetic fields in sextupole lenses excite resonances

which restrict DA. It leads to lower injection efficiency, lower beam lifetime, beam losses during energy ramping. For these reasons magnetic structure in new working points must keep (or improve) machine parameters: injection rate, high stored current, small energy ramping time etc.

SIBERIA-2 structure contains 6 families of quadrupoles (see Fig.1). Lenses F1 and D1 create achromatic bend, F2 determines betatron functions behavior in bending magnets, other lenses in dispersion-free straight section define values of betatron tunes. Sextupoles for chromaticity correction are situated near F1 and D1 quadrupoles. Injection takes place in horizontal plane from inner part of the ring right before F1. Betatron tunes usually equal to $Q_x = 7.77$, $Q_z = 6.70$.

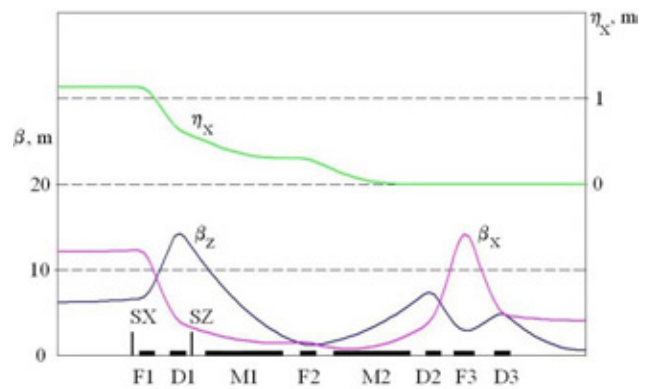


Figure 1: Betatron functions on one-half of the SIBERIA-2 cell (10.34 m = 1/12 of ring circumference). F, D – quadrupoles, M – bending magnets, S – sextupoles.

New magnetic structure may contain achromatic bend or not.

Magnetic Structure with Achromatic Bend

In this case gradients of F1 and D1 must correlate to keep achromatic bend, so emittance is strongly depends on F2 gradient. ϵ_x minimum value corresponds to F2 gradient 3.6 m⁻² instead of 2.8 m⁻² in present structure. New structure has betatron tunes $Q_x = 7.85$, $Q_z = 3.79$ and $\epsilon_x = 66$ nm (all calculations were made by code OPTICK). DA calculations for injection point demonstrate reduction of available aperture from $A_x = 27$ mm (present structure, horizontal plane, ± 40 mm physical aperture) to $A_x = 19$ mm in the new structure. We tried to inject beam into this structure and discovered two times less injection efficiency than in the old structure. As one can see later, this working point have not great advantages in comparison with present one. General properties of the structure are presented in Table 1.

ELECTRON EMISSION AND TRAPPING IN NON-UNIFORM FIELDS OF MAGNET STRUCTURE AND INSERTION DEVICES AT SR SOURCE SIBERIA-2

V.N. Korchuganov, V.I. Moiseev, N.V. Smolyakov, NRC KI, Moscow, Russian Federation

Abstract

In vacuum chamber of SR source, scattered photons provide high intensity flows of photo emitted electrons along the magnetic field lines. The unperturbed electrons reach the opposite walls. The relativistic bunches influence the trajectories of low energy electrons. These electrons can be trapped by non-uniform magnetic field. The low energy electron distributions change the operating settings of the storage ring. For Siberia-2 case, the low energy electrons are evaluated both in quadrupole lenses and in superconducting wiggler on 7.5 T field. The qualitative description of the trapped electrons behaviour was developed. In calculations, the analytical solution was obtained and used for estimations of single impact of relativistic bunch.

INTRODUCTION

The electron storage ring Siberia - 2 is 124 m in length with electron beam energies from 450 MeV up to 2.5 GeV. Beam life time is about 20 -30 hours in regular mode at the electron beam currents above 100 mA. Siberia-2 storage ring is equipped with a superconducting wiggler with magnetic field up to 7.5 Tesla.

This study is initiated by ultrasound measurements at walls of the Siberia-2 vacuum chamber [1]. Ultrasound signals increase with the beam current but appear only if the beam current exceeds some threshold. In this report, an analytical approach is developed for describing trapping and storage of the low energy secondary particles in spatially non-uniform magnetic fields.

In adiabatic approximation, the low energy particle can be considered as a small magnetic dipole with invariant momentum magnitude and oppositely directed to the external magnetic field. Particles oscillate along the magnetic field lines. Relativistic electron beam bunches circularly move in the storage ring. They periodically kick the secondary electrons by its electric field. Being strongly kicked, the secondary electrons move towards storage ring vacuum chamber. We have derived here the analytic expression for transversal component of the secondary electron momentum, which they acquire due to electromagnetic interaction with the electron beam bunch.

LOW ENERGY PARTICLES IN SLOW VARYING SPATIALLY NON UNIFORM MAGNETIC FIELDS

In uniform magnetic fields, particle trajectories are the

*This work was partially supported by the Russian Federation program "Physics with Accelerators and Reactors in West Europe (except CERN)" and by grant of the Russian Ministry of Education and Science (agreement No. 14.587.21.0001).

ISBN 978-3-95450-170-0

regular spirals consisting of the circular transverse motion and the longitudinal motion along the magnetic field line. The transverse motion parameters are illustrated in Table 1 for electrons with 1 eV kinetic energy.

Table 1: Transvers motion parameters for 1 eV electrons

Field, T	0.01	0.1	1
Radius, mm	0.34	0.034	0.0034
Frequency, GHz	0.28	2.8	28

Adiabatic Approximation

In spatially non-uniform slowly varying magnetic field, the equations of particle motion can be averaged over the transverse circular motion of the particles (adiabatic approximation [2]). This approximation provides good results if the transverse trajectory radii are much smaller than the radii of magnetic lines curvature. Time averaging procedure is illustrated at Fig.1. Spatial variation of magnetic field \vec{B} initiates the normal field component B_n which relates the transverse to longitudinal motions:

$$m \frac{dv}{dt} = \frac{qV}{2\pi r} \oint B_n dl, \quad m \frac{dV}{dt} = -\frac{qv}{2\pi r} \oint B_n dl.$$

These equations can be transformed to

$$\frac{dv}{dt} = \frac{vV}{2B} \frac{dB}{ds}, \quad \frac{dV}{dt} = -\frac{v^2}{2B} \frac{dB}{ds}. \quad (1)$$

Directional derivative $\frac{dB}{ds}$ is the magnetic field gradient along the magnetic field line. In mentioned above transformations, resulted from Maxwell equation $\text{div} \vec{B} = 0$ relation $\oint B_n dl = \frac{dB}{ds} \pi r^2$ is used.

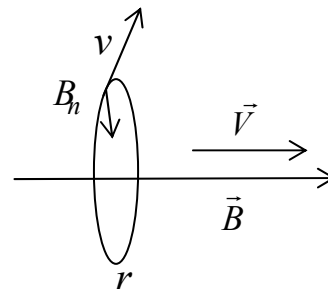


Figure 1: Sketch of an electron motion in magnetic field.

Two values are conserved in adiabatic approximation (1):

$$v^2 + V^2 = \text{const}, \quad v^2/B = \text{const}. \quad (2)$$

Low Energy Particles in Quadrupole Plane field

The magnetic field may be considered as a planar one in the vicinity of the quadrupole lens centre, see Fig. 2.

ANALYSIS OF HIGH ORDER MODES DAMPING TECHNIQUES FOR 800 MHz SINGLE CELL SUPERCONDUCTING CAVITIES*

Ya.V. Shashkov, N.P. Sobenin, National Research Nuclear University MEPhI
(Moscow Engineering Physics Institute), Moscow, Russia
M.M. Zobov, LNF-INFN, Frascati (Rome), Italy

Abstract

The High Luminosity LHC upgrade program foresees a possibility of using the second harmonic cavities working at 800 MHz for the collider bunch length variation. Such harmonic cavities should provide an opportunity to vary the length of colliding bunches. In order to supply the required harmonic voltage several single cell superconducting cavities are to be used. Different cavity designs and several higher order mode (HOM) damping techniques are being studied in order to reduce the cavity HOM impact on the beam stability and to minimize parasitic power losses. In this paper we analyze and compare the HOM electromagnetic characteristics and respective wake potential decay rates for cavities with grooves, fluted and ridged beam pipes. The problem of Lorentz force detuning is also addressed.

INTRODUCTION

At present the project aimed at Large Hadron Collider luminosity upgrade (HL-LHC) is being developed at CERN [1]. The luminosity increase is expected to be accomplished by increasing the currents of circulating beams, by reducing transverse beam sizes at the interaction points (applying smaller betatron functions) and using crab cavities to compensate the geometric luminosity loss in beam collisions [2].

The project considers also a possible implementation of harmonic cavities in addition to the main accelerating cavities working at 400 MHz to increase or to shorten the bunches [3-7]. In order to achieve the desired results a combination of the existing main RF cavities and harmonic cavities operating at 800 MHz is being studied.

In this paper we study electromagnetic characteristics of HOMs for a single cell 800 MHz superconducting cavity. Different techniques for the HOM damping such as beam pipe grooves, fluted beam pipes, ridged beam pipes etc. are investigated and compared.

HIGHER ORDER MODES DAMPING

Basic Design

An initial design of the harmonic cavity has been obtained by scaling (reducing) all the sizes of the LHC accelerating cavity operating at 400 MHz by a factor of 2 [8]. The cavity view is shown in Fig. 1. It is assumed in [8] that higher order modes damping is carried out, as in the case of the LHC accelerating cavity, with four couplers: two dipole and two broadband couplers. These

couplers break the cylindrical symmetry of the electromagnetic field in the structure which gives rise to the transverse component of the electric field (kick-factor) causing a negative impact on the performance of the accelerated beam. Besides, the transient beam loading compensation in LHC requires a very high power main coupler [9]. Placing the robust main coupler and the HOM couplers on the same beam pipe may complicate the final design. That's why different HOM damping techniques were investigated.

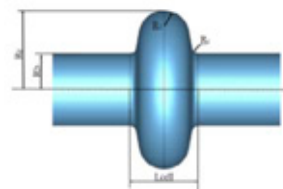


Figure 1: Accelerating cavity.

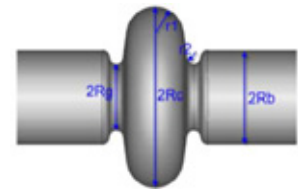


Figure 2: Cavity with grooved beam pipes.

We started our analysis by calculating the resonance frequency and the effective resistance to quality factor Q ratio (parameter R/Q_0) for the cavity shown in Fig. 1 by varying the drift tube radius. It was found that the most dangerous dipole HOM are TE_{111} and TM_{110} . The frequency of these dipole HOMs lie below the cut-off frequency of the TE_{11} wave and therefore cannot propagate along the drift tube [10]. HOMs couplers should be placed as close as possible to the accelerating cavity for the effective damping of such trapped modes.

Beam Pipe with Grooves

Another way to damp the HOMs is to cover the inner surface of the drift tubes with a dissipative material and let the HOMs propagate toward the absorbing load. This method is effective if the higher order mode frequencies become lower than the beam pipe cut-off frequency. Such a task can be accomplished by using grooved structures [11], i.e. cavities with grooves, as shown in Fig. 2.

The main advantage of the grooved structure is its cylindrical symmetry providing the same level of effective damping of HOMs with different polarizations. The absence of HOM couplers makes the design simpler and eliminates eventual negative impact of the couplers on beam dynamics due to the field distortion at their locations.

The results of simulations with ABCI code [12] clearly demonstrate that by choosing the beam pipe radius and the groove geometry in a proper way we have managed to obtain a truly "single mode" cavity. Figure 3a shows the simulated cavity shape, while Figs 3b shows respectively

*Work supported by RFBR grant 13-02-00562/14 and by the EU FP7 HiLumi LHC - Grant Agreement 284404

HIGHER ORDER MODES DAMPING FOR 9-CELL STRUCTURE WITH MODIFIED DRIFT TUBE

A. Mitrofanov, Ya. Shashkov, N. Sobenin, National Research Nuclear University MEPhI (Moscow Engineering Physics Institute), Moscow, Russia,
 V. Zvyagintsev, TRIUMF, Canada, Vancouver

Abstract

This paper is focused on HOM damping in 9-cell superconducting cavities. We are considering HOM propagation outside from the cavity ridged and fluted drift tubes. The analysis of the influence of the parameters of the drift tube on the HOM damping was conducted. The considered methods were analysed and compared.

INTRODUCTION

Development of accelerating structures for modern types of accelerators, such as Energy recovery linacs (ERLs), requires special attention to higher order modes (HOMs) damping. HOMs excitation could create high losses on the cavity walls, beam instability and beam break up (BBU). HOMs couplers are often used in such structures for HOM damping but they could lead to violation of the axial symmetry of the accelerating field and create transverse field components (kick-factor) that can negatively affect on the beam emittance. Also these devices are subject for multipactor discharge and all kinds of pollution. Here we are studying different options of beam pipes to provide better HOMs propagation from the cavity, assuming that they will be dissipated away from the cavity.

INITIAL DESIGN

As a reference point for simulation HOMs propagation was taken 9-cell 1300 MHz superconducting electron accelerating cavity (Fig. 1) [1]. In order to estimate efficiency we decided to calculate HOM electro-dynamics characteristics for the structure without couplers and put at the end of drift tubes RF port boundary conditions, representing ideal loads away from the cavity.

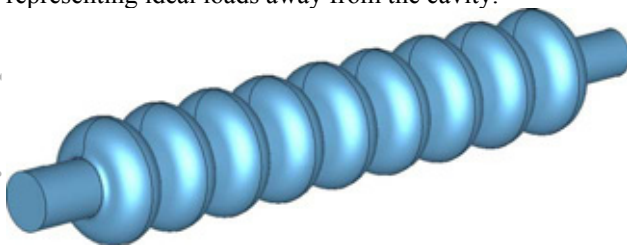


Figure 1: Superconducting 9-cell cavity model.

In order to estimate HOM frequency range, we calculated dispersion characteristics (Fig. 2) for E_{010} modes and HOMs. The most dangerous HOMs for the structure are dipole modes H_{111} , E_{110} , E_{H11} ; quadrupole modes H_{211} and E_{210} and monopole mode E_{011} .

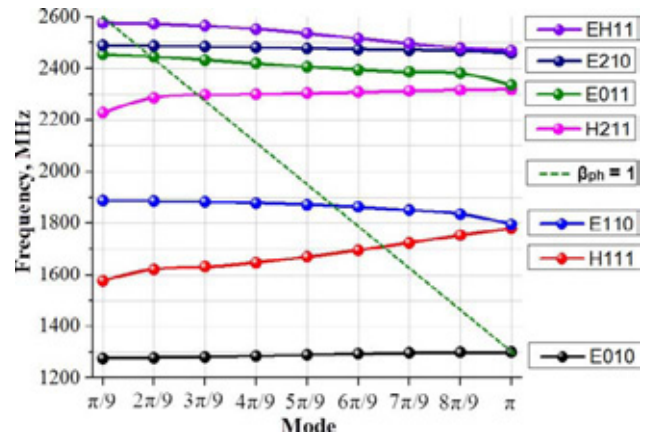


Figure 2: Dispersion characteristics for main wave and for HOMs and β -phase = 1 line.

β -phase = 1 line is shown on the dispersion characteristic on fig 2. Intersection points of dispersion characteristics with β -phase = 1 line (synchronous point) represent modes with the largest interaction between particles and waves and those points need an additional attention.

External Q-factor values for HOMs and operational mode are presented on Fig 3. Q_{ext} values were calculated in CST Microwave Studio [2].

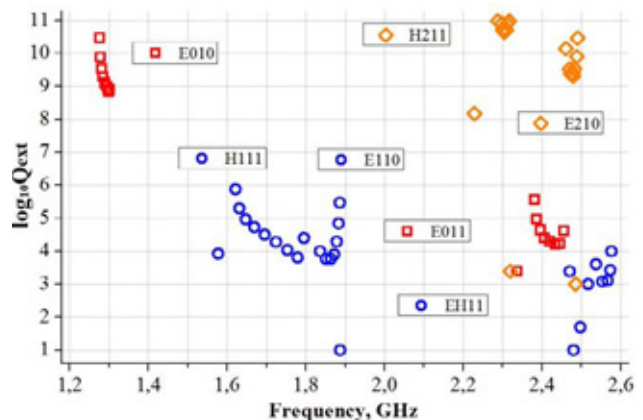


Figure 3: External Q-factor calculations results for HOMs in 9-cell elliptical cavity with beampipes loaded with RF ports. Square (red) – monopole waves, circle (blue) – dipole waves, diamonds (orange) – quadrupole waves.

Comparison of the results with results for similar structures [3] showed that Q_{ext} for operating mode is nearly the same, three orders higher for dipole modes, 4-5 order higher for quadrupole modes and for 2nd monopole HOM it's two times higher.

*Work supported by RFBR grant 13-02-00562/14

SUPPRESSION OF MECHANICAL OSCILLATIONS IN QUARTERWAVE 106 MHz RESONATOR

I.I.Petrushina, I.V. Rybakov, M.A. Gusarova, Ya.V. Shashkov, National Research Nuclear University (Moscow Engineering Physics Institute), Kashirskoe shosse, 31, Moscow, Russia
 V.L.Zvjagincev, TRIUMF, Canada's National Laboratory for Particle and Nuclear Physics, Vancouver, Canada

Abstract

Analytical calculations and numerical simulations have been done for mechanical eigenmodes of quarter wave superconducting resonators with operating frequency of 106 MHz and 80 MHz. A possibility of frequency shift of mechanical modes in 106 MHz resonator has been estimated by application of the damper. We have optimized the damper's position for suppression efficiency. We have also compared the numerical and experimental results.

INTRODUCTION

Superconducting quarter wave resonators (QWR) are used very often in particle accelerators at relatively low particle velocities $\beta < 0.15$. They operate in frequency range from 70 to 160 MHz. The structure of commonly used superconducting QWRs is enough sensitive for mechanical vibrations because of their length of 0.5-1 m made from 2-3 mm thin sheets of Nb. Superconducting cavities inside of cryomodule affected by various factors such as vibrations from environment and vacuum pumps, instant impacts from valves, oscillations of liquid He pressure. Hence, a wide spectrum of mechanical oscillations is applied to the cavity and could excite mechanical oscillations deforming the cavity geometry and providing substantial deviations of resonant frequency. It causes instabilities in cavity operation. There are several ways to mitigate this problem:

- To keep mechanical resonances in higher frequencies region to be far away from strong industrial noise components of 50-60 Hz
- To make cavity structure more rigid to reduce sensitivity for vibrations
- To make operational bandwidth of the cavity higher than frequency deviation caused by mechanical vibrations
- To use mechanical damper [1] to dissipate energy of mechanical vibrations.

The most effective way of microphonics suppression is to develop mechanical dampers for the cavities.

This paper is focused on investigation of mechanical oscillations in 106 MHz [2] superconducting QWR with mechanical damper. The cavity design presented in Fig. 1.

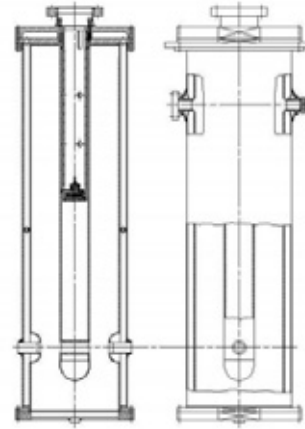


Figure 1: Design of the 106 MHz superconducting Nb QWR with mechanical damper.

ANALYTICAL CALCULATIONS

Inner conductor of the QWR is the most sensitive part to mechanical impacts. Frequencies of mechanical modes f_i of the inner conductor can be roughly estimated by using an approach of a thin-wall cylinder fixed at one edge [3].

$$f_i = \frac{\alpha_i^2 \cdot \sqrt{\frac{E \cdot I}{\mu}}}{2 \cdot \pi \cdot L^2} \quad (1)$$

where E is Young's modulus; L = 685 mm is the length of the inner conductor; μ is the mass of the inner conductor per unit length; α_i is the intrinsic constant of oscillation ($\alpha_1 = 1.875$, $\alpha_2 = 4.694$ for the first and second modes, respectively); $I = \frac{\pi}{4}(r_o^4 - r_i^4)$ is the moment of inertia of a thin-wall cylinder with radii of r_i and r_o .

According to these formulae, the frequencies of the lowest mechanical modes are $f_1 = 46.5$ Hz and $f_2 = 291.2$ Hz for the resonator with an operating frequency of 80 MHz; and $f_1 = 72.7$ Hz and $f_2 = 455.7$ Hz for the resonator with an operating frequency of 106 MHz. According to [3], the frequencies of the first two modes of the inner conductor of 80 Hz resonator are $f_1 = 45$ Hz and $f_2 = 284$ Hz. The difference between results might be explained due to approximation of the theoretical model which did not take into account a complicated shape of the inner conductor.

INFLUENCE OF THE DIFFERENT GEOMETRIC PARAMETERS OF SUPERCONDUCTING ELLIPTICAL CAVITIES ON THE MULTIPACTOR

I.I.Petrushina, M.A. Gusarova, National Research Nuclear University (Moscow Engineering Physics Institute), Kashirskoe shosse, 31, 115409, Moscow, Russia

Abstract

The results of numerical simulations of multipacting discharge in different superconducting elliptical cavities are presented in this paper. The influence of aperture radius, equator shape, iris shape and frequency and electron trajectories for different geometrical parameters of elliptic structures are considered.

INTRODUCTION

Multipacting simulations were carried out using MultiP-M code [1] which provides information about threshold values of accelerating gradient, character and parameters of an electron trajectories and shows the areas of the structure where multipacting discharge occurs. As the result of simulations we obtain a dependence of the of secondary electrons number increase within the cavity vs. accelerating gradient. Example of such graph for various aperture radii is shown in Figure 1.

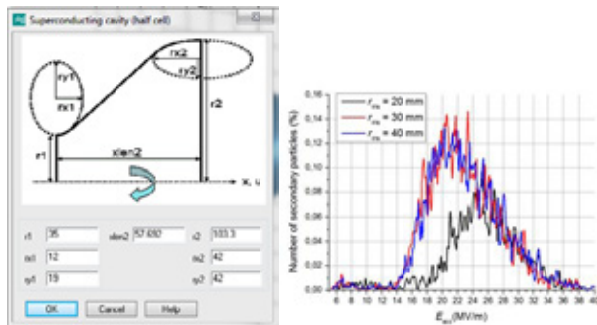


Figure 1: Basic shape of the 1.3 GHz SC cell (left) [2] and the number of secondary electrons as a function of accelerating gradient (right).

This plot doesn't allow obtaining precise values of accelerating gradient when multipacting discharge can occur. The next step of discharge prediction is a detailed analysis of an electron motion.

INFLUENCE OF THE APERTURE RADIUS

Detailed investigation of an electron motion shows that stable multipacting trajectories (1st order at equator region) are obtained in a wide range of an accelerating gradients from 4.3 to 38 MV/m. One can see from Figure 2 that the range of accelerating gradient becomes narrower for larger iris aperture dimensions..

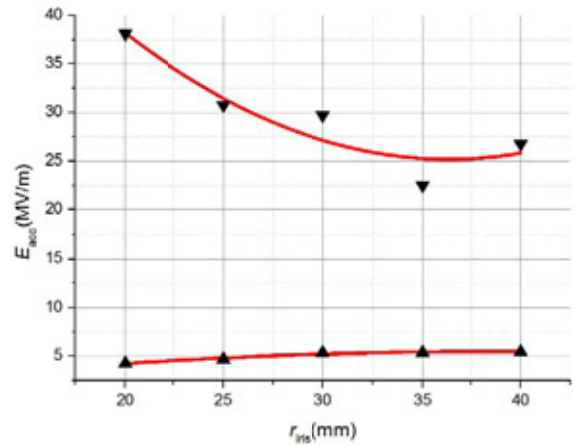


Figure 2: Threshold values of Eacc for various radii.

Q-curve plot (Fig.3) obtained during the vertical test of the standard cell geometry with r_{iris}= 35 mm shows that Q-value starts decreasing at 5-6 MV/m of accelerating gradient which is close to the simulation result.

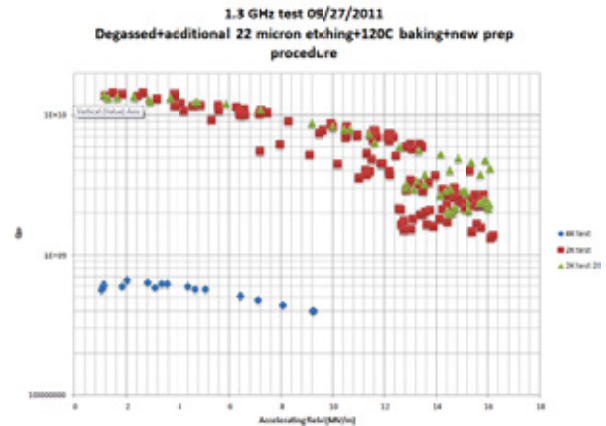


Figure 3: Experimental Q-curve for the standard geometry iris=35 mm. Courtesy of TRIUMF [3].

An example of stable 1st order trajectory is shown in Figure 4. Dependence of main parameters of such trajectories (energy and amplitude) as functions of accelerating gradient for various aperture radii is presented in Figures 5 and 6.

MULTIPACTOR IN ELLIPTICAL CAVITIES 800 MHz

I.I. Petrushina, M.A.Gusarova, National Research Nuclear University (Moscow Engineering Physics Institute), Kashirskoe shosse, 31, 115409, Moscow, Russia

Abstract

The studies of the multipacting discharge possibility in elliptic single-cell cavities at 800 MHz with three types of higher order modes couplers were done. The ranges of the field gradients where the conditions for the occurrence of first order multipacting discharge in the equatorial region, as well as the HOM field levels were determined.

INTRODUCTION

It is known that the equator area in the elliptical shape cavities is of the greatest risk in terms of multipactor discharge development where the first and the second orders stable trajectories could exist. In addition, HOM damping components such as corrugations, ribs and chokes can create additional resonance conditions for the development of a secondary electrons avalanche. The results of the multipactor discharge obtained using the three-dimensional modeling code MultiP-M 3D [1] have been published recently [2]. The number of particles percentage increase as a function of the field gradient for three resonator geometries smooth, fluted beam pipe and demountable damped structure are presented in Figure 1.

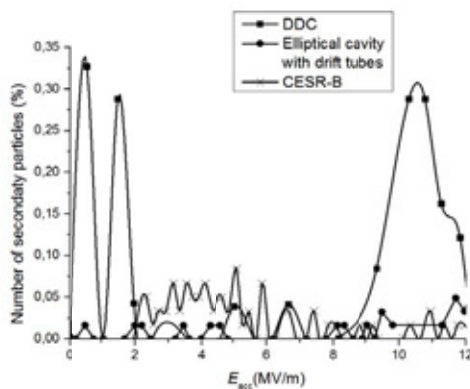


Figure 1: The number of particles percentage increase in the structure as a function of the field gradient for three resonator geometries smooth, fluted beam pipe and demountable damped structure.

For the mentioned structures, the first order trajectories in the equatorial region at low accelerating field gradients of 2–4 MV/m (the numbers may vary slightly depending on the structure type), are of the highest danger of the multipactor discharge. Such trajectories can be eliminated by an additional purification of the cavity surface and subsequent surface conditioning. Beam pipe

geometry doesn't provide any additional resonance conditions to start an avalanche of secondary electrons, except for the notch filter in demountable damped cavity (DDC) structure.

In this paper, we will examine in details the design of DDC and will provide the calculation results of the avalanche increase coefficient for that structure. The calculation was performed in CST Particle Studio [3].

MULTIPACTING DISCHARGE IN DDC

The model and the niobium secondary emission yield (SEY) plot that were used in simulations are presented in Figures 2 and 3. The calculation of the number of particles increase in the structure as a function of time and different field gradients for demountable damped structure was done for 40 RF periods. The results of this calculation are shown in Figure 4.

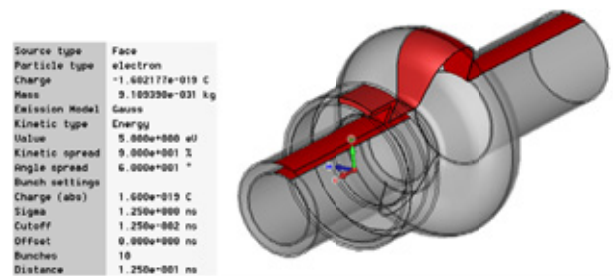


Figure 2: Demountable damped cavity (DDC).

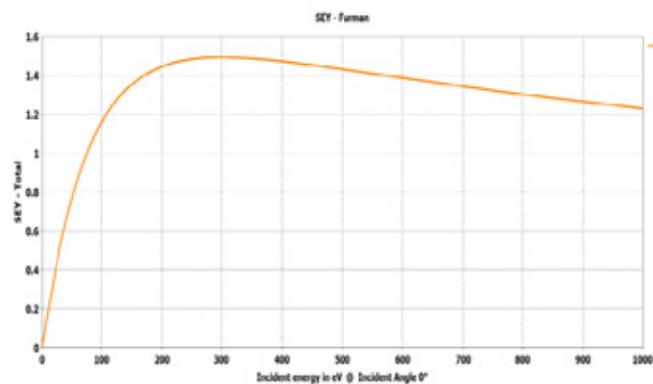


Figure 3: SEY plot for niobium.

UPGRADE OF BPM SYSTEM AT VEPP-4M COLLIDER

E.A. Bekhtenev, BINP, Novosibirsk, and Novosibirsk State University, Russia

G.V. Karpov, BINP, Novosibirsk, Russia

Abstract

Developed in BINP wideband beam position monitor (BPM) electronics has been installed at the VEPP-4M electron-positron collider. The VEPP-4M operates with two electron and two positron bunches. Wide bandwidth of new electronics (200 MHz) allows the separate measurements of electron and positron bunches with time interval between bunches up to 18 ns. 18 BPMs located near four meeting points are supplied with new electronics. The electronics can measure the position of each of four bunches. BPM system works at two modes: slow closed orbit measurements and turn-by-turn measurements. We present details of system design and operation.

INTRODUCTION

Basic scenario of high energy experiments at VEPP-4M provides operation with two electron and two positron bunches [1]. Beam position measurements near four meeting places require high time resolution of BPM electronics. Such electronics with analog bandwidth 200 MHz has been developed and tested at BINP [2]. At present 18 BPMs near four meeting places at VEPP-4M are supplied with new electronics. Positions of these BPMs are shown in Fig.1.

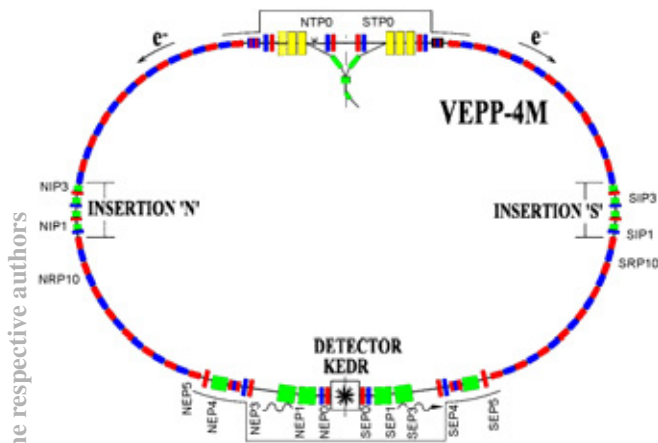


Figure 1: Positions of BPMs with new electronics.

Time intervals between signals of electron bunch and positron bunch for the part of BPMs located close to places of meeting of bunches are given in Table 1.

New electronics design utilizes signal peak sampling with high bandwidth digitizer [2]. The main problem for achieving of required accuracy of a few tens microns is separation the BPM signals of electron and positron bunches. This problem has been solved with two ways: increasing of analog bandwidth to 200 MHz and digital

compensation of the first bunch signal to second bunch signal. Two sets of new electronics have been successfully worked since 2010 year at BPMs NEP0, SEP0. At the end of 2013 year other 16 BPMs are supplied with new electronics. Special software for new BPM system control on base of EPICS has been developed.

Table 1: Time intervals between signals of electron and positron bunches for the part of BPMs

BPM	Time interval, ns
SIP2	2.27
STP0	18.07
NTP0	18.25
NIP3	20.09
NEP0	22.48
SEP0	22.66
NIP1	26.11
SIP1	26.38

BPM ELECTRONICS DESIGN

Functional diagram of the new BPM electronics is presented in Fig.2.

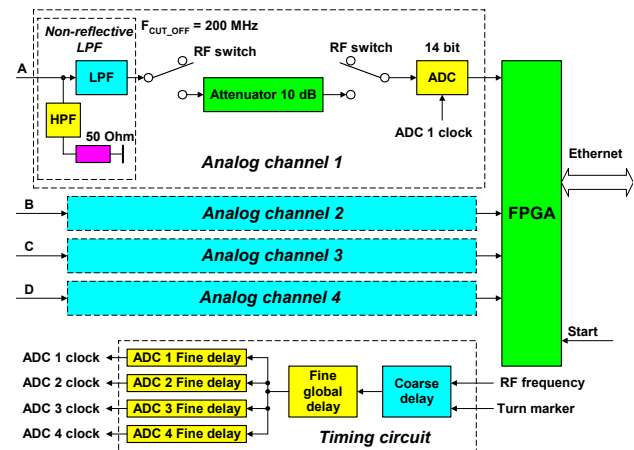


Figure 2: Functional diagram of new BPM electronics.

The electronics consists of four identical analog channels, FPGA, Timing circuit and Ethernet interface. All electronics occupies 1U 19" chassis.

The bandwidth of analog electronics is defined by non-reflective Low Pass Filter (LPF) with cut-off frequency of 200 MHz. Each analog channel has no amplifiers. Linearity and gain temperature stability are defined essentially by ADC.

EXTENDING VEPP-5 CONTROL SYSTEM BY MIDDLEWARE FOR INJECTION/EXTRACTION AUTOMATION

Gusev E.A., Bolkhovityanov D.Yu., Frolov A.R., BINP, Novosibirsk, Russia
Emanov F.A. *, BINP, Novosibirsk, Russia; NSU, Novosibirsk, Russia

Abstract

CX and EPICS are used at VEPP-5 Injection complex. Each system is in charge of some part of accelerator devices. Middleware layer was added in order to make data processing and facility-level control actions more straightforward. Middleware is separated from clients layer by means of additional CX-server. Architectural approach is considered on the example of injection/extraction automation.

INTRODUCTION

In order to provide electrons and positrons for colliders VEPP-5 injection complex [1] in the Budker Institute of Nuclear Physics is being built. This complex includes linear accelerator-based electron-positron source (preinjector) and damping ring. There are two existing injection complex beam users VEPP-4 and VEPP-2000. Charm-Tau Factory project claims the complex to provide positrons [2].

VEPP-4 and VEPP-2000 colliders will require both electron and positron beams with relatively low injection rate. In order to supply users injection complex will switch between users (further switch user) and switch between electrons and positrons (further switch particles type). It is required to store electrons and positrons in damping ring and transfer beam to users on complicated schedule. All mentioned above control actions compose injection complex main loop (machine loop) which is easier to implement by software in this case. Basic-level control was implemented by CX and EPICS software control systems. In order to create facility-level control for injection complex it is required to use both systems. Injection complex synchronization system is in charge of machine loop implementation. Synchronization system hardware was changed in order to support selected operation model. Software and hardware design based on the following principles is discussed:

- existing software and hardware infrastructure is used,
- software is suitable for regular machine operation,
- few copies of any GUI application started on the same or different computers are allowed,
- developers work is minimized.

DESIGN

Requirements

Requirements for injection/extraction automation arise from complex tasks to serve colliders. Let's consider col-

liders injection loops. VEPP-4 injection cycle consists of the following stages: storage to VEPP-3 up to 4^{11} particles, 2^{10} particles/injection, time between injections at least 1 second; acceleration to experiment energy, transfer to VEPP-4 and change VEPP-3 polarity, process duration about 7 minutes; then those stated above are repeated for other particles. Beam for VEPP-2000 is to be injected to BEP. 1.1^{11} 1.4^{11} particles are required to be injected at once. BEP uses 30 s to accelerate, transfer particles and change polarity. VEPP-2000 is expected to require 8 injections of each type of particles as initial collider filling. Refill is to be done in 30-50 s with usual amount of electrons and positrons.

According to beam users working schedule it is required to change machine settings from electrons to positrons or from one user to another one every 30 seconds. Highly automated control has to be implemented to meet this tight machine schedule. Currently injection complex operates with engineering software which presents full set of measurement and control points. Regular machine operation requires dramatic reduction of information amount presented to operator.

In order to avoid additional radiation load on equipment no beam should be accelerated without reason. Continuous start mode with masking was previously used for preinjector. Equipment in this mode can emit undesirable start signals since mask command execution time can be larger than time to next start. Preprogrammed number of starts mode ("counter mode") has to be implemented for preinjector beam systems. Continuous starts mode is being used for high power RF systems since it keeps constant thermal state of accelerating structures.

Start signals for extraction are provided by RF matching system in order to transfer beam to user. Currently this system is under development. Internal start possibility being presented for extraction and transfer channels is required for testing and tuning. RF matching system will continuously generate starting signals. Therefore synchronization hardware has to pass single start on request ("single-pass mode"). Internal starting signals can be provided by any continuous-mode channel of start generator.

Let's summarize requirements for the machine control system changes:

- "counter mode" must be implemented for preinjector beam systems,
- "single pass mode" must be implemented for extraction signals,
- automatic control software must organize user requests processing, beam storage and transfer with all

* F.A.Emanov@inp.nsk.su

DISTRIBUTED BEAM LOSS MONITOR BASED ON THE CHERENKOV EFFECT IN OPTICAL FIBER

Yu.I. Maltseva*, V.G. Prisekin, BINP SB RAS, Novosibirsk, Russia

F.A. Emanov, BINP SB RAS and NSU, Novosibirsk, Russia

A.V. Petrenko, BINP SB RAS, Novosibirsk, Russia; CERN, Geneva, Switzerland

Abstract

A distributed beam loss monitor based on the Cherenkov effect in optical fiber has been implemented for the VEPP-5 electron and positron linacs and the 510 MeV damping ring at the Budker INP. The monitor operation is based on detection of the Cherenkov radiation generated in optical fiber by means of relativistic particles created in electromagnetic shower after highly relativistic beam particles (electrons or positrons) hit the vacuum pipe. The main advantage of the distributed monitor compared to local ones is that a long optical fiber section can be used instead of a large number of local beam loss monitors. In our experiments the Cherenkov light was detected by photomultiplier tube (PMT). Timing of PMT signal gives the location of the beam loss. In the experiment with 20 m long optical fiber we achieved 3 m spatial resolution. To improve spatial resolution optimization and selection process of optical fiber and PMT are needed and according to our theoretical estimations 0.5 m spatial resolution can be achieved. We also suggest similar techniques for detection of electron (or positron) losses due to Touschek effect in storage rings.

INTRODUCTION

VEPP-5 Injection Complex [1] now is under commission and will supply BINP RAS colliders with electron and positron beams. The VEPP-5 Injection Complex consists of 270 MeV driving electron linac, 510 MeV positron linac and dumping ring. Since the Complex is not equipped with any operational beam loss monitor system we proposed to use a distributed beam loss monitor based on the Cherenkov effect in optical fiber.

This type of beam loss monitor has been developed at several facilities such as FLASH (DESY), SPring-8 (RIKEN/JASRI), CLIC Test Facility (CERN) [2–4]. The monitor overview is given by T. Obina [5]. The basic idea behind optical fiber beam loss monitor (OFBLM) is to detect a burst of the Cherenkov radiation (CR) generated in optical fiber by means of relativistic particles created in electromagnetic shower after highly relativistic beam particles (electrons or positrons) hit the vacuum pipe. Some of the Cherenkov photons propagate through the fiber and can be detected by PMT (Fig. 1).

Compared with other distributed beam loss monitors such as long ionization chamber and scintillating fiber, the OFBLM has the following advantages: fast response time (< 1 ns) which allows to detect multi-turn beam losses in

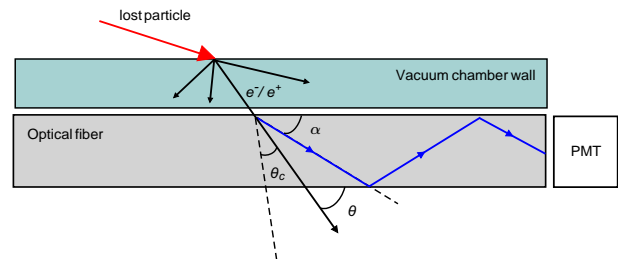


Figure 1: Scheme of beam loss monitor.

a storage ring, near zero sensitivity to background signal (mainly gamma radiation) and synchrotron radiation, unlike scintillating fiber. Moreover, optical fiber is insensitive to magnetic field, but it is susceptible to radiation damage (except quartz fiber), which limits fiber lifetime. Another disadvantage of the OFBLM is an issue with its calibration.

PRINCIPLE OF BEAM LOSS MONITOR

The following physical processes determine the OFBLM spatial resolution.

Electromagnetic Shower

For electromagnetic shower simulation G4beamline code [6] was used. Angular distribution of secondary electrons and positrons relative to beam direction was obtained (Fig. 2).

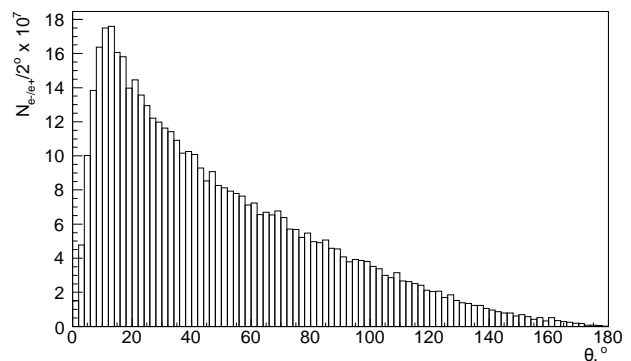


Figure 2: Angular distribution of secondary e^-/e^+ relative to beam direction passing through optical fiber. 270 MeV electron beam with 10^{10} electrons hits 2 mm steel vacuum pipe with 1° incident angle. Fiber is placed at the loss point. Total number of charged particles is $0.5 \cdot 10^{10}$.

* Yu.I.Maltseva@inp.nsk.su

MODERNIZATION OF VEPP-2000 CONTROL SYSTEM*

Yu.A. Rogovsky[#], D.E. Berkaev, O.V. Gorbatenko, Yu.M. Shatunov, BINP SB RAS and
Novosibirsk State University, Novosibirsk, Russia

A.P. Lysenko, A.L. Romanov, A.I. Senchenko, P.Yu. Shatunov, BINP SB RAS, Novosibirsk, Russia

Abstract

Electron-positron collider VEPP-2000 delivered data for the high energy physics since the end of 2009. In the summer of 2013 the long shutdown was started dedicated to the deep upgrade of the wide range of subsystems. The main goal of the improvements is to reach or exceed design luminosity in the whole energy range from 200 MeV to 1000 MeV per bunch.

The hardware of the accelerator complex consists of high current main field power supplies, low current power supplies for steering and multipole magnets, pulsed power supplies for channel's elements, RF subsystems, BPM and some other special subsystems (such as vacuum, temperature, etc.). The control system is based on CANbas, CAMAC and VME devices. The wide range of software corresponding to specific hardware subsystems forms complicated interacting system that manages all parts of the VEPP-2000 accelerator facility. Automation software is running on several TCP/IP connected PC platforms under operating system Linux and uses client-server techniques.

The paper presents general overview and changes made in architecture, implementation and functionality of hardware and software of the VEPP-2000 collider control system.

VEPP-2000 PROJECT

VEPP-2000 electron positron collider [1] was commissioned and spent three successful runs 2010-2013 collecting data at whole energy range of 160÷1000 MeV per beam [2].

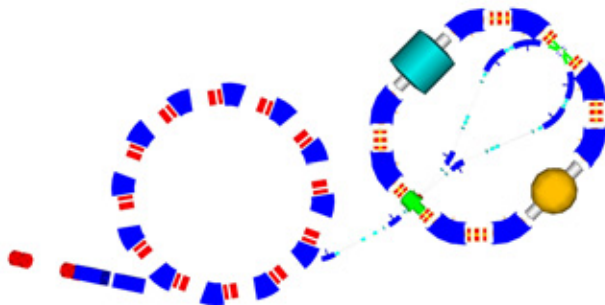


Figure 1: VEPP-2000 facility layout.

During this work VEPP-2000 used the injection chain of its predecessor VEPP-2M which has worked at BINP over 25 years in energy range up to 1.4 GeV in c.m.s. and has collected of about 75 pb⁻¹ integrated luminosity. That machine worked at lower energy (< 700 MeV) and

*Work supported by: 1) Ministry of Education and Science of the Russian Federation, Nsh-4860.2014.2; 2) partly supported by: RFBR grant 14-02-31501

[#]Yu.A.Rogovsky@inp.nsk.su

showed luminosity 30 time lower than designed value of 10³² cm⁻²s⁻¹ for VEPP-2000 at 1 GeV. As a result the positron production rate was not enough to achieve beams intensity limited only by beam-beam threshold. This restriction will be cured by link up via 250 m beamline K-500 [3] to the new injection complex VEPP-5 capable to produce intensive electron and positron high quality beams at energy of 450 MeV. The layout of the VEPP-2000 complex is presented in Fig. 1. The complex consists of Booster of Electrons and Positrons (BEP) and the collider itself with two particle detectors, Spherical Neutral Detector [4] and Cryogenic Magnetic Detector [5], placed into dispersion-free low-beta straights. The main design collider parameters are listed in Table 1.

Table 1: VEPP-2000 Main Parameters (at E = 1 GeV)

Parameter	Value
Circumference (C)	24.3883 m
Energy range (E)	200 ÷ 1000 MeV
Number of bunches	1 × 1
Number of particles per bunch (N)	1 × 10 ¹¹
Betatron functions at IP ($\beta^*_{x,y}$)	8.5 cm
Betatron tunes ($\nu_{x,y}$)	4.1, 2.1
Beam emittance ($\epsilon_{x,y}$)	1.4 × 10 ⁻⁷ m rad
Beam-beam parameters ($\zeta_{x,y}$)	0.1
Luminosity (L)	1 × 10 ³² cm ⁻² s ⁻¹

CONTROL SYSTEM OVERVIEW

The architecture of VEPP-2000 software [6] is based on three-layer structure (see Fig. 2). Specialized services (hardware layer) control one or several CAN or CAMAC buses and allow client applications to have access to hardware. The main application of Middleware layer is VCAS (VEPP-2000 Channel Access Server). Third level is presented with GUI applications, which provides to facility operator powerful and convenient instrumentation for beam tuning and diagnostics of possible systems malfunctioning. For the high loaded data channels like control systems of magnetic structure of storage and collider rings it is possible direct communication between GUI and hardware layers. Another important application in the middleware layer in specially designed Log Server.

DEVELOPMENT OF AUTOMATION SYSTEM OF THE ION SOURCE

A. Koshkarev, Novosibirsk State University, Novosibirsk, Russia

P. Zubarev, A. Sanin, U. Belchenko, A. Kvashnin, Budker Institute of Nuclear Physics,
Novosibirsk, Russia

Abstract

To operate a source of negative hydrogen ions an automatic distributing control system was developed. This system consists of master controller (Slab C8051F120) and a set of peripheral local controllers (PLC) based on microcontroller Slab C8051F350. Using an optical link between PLC and master controller there was created a system resistant to high-voltage breakdown of the ion source.

To control the system, a special programming language has been created. It includes procedures for checking the necessary parameters, setting the value of the physical quantities to simplify the experiment, verifying the lock status and protection. This system provides two programmable timers, as well as procedures in emergency situations, such as: lack of water, poor vacuum. It can be operated in semi-automatic mode, if the script asks operator about preferable actions and then continues the script depending on the response. All scripts are performed in master controller, and this makes system very rapid (for example system response time is 1 ms).

INTRODUCTION

One of the most important stages in the development of new facilities is to automate and connect all control units together. To achieve this goal, the automation of power supply units in the new ion source injector was carried out. The ion source injector is located in a research facility BNCT. This method of treatment is very effective against a number of currently incurable radioresistant tumors, such as glioblastoma multiforme and metastatic melanoma [1, 2]. Frequent changes of control commands and their parameters during experiments cause serious problems. Therefore, the scripting language consisting of control commands was developed. It allows operator to implement all sorts of automatic control algorithms and conduct experiments with minimal outer control. Automation, conducted within the framework of this work, simplifies significantly the operation of the facility.

SUBJECT AREA

The ion injector comprises several high-voltage power sources, temperature and vacuum level nodes, requiring remote control and data capture.

Power sources are controlled by identical and interchangeable modules of programmable logic controller (PLC), receiving commands from a personal computer through a switch. Each PLC has a microcontroller and several analog and digital channels, which are connected via serial interfaces SPI & I2C with the PLC microcontroller. The microcontroller allows

operator to test devices on the board if they are connected with each other. In conditions of high electromagnetic noise the distributed control system with sufficient independence of modules increases the reliability of the entire control system.

The structure of the control system is shown in Fig. 1.

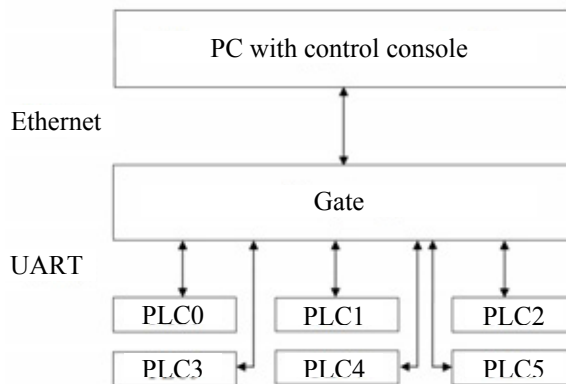


Figure 1: Structure of the control system.

ALGORITHMS

Commands are usually repeated during the experiment and for convenience to operator algorithm scenarios have been developed. Operator can create a certain set of commands once and then these commands can be repeatedly applied. Command can be as unconditional execution of some action, and also it can be a check of channel status. After checking it is possible to jump to another line in the scenario.

The switch algorithms allows user to apply two modes: manual and automatic. In manual mode, the operator can change the values of PLC. On the other hand, automatic mode allows user to run the script, which will perform the control over the experiment without operator. A block diagram of the basic algorithm is presented in Fig. 2.

The developed switch algorithms allow user to control automatically the ion source. Link between the management console and the switch is not required. Accordingly, if the operator console suddenly loses contact with the switch, the experiment will not stop, and the switch will continue to capture the critical parameters of the experiment. If these values are exceeded, the switch takes some measures that were initially set by the user.

SCENARIO

Scenarios – a set of strings that contain parameters such as the block number, channel number, the command, the value of the team and its priority.

The sequence of operations required depends on checking of states and transitions. Therefore, an internal

CONTROLLER FOR RF STATIONS FOR BOOSTER OF NICA PROJECT

G.A. Fatkin, M. Yu. Vasilyev, Budker Institute of Nuclear Physics, Novosibirsk and Novosibirsk State University, Novosibirsk, Russia

A.M. Batrakov, I.V. Ilyin, A.M. Pilan, G. Ya. Kurkin, Budker Institute of Nuclear Physics, Novosibirsk, Russia

Abstract

Intellectual Controller for RF stations based on CPU module SAMA5D31-CM for Booster of NICA Project is presented. Controller measures magnetic field using induction coil and provides corresponding real-time tuning of frequency according to non-linear law with 20 μs period and better than 2·10⁻⁴ accuracy. Controller also allows setting up and monitoring parameters of RF stations. The tester module that generates a sequence of events and signals imitating acceleration cycle is also presented.

INTRODUCTION

RF System for Booster of NICA Project (JINR, Dubna) [1] are created at Budker Institute of Nuclear Physics [2]. It consists of two resonators, two RF stations including power amplification cascades and low-voltage electronic, intellectual controller and tester module. RF system provides ~10 kV acceleration voltage in required frequency range (0.5-5 MHz) on cavity gaps.

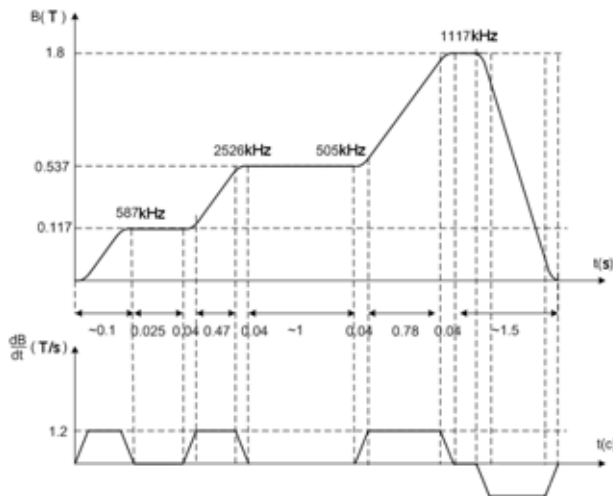


Figure 1: Booster magnetic field and acceleration frequencies.

This article describes the intellectual controller and tester module. Primary function of controller is generation of master frequency depending on the current value of magnetic field. Inaccuracy of frequency setting must not be worse than 2·10⁻⁴. The graphic of magnetic field in booster and corresponding acceleration frequencies for nuclotron injection mode are presented at fig. 1. Magnetic field increase rate in this mode is around 1.2 T/s. Several other acceleration modes are planned including autonomous mode (rising frequency from 0.5 to 5 MHz in 2 s).

Controller also manipulates low voltage electronics, measures and generates all signals necessary for the functioning of RF sections (see tab. 1). Controller must also have means to be integrated in booster control system.

Table 1: Main controller signals

Signal	Channels	Sample Rate	Resolution
Input Signals			
Master frequency	2	50 kHz	24
V resonator	2	50 kHz	12
I anode	2	1 kHz	10
Synchronization	7	N/A	N/A
Output Signals			
Field sensor	1	50 kHz	18
V resonator	2	50 kHz	12
V preamplifier	2	5 kHz	12
I anode	4	1 kHz	12
V rectifier	6	1 Hz	12
V filament	2	1 Hz	12

Currently most of booster elements are in design and manufacturing stages. That is the reason why tester module is created. It imitates signal from magnetic field sensor and necessary synchronization pulses in different acceleration modes. Tester module is intended to allow regular RF system checks at the installation. Both developed devices are 19" 3U modules and are placed in RF stations electronics rack.

CONTROL ARCHITECTURE

The scheme on fig. 3 shows interaction of controller and tester modules with booster instrumentation and RF stations electronics.

Signals from magnetic field sensor and synchronization pulses are provided to the tester module. Tester module allows to interchange between imitation and through-pass modes. Signal from magnetic field sensor is integrated and resulting magnetic field value B is used to calculate frequency according to the following formula:

$$F(B) = \frac{c^2 / LZ / A_n \rho / 10^6 B}{\sqrt{m_n^2 + (Z / A_n \rho c / 10^6)^2 B^2}} \quad (1)$$

MEDIA SERVER FOR VIDEO AND AUDIO EXCHANGE BETWEEN THE U-70 ACCELERATOR COMPLEX CONTROL ROOMS

I.V. Lobov, V.G. Gotman, IHEP, Protvino, Russia

Abstract

The media server was developed that implements the exchange of video and audio streams between control rooms for U-70 technological subsystems. Media server has the possibility of making changes into the intermediate video images to embed current technological information. The media server is implemented as a set of threads of execution, one for each video format conversion module. The media server is a chain of successive transformations of video and audio streams from one format to another: H.264—Y4M—THEORA formats for video, PCM—VORBIS formats for audio. The final video and audio streams are encapsulated into the OGG container stream which is translating into the local network. OGG container has been chosen because of its completely open, patent-free technology and full support in HTML5. Any Web browser with full HTML5 support may be used as OGG stream consumer. The browser client program has written with tag <video> utilization. This allows for client to work on different platforms (Linux, Windows) and get rid of third-party video plug-ins.

INTRODUCTION

The aim of the work was to develop a dispatching system for the organization of audio and video-sharing between different U-70 technological subsystems in IHEP. Requirements for the dispatching system were as follows:

- Simple and convenient instrument of organizing the conversations and conferences.
- The client software must run on different operation systems.
- The software must use open-source free algorithms and libraries.
- Do not use any special designed programs (plug-ins) on the client side.
- The ability to modify the intermediate video images in real time scale.
- To record the video and audio tracks into archive with a possibility of quick search of the desired fragments.
- The ability to transmit media information in conjunction with digital technology data.

DISPATCHING SYSTEM STRUCTURE

The solution of the task lies in the following main ideas (see Fig. 1):

- The dispatching system will use the IP-cameras with video and audio transmit ability instead of connecting to the PC webcams.
- The media server will provide data transmission from IP-cameras to the clients in form of media streams. Thus, instead of a set of programs for different client's operation systems only one dispatching program will be written in.
- To use the benefits of the HTML5 for the client access to the server.

IP-camera which makes your participation in the conference does not need to be connected to the client computer. Thus the client computer does not transmit any media-streams to the server. It simply receives the media-streams. At first, the client makes a connection to the server. Next, the server connects to an IP-camera and starts to receive the media-stream. Finally, the client begins to receive the media-stream from the server.

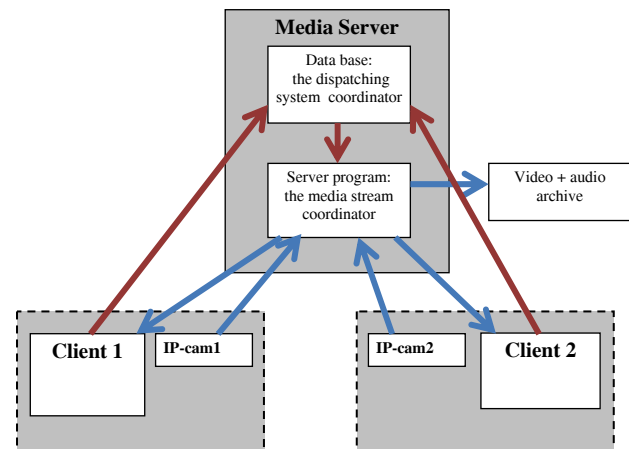


Figure 1: The scheme of the data flow (blue arrows) and the control flow (red arrows).

SOFTWARE INSTRUMENTS AND MEDIA FORMATS STANDARDS

Programming Tools

The server part of the dispatching system was written in Visual Studio 2012.

The libraries used in the project:

- JM 18.6, H.264/AVC Software, Karsten Suehring [1].
- libogg, version 1.3.2, Xiph.Org [2,3].
- libtheora, version 1.1.1, Xiph.Org [4].
- libvorbis, version 1.4.0, Xiph.Org [5].

The client part was written in HTML5 + JavaScript.

U-70 ACCELERATOR COMPLEX: CENTRALIZED ACCESS TO IP-DEVICES WITH EMBEDDED WEB-SERVER

Yu.Milichenko, E.Takaeva, V.Voevodin, IHEP, Protvino, Russia

Abstract

The paper describes our efforts to organize centralized access to IP-devices of specific types. Each device includes proper embedded web-server and is connected to an accelerator department network. Today there are tens of the devices are used to give pictures online.

A device access is carried out by user understandable device names with the aid of accelerator department web-server. Some arisen problems due to increasing number of device users are pointed. Possible manifold forms of on screen presentation of pictures derived from devices are presented.

NEW DEVICES

At last time an accelerator specialists are using increasing number of various digital devices to solve specific tasks of visual monitoring. At present there are tens of the devices. The devices should be connected to local computer network and they give possibility to user to access them by means of web browser.

The types of devices in use are some models of digital multi-channel oscilloscopes, video recorders, IP-cameras, video encoders. The devices are installed in a control and technical rooms of different buildings.

All devices, mentioned above, provide users with online pictures. Web browser may be used to get the digital picture and set some operational parameters of a device, for example, time of the picture renovation. For U-70 accelerator complex this time usually is set to be equal to 10s.

The pictures from video devices first of all give possibilities to see processes of beam injection from linacs, acceleration and beam transfer from booster to main ring. Some of devices used to observe most significant objects, such as radiation dangerous zones, corridors, technological halls and etc.

As a rule, a multi-channel oscilloscope serves signals of a certain technological system or process. It gives possibility to observe processes of acceleration regimes tuning, the quality of a technological system operation.

NETWORKING OF DEVICES

The first devices were directly connected to the same open network together with an accelerator department office PCs. But fast increase in the number of devices and appearance of certain maintenance problems required some centralization and severe discipline to access and control the devices.

The next problems have appeared after short time of operation:

1. Each PC got access to each device and possibility for tuning it up – led to curious situations.

2. Outsiders of accelerator department had direct access to the all devices by printing IP address.
3. A user should to remember set of IP addresses of all the devices he is interested in.
4. Some devices stopped the web service due to exceeding of simultaneously opened web-sessions limit.
5. Some old models of devices do not support classless IP addressing – possible decisions were discussed with support services of the manufacturers.

To solve the problems a network redesign was necessary [1]. It was decided to organize protocol-based virtual network (VLAN) on top of the accelerator department physical office local area network [2]. It became new internal local domain 192.168.0.0/16 including all devices mentioned above. Except devices VLAN combines only those computers, which are installed in the control or technical rooms and assigned to view images from the devices or tuning up them. The usual computer of the office LAN can't access the devices if it is not a member of the VLAN.

CENTRALIZED ACCESS

The centralized access meant for deriving online pictures only. To set operational parameters of the device is possible if user enters directly to web browser the device IP address as web page address.

To centralize and simplify an access to the distributed devices the accelerator department web-server is used. The server was included in the VLAN to get direct access to the devices. It supports two schemes to organize access to the devices from user computers. In both cases the web-server is used as a reference book – a user selects from the corresponding to the scheme list of devices. Each selection list includes names of all available and accessible devices and some comments.

In the first scheme the user web-browser after device selecting request communicates with selected unit directly, so increasing number of clients of the remote device web-server. This scheme is used to access all devices in scale of VLAN only and is showed in Figure 1.

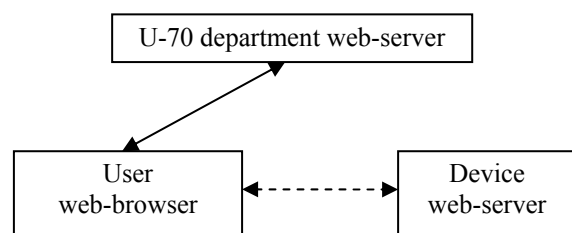


Figure 1: First scheme of device centralized access.

DIGITAL SIGNAL PROCESSING ALGORITHMS FOR LINAC LOW-LEVEL RF SYSTEMS

D.Liakin, S. Barabin, A.Orlov, ITEP, Moscow

Abstract

A set of LLRF systems had been designed for various applications of resonant RF devices such as accelerators or beam deflectors [1], [2]. This report presents compact signal detection algorithms, used in most of developed systems. Application-specific extension of the signal processing procedure allows the system be synchronized to external self-excited oscillator.

SIGNAL AND SYSTEM PARAMETERS

Linear accelerator of charged particles use a resonant principle, where the EM field energy from period to period converted into the energy of accelerated particles. For conversion efficiency, it is important to keep the resonance condition during the system operation cycles. In addition, systems of several resonators need certain and accurate phase difference between oscillations in different resonators. The signal, taken from high-Q resonator, occupies narrow frequency range, defined by the resonator characteristic, shown as an example in Fig. 1. Systems with dynamic phase control use a resonator model to build an efficient feedback transfer function. There is always a trade-off between efficiency on one hand, and resource cost of the signal processor on the other. Normally a first order model describe the resonator very well. However, as it is seen in Fig. 1 the difference is visible.

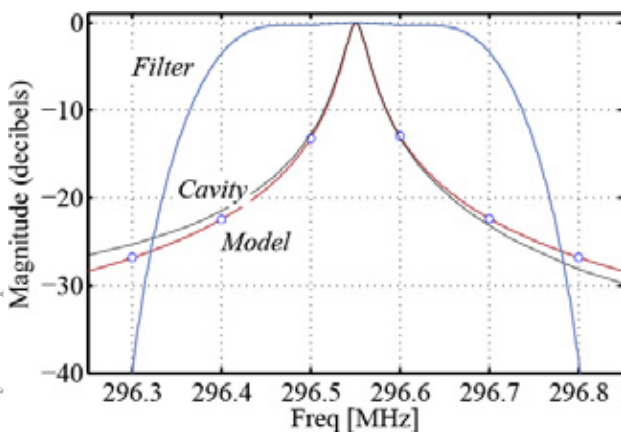


Figure 1: The frequency characteristics of the cavity, 1st order cavity model and overall frequency response of the digital processing unit.

The signal detection needs another compromise. Fig. 1 shows the frequency response of the signal processor. Besides, it shows how ineffective is a resonator as a filtering device. To keep the efficiency the signal processor must reduce the system's sampling rate down to

reasonable low value. For that, it wastes the signal power outside of 500 kHz band.

THE BASE ALGORITHM

Fig. 2 presents the general process used to handle RF signals. The carrier frequency of the RF is higher than the sampling frequency of an ADC or system clock frequency of an FPGA-based digital signal processor (DSP). Because of this the ADC operates in IF mode, working as frequency down converter. The intermediate frequency signal is an input signal for the DSP.

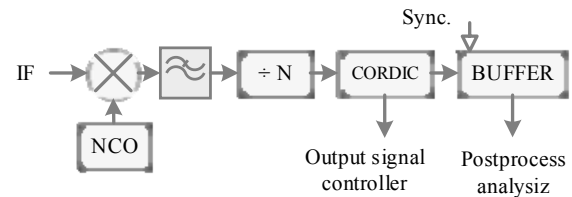


Figure 2: The signal evaluation in the digital domain.

As it is shown in Fig. 2, the first stage of the DSP performs an additional frequency conversion. The system set up defines precisely the frequency shift by a frequency tune word (FTW) of the numerically controlled oscillator NCO. The following low-pass filter suppress image and carrier frequencies existing at the down converter output. The output of the filter is a complex amplitude slowly varying in time. The cost of algorithm is important. To keep the efficiency and effective use of the FPGA resources the data needs to be rarefied according the system bandwidth. Due to the slow signal, the DSP reduces the data rate by factor N, normally down to 1 MSPS. Until this DSP uses a fixed-point arithmetic and Cartesian representation of complex amplitudes. The COordinate Rotation DIgital Computer module converts complex data to the vector form. Then the DSP store the amplitude and phase of the signal in separate buffers.

Fig. 3 gives an example of a system, where the original signal 1 is taken from the master self-excited generator, is used for synchronization of EM-field in the resonator of the novel just designed acceleration section. For successful operation, the digital controller must synchronize two system within 50-microsecond interval after the master-generator start. A distinctive feature of the described system is an oscillation of the amplitude and phase at the rising edge of the reference signal's pulse.

A DIGITAL LOW-LEVEL RF SYSTEM FOR RESONANT BEAM DEFLECTOR OF LAPLAS EXPERIMENT

D. Liakin, S. Barabin, A. Orlov, ITEP, Moscow, Russia

Abstract

A two-resonator heavy ion deflecting system is a part of LAPLAS experiment [1]. ITEP built and put into operation a lightweight prototype of a deflector. Developed high performance radio-frequency control unit provides all necessary options for successful operation in LAPLAS or ITEP installations. The LLRF includes a two-channel reference generator based on a digital signal processing core and resonant frequency control modules, also powered by an appropriate DSP.

frequencies and a phase difference between two resonators. The system uses a set of control signals to stabilize the model near the optimal statement. The main criteria of the proper system operation are accurate phases and amplitudes of EM fields, estimated by measuring of signals taken from control loops 1_X and 1_Y in Fig. 1. Signals 2_X and 2_Y from reflectometers are used while checking the matching criterion.

Fig. 2 presents the structure of the crate of the LLRF module.

RF DEFLECTOR

ITEP develops a radio-frequency deflector of high-energy heavy ion beams as a prototype of the system, assigned to plasma physics experiment in FAIR (Darmstadt, Germany). The operating prototype, shown in Fig.1, consist of two resonators forming orthogonal electromagnetic fields to deflect the beam in vertical and horizontal planes and provide a cylindrical impact volume in solid target body.

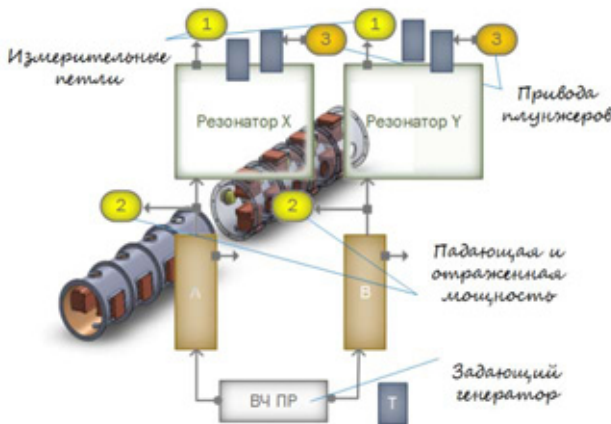


Figure 1: RF system of the beam deflector.

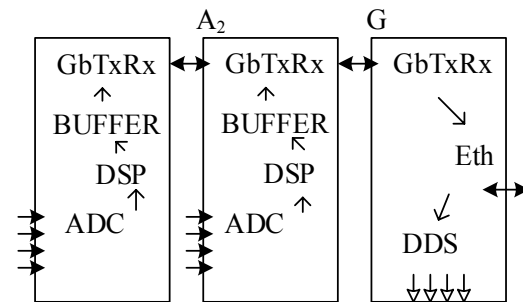


Figure 2: The structure of the LLRF module.

The crate unites two similar four-channel ADC modules A1 and A2, capable simultaneously digitize RF signals in the IF mode, and vector signal synthesizer G with pair of independent two-channel outputs of sinusoidal signals.

GENERATION OF REFERENCE SIGNALS

As shown in Fig. 3, the output signals are generated using the frequency up converter scheme.

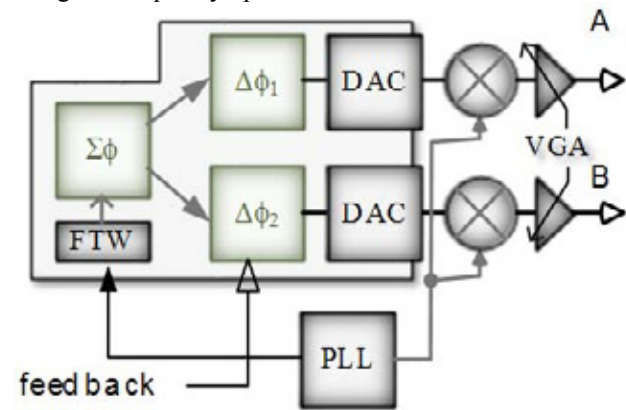


Figure 3: The reference generator.

LOW-LEVEL RF SYSTEM

Fig. 2 shows the LLRF divided into the measurement and generator parts. The LLRF system of the deflector operates in conventional way, similar to LLRF systems of resonant accelerators. As a reference generator, it issues two coherent RF signals, shown as outputs A and B in Fig. 3. When required, the amplitude of signals could be independently set within full-scale range. The ability of the phase difference control between channels is a key option of the reference generator. The phase is adjustable in the 360-degree range. The feedback controller allows phase correction on pulse-by-pulse base.

The model of the RF system of the deflector use three independent parameters describing the system: resonant

Two-channel DDS generates synchronized signals of intermediate frequency. The frequency depends on frequency tune word (FTW) and frequency of the synchronization clock taken from on-board PLL-based synthesizer. The PLL's voltage controlled oscillator (VCO) generates the frequency of 1740 MHz. The clock

QUENCH DETECTOR FOR SUPERCONDUCTING ELEMENTS OF THE NICA ACCELERATOR COMPLEX

E. Ivanov, A. Sidorin, Z. Smirnova, L. Svetov,
JINR, Dubna, Moscow Region

Abstract

A universal quench detector is designed for new superconducting accelerators of the NICA accelerator complex under construction at JINR. The presence of a two channel digital input permits the detector to be used both for comparing voltage across two nearest magnets by a bridge scheme and for separating a resistive constituent of the voltage across a controlled element.

INTRODUCTION

The Nuclotron quench-detection system was modernized in the frames of the Nuclotron upgrade project and commissioned during the runs #46-47 [1]. The detectors are based on a comparison of voltage drops across two identical elements connected in series to the supply circuit using a measuring bridge. The bridge circuit was chosen as the simplest one from the viewpoint of technical implementation. The system (Fig. 1) permits a prompt change in the number of detectors, uniform work with the group and individual detectors and implementation of the total reservation of the line controlling the energy evacuation system. The system provides monitoring of the status of all of its components, as well as signal-testing of external systems, and also indicates malfunctions. The self-diagnostic is provided by apply of pulse signals into measurement circuits between the magnetic field cycles.



Figure 1: Block-diagram of the Nuclotron quench detection system.

Additionally, the system to control quench detectors allows all cases of protection operation to be analyzed, which yields the experimental material for further development of the detector construction. First and foremost this refers to revealing the reasons and excluding the cases of protection operation when

elements do not enter the normal state. The new system permitted safe operation of the magnetic system in the regimes with long plateau of the magnetic field and operation at maximum designed magnetic field. As result, for instance, successive experiments on stochastic cooling and the beam acceleration up to maximum design energy were realized [2].

Further development of the accelerator complex is related with the realization of the NICA (Nuclotron based Ion Collider fAcility) project that presumes creation of two new Super-Conducting (SC) acceleration facilities: booster synchrotron (Booster) and collider rings, and SC transfer line from the Booster to the Nuclotron [3].

The Booster is the fast cycling synchrotron with magnetic system similar to the Nuclotron one. The Booster quench detection system can be based on the same technical solutions and the bridge scheme of the quench detector seems to be optimum.

The collider rings will be operated in the mode of a storage ring (slow beam acceleration is presumed as a reserve option only). The continuous operation is the basic regime for the SC transfer line. Two main detectors of the collider utilize the SC solenoids in a continuous mode. The quench detection is necessary for the test-bench under construction for serial production and tests of the SC magnets for NICA and FAIR facilities where different regimes of the operation are presumed.

In the mentioned cases a method of the quench detection based on separation of a resistive constituent from the measured signal by comparison with the certain reference signal can be more efficient than the bridge one. This method is rather universal: as a reference signal one can use a derivative of the magnetic field with respect to the time that determines the inductive constituent of the voltage drop. It is also possible to use the time derivative of the current flowing through the controlled element. In this case a derivative of the field is defined from the known dependence of the element inductance on the current. A difference in signals of the voltage drop across the controlled element and a signal of the derivative of the field (calculated and analyzed by the electronic circuit) indicates that the normal state is being entered.

In the continuous operation the scheme of the malfunction diagnostic has to be modified also: application of pulse signal in the measurement circuit is impossible in this case.

For use at the NICA accelerator complex and at the bench for testing SC devices, a universal quench detector was developed that is suitable for implementation in both detection schemes required.

EXPERIMENTAL STUDY OF THE SCATTERING OF 7.4 – MEV ELECTRONS INTERSECTING A FOIL AT AN ANGLE OF 5° – 60° TO ITS SURFACE

A.V. Koltsov, A. V. Serov , LPI, Moscow, Russia
 I. A. Mamonov, MEPhI, Moscow, Russia

Abstract

Angular distributions of electrons incident of a planar target at a small angle to its surface have been measured. Electrons have been injected from a microtron with a particle energy of 7.4 MeV. The dependence of the characteristics of beams on the initial energy and direction of injection of particles, as well as on the material and thickness of the target, has been considered. The intersection and reflection of electrons in the target have been investigated. The angle between the trajectory of the particles and the surface of the target was varied in the range of 5° - 60°. Aluminum, lead, and copper foils have been tested. The thickness of the foils was varied from 50 μm to 600 μm.

INTRODUCTION

The solution of some applied problems implies the knowledge of the characteristics of the scattering of particles incident on the surface at an angle much smaller than a right angle. One of such problems is the problem of the excitation of transition radiation by electrons intersecting a dihedral angle [1] or a conical surface [2]. The transition surface can be a thin layer of a certain material (Mylar, metal). In this case, the characteristics of radiation should depend not only on the initial parameters of the beam but also on a change in these parameters when intersecting the thin layer, i.e., on the material and thickness of the intersected surface, as well as on the direction of motion of particles. The smaller the angle between the direction of motion of particles and the surface, the stronger the effect of the properties of the transition surface on scattering. The motion of beams injected at a small angle to the surface was studied in [3]. The aim of this work is to analyse the effect of the direction of injection of particles on the parameters of the beam intersecting metallic foils with various thicknesses.

SETUP OF THE EXPERIMENT

The layout of the experiment is shown in Fig. 1. The z axis is taken along the trajectory of particles and the x axis lies in the horizontal plane. The charge e_d intersecting the target leaved it at the angle of refraction θ_d with respect to the initial direction of motion, whereas the charge e_r reflected by the target moved at the angle ϕ_r to the plane of the target. The point x_b in Fig. 1 is the point at which a straight line in the plane of the target intersects the plane of the detector. The coordinate x_b is determined by the distance L from the target to the detector and the angle of injection α . According to the geometry of the experiment, the coordinates of particles e_d intersecting the

target on the plane of the detector satisfy the condition $x > x_b$ and the coordinates of reflected particles e_r satisfy the condition $x < x_b$.

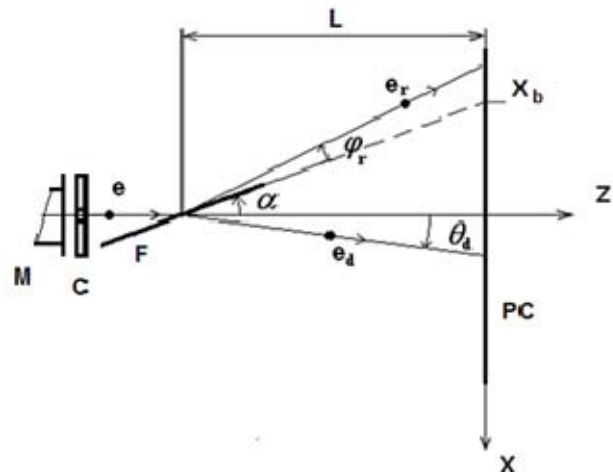


Figure 1: Geometry of the experiment.

In the experiments, it is used 7.4 MeV electron bunches from the microtron. Electrons were extracted to the atmosphere through a 100 μm aluminum foil on the flange of microtron M. Lead collimator C and foil F were placed behind the flange. The 50 mm thick collimator had a hole with a diameter of 3 mm. The foil was rotated with respect to the vertical (y) axis by the angle α . The distribution of electrons was measured by multiwire proportional chamber PC consisting of three 64 × 64 mm frames. The chamber allowed measurements of the distributions of particles in the horizontal (x) and vertical (y) directions. The chamber was located at a distance of $L \sim 150 - 300$ mm from the point of intersection of the foil by the beam. A signal from the proportional chamber was fed to an oscilloscope. Charged particles passing through the layer of the substance undergo numerous collisions; consequently, the spatial distributions of passed and reflected particles are approximated well by a Gaussian distribution. The direction at which the distribution has a maximum was taken as the motion direction of refracted and reflected beams of particles.

EXPERIMENTAL RESULTS

The typical oscillograms of the signals of the chamber are shown in Fig. 2. The first and second pulses of the oscillograms describe the horizontal and vertical distributions of particles, respectively. Figure 2 shows the distributions for the cases where (a) copper foil with a

A PULSE GENERATOR OF X-RAY QUANTS FOR REMOTE RADIATION MONITORING

B.Yu. Bogdanovich, A.V. Nesterovich, A.E. Shikanov,
National Research Nuclear University "MEPhI", Moscow, Russia
B.D. Volchansky, A.V. Ilyinsky, D.R. Khasaya, E.A. Shikanov,
OOO «SPEKTR» Integrated monitoring systems, Moscow, Russia

Abstract

The report presents the development of compact UT, which improved definition x-ray image is ensured by using a diode system with a coaxial geometry acceleration of electrons to the anode electrode internal target and explosive emission cathode. UT used to run a specially designed high-voltage pulse transformer-based "Tesla" with surge sharpener. Describes the design and block diagram interface generator X-ray quanta. Feature is the high stability of the generator is not dependent on the voltage, battery charge. Presented the results of experimental testing of the generator X-ray quanta. Also shows the waveform duration x-ray pulses in the presence of the lead filter and without it.

Modern complex industrial facilities (nuclear reactors, elements of pipeline and rail transports, power plants turbines, heat exchangers, aircraft, etc.) require the implementation of remote penetrant monitoring. At the same time, such monitoring systems are subject to the increased requirements for transportation, portability, expressness of changes.

The best solution for this kind of problems is the application of portable mono-block instruments based on pulse x-ray acceleration tubes (AT). The weight and dimensions of mono-block radiator, the power supply and control panel allow to transfer them easily and quickly mount to take effective measurements. Such radiation sources concerning small dimensions should provide the average exposure rate as ~ 10 mR/s within the distance of $\sim m$ from the target with the minimum area of target's radiating surface. Given parameters are obtained by generating the x-ray quants in the vacuum diode AT operating in the pulsed-periodic mode with the current amplitude of accelerated electrons $\sim kA$, the pulse duration $\sim (1-10)$ ns and the maximum energy of electrons with several hundred keV. For this purpose, the Experimental Plant of Pulse Technique (EPPT) - the subsidiary of OOO «SPECTR»-IMS, with the assistance of Institute for Nuclear Research of the National Academy of Sciences of Ukrainian and NRNU MEPhI, has designed a small-sized AT in which the enhancement of the x-ray image clarity was provided by the diode system with the coaxial geometry of an electrons' acceleration to the internal anode electrode - target [1-2].

This electrodes' geometry allows to produce a cathode plasma spreading to the anode and acting as an intensive source of electrons. The electric field intensity in the anode region can reach up to ~ 108 V/m.

While operating pulse generators of x-ray quants in the field, high requirements are imposed on the mechanical and dielectric strength of AT. And therefore in order to enhance these indicators, the special high voltage ceramic insulator was suggested to be used. By means of computer simulation and physical modelling at a demountable vacuum stand information has been received on optimal geometrical dimensions of a diode acceleration system [3] that formed the basis for designing AT. Fig.1 shows its schematic section and general view.

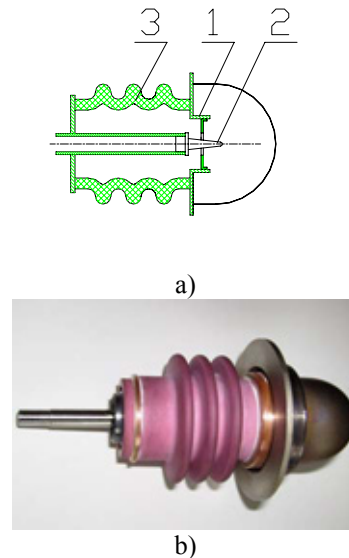


Figure 1: Acceleration tube and its triggering circuit: a) the schematic section of AT. 1- cathode; 2- anode; 3- ceramic corrugated insulator; b) the general view of AT.

Obtained relations of geometric dimensions for a diode system are defined by the following system of inequalities [4]:

$$5 \cdot 10^{-4} m \leq \rho \leq 10^{-3} m, \quad 5\rho \leq r_K \leq 10\rho, \quad 0.2 r_K \leq r_A \leq 0.5 r_K, \quad 0.4 r_K \leq h \leq 1.4 r_K,$$

where ρ - the rounding radius at the anode end, r_K - the radius of a hole in the cathode, r_A - the radius of an anode circular section with the plane passing through the

DEVELOPMENT OF THE SOFTWARE FOR THE ACCELERATING FIELDS IN LINEAR STRUCTURES MEASUREMENT

E. Savin, M. Lalayan, A. Smirnov, National Research Nuclear University «MEPhI»,
Moscow, Russia

A. Zavadtsev, OOO «Nano Invest», Moscow, Russia

Abstract

The software which allows controlling the whole installation to measure electric fields in the linear structures has been developed. The installation consists of linear structure, step motor drive, motor controller, a probe which moves on the string through the structure to perturb the field to use the perturbation measuring method, network vector analyzer and the PC. The software interface is user-friendly, user only needs to write down the length of the structure, a desired step of the probe and push the start button. As a result user can obtain the picture of electric field on the structure axis. It is possible to choose between two measuring methods: by S11 or by S21.

METHOD DESCRIPTION

Information about electrical field amplitude and phase distribution along the axis of the accelerating or deflecting section can be obtained from the measurements, based on non resonant perturbation theory. According to this theory, change of the complex reflection coefficient on the entrance of the structure, when the small perturbing body is in the structure, is proportional to the square of the electric field amplitude in the point where perturbing body is placed:

$$\Delta S_{11} = S_{11}^{pb} - S_{11}^0 = CE^2, \quad (1)$$

where S_{11}^{pb} – is a complex coefficient of the reflection on the structure entrance with perturbing body,

S_{11}^0 – is a complex coefficient of the reflection on the structure entrance with perturbing body,

E – is a complex amplitude of the electrical field in the point of the perturbing body *комплексная амплитуда напряженности электрического поля в точке размещения тела,*

C – is a complex coefficient.

RF field is perturbed by the probe moving along the structure axis. For the accelerating structure with a longitudinal field, the probe geometry is a needle. And for the deflecting structure with a transverse field – it is a flat disk.

Using the measurement results, it becomes possible to calculate reflecting coefficient change $\Delta S_{11}^{(n)} = S_{11}^{pb(n)} - S_{11}^0$ (where n – it is a cell number) and find the ratio between complex amplitudes of electric field in the centers of the neighbor cells.

$$\frac{E_{n+1}}{E_n} = \left[\frac{\Delta S_{11}^{(n+1)}}{\Delta S_{11}^{(n)}} \right]^{\frac{1}{2}}. \quad (2)$$

Let the complex amplitude in the first cell is equal $E_1 = 1$, i.e. its amplitude is equal 1 and phase is equal 0. Then we get following expressions for the complex amplitudes in the cells centers

$$E_{n+1} = E_n \left[\frac{\Delta S_{11}^{(n+1)}}{\Delta S_{11}^{(n)}} \right]^{\frac{1}{2}}, \quad (3)$$

$$E_1 = 1.$$

So, as a result of the reflecting coefficients measurements we get the following data:

$S_{11}^0 = a^{(0)} + jb^{(0)}$ – a complex reflection coefficient with the probe outside the structure (j -is the imaginary unit),

$S_{11}^{pb(n)} = a^{(n)} + jb^{(n)}$ – a complex reflection coefficient with the probe inside the center of the n -cell.

Using the measurement results we can calculate the reflection coefficient change

$$\Delta S_{11}^{(n)} = S_{11}^{pb(n)} - S_{11}^0 = CE_n^2 = C|E_n|^2 \exp(j2\varphi_n)$$

, where $|E_n|^2$ – is a square of electric field amplitude in the middle of the n -cell, φ_n – is a starting phase of electric field amplitude in the middle of the n -cell.

THE INSTALLATION CONSISTANCE

The installation consists of the followings components:

- Directly the measured structure with the thread with probe.
- Step-motor, which controls the thread moving.
- Controller, which is connecting the step-motor with the computer.
- Network analyzer, which is measuring the reflection coefficient and the structure frequency in the defined time moments. It is also connected PC.
- PC with the describing software.

THE INTERFACE

The software is developed in the Lab VIEW, which allows creating the comfortable and intuitive interface. On the Fig. 1 is presented the main window, in which displays

CONTROL SYSTEMS FOR RADIOGRAPHY AND CARGO INSPECTION RF ACCELERATORS

A.N. Ermakov, A.N. Kamanin, V.G. Sayapin, V.I. Shvedunov, D.S. Yurov,
Skobeltsyn Institute of Nuclear Physics, Lomonosov Moscow State University, Laboratory of
Electron Accelerators MSU, Ltd, 119992 Moscow, Russia
I.V. Shvedunov, Laboratory of Electron Accelerators MSU, Ltd, 119992 Moscow, Russia

Abstract

Based on "open technologies" approach to design of control systems for radiography and cargo inspection electron RF accelerators constructed at Laboratory of Electron Accelerators MSU is described. The control system consists of a number of specialized controllers each responsible for separate accelerator subsystem connected via Ethernet interface and Modbus/TCP protocol with control computer which in turn is connected with control panel computer, modulator, power supplies etc. each having its own digital interface. Each controller contains one or several special boards conditioning external analogue and discrete signals and universal microcontroller part providing controller operation and network connection. Both control computer and control panel computer are based on BlueShark SOM (System on a Module) and run Linux operating system. Custom SCADA-like system has been developed to provide proper accelerator operation and operator interface with support for different levels of access to accelerator parameters.

INTRODUCTION

The radiography accelerator UELR-8-2D with beam energy regulated in the range 3-8 MeV and dose rate from 0.5 to 15 Gy/min and cargo inspection accelerator UELR-6-1-D-4-01 with pulse to pulse energy switching between 3.5 and 6 MeV, with repetition rate 400 Hz and dose rate 4 Gy/min were developed and put into operation with the participation of Lomonosov Moscow State University and "Research and Production Enterprise "Toriy" stuff [1]. A compact control system located in the X-ray head cabinet in the vicinity of controlled objects is necessary for proper operation. The control system is built on the hierarchical principle (fig. 1). The top-level computer is connected by Ethernet network and RS232 interface to the operator panel and several subsystem controllers. Subsystem controllers are custom devices implemented using microcontrollers except for klystron modulator which is ready-made device. The control application running on the top-level control computer uses Modbus/TCP protocol to communicate with subsystem controllers that perform data acquisition, actuation and real-time critical tasks. The control application also communicates with the klystron modulator using modulator's own proprietary serial line protocol [2]. The system relies on hardware interlocks to ensure safe operation. The top level computer can query interlocks via Accelerator Controller and other

controllers. Accelerator Controller also uses klystron modulator's hardware interlock inputs to prevent klystron failure in situations such as vacuum loss or cooling system malfunction.

CS STRUCTURE AND OPERATION

All the accelerator systems (fig. 1) are combined into several subsystems: interlocks and alarm signal processing system and synchronization controller (accelerator controller); RF system and cooling system sensors; klystron and accelerating structure ion pumps; sulfur hexafluoride gas delivery system; electron gun supply control; dose rate with ion chamber measurements; cooling module and accelerator power supply control.

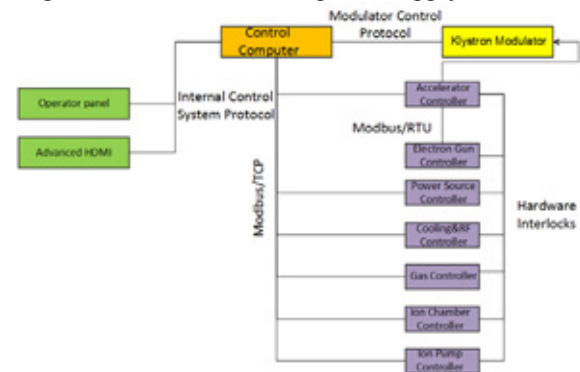


Figure 1: Control system structure.

Each subsystem contains a programmable controller which has the functions of receiving the primary sensor signals, transmitting control signals to actuators, controlling the system operation by incorporated algorithms and communicating with the host computer. The control system also includes a control computer, a network switch and the power source for its own needs.

Operator communicates to the monitor and control system using the control panel located in the control room and connected to the host computer via Ethernet interface. The accelerator network is also connected to the local enterprise network via a router. It can also be connected to a PC running the advanced HMI client program, which provides full access to the host computer and controllers. Local network provides access to the host computer and the individual controllers by the remote terminal over the Internet or private network.

Control computer functions are (1) providing the power supply accelerator on/off procedures and accelerator operation; (2) storing and loading operating parameters of

AUTOMATED CONTROL SYSTEM OF THE TARGET SYSTEM FOR PET RADIONUCLIDES' PRODUCTION

P.A. Gnutov, M.L.Klopenkov, R.M.Klopenkov, A.N.Kuzhlev, A.A.Melnikov, A.P. Strokach,
JSC "D.V.Efremov Institute of Electrophysical Apparatus", St. Petersburg, Russia
B.V. Zabrodin, the St. Petersburg State Polytechnical University

Abstract

An automated control system of target system for production of PET-radionuclids has been designed. The system allows on-line obtaining of the data on the status of the target system and remote control of loading, irradiation and evacuation of the activity to synthesis modules.

According to algorithms available in the software, this system makes possible emergency situations to be prevented and incorrect actions of the operator to be blocked.

INTRODUCTION

Nowadays, the method of positron-emission tomography (PET) is widely used for diagnostics and in medical-biological investigations. This method is the most informative when observing the processes occurring in a human organism [1].

Short-lived and ultra-short lived radionuclides with the lifetime from 13 min to 2 hours are used for PET investigations. Such radionuclides can be produced on proton accelerators located directly in clinics. Cyclotrons of the CC-series [2, 3] designed and manufactured in NII-EFA in its radiation characteristics as well as in overall dimensions completely meet the requirements imposed today on cyclotrons intended for PET. However, until recently, these machines were not equipped with target systems.

At present, our Institute has delivered the 1st model of completely automated target system with the CC-18/9M cyclotron to JSC "NIITFA", Moscow. Fig.1 shows the general view of the target system with the cyclotron.



Figure 1: General view of the target system and cyclotron.

This target system is designed for 5 targets, 3 water and 2 gas, however, delivery with any set of targets is possible. The target system was tested at a beam current of 50 μA , and the target pressure was not more than 8 barr, which confirms a high efficiency of this system. In future, this will allow us to increase the intensity of the proton beam for production of radionuclides. When irradiating H_2^{18}O with beams of accelerated 18 MeV protons, the calculated activity yield was 280 mCi/ μA . In measurements, the activity yield of 200 mCi/ μA was obtained for a 3-ml water target. Below in Table 1 are given activity yields of commercial target devices of leading world manufacturers.

Table 1: Activity yields bading world manufacturers

Manufacturing Companies	Activity Yield
IBA	240 mCi/ μA
NII-EFA	200 mCi/ μA
Triumf	200 mCi/ μA [4]
Kirams	180 mCi/ μA [5]
Syntra	137mCi/ μA

Characteristics of the target system produced in NII-EFA satisfy the world requirements for yield ranges of such systems. In future, when testing the system we plan to increase the target pressure up to 20 barr, which will allow the beam current increase up to 100-120 μA . Works have been started on widening the assortment of water targets; production of 1-ml, 2-ml and an experimental 5ml targets are planned.

AUTOMATED CONTROL SYSTEM OF THE TARGET SYSTEM

The automated control system (ACS) of the target system consists of an operator's workstation and controller unit.

The Mitsubishi GT1275 panel was chosen for the control console of the operator's workstation, which allowed a high-quality user-friendly intuitive operator interface to be designed in the Russian language (see Figs. 2 and 3).

This interface allows remote loading of targets with target materials, unloading of the activity to hot cells and rinsing the target and capillaries connecting the target with hot cells. In the left part of the window, the execution of these programs can be observed in real time, i.e. valves' position, readiness of hot cells, filling of

ISBN 978-3-95450-170-0

SYSTEM FOR REMOTE TARGET REPLACEMENT OF THE TARGET SYSTEM FOR THE CC-SERIES CYCLOTRONS

R.M. Klopenkov, E.N. Abramov, Yu.N. Gavrish, M.L. Klopenkov, K.A. Kravchuck, G.V. Muraviev, A.P. Strokach, JSC "D.V. Efremov Institute of Electrophysical Apparatus", St. Petersburg, Russia

Abstract

An automated system for remote replacement of target devices of the target system for cyclotrons of the CC-series has been designed. The system allows 1 of 5 available targets to be positioned under the beam of the cyclotron at the operator's choice. Such a technical solution allows us to have sufficiently smaller overall dimensions of the equipment and less time for servicing water and gas targets.

Separate system for target replacement is provided for each beam extraction, which allows the cyclotron to be equipped with 10 different target devices, and makes possible simultaneous irradiation of 2 targets.

INTRODUCTION

Nowadays, positron-emission tomography (hereinafter PET) is the most effective method for diagnostics of a wide spectrum of diseases including oncologic cases. This diagnostic method applies radiopharmaceuticals, i.e. substances labeled with radionuclides, which are actively used in various metabolic processes occurring in a human organism.

To produce radionuclides, beams of accelerated particles are used to bombard targets containing target materials. [1]

In clinics and in commercial production of radioisotopes, of the first priority are the operational stability of radiopharmaceuticals' production systems, compactness of their size, multifunctionality, easy maintenance, low radiation exposure of the attending personnel and updating flexibility to meet the requirements of modern medicine and market [2].

In JSC "NIIEFA", energetic works are now underway on designing and preparation of serial equipment for production of radionuclides. Three models of cyclotrons for 12 MeV [3], 18 MeV [4] and 30 MeV [5] as well as target systems for these machines have been designed and constructed.

At the end of 2013 in JSC "NIITFA", Moscow, a system for the production of radionuclides for PET on the basis of the CC-18/9M cyclotron was installed. At the stage of testing of the system, we managed to obtain the target yield ranges comparable with those of the latest-generation equipment of leading producers in the world. The main tasks to be solved when designing target systems are the reliability, easy maintenance-repair and versatility of the target system [6].

SYSTEM FOR TARGET REMOTE REPLACEMENT

To meet the demanding requirements of customers on widening the functionality of the target system, work on designing a system for targets' remote replacement was done. This system is intended for automatic setting of a chosen target under the beam of the cyclotron. The use of this system will allow: optimization of the cyclotron system configuration and minimization its overall dimensions because of possibility to refuse part of ion transport system; possibility to furnish the cyclotron with larger number of targets; remote taking out of target devices from under the beam to reduce the induced activity before its removal and maintenance/repair.

The system for targets' remote replacement consists of 2 systems: a system for disconnection of a vacuum-tight joint between target devices and the ion tube of the cyclotron and system for the transport of target devices (see Fig.1).

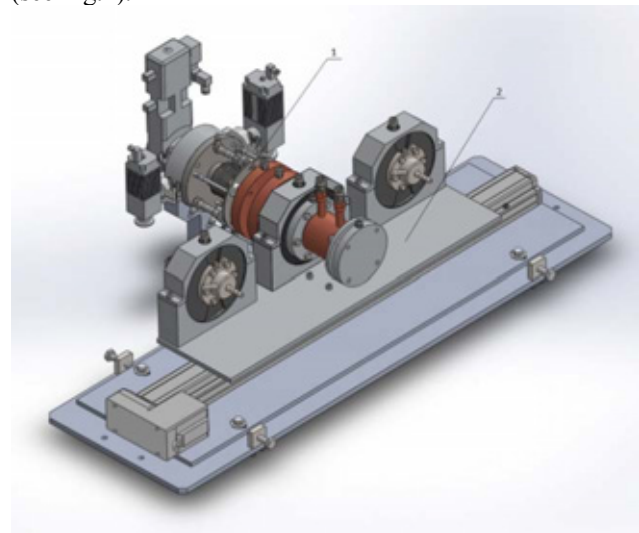


Figure 1: System for targets' remote replacement: 1- system for disconnection of the vacuum-tight joint between target devices and the ion tube of the cyclotron; 2- system for transport of target devices.

The first system provides remote disconnection and connection of the vacuum-tight joint between the end flange of the ion tube and the target device flange. This operation is performed with 3 pneumatic cylinders compressing an intermediate bellow.

The system for transport of target devices consists of a linear electric drive with a step motor and target devices fixed on it. It makes possible transportation of a chosen

MODERNIZATION OF THE AUTOMATED CONTROL SYSTEM IN THE KURCHATOV SYNCHROTRON RADIATION SOURCE USING SitectSCADA

E. Kaportsev, A. Valentinov, V. Dombrovsky, V. Korchuganov, Yu. Krylov, K. Moseev, N. Moseiko, S. Schekochikhin, RRC Kurchatov Institute, Moscow, Russia
Yu. Efimov, CJSC RTSoft, Moscow, Russia

Abstract

The running cycle of Kurchatov Synchrotron Radiation Source (KSRS) includes the injection of electrons with energy 80 MeV from the linear accelerator in the booster storage ring Siberia-1, the accumulation of an electron current up to 400 mA and, then, electron energy ramping up to 450 MeV with the subsequent extraction of electrons in the main ring, storage ring Siberia-2, and accumulation there up to 300 mA, and at last the energy ramping up to 2.5 GeV. [1]

Several years ago, a modernization of the current system of automated control systems (ACS) has started. Modernization has affected the most important parts of the system - the system of data collection and monitoring system. Used advanced solutions based on CAN and VME and modular complexes National Instruments. Currently begins implementation of the SCADA system of Sitect.

In this paper the stages of implementation of the SCADA control system. Showing part of the system, which is already widely used, as well as parts of the system, which is scheduled to launch in the near future.

DESCRIPTION AND OPERATION OF ACS

Appointment of ACS

The current system of automated control systems (ACS) accelerating-storage complex (UNK) "Siberia" - a synchrotron radiation source and the center of collective use of NRC "Kurchatov Institute" was created over 20 years ago on the basis of control equipment in the CAMAC standard. [2] It is physically and obsolete and do not meet modern requirements for speed, accuracy of measurements and speed of data transmission.

Control apparatus of the new ACS UNK with embedded processors, as well as to powerful servers with the operator's computer and network equipment has developed software at all levels of the ACS. [3] All of this should be used to create a modern system of ACS ESC "Siberia" which should significantly increase the speed control parameter stability and reliability of the SR source.

Structural diagram of ACS "Siberia"

Hardware complex (TCC) ACS ESC "Siberia" has a hierarchical structure.

The first (lower) level is the level of local systems. At the level of local systems of CCC ACS UNK transferred command of the actuators, and the level of local systems in CCC ACS UNK receives signals from the sensors parameters of field equipment.

The second level is the level of control. The second level includes a cabinet controller and control panels that form the management team of the actuators, as well as receiving signals from the sensors parameters of field equipment.

The third level is a local area network (LAN), combining the second level control cabinets with cupboard fourth server - the server level. Used for data transmission copper and fiber optic cable lines.

The fourth level includes a cabinet server provides storage and management of data communications between the control cabinets belonging to the third layer structure, on the one hand, and data on the LAN of the upper level, on the other hand.

The fifth level is the top-level LAN, server cabinet combines the fourth level and workstations (AWP) of the sixth level. To transfer data to the LAN using copper and fiber optic cable lines and LAN switches.

The sixth layer is a set of workstations, comprising the following ARM professionals:

- Operator workstation CitectSCADA
- ARM Developer CAN
- ARM developers CitectSCADA
- ARM Developer VME

Structural diagram of ACS "Siberia" is shown on Fig.1.

HARDWARE COMPLEX OF ACS

The composition of program-technical complex (PTC) ACS ESC "Siberia" includes the following products:

- cabinets and equipment;
- basic software (SCADA-system, operating systems);
- application software;
- Spare parts for the warranty period of the PTC.

ELECTROSTATIC PICK-UPS FOR DEBUNCHED BEAMS AT INR LINAC

S. Gavrilov, P. Reinhardt-Nickoulin, I. Vasilyev
 Institute for Nuclear Research of Russian Academy of Sciences, Moscow, Russia

Abstract

Pick-ups are one of the most widespread non-destructive diagnostics at charged particle accelerators. These detectors, also known as beam position monitors, are generally used for the center-of-mass position measurements of bunched beams. The paper describes the research results for infrequent case of debunched beams operation. Measurement peculiarities and distinctive features of electronics are presented. The results of test bench-based measurements and 3D finite element simulations are discussed.

INTRODUCTION

The main idea of pick-ups is to measure the charges induced by the electric field of the beam charged particles on an insulated conductive plates [1]. For a bunched beam the measurement is performed using radio frequency methods [2]. However in case of a debunched beam it is transformed into measurement of quasi-steady-state charge during a macropulse. The name "electrostatic pick-up" is better suited for this application, which became urgent recently at multipurpose research center (MRC) based on the linear accelerator of INR RAS. For some time passed the beam is accelerated up to 209 MeV of 600 MeV and is transported near $L_{Drift} \approx 400$ m to the research facilities without acceleration. Due to the momentum spread ($\Delta p/p \approx \pm 3.5 \cdot 10^{-3}$ at the base) the beam bunch structure ($T_{Bunch} \approx 200$ ps, $f_{RF} = 198.2$ MHz) is lost and the measurements are done for the debunched coasting beam [3].

THEORY FORMALISM

INR electrostatic pick-ups consist of two pairs of cylindrical signal split-electrodes with so-called "linear-cut" (Figure 1). Projection of the cut between adjacent electrodes on the vertical and horizontal planes is a diagonal line. Three guard rings at ground potential minimize asymmetric fringe field effect and reduce cross-talk between pairs.

It is known, that in linear-cut pick-ups induced charges are proportional to the actual plate length at the beam center-of-mass position [1].

In ideal 2D electrostatic approximation for cylindrical split-electrodes with inner radius R beam positions are determined by Difference of the charges over their Sum (DoS) [4]. In practice, because of the capacitive coupling between the adjacent electrodes and asymmetry of the electric field at their edges, positions are:

$$X = K_X \frac{\Delta Q_{Horizontal}}{\sum Q_{Horizontal}} + \delta_X, Y = K_Y \frac{\Delta Q_{Vertical}}{\sum Q_{Vertical}} + \delta_Y,$$

where K_X, K_Y – "pick-up constants" (the smaller the K , the larger the DoS for the same beam position), and δ_X, δ_Y – so-called "pick-up offsets" of the geometrical center with respect to the electrical center, defined by $\Delta Q = 0$.

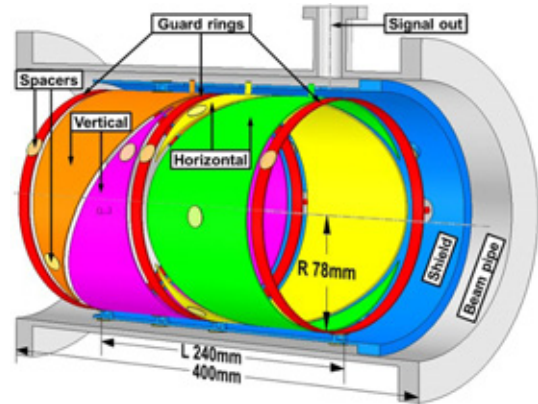


Figure 1: 3D-design of INR electrostatic pick-up.

BENCH-BASED CALIBRATION

Prior to the beam operation it is necessary to map the relationship between the beam position and the DoS, which is actually measured. A simple test bench was assembled for this purpose. The test bench consists of a copper pipe (10 mm diameter) placed between two grid dielectric plates at either sides of the pick-up. The copper pipe rests in two corresponding holes in the front and back grid plates and can be manually positioned accurate within ± 0.5 mm. A signal generator produces a voltage pulse (500 mV, 100 μ s, 50 Hz) at the pipe, imitating the debunched proton beam.

Electronics

Pick-up-based measurements require a conversion of beam-induced charge on detector plates to voltage. Generally, plate charge Q_p is integrated on the total pick-up capacitance C_p , producing voltage $V_p = Q_p/C_p$. Then voltage amplifier (Figure 2a) is used to provide gain. C_p is composed of a pick-up plate-to-ground capacitance (~ 110 pF for INR pick-ups) plus the capacitance of the interconnecting cable.

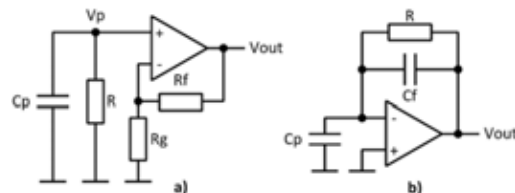


Figure 2: Pick-up electronics operation modes: (a) voltage amplifier, (b) charge amplifier.

DEVELOPMENT OF REMOTE CONTROL SYSTEM FOR H-MINUS IONS SOURCE OF INR LINAC

O.M. Volodkevich, V.N. Zubets, Yu.V. Kiselev, V.S. Klenov
Institute for Nuclear Research, Russian Academy of Sciences, Moscow, Russia

Abstract

A system of remote control of surface – plasma source of negative ions for INR LINAC was designed, constructed and put into operation.

The INR LINAC negative ions injector is based on the accelerating tube at energy of 400 keV and surface – plasma source of negative ions. Galvanic isolation and spatial separation of elements that are at potential 400 kV in the power rack of the ion source and the host computer are carried out by means of fiber-optic USB-interface extender from firms Icron. A set of multifunctional units from National Instruments allows to monitor the oscilloscope signals with up to 50 Ms/s and to control the ions source power settings. The data acquisition devices programming performed in a LabView graphical environment. Algorithm and LabView code for fast and safe “conditioning” of the ion source discharge gap and extractor gap from arcing and breakdowns were developed.

INTRODUCTION

Negative ions injector for INR LINAC is based on the accelerating tube at energy of 400 keV [1]. In this scheme, an ions source with its power supply system is located under pulsed potential of 400 kV. Ions source is a surface-plasma source developed at INP SB RAS (Novosibirsk) [2]. In this source the increase of the negative ions yield achieved by reducing the work function of the electrodes by deposition on its surface the layer of alkali metal (cesium).

A characteristic feature of the source is the presence of several modes, which have different discharge voltage, discharge current and the output of negative ions. "Pure hydrogen" mode of operation is characterized by high discharge voltage (400 V - 600 V) and low discharge currents (1 A - 10 A). The appearance in the discharge of cesium vapor causes decrease in discharge voltage (to 100 V - "low-voltage operation") and increase in the discharge current up to ~ 100 A. Furthermore, in the discharge gap may develop arcs with very low discharge voltage ~ (20 - 40) V and high current. Arcs can lead to significant erosion of the electrodes and are characterized by the absence of negative ions current at the output of the source.

Extraction of the negative ions from the plasma of a gas discharge occurs through the emission hole in the anode by apposition of extracting voltage with amplitude of 16 - 20 kV to the extracting gap with size of about 1.5 mm. Breakdowns in this gap can cause increased erosion of the electrodes and are also characterized by lack of output current of negative ions. Such breakdowns occur with the source electrodes training and during normal operation of the source.

The transition from "high-voltage" discharge mode in the "low-voltage" mode can occur quite quickly. The change in the discharge voltage is an indication of the emergence of cesium in discharge and is usually accompanied by a change in the intensity of H-minus beam.

This rather complex behavior of the discharge and the dependence of the negative ions yield from the history of the source, cause the urgent need for a reliable detailed control of key parameters of the source, which works with a pulse repetition rate up to 50 Hz. To do this, the operator is required to monitor the pulse waveforms of discharge current and discharge voltage, extracting voltage, extracted current of the H-minus ions and others, as well as to control a variety of continuous signals.

The use of the ions source in the injector of LINAC requires some additional conditions on the control system. In particular, it should be possible to integrate it into the control system of the linear accelerator and to choose the different places for the entrance to the source control system, including from the main control room of the LINAC.

STRUCTURE OF THE CONTROL SYSTEM

The control system is based on the connection of multi-function ADC / DAC units to the host computer via the USB-interface. The control system includes multi-function ADC / DAC unit NI USB 6363s, digital oscilloscope unit NI USB 5132, the control computer and fiber-optic extension of the USB-interface Ranger 2224. Block - diagram of the control system is shown at Figure 1.

USE OF FAST MAGNETIC BEAM RASTER SYSTEM FOR INR ISOTOPE PRODUCTION FACILITY

O.Volodkevich, S.Bragin, A.Feschenko, O.Grekhov, Yu.Kiselev, V.Kokhanyuk, V.Mikhailov, A.Mirzojan, V.Serov, Institute for Nuclear Research of RAS, Moscow, Russia

Abstract

Fast magnetic beam raster system for INR isotope production facility is developed and implemented. The system enables to increase the isotope production efficiency by providing a possibility of using a higher intensity proton beam on the target of the isotope production facility. First experimental results of system application for irradiation of the targets are presented.

INTRODUCTION

Interaction of the pulsed proton beam with the irradiated target results in fast (during the beam pulse) local heating of the target material. So the target material density is decreased, consequently, the efficiency of beam interaction with the target is decreased too. This effect causes limitation of beam intensity on the target and restricts the possibilities of isotope production. The problem can be solved by reducing the beam density on the target. But one cannot just increase the cross section of the beam for the existing configuration of the irradiation facility and beam extraction line. Increasing of beam cross section is provided by fast circular or elliptical scan of the beam on the target. Thus, the heating of target material is reduced, consequently, the beam intensity and irradiation efficiency can be increased. Fast beam scanning on the target is done by the Beam Fast Scan System (BFSS), which has been developed [1] and installed upstream the target. Target irradiation is carried out at beam energies from 100 MeV up to 158.6 MeV.

THE STRUCTURE AND PARAMETERS OF THE SYSTEM

Beam scanning is performed by means of its deflection in two mutually perpendicular alternating magnetic fields having the same frequency and quarter period phase shift. Mutually perpendicular alternating magnetic fields are created by two windings. Each winding consists of two symmetrical coils connected in series. Winding X deflects the beam in the horizontal direction, winding Y deflects the beam in the vertical direction. Frequency of fast beam scanning is about 5 kHz. One scan cycle takes one beam pulse of 200 μ s. The angle of beam deflection in this system has been calculated according to the results of magnetic field calibration for windings X and Y. It equals to 1.5 mrad at nominal winding current and beam energy of 158 MeV. Corresponding deflection of the beam on the target is equal to 4.5 mm in both planes. This system gives the possibility to vary the beam size and the beam scan radius on the target in wide range. BFSS consists of electromagnetic windings and control system.

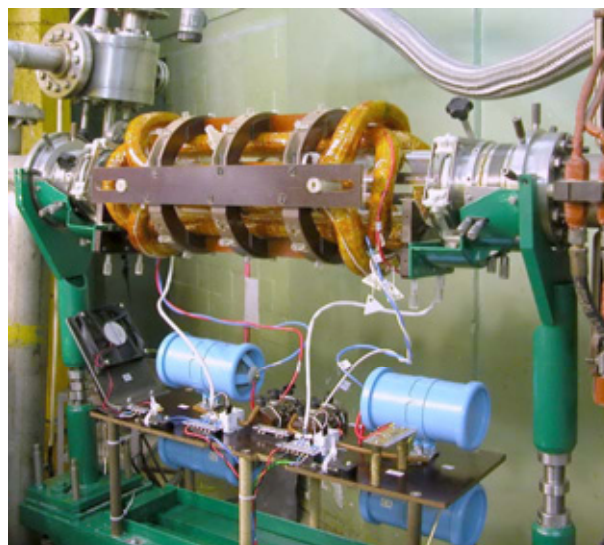


Figure 1: Windings assembly with the capacitor bank.

The windings are designed for vertical and horizontal deflection of the beam and are arranged one above the other on the outside of a glass chamber, which is a part of beam transportation line (Fig. 1). Each winding is included in parallel resonant circuit. The main characteristics of the system are given in Table 1.

Table 1: The main parameters of the system

Supply voltage	$\sim 220\text{V}, 50\text{Hz}$
Power consumption	$\leq 500\text{ W}$
Resonant circuit X	
Amplitude of deflecting magnetic field	71.5 G
Amplitude of nominal current	4.4 A
Effective magnetic length of winding	40.7 cm
Number of turns of the winding	309
Inductance of the winding	36 mH
Resonant circuit Y	
Amplitude of deflecting magnetic field	55.7 G
Amplitude of nominal current	3.8 A
Effective magnetic length of winding	52.3 cm
Number of turns of the winding	282
Inductance of the winding	36 mH
Control	
Number of channels	2
Output signal shape	Sinusoidal
Range of frequency adjustment	$4.6 \div 5.0\text{ kHz}$
Maximum output current	10 A
Current adjustment range	$0 \div 10\text{ A}$
Phase adjustment range	$\pm 90^\circ$

SIMULATION AND OPTIMIZATION OF ION OPTICAL EXTRACTION, ACCELERATION AND H⁻ ION BEAM MATCHING SYSTEMS

B.A.Frolov[#], National Research Centre “Kurchatov Institute” State Research Center of Russian Federation – Institute for High Energy Physics, Protvino, Moscow Region, Russia
V.S.Klenov, V.N.Mihailov, O.M. Volodkevich, Institute for Nuclear Research, Russian Academy of Science, Moscow, Russia

Abstract

The source of negative hydrogen ions for the implementation of multiturn charge-exchange injection to increase the intensity of IHEP buster is developed. Surface-plasma ion source with Penning discharge is selected as a source of H-minus ions. A high-current extraction system with downstream electron dumping has been designed. A three-dimensional ion optical code IBSimu has been utilized for simulation and optimization the extraction system and ion beam acceleration to energy of 100 keV. A magnetic low energy beam transport line consisting of two solenoids has been designed to match the beam with RFQ. TRACE 2D code was used to optimize LEBT. A deflecting magnet with small angular deflection (10^0) has been installed between solenoids to eliminate forward tracing of neutral atoms from ions source to RFQ.

INTRODUCTION

The beam intensity increase is one of the main tasks of modern proton accelerators' development. In the leading acceleration centers of the world the charge-exchange injection H-minus (H⁻) ions to accelerators is being used for this purpose. Such methodology is planned to be used in the IHEP booster storage ring which will allow to several times raise the intensity of U-70 complex acceleration (up to 10^{13} protons per cycle). It will be necessary to develop the highly effective and reliable source of H-minus ions. The collaboration of IHEP and INR is developing the H-minus ions source which should produce the H⁻ beam with the following parameters: H-minus current ≥ 50 mA, pulse duration – 25 μ s, repetition rate -25 Hz, energy of ions -100 keV, normalized rms emittance $\leq 0.25 \pi$ mm-mrad, e/H⁻ ratio < 5. Basing on the experience of working with the negative ions source in INR RAS [1] and BINP SB RAS [2], and also on the analysis of publications about the work of negative ions sources in BNL [3], ISIS [4], FNAL [5], CERN [6] the surface-plasma source with the Penning gas-discharge chamber with axially symmetric emission aperture at the ion source output was chosen as a source of H-minus (H⁻) ions. To extract ions from plasma, accelerate and form the beam with minimal aberrations and match the optical parameters of ion beam with the RFQ entrance the high effective ion-optical system (IOS) and low energy beam transportation system (LEBT) are needed. The numeric

modeling results of IOS of extraction, acceleration and H⁻ beam matching are described below.

EXTRACTION AND ACCELERATION SYSTEM

The three-electrode IOS is used to extract ions from plasma and accelerate to the energy of 100 keV. It is formed by plasma, extraction and acceleration electrodes. Plasma electrode works as gas discharge anode and the gas-discharge chamber of source itself is under potential of 100 kV. Emission aperture diameter equals to 3 mm. Extraction voltage is 20 kV, extracting electrode diameter is 4 mm. The acceleration of negative hydrogen ions up to energy of 100 keV happens in the second gap. The lengths of extracting and accelerating gaps were chosen basing on the detailed calculation series on the condition of getting minimal rms emittance at the matching line entrance. The drift space of 140 mm before the matching line entrance is provided after the accelerating electrode. It is meant for gas evacuation, magnet corrector and diagnostic device allocation. Penning gas-discharge chamber is located in the magnetic field with the induction of around 0.1-0.15 T. The ion source magnetic field protrudes to the extraction and acceleration area. The negative ions are deflected from the axis by the gas-discharge chamber magnetic field in the extraction and acceleration gaps. Therefore the corrector is required to compensate the H⁻ beam deflection.

The three-dimensional code IBSimu (Ion Beam Simulation) was used for the H⁻ beam extracting, focusing and accelerating simulation [7]. Self-consistent procedure of plasma sheath calculation takes into account fast and thermal positive ions, negative ions and electrons. IBSimu is used in several acceleration centers (like CERN, SNS, etc.) for modeling of negative ions extraction from plasma and beam transportation processes. IBSimu describes the experimental results with good accuracy [8].

The extraction system was simulated with ion source producing H⁻ beam current of 50 mA and co-extracted electrons current of 150 mA. In simulation the ions and electrons transverse temperature was set to 2 eV, plasma potential to 10 eV, the initial energy of particles to 5 eV, number of each sign particles to 30 000. The electron component was deflected from the ion beam on the extraction electrode by the source residual magnetic field. The simulation has been carried out with gas-discharge

[#]bfrolov.ihep@list.ru

PRODUCTION OF METAL ION BEAMS FROM ECR ION SOURCES BY MIVOC METHOD*

S. Bogomolov, A. Bondarchenko, A. Efremov, K. Kuzmenkov, A. Lebedev, K. Lebedev, V. Lebedev, V. Loginov, N. Yazvitsky, JINR, Dubna, Moscow Region, Russia
Z. Asfari, B.JP. Gall, IPHC, Strasbourg Cedex 2, France

Abstract

The production of metal ion beams with ECR ion sources using MIVOC method is described. The method is based on the use of metal compounds having a high vapor pressure at room temperature: for example, $C_2B_{10}H_{12}$, $Fe(C_5H_5)_2$ and several others. Intense ion beams of B and Fe were produced at the FLNR JINR cyclotrons using this method. The main efforts were went into production and acceleration of ^{50}Ti ion beam at the U-400 cyclotron.

The experiments on production of ^{50}Ti ion beam were performed at the test bench with the natural and enriched compounds of titanium $(CH_3)_5C_5Ti(CH_3)_3$. In the experiments at the test bench the beam currents of $^{50}Ti^{5+}$ - 80 mA and $^{48}Ti^{11+}$ - 70 mA were achieved at different settings of the source. After successful tests two 3 weeks runs with Ti-50 beam were performed at the U-400 cyclotron for the experiments on spectroscopy of super heavy elements. The intensity of the injected beam of $^{50}Ti^{5+}$ was about of 50-60 μA , during experiment the source have shown stable operation. The compound consumption rate was determined to be about of 2.4 mg/h, corresponding to ^{50}Ti consumption of 0.52 mg/h.

INTRODUCTION

The most heavy target, with which it is possible to carry out experiments on the synthesis of super heavy elements in heavy-ion reactions is ^{249}Cf , and the further progress in the area of the elements with $Z > 118$ requires the production of intense beams of accelerated neutron-enriched isotopes such as ^{50}Ti , ^{58}Fe , ^{64}Ni and others. The use of each new isotope for production of the accelerated beam requires investigations directed on optimization of the ECR source operation mode and development of technique for material feed into the source.

The method of solid materials feed into an ECR ion sources strongly depends on the specific properties of materials.

Several methods for production of ions of solids from ECR sources have been developed. Solid material can be evaporated by resistor or inductive oven, which is inserted into the source chamber [1]. Refractory metals can be sputtered by plasma ions [2] or inserted into the plasma and heated by energetic plasma electrons ("insertion technique") [3].

The other possibility for production of ions of solids is the feeding of the plasma with an organometallic compound through the Metal Ions from Volatile Compounds (MIVOC) method [4].

*Work supported by Russian Foundation for Basic Research under grant number 13-02-12011

PRODUCTION OF IONS OF METALS BY MIVOC METHOD

MIVOC method is based on the use of organometallic compounds having a high vapor pressure at room temperature: for example, $C_2B_{10}H_{12}$, $Fe(C_5H_5)_2$ and several others.

First time in FLNR the MIVOC method was used for production of intense beam of $^{11}B^{3+}$ required for generation of secondary beams of 6He and 8He at the U400M cyclotron [5]. The compound $C_2B_{10}H_{12}$ which has the vapor pressure of about 1-2 Torr at the room temperature has been used. The ion source operated stable without addition of support gas.

The maximal current of $^{11}B^{3+}$ up to 200 μA was produced from DECRIS-2 [6] ion source. The material consumption measured at 100 μA current of $^{11}B^{3+}$ constitutes 2,2 - 2,8 mg/h.

Later this method was successfully applied for production of iron, cobalt and chromium ion beams using the ferrocene, cobaltocene and chromocene as a working substances. The results, obtained at the test bench are presented in the Table 1.

Table 1: Intensity (μA) of Metal Ion Beams Produced by MIVOC Methods at the Test Bench (* - intensity optimization)

	Fe	Co	Cr
6+	43	57	70*
7+	93	80	60
8+	125	86	37
9+	172	80*	17
10+	145*		7
11+	114	82*	
12+	73	25	
13+	45		

At the U-400 cyclotron the beam of ^{58}Fe was accelerated using the same technique. The intensity of injected $^{58}Fe^{7+}$ beam was 40-50 μA (6 - 7 μA), and the $^{58}Fe^{23+}$ beam intensity at the target constitutes 15 - 17 μA (~ 0.7 μA). The consumption of ^{58}Fe constitutes about of 1,5 mg/h.

PRODUCTION OF TITANIUM ION BEAM

The experiments on production of Ti ion beams were carried out at many laboratories with the use of different methods.

The production of Ti ion beams by evaporation from the resistor oven was studied at GSI [7]. The evaporation

HYDROGEN NUCLIDES ACCELERATION FROM LASER PLASMA IN THE DIODE WITH MAGNETIC INSULATION OF ELECTRONS

K.I. Kozłowski, E.D. Vovchenko, V. L. Shatokhin, A.E. Shikanov, National Research Nuclear University "MEPhI" (Moscow Engineering Physics Institute), Moscow, Russia

Abstract

The results of an experimental investigation of the deuterons acceleration from laser plasma in a compact magnetically insulated ion diode are reported. The experiments were done in a pulsed mode ($U \leq 300$ kV, $I_{\max} \leq 600$ A, $\tau \leq 500$ ns) at a pressure of 0,01 Pa. The deuterium laser plasma was produced at the anode during irradiation of a TiD target with a laser pulse (wavelength $\lambda = 1060$ nm and intensity $q \sim 5 \cdot 10^{14}$ W/m²). The positive accelerating voltage was created by means of a 20 stage Marx generators with air spark gap-switched circuit. The ion diode has an axially symmetric geometry of the anode-cathode gap. A hollow cylindrical cathode made of a permanent magnet with induction on an axis up to 0,4 T. Magnetic insulation of electrons in the accelerating gap leads to suppression of the electronic components of the total current in 4-5 times.

INTRODUCTION

Plasma diodes are widely used for producing intense beams of electrons and ions with currents up to 100 kA and energy 100÷500 keV. Such high-energy dense beams of charged particles are applied in various fields of science and technology (for example, in ion implantation materials, injection of charged particle accelerator, neutron and x-ray radiation). In this work we discuss only the ion diodes developed for the generation of neutron radiation.

Currently, new technologies are being developed on the basis of compact pulsed neutron generator (PNG), such as screening and detection of dangerous substances and items, neutron logging oil and mineral deposits, neutron activation analysis [1]. Much attention in this research is given to the hydrogen nuclides acceleration on the basis of vacuum and gas-filled pulse diode and the optimization of their design, aimed at increasing resource and neutron yield. In this case work with the sealed designs on tritium gives an increase in the neutron yield by two orders of magnitude, however due to of high radiation danger their application is extremely limited. The main part of basic researches is carried out on a deuterium.

Good prospects for the development of compact PNG provides the use of the diode with magnetic insulation of the electrons and the laser-plasma source of deuterons [2, 3]. In environments with strong magnetic fields, the electrons move along the trajectories of the cycloid, not already captured the anode plasma and does not overlap the accelerating gap. According to preliminary estimates in such laser-plasma diode can be achieved density of the ion current up to 10^6 A/m². Such scheme has high efficiency for radial extraction of deuterium ions from the

side surface of a laser-induced plasma cloud and provides higher emission characteristics compared to the vacuum-arc ion sources. It is simple and convenient to install the laser target on the high-voltage electrode. In addition, the laser-plasma diode allows to vary the initial parameters of the plasma by changing the intensity of the laser radiation.

Neutron generators on the basis of laser deuterons sources began to be developed for a long time, about 30-40 years ago [4, 5] (in MEPhI, JINR (Dubna), All-Union Scientific Research Institute of Nuclear Geophysics and Geochemistry, some other research centers). However, these experimental studies have significantly limited the absence of laser technology with high performance. At the same time had no active development of the idea of magnetic insulation of electrons. The main part of neutron generators based on the laser-plasma diode with magnetic insulation of electrons remained as experimental models. Now, this work is continued in National Research Nuclear University MEPhI again, due to the possibility of using compact new lasers and new super-strong permanent magnets.

THE EXPERIMENTAL SET-UP

Experimental investigations carried out on the model of laser-plasma diode with direct acceleration of deuterium ions from anode laser plasma to the cathode-target, forming neutrons (DD reaction). The diode has an axially symmetric geometry of electrodes (Fig. 1) with the internal high-voltage anode and the external hollow cylindrical cathode. At the anode is installed laser TiD target. Electrodes are established in the vacuum chamber equipped with means of pumping for obtaining residual pressure to $5 \cdot 10^{-2}$ Pa. For connection of the high voltage anode with Marx generator is used the vacuum electrical connector. It isolator is designed for an operating voltage up to 500 kV.

In the diode, for the purpose of increase in ion acceleration effectiveness, the scheme with magnetic insulation of electrons is applied. The magnetic field is created by the permanent magnet which is at the same time the cathode of the diode. The cathode has a form of the hollow cylinder with an internal radius of 0,02 m and 0,06 m high. The required induction value B was estimated from a comparison of the Larmor radius r_L of accelerated electrons with the distance between the plasma anode and cathode. From a condition of

$$r_L = [(2mU)/(eB^2)]^{1/2} < 5 \cdot 10^{-3} \text{ m}, \quad (1)$$

where $U = 300$ kV – the accelerating voltage, m and e – the mass and elementary charge of electron, follows $B \approx$

ISBN 978-3-95450-170-0

HYDROGEN NUCLIDES EXTRACTION FROM PULSE PLASMA FORMATION

B.Yu. Bogdanovich, A.V. Nesterovich, A.E. Shikanov, V.L. Shatohin,
National Research Nuclear University «MEPhI», Moscow, Russia

Abstract

The features of hydrogen nuclides extraction from vacuum-arc plasma and laser sources by electric field research results are presented in the report. Such sources can be used in accelerators injection systems and in neutron generators. These processes, found, are strongly influenced by electrostatic oscillations in the plasma boundary, which position continuously varies, in addition to the ions thermal motion. Such movement kinematics determined by the velocity field in plasma formation and its concentration reducing because of the ions extraction. On the basis of this model it shows that plasma boundary moves initially in the direction to the ejection electrode, then stops and begins quickly move back. An equation for the nuclides emission current density from hydrogen plasma surface for their quasiplanar extraction geometry is obtained.

At present sources of hydrogen nuclides based on an arc discharge in a vacuum or a laser-produced plasma are used in pulse neutron generators (PNG) [1,2]. PNG contains a small-sized pulsed ion diode placed in a sealed vacuum containing hollow cylindrical anode and cathode. Between them deuterons are accelerated to the maximum energy not exceeding 150 keV by a pulse electrostatic field. The operating pressure in diode's volume comprises about 10^{-2} Pa.

The reactions $T(d,n)^4\text{He}$ and $D(d,n)^3\text{He}$ undergoing inside the target located in the cavity of a cathode electrode are used for obtaining neutrons. The target represents a metal film effectively dissolving hydrogen (Ti, Sc, Zr), evaporated onto a metal substrate and containing occluded deuterium or tritium.

Fig. 1 shows the schematic section in one embodiment of the vacuum arc deuterium source (VADS) described in works [1,3].

The anode and cathode of the source in question are made of deuterated zirconium.

The processes of deuterium plasma formation are defined by properties of an arc discharge in a vacuum [3,4]. The formation of an arc is preceded by high voltage discharge in the interelectrode space. During the build-up of the discharge current under the influence of a self-generated magnetic field, pinching of the discharge channel occurs in the cathode and anode regions where current densities can exceed 10^{10} A/m². Fast local heating of electrodes, deuterium desorption and evaporation of the metal carrier (Zirconium) take place in the pinch zones. And in this medium the formation of an arc occurs. An ignitor discharge over the surface of a hollow disk shaped insulator is used for the enhancement of an arc.

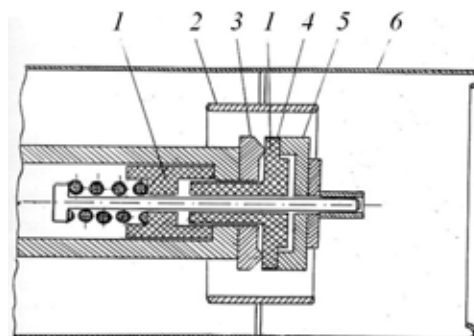


Figure 1: A three-electrode VADS: 1- insulators; 2- anode; 3- cathode; 4- semiconducting coating ; 5- igniter electrode; 6- shielding electrode

This discharge arises due to intensive field emission in the region of the triple point (insulator-metal-vacuum) characterized by abnormally high value of the electric field intensity. The breakdown of a vacuum gap between cathode and igniter electrode leads to the heating of the cathode's part followed by deuterium desorption. As a result, a partially ionized cloud of deuterium vapour rapidly spreading into the space between the cathode and anode of an ion source is formed.

The process of an arc formation is accompanied by the establishment of anode and cathode spots in the regions of its pinching over a period of time about 10^{-8} c.

The temperature of electrode spots can reach several thousand degrees. This provides a continuous deuterium desorption and evaporation of the metal carrier. After filling the discharge gap by metal pairs, they become the base medium of arcing since the ionization potential of the metal carrier is sufficiently lower than the deuterium potential. Therefore it should be assumed that the main suppliers of deuterons to VADS are not the body of an arc but its cathode and anode spots. Plasma is injected by electrode spots of an arc in the form of jets moving at a velocity of shock wave propagating in a vacuum. Estimates and the experimental data show that this velocity is equal to $\sim 10^4$ m/s [5].

The emission of laser jets by the electrode spots is a random process. There is also a significant variance of laser jets directions from pulse to pulse. However, as a result of internal anode reflections of a VAT (Vacuum acceleration tube) diode system, a laser jet is partially symmetrized.

One of the factors that shall affect the current value of deuterons extracted from VADS is the atomic weight of the metal carrier. To illustrate this effect it can be easily drawn an analogy to a simpler laser deuterium source (LDS) [1,6], which can be regarded as a physical model

NEUTRON ACCELERATING TUBES WITH MICROWAVE DEUTERONS SOURCE USING ELECTRON-CYCLOTRON RESONANCE EFFECT

Didenko A.N., Bogdanovich B.Y., Nesterovich A.V., Shikahov A.E.,
Kozlovskiy K.I., Prokopenko A.V., Shatokhin V.L.

National Research Nuclear University (Moscow Engineering Physics Institute)
Moscow, Russia

Abstract

The physical principles of increased efficiency neutron accelerating tubes based on the microwave sources of heavy hydrogen nuclides, using the electron-cyclotron resonance effect (ECR) are considered. The authors' theoretical results consist of electromagnetic oscillations generation in the working volume of the ion source of the accelerating tube with the boundary excitation of a microwave discharge. Resonator and waveguide modes for ECR-plasma excitation are examined. Features of neutron generation in these accelerator neutron tubes based on microwave source of heavy hydrogen nuclides are analyzed. The algorithm is developed and numerical simulation of neutron pulse formation in neutron generators based on microwave source is done taking into account target shape and the possible deuterons resonant recharge. Frequency dependences of the energy flux density transmitted from an alternating electromagnetic field to the electron component of the plasma are obtained. They depend on the constant longitudinal magnetic field induction and pressure in the discharge chamber. The results of these studies could form the basis for the efficient domestic portable neutron generators development based on accelerating tubes with microwave hydrogen nuclides sources.

Modern development of several areas of science and technology requires a new generation of compact electro-physical neutron sources - neutron generators [1, 2]. The main units of neutron generator are accelerating tube, high-voltage source, as well as of its operation and energy supply systems. Accelerating tube consists of an ion source of heavy hydrogen, the target, accelerating and focusing electrode system. In an accelerating tube for receiving hydrogen ions Penning sources with heated, cold or hollow cathodes, duoplasmatron, sources with high-frequency and superhigh-frequency (microwave) discharges, vacuum-arc discharge or laser plasma could be used [2-4]. The results of studies related to the development and production of neutron generators with the microwave oven sources of nuclides of hydrogen, in which the effect of an electron-cyclotron resonance (ECR) is realized, were published at [5-6].

The presence of the ECR and the magnetic constriction of the discharge allow to the increase of energy input into the plasma to achieve and maintain a high degree of ionization k (70%) with electron temperature θ (up to 10 eV) and the ion concentration n (to $\sim 10^{19} \text{ m}^{-3}$). Thus

intense beams of nuclides hydrogen with output source current density $0.1 - 10 \text{ kA/m}^2$ are formed;

$$j = \left(\frac{e^3}{2\pi M} \right)^{1/2} n \left(\frac{\theta}{A} \right)^{1/2}. \quad (1)$$

where e - elementary electric charge, M - the mass of a proton, A - the atomic mass of a nuclide of the hydrogen extracted from plasma.

Plasma generation in a microwave ion source is carried out in the course of cyclotron acceleration of electrons in the field of electro-dynamics cavity or waveguide. Thus dynamics of an electron in considered local area of the resonator will be defined by the following differential equation:

$$m \frac{d^2 \mathbf{r}}{dt^2} = -m\omega_e^2 \mathbf{r} - e\mathbf{E} \cos 2\pi ft - e \left[\frac{d\mathbf{r}}{dt}, \mathbf{B} \right] - mv \frac{d\mathbf{r}}{dt}, \quad (2)$$

where m - electron mass, \mathbf{r} - radius vector in the local coordinate system, \mathbf{E} , \mathbf{B} - vectors of the electric field and the magnetic field at a given point of the resonator, f - microwave generator frequency, v - the average electron collision frequency. The influence of an alternating magnetic field in equation (2), as shown by computer simulations carried out, can be neglected, if the power of the microwave generator does not exceed 1 kW. Equation (2) can be solved by an equivalent system of differential equations. To the electrons of the plasma which are in the set unit of volume, energy of an electromagnetic field will be transferred in unit of time ($\text{J} \cdot \text{m}^{-3} \cdot \text{s}^{-1}$):

$$q(f, p, b, z) = en\mathbf{E}(z) \left\langle \frac{d\mathbf{r}}{dt} \cos 2\pi ft \right\rangle.$$

This function has a resonant character. On Fig.1,2 as an example, shows the calculated dependencies $q(f,p,1,0)$ and $q(f,0.25,b,0)$. The point $z = 0$ corresponds to the center of the discharge space. The calculation of these temperature dependencies of was chosen at $\theta \approx 10 \text{ eV}$. Such temperature is typical for ECR plasma, obtained as a result of the probe measurements (see, for example [7]). On these curves can be clearly seen two peaks. Their presence is a consequence of the ECR. Calculations show that the presence of two such peaks occurs at commensurability of Larmor and Langmuir frequencies.

ION SOURCE DEUTERON BEAM ACCELERATION IN GAS-FILLED ION-OPTIC SYSTEM

V.I.Rashchikov, NRNU(MEPHI), Moscow, Russia

Abstract

Computer simulation of deuteron beam from ion source acceleration in gas-filled neutron tube has been fulfilled. Fully relativistic electromagnetic particle-in-cell finite difference, time-domain code SUMA [1-2] has been used to investigate the ionization and knock on processes and their influence on deuteron beam and output neutron flow parameters. When deuteron and ionized particles space charge self-field forces become the same order of magnitude as external one, virtual cathode may occur. It happens because of injected from ion source deuterons cannot overcome their own space charge potential wall and move in transverse direction. However, electrons, produced by ionization, are trapped within the deuteron beam space charge potential wall and decrease it significantly. Thus, space charge neutralization of deuteron beams by electrons, may considerably increase target current and, as a result, output neutron flow. The data obtained were compared with experimental results.

COMPUTER SIMULATION

To design neutron tube with assigned flow value and other parameters such as size, service life and so forth, preliminary computer simulation should be fulfilled. PIC code SUMA was used for ion optic system modeling and investigation of ionization processes influence on deuteron beam dynamics and output data of gas-filled neutron tubes. The code is a 2.5 dimensional time dependent model that may self-consistently describe the charged particles dynamics at various coordinate systems.

As a sample typical gas-filled pulse neutron tube has been studied (see Fig. 1).

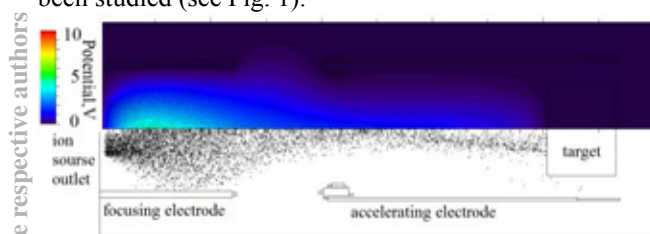


Figure 1: Deuterons distribution (lower) and their self-field potential (upper) in neutron tube.

Accelerated electrode is under -85kV potential, target -83kV , focusing electrode is grounded.

Preliminary ion source deuteron beam parameters have been obtained experimentally. For this purpose alone Langmuir probes, multi-electrode energy analyzer and Faraday cup were used. We obtain following deuteron beam parameters: longitudinal energy $1.7\pm 0.4\text{ keV}$, current $\sim 150\mu\text{A}$ for initial gas pressure $0.5\cdot 10^{-3}\text{ Torr}$. Moreover, some beam density distribution measurements were

ISBN 978-3-95450-170-0

fulfilled. Nevertheless, it was not enough data for computer simulation. Therefore, the attempt to solve inverse problem was made. As the result to be obtained the experimental deuteron current density distribution on target shown on Fig. 2a was used.

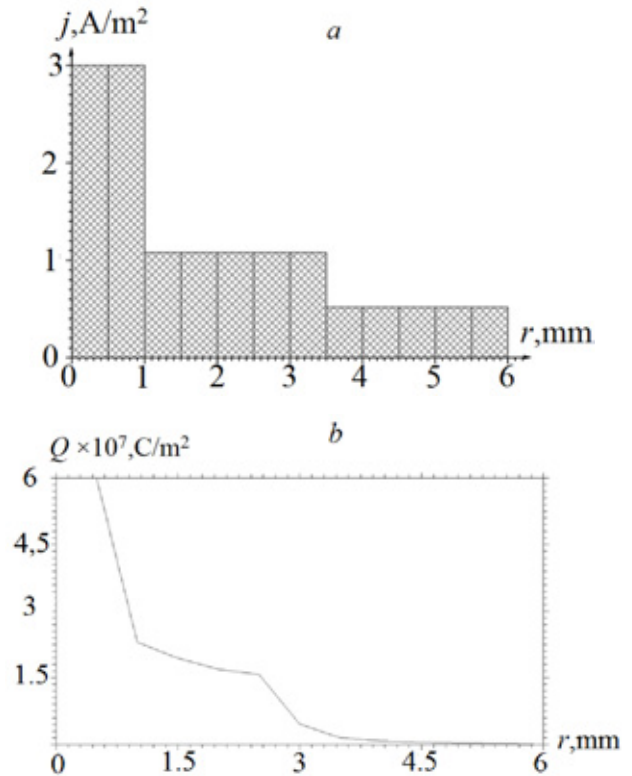


Figure 2: Current density (experimental, *a*) and charge distributions (simulation, *b*) on the target.

Experimental data were rebuilt from target depth erosion and target sputtering calculation.

Computer simulation shows that for the following input beam data, experimental and calculated distributions are close to each other: longitudinal energy $1.9\pm 0.1\text{ keV}$ and transverse energy distribution $\sim 120\text{ eV}$, current $\sim 150\mu\text{A}$ (see Fig.2b).

Passing through the gas, deuteron beam produces plasma, which consists of electrons and slow ions. Their densities under considered gas pressure range approximately equal each other (see Fig. 3.) [3].

DYNAMICS OF PLASMA-BEAM FORMATIONS IN THE ACCELERATION GAP OF THE PULSE NEUTRON GENERATOR-BASED VACUUM NEUTRON TUBE

A.V. Agafonov, The Lebedev Physical Institute of the Russian Academy of Sciences, Moscow, Russia

S.G. Kladko, S.P. Maslennikov, E.Y. Shcolnikov, NRNU MEPhI, Moscow, Russia

Abstract

The analysis of dynamics of plasma flows containing deuterium, zirconium ions and electrons in the accelerating gap of the pulse neutron generator-based vacuum neutron tube (VNT) [1] is presented in the paper. The investigations have been carried out using the code KARAT [2] for the two-dimensional non-stationary mode. The limiting currents of each component for the real accelerating gap geometry have been determined. The differences between the values of these currents and those ones determined by the Child-Langmuir equation have been demonstrated.

The analysis of plasma emitter dynamics in the gap has been performed by the model of VNT with the accelerating voltage amplitude of 120 kV and the pulse duration of 1.2 μs. It has been shown that the value of the current entering the gap from the source of ions can be very different from the current value at the target. To increase this value the accelerating gap partition using the conductive grid which is transparent for a beam and has several geometric configurations has been proposed. The ring configuration of the emitter has been considered for the same purposes. The calculations have shown that the combination of these two methods described above can allow transporting the current of deuterons from the anode grid to the target without losses.

INTRODUCTION

All set of physical processes accompanying the operation of VNT can be structured as follows. Firstly, these are processes in the vacuum arc discharge including in particular the production of an erosion mass from the discharge gap electrodes. Secondly, these are processes accompanying the expansion of plasma products emitted by a vacuum arc. Thirdly, this is the transmission of a plasma flow through the anode grid of VNT and the acceleration of deuterium ions in the accelerating gap and, fourthly, these are the processes in the target accompanied with the generation of neutrons.

Modelling of the plasma dynamics in the accelerating gap has been carried out using the code KARAT. Initial data for plasma parameters were obtained from the designed model of VNT [3]. A voltage supply to the accelerating gap has been modelled using a TEM wave, therefore the diode has been shown as a shorted coaxial transmitting line. All computational region is divided into cells, a set of which forms a rectangular grid. The basic

parameters for choosing the size of a grid unit cell are the Debye length λ_D and the collisionless skin depth. The above mentioned values of plasma parameters are:

$$\lambda_D = 2,35 \times 10^{-4} \text{ cm}, \tag{1}$$

$$\frac{c}{\omega_{pe}} = 1,68 \times 10^{-1} \text{ cm}.$$

where ω_{pe} – the electronplasma frequency

The increase in the number of cells extends the running time. As a non-stationary process is under consideration and the Debye length is more statistic parameter, in this case, the collisionless skin depth is the characteristic scale. On that basis, the number of divisions is selected in such a way that a unit cell is a square with a side of $1,24 * 10^{-2}$ sm. The time step for every iteration is automatically selected by a code and comprises $1,87 * 10^{-4}$ ns that is agreed with the period of electron component oscillations of this plasma $\sim 10^{-2}$ ns.

To estimate the space-charge limited current in a planar diode with the distance d between electrodes and the emitting surface of R, the Child-Langmuir equation can be used:

$$I_{CL} = \left(\frac{R}{d}\right)^2 \frac{\sqrt{2}}{9} \frac{mc^3}{e} \left(\frac{\varphi_a}{mc^2/e}\right)^{3/2} \tag{2}$$

where φ_a - the voltage across the diode, m – the mass of accelerated particles.

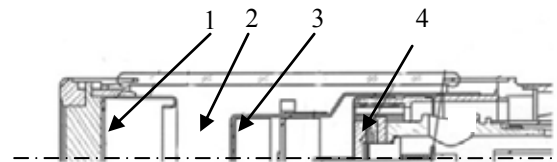


Figure 1: The design of VNT: 1 - the target, 2 – the accelerating (cylindrical) electrode, 3 – the anode grid, 4 – the ion source.

The code KARAT has been used to calculate limiting currents of each plasma component in the real geometry of the accelerating gap.

The design of typical VNT developed in All-Russia Research Institute of Automatics named after N.L. Dukhova is shown in Fig. 1. The plasma flowing comes from the ion source (4). The accelerating gap itself represents a space between the anode grid (3) and the target electrode (2).

THE NG-10 NEUTRON GENERATOR FOR PRODUCTION OF NEUTRON FLUXES IN CONTINUOUS AND PULSE MODES

D.A. Solnyshkov[#], A.V. Antonov, G.G. Voronin, A.N. Kuzhlev,
N.P. Mikulinas, A.V. Morozov, JSC “D.V. Efremov Institute of Electrophysical Apparatus”,
St. Petersburg, Russia

Abstract

The neutron generator is designed for a neutron yield of 1×10^{11} n/s in the continuous operation mode. It consists of an ion accelerator with an accelerating voltage continuously adjustable in the range of 120-150 keV and beam current of atomic deuterium ions up to 2 mA and a set of target devices, in which Ti-T and Ti-TD targets of different diameters are used. In addition to a high and stable in time yield of neutrons when operating continuously, the generator also provides the pulsed mode over a wide range of pulse widths and repetition rates. By modulating the discharge current of the ion source, the neutron generator is switched into the pulsed mode. A unique system of the discharge power supply allows operation both in continuous and pulse modes. In this case, a smooth adjustment of the pulse width and repetition rate is possible. Switching from the pulse mode to DC can be promptly made from the host computer.

A wide range of available neutron sources and instruments for measuring neutron flux parameters calls for creation of systems of apparatus for calibration and certification of such products. The NG-10 neutron generator designed in NIIIEFA can be used as an apparatus producing reference neutron fluxes in such systems. In addition to a high and stable in time neutron yield in the continuous mode, such a generator will ensure the pulse operating mode when pulse durations and repetition rates vary over a broad range.

This generator can be widely used for the neutron-activation analysis in different fields of science and engineering as well as in highly efficient systems intended for control of fissionable substances, detection of explosives, toxic substances and drugs. The NG-10 neutron generator is designed for a neutron yield of 1×10^{11} n/s in the continuous operating mode. It includes an ion accelerator with an accelerating voltage continuously adjustable in the range of 120-150 keV and beam current of atomic deuterium ions up to 2 mA and 4 target devices, in which Ti-T and Ti-TD targets of different diameters are used.

An ion beam produced by a duoplasmatron - type source is accelerated up to 150 keV in a sectionalized accelerating tube, separated in mass with an electromagnetic mass-separator and then is focused to a target with a doublet of quadrupole electromagnetic lenses. General view of the ion accelerator is shown in Fig. 1.

The power supply system of the ion source is installed in a high-voltage terminal and consists of a unit for data receive and transfer, hv sources of extraction and focusing voltage and power supply unit housing power supplies of the discharge, electromagnet, cathode filament and Pd leak valve.

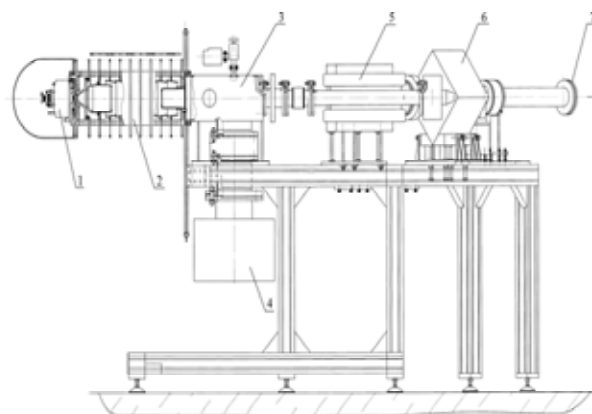


Figure 1: Ion Accelerator. General View. 1-ion source, 2-accelerating tube, 3-vacuum chamber, 4- ion pump, 5- electromagnetic mass-separator, 6- quadrupole lens, 7- target device.

All power supply systems are stabilized and operate at a frequency of 40-50 kHz, which allows its overall dimensions to be reduced and the ion beam current stability of about 1% to be attained. Power supplies under high potential are controlled through fiber-optic communication lines.

By modulating the discharge current of the ion source the neutron generator is switched into the pulse mode. For this purpose a unique system of the discharge power supply was designed, which allows operation both in continuous and pulse modes. In this case smooth adjustment of the pulse width and repetition rate is possible. Switching from the pulse mode to DC and vice versa can be promptly made from the host computer. The structural diagram of the discharge power supply is shown in Fig. 2.

The discharge power supply is a serial pulse current controller based on V1, V3 components and operating at a frequency of 40 kHz. Choke L1 serves to smooth current ripples and to store energy. The current from the controller output enters a load through the connector X1. Transistor V4 is connected in parallel with the current controller output. In the continuous mode of the power supply this transistor is cut off and does not affect its operation. When switched into the pulse mode, the

IMPROVEMENT OF THE BEAM TRANSMISSION IN THE CENTRAL REGION OF WARSAW U200P CYCLOTRON

O. Steczkiewicz[#], J. Choinski, P. Gmaj, HIL, Warsaw, Poland
V. Bekhterev, I. Ivanenko, JINR, Dubna, Moscow Region, Russia

Abstract

To date, Warsaw U200P cyclotron exploited a mirror inflector to feed heavy ions extracted from ECR ion source (10 GHz, 11 kV) to the central region of the cyclotron. However, in such configuration very low transmission was reachable after many optimizations. Additionally, the new ECR ion source (14,5 GHz, 14-24 kV) was installed, which offers energies exceeding the energy acceptance of the currently operated inflector and central region. To avoid these obstacles, we have developed a spiral inflector and redesigned central region of the cyclotron. It was a very challenging task, bearing in mind limited volume of central region in our compact machine, to carve these elements suitably for decent versatility of ion beams offered by Warsaw cyclotron. This project was executed in the collaboration with FLNR in Dubna, Russia. The cyclotron equipped with the new central region works in the "constant orbit" regime. Here we present the results of both computational simulations and measurements of the beam transmission in upgraded central region.

COMPUTATIONAL SIMULATIONS

Introduction

The basic informations of U200P cyclotron are described in Refs. [1,2]. U200P cyclotron is an isochronous cyclotron (with four – sectors magnetic structure) equipped with two 45 degrees dees. The range of RF system's frequency is from 12 MHz to 18 MHz. The ions are accelerated using second and third harmonic with the range of the dee voltages from 50 kV to 70 kV. The scope of ions, which can be accelerated in U200P cyclotron is from $A/q=4$ to $A/q=6,7$, where A is a mass number and q is a charge state of the ion. The average magnetic field in the cyclotron amounts to 2T. The measured form of the magnetic field map used in all calculations and simulations is shown in Figure 1.

Spiral Inflector

A spiral inflector consists of two coaxial, spirally twisted electrodes, placed in the magnetic field.

According to the scope of the accelerated ions and the range of the injection voltage of the ECR ion source (14kV – 24kV), following parameters of the spiral inflector were chosen. To avoid the sparking effect the maximum potential on each electrode has to be not higher than 10kV. The height of the inflector is limited by the existing geometry in the central region of the cyclotron and equal to 40mm. The electric radius, which

corresponds to the energies of the ions produced in the ion source, amounts to 25mm. Taking into account the electric radius and the maximum voltage on the electrode, the aperture of the inflector has to be equal 10mm. The width of the electrodes amounts to 20mm, due to the fact, that the ratio between the width and the spacing of the electrodes should be equal 2 to minimise the fringe field effect. According to all above mentioned parameters, the appropriate magnetic radius of the designed spiral inflector should amount to 2,16 cm. The main influence on the trajectory of the ions inside the spiral inflector and at the first accelerating gap has a minimum and the maximum injection voltage (14kV and 24kV) and the adequate level of the magnetic field in the cyclotron centre.

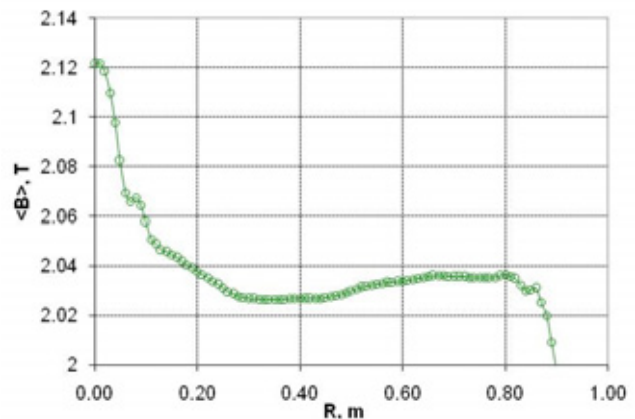


Figure 1: Magnetic field map of U200P cyclotron.

Calculations

All calculations were done for two extreme regimes for U200P cyclotron, which means the minimum and the maximum injection voltages and A/q ratio. These two cases are listed below:

- $^{16}\text{O}^{4+}$; $U_{inj} = 23,3\text{kV}$; $U_{dee} = 65\text{kV}$; $B_0 = 2,037\text{T}$; $2h$; $f = 15,33\text{MHz}$
- $^{20}\text{Ne}^{3+}$; $U_{inj} = 14\text{kV}$; $U_{dee} = 65\text{kV}$; $B_0 = 2,037\text{T}$; $3h$; $f = 14\text{MHz}$.

The spiral inflector and the new central region is designed to work in the "constant orbit" regime. Each ion has the same trajectory in the spiral inflector and before the first acceleration gap, which is secure by varying the injection voltage of the ion source and the potential at the inflector's electrodes. For both calculation regimes the transverse emittance at the entrance of the spiral inflector was defined as $150 \pi \text{ mm mrad}$.

COOLING STORAGE RING CR OF THE FAIR FACILITY - STATUS AND PERSPECTIVES*

Yu. Rogovsky[#], D. Berkaev, A. Kasaev, E. Kazantseva, I. Koop, A. Krasnov, A. Semenov, P. Shatunov, D. Shwartz, A. Starostenko, BINP SB RAS, Novosibirsk, Russia
U. Blell, C. Dimopoulou, A. Dolinskii, O. Gorda, U. Laier, H. Leibrock, S. Litvinov, I. Schurig, U. Weinrich, GSI, Darmstadt, Germany

Abstract

In 2014 BINP takes full responsibility on the design and construction of the Collector Ring of the FAIR facility. Still few work-packages remain to be on the supervision of GSI's team. In this paper the current status of the CR project is presented and future plans are discussed.

INTRODUCTION

The Collector Ring (CR) at FAIR [1,2] is a dedicated storage ring which will fulfill the following tasks (next column). Its layout and location of subsystems are shown in the Fig. 1, parameters are presented in the Table 1.

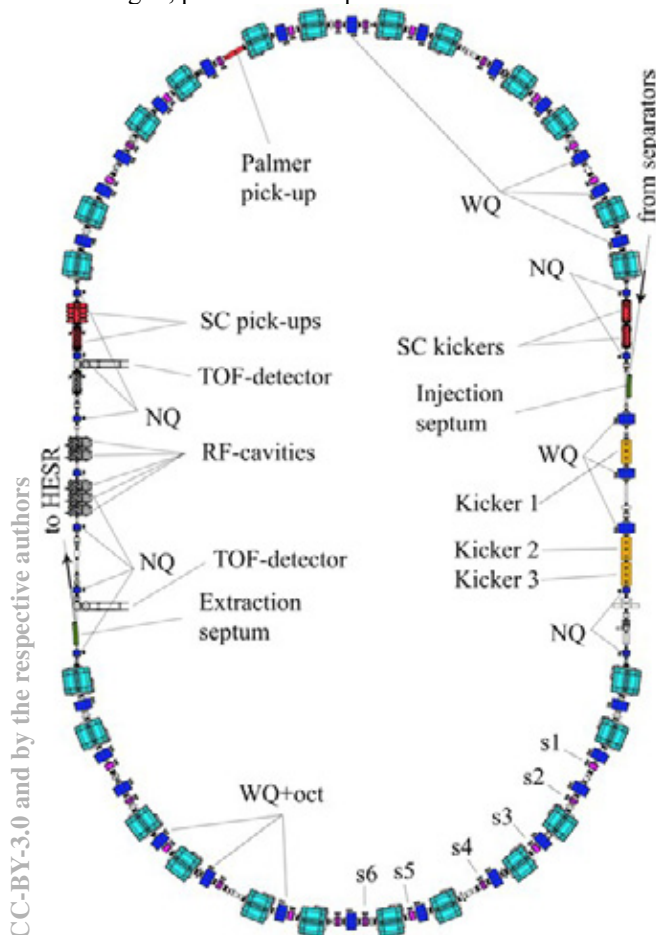


Figure 1: Layout of CR ring.

Main tasks for Collector Ring operations:

- Stochastic cooling of antiprotons coming from the antiproton separator, to be delivered to the HESR (later to RESR) storage ring.
- Stochastic cooling of rare isotope beams (RIB) coming from the Super-FRS fragment separator, to be delivered to RESR.
- TOF measurements of masses of short-lived secondary rare isotopes in the isochronous mode.

Table 1: Main parameters of Collector Ring

Circumference	221.45 m		
B·ρ	13 Tm		
Mode	p-bar	RIB	Isochronous
Max. N	10 ⁸	10 ⁹	1-10 ⁸
Kinetic energy	3 GeV	740 MeV/u	400-790 MeV/u
Lorentz γ	4.20	1.79	1.43 – 1.84
Transition γ _{tr}	3.85/4.84	2.71/2.95	1.43 – 1.84
Slip factor η	0.011	0.178	0
Acceptance	240	200	100
Max Δp/p	±3%	±1.5%	±(0.22–0.62)%

LATTICE

The lattice of the CR consists of two 180 degree arcs separated by two long straight sections. Because of the large acceptance of the CR, it is important to use large aperture magnets only where they are needed. In order to minimize both the production and operating costs, wide aperture quadrupole magnets with useful aperture 400mm by 180 mm are used for the injection section and in the arcs of the CR. The narrow quadrupole magnets with reduced horizontal good field region (useful aperture 180 mm by 180 mm) are installed only in the straight sections.

A list of magnetic elements includes:

- 24 dipole magnets
- 29 wide aperture quadrupoles (WQ) and 11 narrow aperture quadrupoles (NQ) will be used.
- 6 families of sextupoles (s1-s6) will be applied to control the chromaticity and the dispersion in the arcs.
- 3 families of octupole correctors embedded into wide quadrupoles (WQ+oct) are needed for corrections of mass measurement accuracy.
- Orbit correctors in dipoles and in drifts

According to the list of tasks, there were developed 2 basic optical schemes: one for antiproton beam cooling,

*Work is supported by SAEC "Rosatom" and Helmholtz Association
#rogovsky@inp.nsk.su

TIME DEPENDENCE OF ION BEAM TRANSVERSE PHASE-SPACE PORTRAIT ORIENTATION DURING LINAC PROTON INJECTOR PULSE

O.T. Frolov, A.S. Belov, S.E. Golubovskiy, E.S. Nikulin, V.N. Zubets,
Institute for Nuclear Research of RAS, Moscow, 117312, Russia

Abstract

It is shown that turn-on transients of the 400 kV column intermediate electrode potential is one of main processes responsible for change of beam phase-space portrait orientation during 200 μ s, 50 Hz proton injector high voltage accelerating pulse. It has been found that significant variation of this potential takes place due to transition process during a pulse in the resistive-capacitive voltage divider of the accelerating tube. The divider capacitors matching procedure has been performed. The beam emittance measurement results presented have shown significant decrease of a beam transverse phase-space portrait orientation change during injector pulse with the accelerating tube voltage divider being compensated.

The INR RAS linac proton injector provides a pulsed beam with the following parameters:
peak current – (65 \pm 100) mA; duration – 200 μ s; pulse repetition rate – 50(100) Hz; energy of ions – 400 keV. Schematic drawing of the accelerating tube is shown in Fig. 1. A beam of hydrogen ions is generated in the duoplasmatron type ion source.

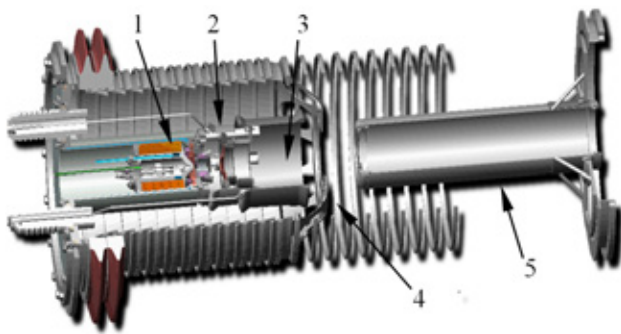


Figure 1: Schematic drawing of the accelerating tube: 1 - ion source, 2 - extracting electrode, 3 - focusing electrode, 4 - intermediate electrode, 5 - grounded electrode.

A beam is accelerated in the tube of about 1600 mm long with external surface being positioned in the open air. For decreasing of influence of coulomb repulsion of ions in beam a total length of inner accelerating gaps in vacuum have to be a minimal one, so the ion source and the grounded electrode are deeply in the tube (Fig. 1). The column has two inner accelerating gaps with a summary length of 220 mm: a) the first accelerating/focusing gap (100 mm) in which an ions have reached an energy about 95 keV; b) in the second gap (120 mm) an ions have been accelerated to an energy of 400 keV. The intermediate electrode (IE) is positioned at joint between two gaps.

Focusing electrode and IE diaphragm represent electrostatic lens which determine the beam focusing/crossover location at LEBT channel entrance when focusing electrode potential being changed.

A high accelerating voltage is distributed along the tube by means of water divider with a total resistance about 1.5 M Ω . At nominal voltage of 400 keV a current through the divider is about 0.27 A; this value more than 3 times exceeds usual beam current of 80 mA. This is important for reliable distribution of voltage along the tube and full elimination of high voltage breakdowns. The IE is connected with the divider point where high accelerating voltage is divided in approximate ratio of 1:3.

Emittance measurements for ion beam at the injector exit show significant phase-space portrait orientation change during 200 μ s injector high voltage pulse [1, 2].

Study of ion beam transport in the proton injector has been performed using Trak and SpaceCharge package developed at Field Precision LLC [3]. The numerical simulation takes into account plasma boundary formation at ion source expander, space charge effects for ion beam extracting, accelerating and transporting.

It has found that the causes of observed position/shape phase portrait changes during high voltage injector pulse can be as follows: instability of high voltage pulse; possible changes of the injector ion beam current; dynamic of ion beam space charge compensation process; the IE potential changes.

As a result of some efforts which have been made in recent times with the aim to decrease the injector accelerating voltage instability the latter is now not worse than $\pm 0.085\%$ (see Fig. 2). Pulse-to-pulse voltage instability does not exceed $\pm 0.04\%$ [4]. So the summary instability equals value of $\pm 0.125\%$ or less.

The beam transport simulation performed shows that such a change of high voltage amplitude during pulse has no influence on the ion beam transverse phase-space portrait orientation.

Influence of ion beam current changes on phase-space portrait orientation is especially important in the case of “noisy” mode of an ion source operation because of ion beam current fast variations which can reach tens percent of maximal value during a pulse. However, the present duoplasmatron source has “noiseless” operation mode [5]. As we can see from Fig. 2, beam current transients up to $\pm 8\%$ result in notable change of beam phase-space portrait orientation when beam current is about 65 mA.

Additionally to improve stability of beam current during a pulse and pulse-to-pulse stability the transistor stabilized arc modulator (instead of the thyristor unit based on pulse forming network) with no more than $\pm 0.5\%$ dis-

ELECTRON AND POSITRON BEAMS TRANSPORTATION CHANNELS TO BINP COLLIDERS*

I.M. Zemlyansky[#], D.E. Berkaev, V.A. Kiselev, I.A. Koop, A.V. Otboev, A.M. Semenov, A.A. Starostenko, Budker Institute of Nuclear Physics, Novosibirsk, Russia

Abstract

There are two accelerator complexes VEPP-2000 and VEPP-4M in BINP. There is preparatory work for building of new accelerator – Super Charm-Tau Factory. As an injector of positrons for Super c- τ Factory the existing injection complex VEPP-5 will be used. Existence of the powerful injection complex provokes the desire to use it for needs of the working accelerator complexes VEPP-2000 and VEPP-4M. Replacement of the existing injection subsystems with the injection complex VEPP-5 will allow us to increase the speed of accumulation of positrons at the accelerator complexes VEPP-2000 and VEPP-4M in 1000 and 100 times respectively. For VEPP-2000 this improvement has a great significance as the existing conversion system doesn't provide the demanded quantity of positrons for designed luminosity of a collider $1 \times 10^{32} \text{ cm}^{-2} \text{ s}^{-1}$.

In the article the short review of transportation channels from the injection complex VEPP-5 to the accelerator complexes VEPP-2000 and VEPP-4M, time sequence of an injector's work for both complexes are given. The transportation channel from the injection complex VEPP-5 to the booster ring BEP of the accelerator complex VEPP-2000 is described in details.

BINP COLLIDERS AND INJECTION COMPLEX

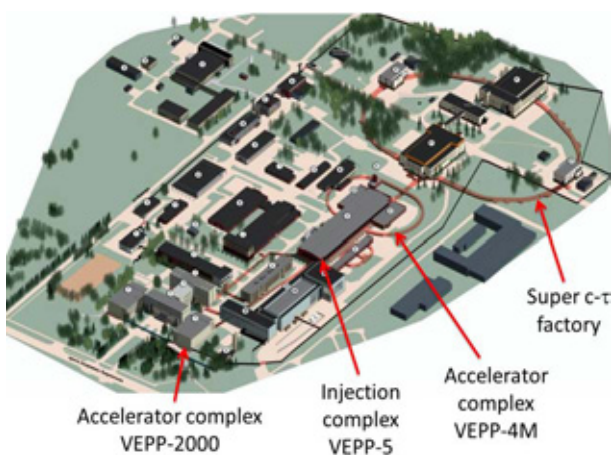


Figure 1: Colliders and Injection Complex in BINP.

In Figure 1 the arrangement of colliders and the injection complex in the territory of BINP is shown. Their detailed schemes are submitted in Figures 2-4.

The existing injection system of VEPP-2000 provides

2×10^7 positrons per second that allows us to reach luminosity $5 \times 10^{30} \text{ cm}^{-2} \text{ s}^{-1}$ at energy 1 GeV in one bunch. Achievement of designed luminosity $1 \times 10^{32} \text{ cm}^{-2} \text{ s}^{-1}$ requires 1×10^8 positrons per second.

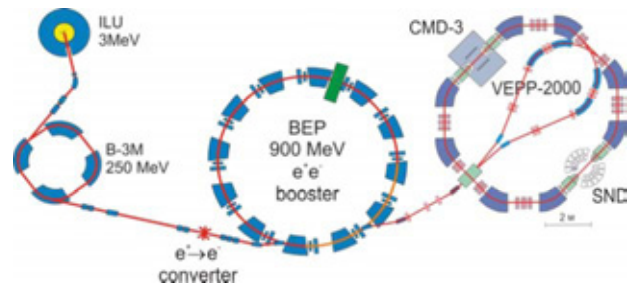


Figure 2: Accelerator Complex VEPP-2000.

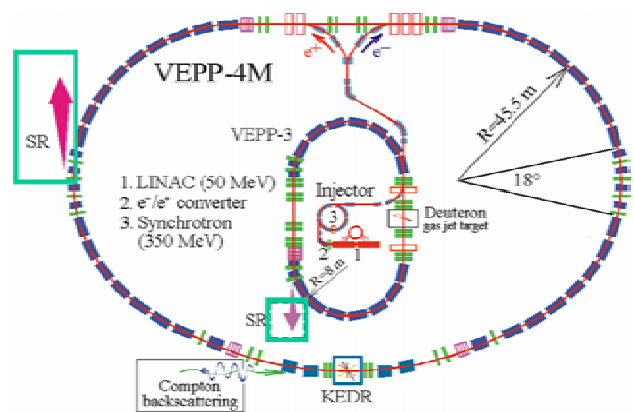


Figure 3: Accelerator Complex VEPP-4M.

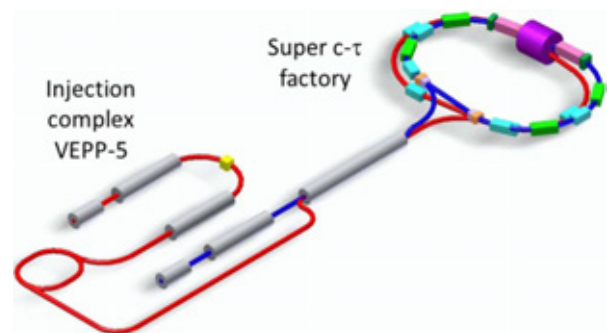


Figure 4: Super Charm-Tau Factory and Injection Complex VEPP-5.

The existing injection system of VEPP-4M makes 2×10^8 positrons per second that allows us to reach luminosity $2 \times 10^{30} \text{ cm}^{-2} \text{ s}^{-1}$ at energy 1.8 GeV in one bunch. Achievement of the future designed luminosity $8 \times 10^{31} \text{ cm}^{-2} \text{ s}^{-1}$ at energy 5.5 GeV in one bunch requires 2×10^{10} positrons per second.

*Work supported by the Ministry of Education and Science of the Russian Federation, NSh-4860.2014.2
#I.M.Zemlyansky@inp.nsk.su

PROBLEMS AND PROSPECTS OF THE TANDEM ACCELERATOR WITH VACUUM INSULATION*

D. Kasatov, A. Koshkarev, A. Kuznetsov, A. Makarov, Yu. Ostreinov, I. Sorokin, I. Shchudlo, S. Taskaev[#], Budker Institute of Nuclear Physics, Novosibirsk, Russia,

Abstract

A tandem accelerator with vacuum insulation for development of the technique of boron neutron capture therapy (BNCT) is proposed and constructed. The accelerator is characterized by rapid acceleration of charged particles. The article describes the problems of the new type of accelerator, both solved and remain to be solved. Also research plans and prospects for the use of the accelerator are presented and discussed.

INTRODUCTION

Presently, Boron Neutron Capture Therapy (BNCT) is considered to be a promising method for the selective treatment of malignant tumours [1]. The results of clinical trials, which were carried out using nuclear reactors as neutron sources, showed the possibility of treating brain glioblastoma and metastasizing melanoma incurable by other methods. The broad implementation of the BNCT in clinics requires compact inexpensive sources of epithermal neutrons. At BINP the source of epithermal neutrons based on Vacuum Insulation Tandem Accelerator (VITA) and neutron generation through ${}^7\text{Li}(p,n){}^7\text{Be}$ reaction was proposed [2], created and operated [3-5].

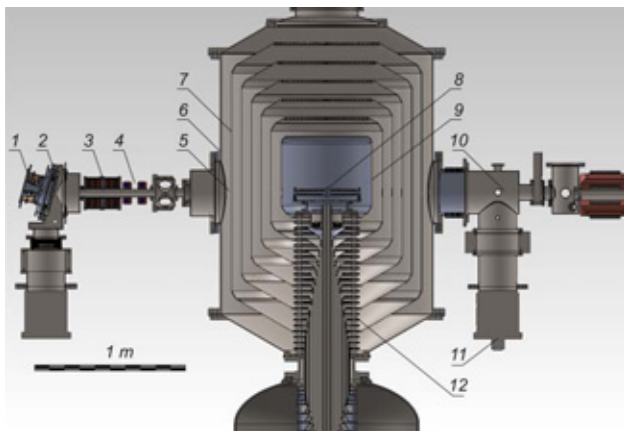


Figure 1: Vacuum insulation tandem accelerator. 1 – H^- ion source, 2 – diaphragm, 3 – magnetic lenses, 4 – corrector, 5 – a temporary location of the beam detector, 6 – accelerator, 7 – electrodes, 8 – high voltage electrode, 9 – stripper, 10 – high energy beam transport, 11 – turbo molecular pumps, 12 – bushing insulator.

General view of the accelerator is shown in Fig. 1. Negative hydrogen ions are injected and accelerated up to 1 MeV by potential applied to the electrodes, then H^- turn

into protons in the gas stripping target and at last the protons are accelerated up to 2 MeV by the same potential. Pumping of the stripping gas is carried out by cryogenic and turbomolecular pumps through the jalousies. The potential of the high-voltage and five intermediate electrodes is supplied by a high-voltage source through the bushing insulator which has a resistive divider.

PROBLEMS

The main problem of accelerators is high-voltage strength of vacuum gaps. Because of the large square of the electrodes, great energy is stored in the gaps and the inevitable breakdowns could lead to the gap detrainning. The high-voltage strength of 45-mm and 66-mm vacuum gaps was studied. It was found out that the breakdowns at stored energy of 50 J did not lead to the gaps detrainning. The stored energy in this accelerator did not exceed 26 J. Training by breakdowns allowed to obtain the required voltage of 1 MV [6].

Another problem of accelerators is strong input electrostatic lens. To provide passage of the beam through the stripping target it was necessary to refocus the beam before the lens without a significant increase in the emittance. To study H^- beam injection, the 22-channel detector has been produced and mounted in front of the first accelerating electrode. It has been determined that the best agreement with the numerical calculation is achieved by assuming the full compensation of the space charge in the transport channel and setting the transverse ion temperature equal to 1 eV at the plasma boundary of the ion source. This study described in detail in [7] resulted in better focusing of the beam required for acceleration of the beam without significant losses.

On the accelerator, stationary proton beam with 2 MeV energy, 1.6 mA current, 0.1% energy monochromaticity and 0.5% current stability was obtained [8]. To conduct BNCT, it is planned to increase the beam parameters to at least 2.5 MeV and 3 mA.

Not good enough vacuum conditions in the beginning of the acceleration of the ion beam seem to be the main current problem. Injected beam ionizes residual and stripping gas mainly in the area before a strong input lens. The born electrons are accelerated to the full voltage of 1 MV and absorbed by construction materials lead to significant power bremsstrahlung [9]. The resulting positive ions were registered by the detector mounted on inlet flange of the accelerator at beam periphery [10]. The magnitude of the current of charged particles reaches 25 % of the current of the accelerated ion beam. Probably, it is the presence of a beam of charged particles in the

* Work is financially supported by the Russia through the Ministry of Education and Science of Russia (project RFMEFI60414X0066)

[#] taskaev@inp.nsk.su

DYNAMICS OF PROCESSES IN SUBCRITICAL REACTOR DRIVEN BY LINEAR ACCELERATOR*

A.G. Golovkina[#], I.V. Kudinovich, D.A. Ovsyannikov, Yu.A. Svistunov
Saint-Petersburg State University, Saint-Petersburg, Russia

Abstract

In this paper dynamics of processes in accelerator driven subcritical reactor (ADS) is considered. ADS operates at subcritical level and the necessary neutron supply comes from the interaction of a charged particles beam with a heavy atom nucleus (spallation reaction). Mathematical model of dynamics of subcritical reactor controlled by linear accelerator is presented. Calculation results of transient processes in the reactor core taking into account fuel feedback. The reactor power level control is carried out through the regulation of linac current impulses frequency.

INTRODUCTION

The subject of research in the paper is subcritical reactor driven by proton linac. Currently, research in this field purposes is carried out in many scientific centers all over the world. They are focused on the problem of ADS design for transmutation of radioactive waste and safe energy production. The proposed projects are mostly supposed the use of accelerator with output energy about 1-2 GeV, that substantially defines the facility high price. In this paper proton linac with lower beam characteristics [1] ($E = 300$ MeV, $I = 5$ mA, duty factor 10%, $W = 1.5$ MW) is considered as an ADS driver.

The ADS control strategy should differ from traditional critical reactors control. In traditional reactors the reactivity effects are compensated by neutron absorber that guarantees the reactor maintenance in the critical condition. But there is no control impact on the subcritical reactor reactivity in ADS, the system power level is regulated only by accelerator.

POSSIBLE CONTROL SCHEMES FOR ADS WITH PROTON LINAC

Thermal power for the reactor core is defined by the following formula

$$N_T = \frac{E_f S k_{ef}}{\nu(1 - k_{ef})}, \quad (1)$$

where E_f - energy, released per a fuel nuclei fission, k_{ef} - effective multiplication factor, S - external neutron source generation intensity:

$$S = \frac{I_p m_0}{e},$$

where I_p - the accelerator average current, m_0 - neutron

yield (the average number of neutrons generated in the target by one accelerated charged particle, depends on charged particles beam energy, target composition and sizes), e - the charge of an accelerated particle.

ADS Power Level Regulation

The ADS power level control can be realized by variation of external neutron source generation intensity which depends on the average accelerator current and charged particles beam energy.

The average current regulation is possible because of pulse current value or pulse repetition rate variation.

Pulse current can be increased by raising current at the exit of plasma ion source (for example, because of increasing the emissive aperture diameter), but the beam emittance grows meanwhile, system of beam formation for injection to the acceleration channel gets more complicated, transient processes in resonators and beam dynamics change. That is the accelerator design and adjustment becomes more complicated in comparison to accelerator with fixed output parameters.

Increasing of average current by increasing pulse repetition rate is a simpler decision because particle dynamics in accelerating tract doesn't change. The effect is achieved due to the control system of rf and injector feed lines.

Increasing of proton energy can be fulfilled by activating additional resonators at the end of the accelerating channel. In should be noted that when the resonators are turned off, the beam output characteristics will get worse.

Thus, the most suitable way to control ADS is the accelerator average current variation by pulse repetition rate change.

It should be noted that because of resonators high quality factor the transient processes in them will have quite large duration. As well known, the process of rf electrical field amplitude stabilization is characterized by the following expression:

$$E = E_\infty (1 - \exp(-t/\tau)),$$

where $\tau = Q/\omega$ - magnitude which characterize transient (taking into account generator impact); t - time, Q - quality factor, E_∞ - steady value of rf field in resonator (for $t \rightarrow \infty$).

The field stabilization time can be comparable with the current pulse duration or exceed it in several times. This can lead to the additional short pulsations of source neutron power.

*Work was partly supported by SPbSU, grant No. 9.38.673.2013
#golovkina.a@gmail.com

ACCELERATORS APPLICATION FOR RADIATION PROCESSING OF FOODSTUFFS

A.Yu. Gracheova, M.A. Zaviyalov, V.V. Kondratenko, V.P. Filippovich, Russian Research Institute of Canning Technology, Vidnoye, Moscow area, Russia

Yu.S. Pavlov, Institute of Physical chemistry and Electrochemistry RAS, Moscow, Russia

A.V. Prokopenko, National Research Nuclear University (MEPhI), Moscow, Russia

Abstract

During last couple decades in Russia an interest in the electron-beam sterilization technology has been significantly renewed. The electron beam irradiation occurs at electron energies in the range from 3 up to 10 MeV with dose of 30 kGy. A special research interest is an exploring the possibility to reduce electron energy and dose characteristics upon foods irradiation. The aqueous suspensions with *Escherichia coli* and *Staphylococcus aureus* have been used as the research objects.

Whole treatment process has been carried out on an industrial electron accelerator UELV-10-10-C-70 located in the A.N. Frumkin Institute of Physical chemistry and Electrochemistry at the Russian Academy of Sciences. Beforehand partially filled and sealed 10 ml vials containing the sample suspensions with microorganisms have been installed on an accelerator line in two different positions: vertical and horizontal. The samples were irradiated with doses of 3, 5, 7 and 10 kGy. Microbiological investigations of irradiated objects have been carried out in accordance with the Russian State Standards 30726-2011 and GOST 10444.2-94 by the most probable number of colony forming units (CFU) method.

As an investigative result, the microorganism radioresistance index D10 has been determined. It makes it possible to evaluate amount of these microorganism types upon contaminated foodstuffs irradiation. It has been established that during exposure the horizontal position of the vials was more effectively. It may be explained due to simultaneous influence of two different though interrelated reasons: the direct radiation and radiation-induced ozone.

In recent years, Russia has been a renewed interest in radiation technologies. The application of radiation technologies at agriculture and food industry is a global trend [1]. Radiation sterilization technology and food processing have a high degree of efficiency, high performance, accuracy of dosing radiation and possibility to irradiate packaged products. Radiation processing occurs without significant heating of the product, which allows to sterilize thermolabile objects. Radiation facilities have low operating costs and compliance with accepted environmental standards. According to the International Commission on Radiological Protection every year on Europe market receives more than 200 000 tons of irradiated foods.

In the USSR, feasibility studies on radiation processing of food began with the beginning of the 60s of the last century. The studies were conducted at the 'A.N. Bach Institute of Biochemistry' of Academy of Sciences, in research institutes of Union Academy of Agricultural Sciences of the USSR, 'Institute of Nutrition' of Academy of Medical Sciences and 'F.F. Erisman Research Institute of Hygiene'. At that time, the lead organization for the study of radiation effects on the food served Institute of Canning and Vegetable Drying Industry (now Russian Research Institute of Canning Technology), which had gamma-installation based on the activity of the ^{60}Co irradiator 300 Curie. The investigations [2, 3] have shown promising applications of radiation method to prolong the shelf life of food products. At [4] it was shown the relevance and timeliness of the use of electron-beam sterilization technology using high current electron accelerator.

In contrast to sterilization by gamma radiation, electron radiation does not use radioactive isotopes. Electron accelerators have appeared in the 50s of the last century, but their use at that time was not economically justified. With the development of technologies for the creation of high-current electron accelerators (energy, beam current and pulse duration increase) value of electron beam sterilization decreased to quite an acceptable level. This has caused interest in the electron beams from the food industry. Irradiation occurs when the energy of the electrons in the range of 3 to 10 MeV. At these energies electrons no education isotopes in food and the penetration depth of the electrons is sufficient for their penetration into the product packed in containers ready for shipment.

High dose rates of electron irradiation allows to influence them for several seconds as opposed to hours of exposure to the product with gamma radiation. Short-term impact of accelerated electrons reduces the possible effects of oxidation product. This minimizes radiation and thermal disturbances in products and packaging material. Accelerators it is possible to vary the energy of the electrons and bremsstrahlung. Reduction of energy leads to the minimization of damage to the products during radiation treatment. In addition, the cost of operation of the accelerator and the capital cost of the creation of radiation-accelerator center is much smaller.

In Russia since 1980 designed and built for industrial radiation processes over 200 accelerators (excluding accelerators for medicine, fault detection and imaging). At the moment are in operation for more than 80 linear electron accelerator. In [5] provides an overview of the